Commission of the European Communities

technical steel research

Properties and service performance

RESEARCH INTO THE MECHANICAL BEHAVIOUR OF COLD-FORMED SECTIONS AND DRAFTING OF DESIGN RULES

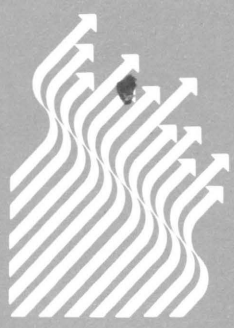

Report
EUR 11670 EN

Blow-up from microfiche original

Commission of the European Communities

technical steel research

Properties and service performance

RESEARCH INTO THE MECHANICAL BEHAVIOUR OF COLD-FORMED SECTIONS AND DRAFTING OF DESIGN RULES

[1]J. RHODES, [2]A.W. TOMÀ, [2]F. SOETENS

[1]UNIVERSITY OF STRATHCLYDE
Department of Mechanical and Process Engineering
Division of Mechanics of Materials
James Weir Building
75, Montrose Street
GB-GLASGOW G1 1XJ

[2]TNO
Institute for Building Materials and Structures
P.O. Box 49
NL-2600 AA DELFT

Contract No 7210-SA/608
(1.7.1983 – 31.12.1986)

FINAL REPORT

Directorate-General
Science, Research and Development

1988 EUR 11670 EN

Published by the
COMMISSION OF THE EUROPEAN COMMUNITIES

Directorate-General
Telecommunications, Information Industries and Innovation

L-2920 LUXEMBOURG

ABSTRACT

This report details the research carried out at the University of Strathclyde on ECSC Contract No 7210/SA/608.

The theoretical and experimental projects on the behaviour and load carrying capacity of unstiffened elements, edge stiffened elements and intermediately stiffened elements of cold formed steel sections is outlined.

Design rules governing the behaviour of the three types of elements investigated are presented.

Comparisons are made with the predictions of the European Recommendations.

RESUME

Ce rapport décrit en détail la recherche effectuée à l'Université de Strathclyde dans le cadre du contrat CECA n° 7210-SA/608.

Il décrit les projets théoriques et expérimentaux relatifs au comportement et à la capacité de charge des éléments assouplis, des éléments renforcés aux arêtes et des éléments renforcés intermédiaires des profilés d'acier formés à froid.

Le rapport présente les règles de conception régissant le comportement des trois types d'éléments étudiés.

Il effectue des comparaisons avec les prévisions des recommandations européennes.

ZUSAMMENFASSUNG

Der Bericht schildert ausführlich die an der Universität Strathclyde im Rahmen des EGKS-Vertrages Nr. 7210-SA/608 durchgeführten Forschungsarbeiten.

Es wird über die theoretischen und experimentellen Untersuchungen über das Verhalten und die Tragfähigkeit unversteifter, randversteifter und zwischenversteifter Elemente aus kaltverformten Stahlprofilen berichtet.

Vorgestellt werden die für das Verhalten der drei untersuchten Elementtypen maßgeblichen Bemessungsregeln.

Außerdem werden Vergleiche mit den Angaben der europäischen Empfehlungen angestellt.

CONTENTS

		Page
1.	GENERAL	1
2.	UNSTIFFENED ELEMENTS	4
3.	EDGE STIFFENED ELEMENTS	12
4.	INTERMEDIATEY STIFFENED ELEMENTS	34
5.	PROPOSED DESIGN RULES GOVERNING ELEMENT BEHAVIOUR	50
6.	COMPARISON WITH EUROPEAN RECOMMENDATIONS	59
7.	SUMMARY	63
8.	REFERENCES	65
TABLES 1 - 13		67
FIGURES 1 - 117		106

1. GENERAL

This report summarises the work carried out at the University of Strathclyde on RESEARCH INTO THE MECHANICAL BEHAVIOUR OF COLD FORMED SECTIONS AND DRAFTING OF DESIGN RULES as part of ECSC contract No 7210/SA/608.

The main aims of this part of the research programme were to examine the behaviour of specific types of elements of cold formed sections. The types of elements are as follows:-

(a) Unstiffened elements

(b) Edge stiffened elements

(c) Intermediately stiffened elements.

From the examination of these types of behaviour the aims were to provide simple user friendly design rules governing the behaviour of such elements.

Each type of element was subjected to comprehensive examination on the basis of theoretical analysis and experimentation. The theoretical investigations of each case are of necessity extremely complex. Since protracted expositions of mathematical derivations do not convey the physical realities of the problems, the theoretical aspects are only outlined in this report. The work of this project has resulted in the attainment of three PhD degrees (1) - (3) and one MSc degree (4) as well as forming the basis of a number of BSc research projects. Full details of the theoretical aspects of each problem are given in Refs (1) - (4).

In deriving the design rules applicable to each type of element recourse was made to the theoretical findings to determine the general form of the design rules, and to some extent simplified theoretical models were set up. However, the factors used in the relevant equations were based to a large extent on the experimental findings.

Two points of note became clear during the investigations. It is worthwhile mentioning these points early in this report, as they are of substantial importance:-

(i) The applicability of a set of design rules for a specific type of element is dependant on the design system used as a whole. If it is desired to accurately assess the effects of individual elements on section behaviour then the assessment of the complete section behaviour must follow a prescribed pattern.

(ii) The real behaviour of an element cannot accurately and generally be specified in isolation. Element behaviour is dependant on the geometry of the complete section and the type of loading applied to the complete member (e.g., bending or compression). Design specifications at the present time rely substantially on design rules which are applicable to elements in isolation and because of this they are able to specify very simple rules. While simplicity of the design rules is an important prerequisite at this time, and in this project, it should be realised that "simplicity" and "generality" are not in this case synonymous. Design rules which are too simple can only be accurately applied within a narrow range, and to cater for wider applicability, with accuracy, a

greater degree of sophistication must be introduced into the rules.

In this report, to take point (i) into account, element design rules are presented for elements not specifically covered by this investigation. These are required in order to assess the behaviour of individual elements on the basis of tests carried out on complete sections.

The design rules used in this report for dealing with ancillary elements are not the same as those of the European Recommendations (5). This arises largely because the European Recommendations were not completed, and therefore subject to change, until the project was far advanced. The rules used for ancillary elements are specified in the report.

With regard to point (ii) the design rules presented in this report have been kept simple, and areas in which there is doubt as to their applicability are mentioned at the relevant stages.

During this investigation a large number of tests, over 350, were carried out on elements and sections and as time progressed various avenues of investigation not initially envisaged were explored. As would be expected the results of these investigations highlighted areas in which present knowledge is not sufficient, but which could not be completely covered in this programme. Although this is the final report it should be mentioned that the work on various aspects of this project is continuing with a view to producing a more comprehensive coverage of the design aspects of cold formed steel sections.

In the following sections the investigations of the three different types of elements are recounted. The investigation of the first type of element, unstiffened elements, extended a previous project sponsored by the British Cold Rolled Sections Association.

2. UNSTIFFENED ELEMENTS

Unstiffened elements, i.e., elements supported on one edge only, have low local buckling resistance in comparison to stiffened elements. However these elements can have substantial postbuckling carrying capacity. After local buckling an unstiffened element loses all its effectiveness near the free edge, and further compression resistance only occurs near the supported edge as shown in Figure 1. Because of this the effective cross-section becomes narrow, and the in-plane bending resistance is substantially reduced. Due to this behaviour unstiffened elements can have detrimental effects on the load capacity of columns and beams containing such elements. This has led to mistrust of the postbuckling capacity of unstiffened elements, and the AISI specifications prior to the most recent (6) have severely restricted the use of the postbuckling capacity of such elements. Despite this, there can be substantial postbuckling capacity and a variety of attempts have been made to postulate design approaches which predict the behaviour of such elements. Approaches using the concepts of "effective thickness" "varying effective thickness" and "effective width" as illustrated in Figures 2, 3 and 4 have been postulated in the past. In the new British Specification (7), and in the new AISI Specification and the new European Recommendations effective width approaches have been used. In the European Recommendations the parts of the elements in tension are considered to be fully effective, and the effective width expression takes this into account.

In the British Code increased effective widths are specified for unstiffened elements.

2.1 Outline of theoretical approach

Theoretical examination of unstiffened element behaviour has been carried out by the writer prior to the start of this investigation (8) on the basis of an elastic postbuckling analysis using the semi-energy approach originally derived by Marguerre (9). This examination suggested that in the elastic range an unstiffened element bent in such a way that the free edges were in compression had postbuckling capacity, but the flexural rigidity was significantly reduced by local buckling.

The flexural rigidity was reduced to about 0.09 of its prebuckling value if the supported edge was simply supported, and to about 0.14 of its prebuckling value if the supported edge was fixed.

Further investigations carried out during this project suggest that these values are reasonably accurate in assessment of the postbuckling behaviour of unstiffened elements, and that the bending behaviour of unstiffened elements could adequately be described using an "effective width" approach provided that the effective width formulation was suitable.

The von Karman effective width equation for stiffened elements is

$$\frac{b_e}{b} = \sqrt{\frac{\sigma_{CR}}{\sigma_Y}}$$

where b_e is the effective width, b is the real width, σ_{CR} is the critical buckling stress and σ_Y is the yield stress. Von Karman obtained this equation on the basis of simplified analysis, and this equation has since been modified for use in many design codes.

Using a similar simplified analysis for unstiffened elements yields the result

$$\frac{b_e}{b} = \left(\frac{\sigma_{CR}}{\sigma_Y}\right)^{1/3}$$

In the presence of imperfections and in the light of experimental findings this equation can be modified to

$$\frac{b_e}{b} = C\left(\frac{\sigma_{CR}}{\sigma_Y}\right)^{1/3}$$

where c is obtained on the basis of experiment.

2.2 Experimental Investigations

In the experimental investigations, cold formed steel sections containing unstiffened elements were loaded as beams, with the unstiffened elements comprising the bending elements of these beams.

A number of different series of tests were carried out on plain channel, angled channel and angle section beams to investigate different aspects of their behaviour.

The general set up of the test rig used in these investigations is shown in Figure 5. This test rig was used in a Tinius Olsen testing machine and

applied uniform moment to a beam over the central span. For most of the tests the central span was set at 700 mm, but this could be varied as required.

A total of 115 tests were carried out on sections of general plain channel shape, having the flanges either perpendicular to the webs or at some angle θ to the webs. Of these tests, 91 were carried out on channels bent in such a way that bending caused compression of the flange free edges, and 24 were bent in the opposite direction, i.e., causing tension of the flange free edges.

Details of the specimens tested and the experimental failure moments are given in TABLE 1. Specimens which have T appended to their number were tested with the flange free edges in tension.

A total of 36 tests were also carried out on Vee sections with large angles between the legs of the Vee. These tests were carried out largely to examine the effects of large corner angles on the section behaviour, (as were some of the channel tests), and the tests were carried out on a modified test rig similar to that used for the channels. Of these tests half were carried out in bending to cause compression of the free edges of the elements, and half in the reverse direction. The dimensions and failure moments of these sections are given in TABLE 2. In this table the letters "C" and "T" used in the section number specify the free edge compression or tension conditions under the test loading. All specimens were manufactured in the University, and for each different sheet of material used tensile test specimens were cut and tested.

Typical moment-deflection curves are shown in Figures 6, 7 and 8 for channels having flange perpendicular to the webs. For relatively thick material, Figure 6, the nonlinearity near the maximum moments is due to plasticity, while for very thin material, Figure 8, the nonlinearity is due to local buckling. For the deeper sections in this figure local buckling occurs theoretically at a moment of around 20 Nm, and this indicates the high degree of postbuckling capacity. The deflections recorded here were the total deflections, including deflections of the overhangs between supports and end loads. An indication of the effects of flange angle from the vertical is given in Figure 9, for angled channels.

Figure 10 shows non dimensional values of experimental failure moment for all channel section tests where the flange angle is 60^{o} or less and the flange free edges are in compression. Also shown on this figure are values of fully plastic and first yield moments for different flange/web ratios. Points immediately apparent from this figure are:

1. The specimens tested can withstand the full first yield moment if the flange width to thickness ratio is less than about 29. This indicates significantly greater strength than given in most current design codes.

2. For flange width to thickness ratios less than about 16 the fully plastic moment, or greater resistance, was attained. No design code for cold formed steel known to the writer permits any degree of compression plasticity in unstiffened elements with b/t greater than 10, whereas

these tests indicate partial plastic capacity for b/t up to 29, and full plastic capacity for b/t less than 16 for the conditions considered.

Comparisons of the experimental failure moments with those predicted using the British Code and the European Recommendations are shown in Figure 11. The predictions of both codes are over conservative. The AISI code cannot be used to examine this case as the effective width in that code is governed by the stress at the supported edge, which for this case, tensile.

Figure 12 shows comparisons of the experimental failure loads with the proposed design rule of this report. This is as follows for b/t > 30

$$\frac{b_e}{b} = 0.9\left(\frac{\sigma_{CR}}{\sigma_Y}\right)^{1/2}$$

where $\sigma_{CR} = 185000\, K \left(\frac{t}{b}\right)^2$

and $K = 3.4/(2 + h/(1+h))$ for the plain channels considered

The expressions for σ_{CR} and K are taken from the British Code. The σ_{CR} expression is simply obtained using standard buckling formulae and the material constants for steel. The expression for K was derived in the course of the work reported here. From Figure 12 it may be claimed that the design formulae give reasonably good, slightly conservative estimates of failure for members with b/t > 30.

For relatively thick members, i.e, b/t < 30, the effects of post compression yield can be taken into account using an elasto-plastic stress distribution together with the assumption that failure occurs at the point of plastic

buckling in the flange. A perhaps simpler approach is to use an interaction formula in the range where σ_{CR} is greater than Ys. The interaction formula suggested is

$$\text{for } \sigma_{CR} > \sigma_Y \qquad M_{ULT} = M_P - \frac{\sigma_Y}{\sigma_{CR}} (M_P - M_Y)$$

where M_P is the fully plastic moment, M_Y is the moment to cause first yield and M_{ULT} is the ultimate moment. The failure predictions obtained using this equation are given in Figure 12, showing conservative agreement with test results.

The effects of large corner angles is shown in Figure 13. This plots the comparison of failure moments obtained using the design approach proposed here with the results of those tests which were carried out on specimens with large corner angles. As may be observed from the figure, at corner angles less than about 60°, the experimental results are in good agreement with the design predictions. For greater corner angles the experimental results are less than those predicted by the design analysis. This was expected, due to the high order effects which arise for large corner angles, and is the subject of a continuing research project. However, from the results shown it can be stated that the design rules proposed are adequate for corner angles of 45° greater than the right angle, with something in reserve.

In the case of unstiffened elements bent in such a way that the free edges are in tension, the results obtained showed that a partially plastic failure criterion, as used in the European Recommendations, is applicable. This is illustrated in Figure 14 which shows variation of experimental failure moment with variation in flange-web angle. The proposed design procedure in this case is to treat the unstiffened element as if it were a stiffened element.

The stress distribution was assumed to be elasto-plastic as illustrated in the figure and failure was assumed when the stress on the effective width of the compression element reached Ys. The effective width was evaluated using the expression given in Section 5 with the buckling coefficient for the compression element taken as 5.34 as calculated theoretically.

As may be observed the design rules predicted the maximum moment with some conservatism for corner angles less than about 50^{o}. For large corner angles, as expected the predictions are non-conservative. This graph also therefore justifies a limit of 45^{o} corner angles for safe application of the design rules.

Although the failure moments are predicted accurately by the methods described here, for thin elements the experimental deflections before failure could be substantially greater than predicted using the effective width approach. This can be explained on the basis of two strain investigations carried out on sections bent to cause compression of the flange free edges. In these investigations, strain gauges were laid on one flange as indicated in Figure 15. Readings of the strains for specimen No 18, of relatively thick material, and specimen No 32, of very thin material, are shown in Figures 16 and 17. The variation of strain on the tension side very adequately shows the significant movement of the neutral axis towards the web as predicted by the effective width approach. On the compression side, however, for the thinner element, the large buckling deformations affect the strains (and stresses) very substantially. So much so that for the thinner element of Figure 17, at high moments, the strain and stress on the compressed free edge becomes tensile. This reduction in strain and stress is

also very noticeable at the point of maximum strain, and indeed the maximum membrane strain is much less than the yield value when failure occurs. This is in agreement with theoretical analysis, and indicates that failure occurs due to the combination of membrane and out of plane bending stresses reaching yield. Under these conditions, although an effective width approach can give accurate predictions of failure it is not really modelling the failure mechanics. To investigate this further, a plastic mechanism analysis was employed whereby plastic failure was assumed to occur at "hinge lines" as illustrated in Figure 18. This produced very good agreement with experimental results. However, since the effective width approach gives simple and accurate assessments of failure load, and no clear way could be seen to produce quite so simple equations using the mechanism approach it was decided not to pursue this approach with regard to design analysis at the present time.

3. EDGE STIFFENED ELEMENTS

Edge stiffeners are used to avoid the problems of early buckling which arise in unstiffened elements, and to make such elements behave as if they were stiffened. In order to achieve this an edge stiffener must have a specified minimum flexural rigidity. Until recent years it was assumed that the required flexural rigidity of an edge stiffener was such that it increased the buckling coefficient of its associated element to be equal to that of a stiffened element. This is now known to be an unsatisfactory and insufficient criterion. For elements which have an edge stiffener, an adequate stiffener must support the edge not only at the point of buckling, but throughout the postbuckling range until the element fails as a stiffened element.

In the research reported here theoretical and experimental investigations were initially carried out on individual elements. The stiffener rigidities required for such elements were substantially greater than those used in design codes and it became clear that the support from adjacent elements had a substantial effect on the required stiffener rigidity. Further series of tests were carried out on edge stiffened elements as parts of compressed sections and as elements of beams.

3.1 Outline of theoretical approach

In the theoretical investigation of edge stiffened elements the semi-energy method approach was again used. The possibility of plate initiated buckling (local buckling) and stiffener initiated buckling (torsional buckling) occurring either individually or simultaneously was considered. The types of buckling and the nomenclature used are illustrated in Figure 19. In order to simulate the effects of adjacent elements it was assumed that rotations of the supported edge of the element were resisted elastically, with the rotational stiffness, R, being different for the local mode than for the torsional mode as occurs in actual sections. Full details of the investigation are given in Ref (1), and only the general findings are mentioned here. These are:

1. For elements with simply supported edges the buckling loads obtained from the analysis were in fairly good agreement with, as indicated in Figure 20, but less than those obtained by Kloppel (10). This indicated that the present analysis was more accurate than Kloppels.

2. In consideration of a single half wavelength of the torsional buckling mode it was found that there were strongly directional effects, i.e., buckling in one direction was easier than in the opposite direction. The directionality was affected by the edge stiffener geometry and by the presence of local buckling.

3. The minimum resistance to torsional (stiffener initiated) buckling of a given edge stiffened element is extremely dependant on the restraint against rotation of the supported edge. If this edge is simply supported then the torsional buckling load decreases with increase in length of the element, and the minimum buckling load of an edge stiffened element eventually becomes less than that of an unstiffened element. This seemingly strange result had been earlier found by Bulson (11). It follows from this that the adjacent elements of a section, and the loading applied to the section, have a substantial effect on the buckling load of the edge stiffened element.

3.2 Experimental investigation

In the experimental investigation of edge stiffened elements tests were carried out on individual elements with simple right angle lips, elements with angled lips and elements with compound lips. Tests were also carried out on compressed sections having elements with simple and compound edge stiffeners and on beam sections with simple lip edge stiffeners. Apart from one series of compression members with simple lips all elements and sections were manufactured in the University. Tensile test specimens were cut and tested from all sheets of material used, so that each specimen could be

analysed on the basis of the true yield stress for that specimen. The types of elements and members tested are illustrated in Figure 21.

To test individual elements a test rig was designed and manufactured in the University. This test rig is shown diagramatically in Figure 22 and different elevations and cross-sections in Figure 23. Detail drawings have been omitted. This test rig accommodated L shaped specimens of total length 985 mm and overall width 75 mm. Three holes were drilled at the top and bottom of each specimen and the specimen was fixed to the loading heads of the test rig through these holes. Thus in the test the specimen ends were fixed, and the free length of element between the supports was 915 mm. The supported edge was held in place by knife edge supports which provided simple support conditions. In the case of elements with simple lip edge stiffeners the specimens were manufactured with 5 different lip widths of nominal dimensions 0, 6.25 mm, 12.5 mm, 18.75 mm and 25 mm.

To facilitate measurement of deflections of these specimens, and to examine the initial imperfections of the specimens a deflection measuring device ~ DMD ~ was designed and manufactured in the University. This device was designed to provide a magnified plot of deflection against distance along the specimen. The DMD is shown in Figure 24. This consists of a linearly variable differential transformer (LVDT) which is used as a contact probe, positioned in a holder which is mounted onto two longitudinal stainless steel tubes and can move freely along these tubes. The longitudinal tubes are in turn mounted on transverse tubes at each end, so that the probe can be positioned at any point in a plane. The frame of the DMD is made of slotted angle, and the length and width of the DMD can be varied by the use of longer

or shorter tubes and framing angle. The position of the contact probe along the longitudinal tubes is measured by a position transducer. The contact probe is moved remotely by means of a wire and pulley arrangement through a handle positioned along one of the edge framing angles. This ensures that measurement of the deflections is accomplished without applying any force to the specimen other than the spring force of the contact probe. The signals from contact probe and position transducer are fed to an XY plotter to produce a plot of deflection distance along the specimen. During test the DMD was attached to the test rig through its slotted angle frame.

The DMD was made with easy adjustability so that this device could be used with a variety of test rigs, and this allowed the use of this device with subsequent compressed section tests and intermediately stiffened element tests.

The stiffened element tests were carried out in the Tinius Olsen test machine. A total of 75 tests were carried out on elements with simple right angled lip stiffeners. A further 6 tests were carried out on angled lip stiffeners and 24 tests were carried out on compound lip stiffeners, making a total of 105 tests on individual elements. The specimen dimensions and failure loads are given in TABLE 3.

Figure 25 shows typical measurements of initial imperfections in the torsional and local modes measured on an unloaded specimen by the DMD.

Figure 26 to 28 show typical variations of deflections along the centre line of loaded edge stiffened elements. The elements shown in Figure 26 have

small thickness and large lips, and in such a case local buckling, indicated by the short wavelength deflections, occurs initially. Failure in these cases is largely due to local buckling.

The specimens of Figure 27 have no lip and a very small lip, and here torsional buckling in a single half wave occurs. Note that the end fixity is clearly shown. It is also of note that the specimen with no lip shown here developed shorter have wavelength buckles on the long wavelength buckle as loading progressed.

The specimens shown in Figure 28, despite having relatively large lips, underwent torsional buckling initially. It is of interest to note from this figure that torsional buckling does not produce immediate failure, and in fact there can be a substantial post-torsional buckling range. It is also of interest to note that, as predicted theoretically, local buckling can occur after the elements have buckled torsionally.

Figure 29 shows plots of load against end shortening obtained from a series of specimens having the same material thickness and different lip sizes. The full lines shown in this figure were directly obtained from the Tinius Olsen test machine plotter and the various dots and other symbols represent the results of dial gauges which were used to check various aspects of the machine measurement system. As would be expected, increasing the stiffener size increases the load capacity.

Figures 30 and 31 show comparisons of the theoretical and experimental load-end shortening curves, indicating reasonable agreement.

On one specimen a strain investigation was carried out. Two bands of strain gauges were positioned on the specimen at the locations shown in Figure 32. The top band location was specified to coincide with a position on the specimen where the local imperfections had a maximum value, and the bottom band was located on the mid-length of the specimen. Each band of gauges consisted of 10 two gauge rosettes placed on each side of the material, from which membrane strains and stresses could be obtained. The total number of gauges used in the two bands was 80.

Figures 33 and 34 show the variation of stresses obtained from the strain gauge readings for a number of applied loads. The specimen examined was of thin material and had a large lip. The well known effects of reducing stress towards the centre of the main element and towards the free edge of the lip are clearly observed. It may also be observed that the stresses at the lip-main element junction are slightly less than those at the supported edge. This is due to small out of plane deformations of the junction.

The variation of experimental failure loads with variations in element width to thickness ratio is shown in Figure 35. The failure loads are plotted in non-dimensional form. Main points of note from this figure are:-

1. For all material thicknesses the failure load increases with increase in lip size until the lips are large in width. For lip sizes of approximately one quarter of the plate width and one third of the plate width the failure stresses are similar for most of the range. Thus for the elements tested the required lip width for adequate support is about one quarter of element width. This is not quite true for the lower

width to thickness ratios, where there is still some increase in failure stress as the lip size increases. Thus for adequate support the lip sizes for thicker elements require to be somewhat larger than quarter of the element width.

2. For the highest b/t ratio tested, i.e, 108, the non dimensional experimental failure loads show a reduction from those which would be expected, and the curves show a downward trend. This caused some speculation as to whether there was some unforeseen problem with the test rig, or some high order effects which became manifest at this stage. However, the major reason for the low failure stresses for this b/t ratio lies simply in the fact that the material of this thickness which was used had a very low yield stress, 174 N/mm^2, in comparison with all the other material thicknesses.

3.2.2 Compression members

In order to examine the effects of adjacent elements on the behaviour of edge stiffened elements, tests were carried out on outwardly turned lipped channel, or top hat section compression members. A total of 22 specimens were tested, 18 having simple lip stiffeners and 4 having compound lip stiffeners. For the simple lip specimens, all specimens had flanges and webs of 77 mm nominal width. Three different thicknesses of material were used and for each thickness 6 different lip widths were tested ranging from 0 to 32 mm in approximately equal steps. Details of the specimen geometries and dimensions are given in TABLE 4.

The specimens were tested between flat plattens in the Tinius Olsen test machine, and the test arrangement is shown diagrammatically in Figure 36. Prior to test the ends of the formed specimens were carefully milled and ground to ensure a flat and plane surface perpendicular to their longitudinal axes. Aluminium plates of 0.8 mm thickness were glued to the open ends of the specimens using quick setting Araldite 2002. This procedure had been carried out on earlier tests of thin-walled sections, and proved successful in eliminating any slight irregularities in the specimen ends which may still exist after machining and in ensuring that the specimen ends did not warp. Strain gauges were attached to each specimen at mid height in the positions indicated in Figure 37. These gauges were used to ensure that uniform compression was applied across the section, to determine the local buckling load if required, and to assess the behaviour of the stiffener-flange junction for future study. The strain gauge results are not presented in this report, but are available in Ref (1) if required.

Out of plane deflections of the edge stiffened element were measured at the position shown in Figure 38. The deflection plots at different loads are shown for all specimens of a single thickness in Figures 39-41. As for the individual elements it can be observed that small lips do not prevent long wave torsional buckling deflections whereas with larger lips these are prevented, and short wave local buckles are more in evidence.

Failure loads for all the specimens tested are given in TABLE 5.

3.2.3 Bending members

The behaviour of edge stiffened elements under bending such that the edge stiffeners are in tension is well known, and needs no examination. In the case of elements bent to cause compression of the edge stiffeners, however, some investigation was considered worthwhile. A series of tests were therefore carried out on top hat sections loaded as beams in which the edge stiffeners were subjected to compression.

This series consisted of 8 tests on top hat sections having nominal flange and web dimensions of 52 mm and of thickness 0.87 mm. The lip dimensions were varied from zero to 27 mm. Complete dimensions of the specimens tested are given in TABLE 6.

The specimens were tested under 4 point bending on the bending test rig used for the examination of unstiffened elements, with the edge stiffened elements comprising the bending elements, and the loading applied such that the stiffeners were in compression.

Two of these specimens failed by local crushing of the webs. This type of failure was avoided in the remainder of the tests by providing more substantial load spreaders at the supports and loading points. Typical moment-deflection curves are shown in Figures 42 and 43, and the failure loads of all specimens are given in TABLE 7.

3.3 Formulation of design approach

To facilitate the formulation of a set of rules governing the behaviour of edge stiffened elements a simplified analysis procedure was set up. In this

procedure the torsional buckling behaviour of an edge stiffened element was assumed to consist of rotation about the supported edge as illustrated in Figure 44. This rotation is resisted by elastic restraining forces R as shown in the figure, where R is equal to $\frac{M\,b}{\theta\,D}$.

By evaluating the total potential energy of the system, minimising and setting this equal to zero the value of the stress to cause torsional buckling of an element with simply supported ends can be derived as

$$\sigma_{CR} = K_T \cdot \frac{\pi^2 D}{b^2 t} = K_T \cdot \frac{\pi^2 E}{12(1-\nu^2)} \left(\frac{t}{b}\right)^2 = 185000\, K_T \left(\frac{t}{b}\right)^2 \qquad 3.3.1$$

where

$$K_T = \frac{\left[\left(\frac{b}{\ell}\right)^2 \left(1+\left(\frac{A_s}{bt}\right)^3\right) + \frac{6(1-\nu)}{\pi^2}\left(1+\frac{A_s}{bt}\right) + \frac{3t}{\pi^4}\left(\frac{\ell}{b}\right)^2 R + \frac{3E\bar{I}}{Db}\left(\frac{b}{\ell}\right)^2\right]}{\left(1+3\,\frac{A_s}{bt}\right)} \qquad 3.3.2$$

In this expression As is the stiffener area, D is the plate flexural rigidity factor and $\bar{I}$ is the equivalent stiffener flexural rigidity.

For a lip stiffener of width b_1

$$\bar{I} = I_s \times \frac{b^2 + 5.6\,b_1 + 4\,b_1^2}{b^2 + 8.6\,b_1 + 16\,b_1^2} \qquad 3.3.3$$

where I_S is the stiffener second moment of area about the plate middle surface. The numerator of the expression for K_T is obtained from the bending energy of plate and stiffener, and the denominator is obtained from the potential lost by the applied loading. If the stiffened element has undergone local buckling prior to torsional buckling the numerator remains unchanged. The denominator changes, and to take this into account it is assumed that the effects of local buckling are to induce an effective width of the main element, b_{eff} which is equal to ρb , and an effective area of stiffener, A_e. If the plate effective portions are equally situated at both edges as shown in Figure 45 then

$$1 + 3\frac{A_S}{bt} \quad \Longrightarrow \quad \frac{1}{4}\eta(6 + \eta^2 - 3\eta) + 3\frac{A_e}{bt} \qquad 3.3.4$$

In the case of the individual elements examined, with simply supported loaded edges, R = 0 and the expression for K_T can be written

$$K_T = \frac{\left(\frac{b}{t}\right)^2\left[1 + \left(\frac{A_S}{bt}\right)^3\right] + \frac{6(1-\nu)}{\pi^2}\left(1 + \frac{A_S}{bt}\right) + \frac{3E\bar{I}}{Db}\left(\frac{b}{t}\right)^2}{\frac{1}{4}\eta(6 + \eta^2 - 3\eta) + 3\frac{A_e}{bt}} \qquad 3.3.5$$

If it is assumed that failure accompanies torsional buckling then the torsional buckling stress must be equal to, or greater than the material yield stress if the stiffener is adequate

Thus $\quad 185000\left(\frac{t}{b}\right)^2 K_T \geqslant Y_S$

$$\text{i.e } K_T = \frac{Y_S}{185000\left(\frac{t}{b}\right)^2} \qquad 3.3.6$$

If yield and torsional buckling coincide.

Nominating this value of K_T as K_Y and rearranging the governing expression for K_T gives

$$\frac{\bar{I}}{Db} = \frac{1}{3}\left\{\left[K_r\left[\tfrac{1}{4}\eta(6+\eta^2-3\eta)+3\frac{A_e}{bt}\right]-0.425\left(1+\frac{A_s}{bt}\right)\right]\left(\frac{\ell}{b}\right)^2-1\right\} \qquad 3.3.7$$

For a lip stiffened plate, this can be rewritten

$$\frac{\bar{I}}{b^3t} = \frac{\left\{\left[K_r\left[\tfrac{1}{4}\eta(6+\eta^2-3\eta)+3\frac{A_e}{bt}\right]-0.425\left(1+\frac{A_s}{bt}\right)\right]\left(\frac{\ell}{b}\right)^2-1\right\}}{36(1-\nu^2)\left(\frac{b}{t}\right)^2} \qquad 3.3.8$$

Note that in the formulation of the above equation the term $\left(\frac{A_s}{bt}\right)^3$ was omitted, as this has quite a small value for normal stiffener dimensions. Note also that as 1/b increases the numerator increases so that for very long elements the required stiffener rigidity becomes extremely large. This is due to the lack of restraint on rotation of the supported edge of the plate.

For the unstiffened elements tested the end supports were fixed. Therefore the effective length should be taken as half the total length. However, since full fixity cannot be achieved it was decided to take the effective length as 0.6 times the total length.

Equation 3.3.8 cannot be solved directly because A_s, A_e and $\bar{I}$ are interdependent. However this equation can be solved very quickly by iteration methods to yield the required value of I for a given set of conditions. Knowing the value of $\bar{I}$, the corresponding value of I_s and the corresponding minimum lip width can be obtained using equation 3.3.3 and the relationship

$$I_s = \frac{b_p^3 t}{3} \qquad 3.3.9$$

By this means the minimum required value of the rigidity of an edge stiffener, and the minimum lip width, can be obtained to provide adequate support to the stiffened edge. For elements having adequate support then stiffened plate design analysis can be used.

For elements without an edge stiffener the failure loads and stresses can be obtained using unstiffened element analysis.

For elements having stiffeners which have rigidity less than adequate the failure load lies between the unstiffened and stiffened element analyses, and to establish the behaviour of such elements examination of the experimental results is beneficial.

Figures 46 to 50 show the variations of ultimate loads obtained experimentally (plotted in non-dimensional form) from the tests on 5 different thicknesses of elements, In each figure, two curves, are also shown. The curve to the right of each figure is for adequate stiffener analysis, and starts from the minimum required lip width and plots the ultimate load using the stiffened element analysis given in this report. The curve to the left of each figure is for inadequate stiffener analysis and is a straight line drawn from the calculated capacity of an unstiffened element (with h=o) to the point where the stiffener is just adequate and stiffened element analysis can be employed. These curves show quite good agreement with the experimental ultimate loads in all cases, both for adequate and inadequate stiffeners.

In the case of elements of compression members, which is the practical condition, interaction between elements arises, and torsional buckling of an edge stiffened element is generally resisted, this resistance being specified by the coefficient R. The act of restraining the supported edge prevents the torsional buckling stress from decreasing indefinitely with increase in length, and a minimum value of K_T arises at a particular l/b ratio. The maximum value of K_T can be determined by differentiating equation 3.3.2. with respect to R, thus obtaining the value of l/b at which the minimum K_T is obtained, and thereafter substituting this l/b value into equation 3.3.2. to get K_{TMIN}. Now by setting K_{TMIN} equal to K_Y the following minimum stiffener rigidity requirement is obtained.

$$\bar{I} = \frac{Db}{3E}\left\{\frac{\pi^4}{12R}\left[K_Y\left(1+3\frac{A_s}{bt}\right) - 0.425\left(1+\frac{A_s}{bt}\right)^2\right] - 1\right\} \qquad 3.3.10$$

In the presence of local buckling the term $\left(1+3\frac{A_s}{bt}\right)$ is replaced as given by equation 3.3.4.

Performing this replacement and considering the case of lip stiffeners yields the following expression

$$\frac{\bar{I}}{b^3t} = \frac{\left\{\left[K_Y\left(\frac{1}{4}\eta(6+\eta^2-3\eta)+3\frac{A_e}{bt}\right) - 0.425\left(1+\frac{A_s}{bt}\right)\right]^2 \times \frac{\pi^4}{12R} - 1\right\}}{36.(1-\nu^2)\left(\frac{b}{t}\right)^2} \qquad 3.3.11$$

It should be mentioned here that owing to the simplified deflected form used in this analysis the above equation only holds if the value of R is not very large. For channel or hat type sections under relatively long wavelengths

torsional buckling conservative evaluation of the magnitude of R can be obtained on the basis of simple beam analysis which gives

$$R = 2\frac{b}{b_2} \qquad 3.3.12$$

where b_2 is the width of the web of the section as indicated in Figure 51.

Equation 3.3.11. can be solved iteratively to evaluate the minimum required stiffener rigidity, and lip width for a given section geometry.

Comparison of the failure loads for top hat sections of different material thicknesses is shown in Figure 51. The curves to the right of the figure are for adequately stiffened sections and those to the left are for inadequately stiffened elements. In deriving these curves the same procedure was used as for the individual elements discussed previously. The unstiffened element loads were obtained, for the case h=o, on the assumption that K=0.425.

The agreement between the theoretical and experimental failure loads is in general very good, therefore it can be claimed that the approach used accurately models the behaviour of edge stiffened elements. However, equation 3.3.11, which requires an iterative solution, cannot be said to be "simple", and some simplification would be beneficial.

From equation 3.3.11. it can be seen that the coefficient R has a significant effect on the required stiffener rigidity, and as R depends on section geometry it is therefore the case that the required stiffener rigidity depends on section geometry rather than on the individual element which is being stiffened.

3.4 Finite strip investigation

As design codes at present takes no account of section geometry effects it was decided to further check this conclusion using finite strip analysis. The finite strip approach used only considered the initial buckling load, and could not therefore be used directly to take the effects of local buckling on torsional buckling into account. However this can be accomplished indirectly using equation 3.3.4. This equation can be rearranged to give a multiplication factor to relate, approximately, values obtained on the basis of neglect of local buckling effects to the corresponding values which take local buckling into account.

The rearrangement gives

$$K_R = \frac{K_Y \times \eta/4\,(6 + \eta^2 - 3\eta) + 3\,\frac{A_e}{bt}}{1 + 3\,\frac{A_s}{bt}} \qquad 3.3.13$$

where K_R is a ficticious yield coefficient.

In the finite strip analysis, three different edge stiffened elements were considered, (1) an element of a channel having web width equal to twice the flange width, (2) an element of a channel having equal flange and web widths, and (3) an element fully fixed on its supported edge. The edge stiffened elements in each case had a "simple" lip of width one fifth of the element width.

Figures 52, 53 and 54 show comparisons of the torsional buckling loads for each element for three different width to thickness ratios. Bearing in mind

the fact that in each case the element in question is identical the differences in torsional buckling resistance are great. The required minimum buckling coefficient for an adequate stiffener is shown in each case. The fixed edge element is more than adequately stiffened in all circumstances. The element of the square channel is inadequately stiffened for the largest width to thickness ratio while the 2:1 channel is only just adequately stiffened for the smallest width to thickness ratio. This clearly demonstrates the difference in stiffness requirements for different geometries of section.

3.5 Design rules

In the light of the findings to date, it can be said that for accurate assessment of stiffener adequacy some method of taking the interaction between different elements into account should be used. Equation 3.3.11 does this, but requires an iterative solution and so is not very suitable for design. To make this equation more suitable, use can be made of the fact that it is a very quickly converging equation, and so as an initial guess it can be assumed that the ratio of stiffener to plate area is equal to 0.2. Substituting this into equation 3.3.11 gives a solution of acceptable accuracy on the first iteration. To make the solution simpler and at the same time to apply a small degree of conservatism the term of unity at the extreme right hand side of equations 3.3.10 and 3.3.11 can also be neglected. The quantity K_Y can also be written in the form

$$K_Y = \frac{Y_s \left(\frac{b}{t}\right)^2}{185000} \qquad 3.5.1$$

Substituting this into equation 3.3.10, performing the simplications mentioned and rounding the resulting numerical factors in such a way that conservatism is assisted, yields the following design equation corresponding to equation 3.3.10 for an element not subject to local buckling.

$$\frac{I}{t^4} = \frac{b}{t}\left[\frac{Y_s}{280} \times \frac{\left(\frac{b}{t}\right)^2}{2000} - 0.08\right]^2 \times \frac{10}{R} \qquad 3.5.2$$

To cover the situation when the element has buckled, a very simple approximation to the effective width of a stiffened element is used, i.e, for $b/t > 40$ then $b_e = 40/(b/t)$.

Assuming also that the stiffener effective area can be given by $Ae = 0.2 \times b_e t$, for the purposes of setting up the equation results in the equation, for an element subject to local buckling, $b/t > 40$.

$$\frac{I}{t^4} = \frac{b}{t}\left\{\frac{Y_s}{280}\left[\frac{(b/t)^2}{10000} + \frac{(b/t)}{62.5}\right] - 0.08\right\}^2 \times \frac{10}{R} \qquad 3.5.3$$

Equations 3.5.2 and 3.5.3 cover the case of locally unbuckled and locally buckled elements. If b/t is about 12.65 then I = 0, and for elements of lower width to thickness ratios no stiffener is required.

In the stiffener adequacy equations b is the flat width of the element and I_A is the second moment of area of the stiffener about the plate middle surface. The restraint coefficient, R, is taken as given by equation 3.3.12, i.e,

$$R = \frac{2b}{b_2} \qquad 3.5.4$$

where b is the width of the element to be stiffened and b_2 is the web width.

The value of R should not be taken as greater than 6 in any circumstances. Also, R need not be taken as less than 0.4 if there is a web to resist twisting of the edge stiffened element. Note that these rules apply only to an element which has a web on its supported edge. Comparison of the predictions of these rules, together with the other design rules proposed in this report, with the experimental findings of the investigation on channels are given in Figure 55, (identical to Figure 51), which shows good agreements.

The prescribed stiffener rigidities given here are quite substantially different from those of both the AISI specification and the European Recommendations, which are both very similar, following from the research of Desmond, Pekoz and Winter[11]. Quite apart from the fact that these specifications do not differentiate between the stiffener requirements for different section geometries, the actual requirements are substantially different for a typical case.

In the case of thin elements, the requirements of the European Recommendations are based largely on test results. However, as mentioned previously, in order to assess the results of tests it is not only the specific element under examination which contributes to the behaviour, but also the other elements of the section, so that the apparent results of element examination are dependant on the complete design approach used.

In order to further assess the validity of the equations produced here, together with the other design formulae presented in this report, an

examination of the experimental results of Desmond et al[11] was carried out. Comparison of the experimental failure loads of Reference (11) with the calculated failure loads using the adequacy requirements and other design formulae of this report is shown in Figure 56. The agreement is fairly good in all cases. For the specimens of E-23.9 and E-21.4, backing plates were glued and rivetted to the webs to make the webs fully effective. If the webs are fully effective the analysis results slightly overestimate the load capacity, as shown in the Figure. Since the backing plate was very thin, re-analysis was undertaken assuming that the backing plate behaves as a stiffened element. The resulting analytical failure loads, shown by the dotted curves for these specimens, are close to the test loads.

It may be also considered that the stiffener adequacy requirements set out in equations 3.5.2 and 3.5.3 can be applied with adequacy for any loading condition, if Y_S is replaced by σ_S where σ_S is the stress on the stiffener at failure. Thus in the case of elements loaded in combined bending and axial load, if the stress on the stiffener is greater than that at the supported edge then $\sigma_S = Y_S$. If the stress on the stiffener is less than that at the supported edge then $\sigma_S < Y_S$, and the stiffener rigidity required for adequacy is reduced. In the case of sections bent in such a way that the stiffener is in tension, then no stiffener is required for the element to behave as a stiffened element, and this was borne out by the results of the tests carried out on plain channels loaded to cause compression of the web.

In the case of stiffeners bent in such a way that the stiffeners are in compression then at failure $\sigma_S = Y_S$ and the adequacy requirements are as given by equations 3.5.2 and 3.5.3. However, the tests on sections bent in

this way highlighted important differences for such a case. For a light gauge element with an edge stiffener under bending as shown in Figure 57, the stresses are relayed to the edge stiffener via shearing forces at the element stiffener junction, as indicated. In such a case there is the tendency for the stiffener to bend in plane and the stress system induced across the stiffener varies from tension to compression as shown in the figure, even if the stiffener is perfectly adequate.

Under these conditions the load carried by the stiffener is equivalent to the load carried by the uniformly stressed stiffener of width one quarter of the actual stiffener width. If the bending was applied in such a way as to cause tension in the stiffeners then beam action would counteract this effect and nullify this tendency, thus inducing more or less fully effective stiffeners. However bending which causes compression of the stiffeners does not inhibit this tendency and indeed may tend to exacerbate this types of behaviour.

The failure moments on channel beams obtained from the tests which caused compression of the edge stiffeners are shown in Figure 58 in comparison with the ultimate moments calculated using the stiffener adequacy requirements given here and assuming that the lips are either completely effective or only 25% effective. The 6 tests in this series which were not affected by web crippling are shown here, and as can be observed the 4 specimens with adequate stiffeners failed at loads very close to those obtained on the basis of 25% effective stiffeners. Thus this hypothesis is confirmed, and in design only 25% of the stiffener width should be counted for such a case. It is also noteworthy that in the case of inadequate stiffeners the straight line variation in stiffener effectiveness between zero stiffened and adequate

stiffener does not seem to hold in this case, and if the stiffener is inadequate then for safety its contribution should be discounted completely.

4. INTERMEDIATELY STIFFENED ELEMENTS

Intermediate stiffeners are used to reduce local buckling effects in stiffened elements by using stiffeners to minimise deflections at the stiffener location. The general nature of the behaviour of intermediate stiffeners has substantial similarities to that of edge stiffeners, i.e, the stiffeners require to have a certain minimum rigidity if they are to fulfill their function properly. As with edge stiffeners, early research concentrated on specifying the stiffener rigidity required to support the stiffener location at buckling. However, the work of Desmond (12) showed that, as with edge stiffeners, this is not the correct criterion. Instead, an adequate intermediate stiffener must support its associated plate elements until local plate failure occurs, which may be at a load less than or greater than the buckling load of the stiffened sub-element.

The research carried out in this programme involved theoretical analysis of stiffened elements with a single intermediate stiffener, and experimental investigations of the behaviour of simply supported intermediately stiffened elements in compression and of beams having intermediately stiffened compression elements.

4.1 Outline of theoretical approach

The main theoretical approach again used the semi-energy method. The cross section of the intermediately stiffened element studied was of the form shown in Figure 59 and stiffener and plate buckling modes as shown in Figure 60(a)

and 60(b) were considered. One half of an intermediately stiffened element was analysed, assuming symmetry about the stiffener centre line with regard to stiffener initiated buckling, and anti-symmetry with regard to plate initiated buckling as indicated in Figure 61.

As in the case of edge stiffeners it was found that directional effects arose with regard to the stiffener buckling behaviour, and these were affected by the presence of local buckling. For intermediate stiffeners the effects of rotational restraint on the element edges is not so pronounced as for edge stiffeners, and for long intermediately stiffened elements the stiffener buckling mode may consist of several waves rather than a single half wavelength.

4.2 Experimental Investigations

Two main investigations were made into the experimental behaviour of intermediately stiffened elements; one investigation into individual elements and the other into compression elements of beams. All specimens tested were manufactured in the University, and tensile tests were made on all sheets of material used in their manufacture. The types of elements and members tested are shown in Figure 62.

It was required, for both investigations, that stiffeners of a variety of different depths be formed in the specimens. To accomplish this a press rig was made up using hot rolled channel and T beams. The general arrangement of the press rig is shown in Figure 63, and cross-sectional views are shown in Figure 64. This rig could produce formed intermediate stiffeners of overall

width from 6 mm to 11 mm and of any desired depth and used the Tinius Olsen test machine to provide the following loads.

4.2.1 Individual Elements

A total of 42 individual elements were tested to failure, 35 intermediately stiffened elements and 7 elements without intermediate stiffeners. The geometry of the elements is shown in Figure 65 and all elements were nominally 950 mm in length. Details of the dimensions of the elements are given in TABLE 8.

A test rig was designed and manufactured in the University for testing of the elements. This rig was built to apply uniform compression to elements of length between fixed ends of 950 mm and width between knife edge supports of 160 mm. An isometric view of the test rig is shown in Figure 66 and plan and elevations are shown in Figure 67. A typical set of load-end shortening curves for specimens of a single thickness is shown in Figure 68. The stiffener depths for the specimens shown here varied from 2.9 mm to 25.2 mm, and the plots show that the strength and stiffness of the element increased as the stiffener depth increases. It should be mentioned here that as the stiffener depth increases the element cross-sectional area increases, so that part of the increase in load capacity is simply due to increase in cross-sectional area. For example, in this figure the specimen SP5 had a cross-sectional area 15% to greater than that of specimen SP4. While the total failure load of SP5 was 26% greater than that of SP4, the increase in efficiency was therefore much less.

Figures 69 to 72 illustrate the deflection behaviour exhibited by the

elements. The deflections of a flat element without an intermediate stiffener are shown in Figure 69. This shows that from an initially imperfect condition the element developed more or less symmetrical buckles, approximately equal in half wavelength to the total width between knife edge supports. For small depth stiffeners Figure 70 shows that stiffener initiated buckling occurs, with three half wavelengths over the element length. With slightly larger stiffeners, Figure 71, local buckling and stiffener buckling, are both present. The local buckles have less than half the wavelength of those in the flat plate while the stiffener buckle half wavelength has increased so that now only two half wavelengths occur rather than three as for the smaller stiffeners. It is noteworthy that the local buckles increase in amplitude where the stiffener buckling deflections are upwards in Figure 71, and decrease in amplitude when the stiffener buckling deflections are downwards. This is due to the fact that the stiffener buckling upwards increases the plate stresses, while downward buckling of the stiffener decreases the plate stresses. This is part of the directionality effect mentioned earlier. With larger stiffeners the buckling is mainly local, as shown in Figure 72. However, as is found theoretically, it is in general not possible for local buckling to occur without also inducing overall deflections.

For two specimens strain gauge investigations were undertaken. Each investigation used 56 gauges laid in two bands across one symmetrical half of the element. Layout of the gauges for one test are shown in Figure 73 and the position of the strain gauge bands are shown superimposed on a plot of the deflections along the specimen tested in Figure 74. Band (1) and Band (2) of the gauges lay on sections which buckled in two different directions

as may be observed from the figure, although the deflections at Band (1) are less than those of Band (2). The membrane stress distributions obtained from this test are shown in Figure 75. The figure clearly shows that at Band (1), where the stiffener buckled inwardly the membrane stresses in the plate in the region of the stiffener are significantly less than for Band (2), where the stiffener buckled outwardly. This shows the effects of stiffener bending, which is in reality stiffener/plate bending.

Full details of all strain gauge readings may be obtained from Ref (2).

In addition to the two strain gauge investigations mentioned all specimens tested had two strain gauges affixed to them to facilitate evaluation of the initial buckling load for comparison with theory. The positioning of the strain gauges was determined on the basis of the theoretical analysis. For specimens in which the initial buckling mode was local the strain gauges were positioned in the centre of the sub-element, i.e, the flat part between stiffener and support. For specimens in which the initial buckling mode was stiffener initiated.

Figure 76 shows the strain gauge positions and variation of the strains for two tests. In these tests the expected mode of initial buckling was local. The buckling load was evaluated using the well known method of taking the intersection of the tangents to the pre and post buckling membrane strains as illustrated in the figure.

The experimental buckling loads so obtained are shown in comparison with theoretical values, in the form of non-dimensional buckling coefficients, in

Figure 77. The x-axis in this figure is I_s/I_s^* where in this case I_s is the stiffener second moment of area about its own centroidal axis parallel to the plate, and I_s^* is that value of I_s which will make stiffener buckling and plate buckling occur simultaneously. The experimental results are in reasonable agreement with theory in all circumstances, both for plate initiated buckling, $I_s > I_s^*$, and stiffener initiated buckling, $I_s < I_s^*$.

Figure 78 shows a comparison of the load-end shortening curves obtained theoretically and experimentally for a flat plate test. The flat plate tests were carried out partially to give results for the situation of zero stiffener rigidity and also to check that the rig was capable of reproducing behaviour which could be checked by widely available theoretical methods. The theoretical analysis had the facility to allow the buckle half wavelength (BW) to change continuously after buckling, to achieve absolute minimisation of the Potential Energy, or to remain at the half wavelength corresponding to the minimum buckling load. From the figure it may be seen that if the buckle half wavelength is allowed to change then almost perfect agreement with the experimental results is attained. This corroborates the findings of tests carried out earlier on plate behaviour.

Typical comparisons of experimental and theoretical load-end shortening curves for intermediately stiffened elements are shown in non-dimensional form in Figures 79 and 80.

The theoretical failure criteria used was that failure was assumed to occur due to either of two incidences.

1. If any part of the stiffener has yielded then the system can sustain further load only until the maximum plate membrane stress reached yield.

2. If the stiffener has not reached yield then the system can sustain load until the average membrane stress on the plate supported edges reaches yield.

Plastic behaviour was taken into account in the theoretical analysis in an approximate way.

In Figure 79 the first criterion applies and in Figure 80 the second criterion applies. Two theoretical curves are shown in each case, one corresponding to perfect plate behaviour and the other corresponding to specified local and overall imperfections. The magnitude of these imperfections were not measured but were in fact chosen to obtain agreement with the experimental curves. It is not really surprising, therefore, that good agreement is obtained between the theoretical imperfect plate analysis and the experimental results. However, the curves do indicate that the theoretical analysis can closely model the actual behaviour.

The theoretical curves are terminated at the point dictated by the failure criteria discussed, and show good agreement with experimental failure loads.

Figure 81 shows the variation in non-dimensional failure loads with variation in stiffener rigidity for all material thicknesses tested. In this figure I_p is the stiffener second moment of area about the plate middle surface, and I_p adequate is the minimum stiffener rigidity suggested in Reference (13).

4.2.2 Compression elements of beams

The investigation of intermediately stiffened beam compression elements involved tests on beams manufactured from material of six different thicknesses.

Tests were carried out on 32 beam specimens of lipped channel section, which had intermediate stiffeners formed in their compression flange using the press rig described earlier. The length of the press rig limited the overall length of beam to 1060 mm. The general geometry of the test beams is shown in Figure 82, and the nominal cross-sectional dimensions were 152 x 76 x15 mm lips. Full dimensions of all specimens are given in TABLE 9. In order that the maximum length of the beams could be tested under 4 point bending end extension pieces were manufactured from hot rolled channels as illustrated in Figure 83. A 12.7 mm slot was milled in the web of the channels to accommodate the intermediate stiffener and the flanges were stepped to eliminate contact with the lips of the test specimens during test. These extension pieces were fitted to both ends of the specimen to be tested.

The bending test set up is shown in Figure 84. Loading and support points were on the extension pieces, so that the test specimens were subjected to pure moment. Strain gauges were fitted to specimens in the A, B and C series (see TABLE 9) to determine the experimental buckling moments and buckling coefficients.

Moment-central deflection curves for each test series are shown in Figures 85 to 90. These curves terminate at the maximum moment. From the curves it would be difficult to tell which beams had large stiffeners and which had

small stiffeners. There is a substantial difference between the pattern of behaviour observed in the beam tests from that observed in compression tests. Whereas for the compression tests the load generally showed a slight increase with increase in stiffener size even for stiffeners which were much more than adequate, the same is not true for the beam tests. In the beam tests, the use of stiffeners produced relatively small load increases provided the stiffener dimensions were not large. With further increase in stiffener dimensions the moment capacity tended to decrease. These differences in characteristics should be taken into account in the design rules.

The failure moments and buckling moments obtained from these tests are shown in TABLE 10.

4.2.3 Formulation of design approach

(a) Stiffener Adequacy Requirements

The requirements for the minimum required rigidity of an intermediate stiffener to adequately stiffen the sub-elements were based largely on the test results. The tests suggested that the requirements suggested in Reference (13) were reasonable, but could be improved upon. The requirements finally arrived at on the basis of the tests were as follows:-

For $w/t < 50$, $I_{min}/t^4 = 0.3\left(\frac{w}{t}\right)^2 \cdot \frac{\gamma_s}{280}$

For $w/t > 50$, $I_{min}/t^4 = [0.15\left(\frac{w}{t}\right)^2 + 375]\frac{\gamma_s}{280}$

where w is the width of the sub-element.

The failure loads obtained on from the tests on compressed plates are plotted in Figure 91 against the ratio of stiffener rigidity to adequate stiffener rigidity as given by the above equations. This figure indicates that the requirements given indicate a reasonable approximation to the stiffener rigidity at which the element is adequately stiffened. For rigidities less than this there is quite significant reduction in load capacity. For rigidities greater than this the increase in load capacity is only that which could be expected due to the increase in stiffener area. It should be mentioned also that if the total element width is less than about 30 times its thickness then it will be fully effective without an intermediate stiffener.

(b) Elements of Compression Members

The compression tests on individual elements could be expected to provide conservative estimates of the behaviour of intermediately stiffened elements as components of compression members. For intermediately stiffened elements, there is always some deformations of the stiffener, even if this is of adequate rigidity. To take this into account, the effective width equation used for stiffened elements is modified for intermediately stiffened elements, having adequate stiffeners, to take the form

$$\frac{w_e}{w} = \left[1 + 14 F_r \left(\sqrt{\frac{Y_s}{\sigma_{CR}}} - 0.35\right)^4\right]^{-0.2}$$

where w_e is the effective width of an adequately stiffened element, σ_{CR} is the local buckling stress of the individual sub-element and F_r is a factor which takes account of the loss of strength due to stiffener

deformation. The expession derived empirically for F_r is

$$F_r = 1 + 0.11\sqrt{\frac{Y_S}{\sigma_{CR}}}$$

An adequate stiffener may be assumed to remain fully effective for the purposes of assessing its contribution of the load capacity of the intermediately stiffened element.

In the case of stiffeners which do not have adequate rigidity the ultimate load, or the effective width is determined on a similar basis to the edge stiffened elements. Thus, at failure of an inadequately stiffened element the load is given by

$$P_{ULT} = P_S + (P_{SA} - P_S) \quad (I/I_{min})^{1/3}$$

where P_S is the ultimate load for a stiffened element without an intermediate stiffener and P_{SA} is the ultimate load for a stiffened element with an intermediate stiffener of just adequate rigidity.
This can also be written in terms of the effective widths as

$$b_e = b_{es} + (b_{eSA} - b_{eS}) \quad (I/I_{min})^{1/3}$$

where b_{eS} and b_{eSA} refer to an element without a stiffener and element with an adequate stiffener respectively. For an inadequate stiffener the effective area may be taken as

$$A_e = A_S \times I/I_{min}$$

where A_s is the full cross sectional area of the stiffener

Figures 92 and 93 show comparison of the non-dimensional failure loads predicted using these design rules with the results obtained from the tests. Reasonable, conservative, agreement with the experimental results is shown in all cases. The overall picture is shown in Figure 94 which plots the ratio of experimental to calculated failure loads to a base of the ratio actual to adequate stiffener rigidity. Again this indicates quite satisfactory agreement throughout the range, with the bulk of the experimental results being above the datum line, at unity, which indicates a slight degree of conservatism.

Comparison of the results with some existing design codes is shown in Figures 95 and 96. Demonds (12) analysis has been incorporated as the basis of the AISI code and the European Recommendations. Figure 95 indicates that in the analysis of intermediately stiffened elements of compression members this is somewhat non-conservative, largely because there is no provision for any reduction in effective width due to the deformations of an adequate stiffener.

The British code seems, from Figure 96, to be very conservative in its assessments of load capacity. This code contains substantial information from the 1980 AISI specification with regards to intermediate stiffeners, and incorporates from that specification reduction factors which are in reality more applicable to compression elements of beams, as will now be discussed.

(c) Compression Elements of Beams

The adequacy requirements of intermediate stiffeners in beam compression elements can be taken as those already specified for elements of compression members. With regard to the effective width the same expression as for elements of compression members is also applicable. However, in the effective width equations the value of K for a sub-element is normally greater for elements of compression members. For the channel beams tested, K for each sub-element was found from the expression

$$K = 5.4 - \frac{1.4H}{0.6+H} - 0.02H^3$$

where H is the ratio of sub-element width to beam web width.

The major difference between the behaviour of intermediately stiffened compression elements of beams and their counterparts in compression members lies in the phenomenon of cross-section curvature found in thin-walled beams. This effect causes wide compression (or tension) elements to displace towards the neutral axis. The phenomenon is well known, and design codes give formulae to determine the amount of displacement. However its effect on beam capacity and behaviour is generally neglected. The presence of intermediate stiffeners can be shown theoretically to exacerbate this effect, and even for large stiffeners the movement towards the neutral axis can very substantially reduce the stiffener's contribution towards the beam strength. To take this into

account, the effective area of any stiffener in a beam compression element should be reduced. A suitable reduction factor, in the case of an adequate stiffener -is obtained by using the following expression for the effective area of an adequate stiffener in a beam compression element.

$$A_e = A_S \times \frac{\sigma_{CR}}{\gamma_S}$$

where σ_{CR} is the local buckling stress for the sub-element.

In the case of inadequate stiffeners, these are already reduced for elements of compression members, and should be further reduced to

$$A_e = A_S$$

The rules given here were used, together with the general approach to beam analysis outlined in Section 5.6 to predict the capacity of the beams tested in the experimental programme. Comparisons of the experimental results with the predictions of the design analysis are shown in Figures 97 to 100. In all cases except for those of the thinnest material the design analysis gives conservative but reasonably accurate predictions of the moment capacity. The overall picture is shown in Figure 101 which gives the ratio of experimental to calculated failure moments for all specimens tested. In the case of the thinnest material, with w/t = 180, the experimental failure moment was consistently less than that obtained from the design analysis, and this caused some concern.

For the thicker specimens, particularly those having w/t of 94 and 60 the results are very conservative, of the order of 10% to 30%. The materials of these specimens were of the gradual yielding type with no specific yield point, and the 0.2% proof stress was used in analysis. For the thicker specimens, yield occurred in tension before failure. Tensile yield does not cause failure, and when tensile yield occurs, analysis may be carried out on an elasto-plastic basis. This was used in the design analysis performed.

As a further check on the design analysis beam test results of other authors, namely Desmond (12), Konig (14) and Skaloud (15) were analysed. The specimens and details of the specimen dimensions for these tests are given in TABLES 11 to 13. Comparison of the calculated capacity and the experimental results of these researchers is shown in Figure 102. There is in general reasonable agreement, with the design analysis in the main conservative. Very good agreement with Konig's tests may be observed. Since these tests were on very thin specimens, any doubts which arose over the low failure loads of the thinnest material beams of this investigation were to some extent assuaged. The agreement between the design analysis and the experimental results of Desmond is reasonable, but consistently conservative. This is most probably due to the fact that Desmonds specimens had a screwed tension flange attached, which effectively closed the sections and inhibited the tendency to cross-section distorsion discussed earlier. As most thin walled beams in practice will not be closed it is somewhat dangerous to use such types of test specimens to provide analysis which will then be applied to more general circumstances. Comparison with Skaloud's test also showed

consistent conservatism. This was perhaps because Skaloud's test specimens were all manufactured from gradually yielding material with no defined yield point.

In order to provide some additional information, the analysis of Desmond, which formed the basis of both the new AISI and European Recommendations design rules for intermediate stiffeners, was compared with the various test results. The comparisons are shown in Figures 103 and 104. Comparison of Desmond's analysis with the results of the tests of this programme are shown in Figure 103 to be very scattered, with analytical results very much underestimating the capacity of the thicker beams, while overestimating the capacity of the thinner beams.

The reason for the underestimation of the capacity of the beams of thicker material is not really because of inaccuracy in the analysis of intermediately elements, but mainly because of neglect of post tensile yield capacity of the beams.

Comparison of Desmond's analysis with his own tests in Figure 104 shows very good agreement. Comparison with Skaloud's tests shows consistent conservatism, as for the proposed analysis. Comparison with Konig's tests shows substantial non-conservatism, due to neglect of the cross beam curvature effects.

Figure 105 illustrates the degree of conservatism which can arise if failure is assumed at first yield, when first yield is in tension. This figure was drawn considering beams of the thickest material used in the

present investigation, having w/t = 47. As can be seen, the differences between the failure loads predicted on the basis of first yield and those predicted allowing tensile yield and using elasto-plastic analysis are substantially greater than the differences caused by stiffener considerations.

In general it can be said that the design rules proposed here for intermediate stiffeners are in reasonable agreement with the results of the tests carried out in this investigation and with those of other experimenters. The general applicability of the proposed rules would seem to be better than that of the rules of existing specifications.

5. PROPOSED DESIGN RULES GOVERNING ELEMENT BEHAVIOUR

In this section all design rules used in the analysis of the sections and elements tested are detailed. Although only unstiffened elements, edge stiffened elements and intermediately stiffened elements were the subject of investigation in the project, it was also necessary to analyse ancillary elements, such as simple elements and beam webs. Since during the period of investigation the European Recommendations were in a state of flux it was necessary to set design rules for the ancillary elements to facilitate evolution of the rules for the elements under investigation.

For the ancillary elements the design rules used are based on the work of Ref 13. The rules used are given in Section 5.2.

Comparison of the design rules proposed here with the experimental results and with the European Recommendations is shown in Section 6.

5.1 Classification of Elements

Elements of a section are classified as stiffened elements, unstiffened elements, edge stiffened elements or intermediately stiffened elements.

Where effective width formulations are used then in the case of stiffened elements the effective width is presumed to be located next to the supported edges, equally disposed between these edges, for the calculation of section properties. In the case of unstiffened elements the effective width is presumed to be located next to the single supported edge.

In all cases except those specifically declared to the contrary the determination of effective width should be based on the mid-line dimensions of an element.

5.2 Effective Width of Stiffened Elements, b_e

$$\frac{b_e}{b} = \left[1 + 14\left(\sqrt{\frac{\sigma}{\sigma_{CR}}} - 0.35\right)^4\right]^{-0.2} \qquad \text{(i)}$$

where σ is the applied stress on the effective width

b is the element width and σ_{CR} is the local buckling stress given by

$$\sigma_{CR} = 185000\ K \left(\frac{t}{b}\right)^2 \qquad \text{(ii)}$$

K is the buckling coefficient which may be taken as having a minimum value of 4, or greater if greater values can be justified. Suitable values for K for various elements are given in Ref (13).

For an element subjected to stress gradient, if the stress on both supported edges is compressive then equation (i) gives the effective width if σ_m, the mean or average compressive stress, is used in place of σ.

If the stress varies from tension to compression, such as the stiffened web of a beam then the element is considered wholly effective, and a limiting value of the compressive stress on the web is used. The limiting value, p_C, is

$$p_C = \left(1.13 - 0.0019\ \frac{D}{t}\sqrt{\frac{Y_s}{280}}\right) Y_s \quad \text{but } p_C \not> Y_s \qquad \text{(iii)}$$

where D is the web depth and Y_S is the material yield strength.

5.3 Effective Width of Unstiffened Elements, b_{eu}

$$\frac{b_{eu}}{b} = 0.73 \left(\frac{\sigma_{CR}}{\sigma}\right)^{1/3} \qquad \text{(iv)}$$

In evaluation of b_{eu}, the buckling coefficient, K, may be taken as having a minimum value of 0.425, or with higher values if these can be justified.

For elements subjected to a stress gradient then K may be taken as

$$K = \frac{1.7}{3 + R_S} \qquad (v)$$

where R_S is the ratio of stress at the supported edge to stress at the free edge, compressive stresses being taken as positive, and σ being taken as the compressive stress at the free edge. Higher values of K may also be used if these can be justified.

In the case of unstiffened webs of beams, bent to cause compression of the free edge

$$\frac{b_{eff}}{b} = 0.9 \left(\frac{\sigma_{cr}}{\sigma}\right)^{1/3} \qquad (vi)$$

It should be emphasised here that the stress σ in this case is the Maximum compressive stress on the effective width, i.e, at the free edge of the effective element.

If an unstiffened web is bent to cause tension of the free edge, it can be treated as a stiffened element.

Note Equation (iv) was derived to be of similar form to equation (vi), and has been checked with the results of this test programme and found to be satisfactory.

5.4 Edge Stiffeners

Requirements for adequacy.

For an element of width to thickness ratio less than 40, an edge stiffener has adequate rigidity if

$$\frac{I_{min}}{t^4} = \frac{b}{t}\left[\frac{Y_s}{280}\frac{(b/t)^2}{2000} - 0.8\right] \times \frac{10}{R} \qquad \text{(vii)}$$

where I_{min} is the second moment of area of the stiffener about the plate middle surface

R is the rotational restraint factor given by $R = \frac{2b}{b_2}$, where b_2 is the web width. The maximum value which may be taken for R is 6.

R need not be taken as less than 0.4 for sections in which a web restrains the edge stiffened element.

If b/t > 40 then for adequacy of an edge stiffener

$$\frac{I_{min}}{t^4} = \frac{b}{t}\left\{\frac{Y_s}{280}\left[\frac{(b/t)^2}{10\,000} + \frac{(b/t)}{62.5}\right] - 0.8\right\}^2 \times \frac{10}{R} \qquad \text{(viii)}$$

If an edge stiffened element has adequate rigidity then the element can be treated in analysis as a stiffened element. The stiffener should be treated as an unstiffened element in its own right if it is a simple lip, or as a combination of individual elements if it is other than a simple lip.

For inadequate stiffeners, if the stiffener is a simple lip the load capacity can be obtained from

$$P_{ULT} = P_U + (P_S - P_U) \times \frac{b_s}{b_{sa}} \qquad \text{(ix)}$$

where P_U is the ultimate load for an unstiffened element of the same width and thickness, P_S is the ultimate load for an adequately stiffened element of the same width and thickness, b_S is the stiffener width and b_{SA} is the minimum width of an adequate stiffening lip. This can alternatively be written in effective width form as

$$b_e = b_{eu} + (b_{es} - b_{eu}) \frac{b_s}{b_{SA}} \qquad (x)$$

where b_e is the effective width of the actual element, and b_{eu} and b_{es} are the effective widths obtained for an unstiffened element and a stiffened element respectively. Note that b_{es} includes the contribution of the stiffener effective area.

In the more general case of an element other than a simple lip the equivalent equations are

$$P_{ULT} = P_U + (P_S - P_U) \times \left(\frac{I}{I_{min}}\right)^{1/3} \qquad (xi)$$

$$b_e = b_{eu} + (b_{es} - b_{eu}) \times \left(\frac{I}{I_{min}}\right)^{1/3} \qquad (xii)$$

where I is the second moment of area of the actual stiffener about the element middle surface and I_{min} is the minimum required value of I for adequacy.

If an edge stiffened element is bent in such a way as to cause tension of the stiffener then the element can be treated as a stiffened element regardless of the stiffener dimensions.

If an edge stiffened element is subjected to a combination of bending and axial load which causes the stress on the stiffener, σ_s , to be compessive but less than that on the supported edge at failure, Y_s, then the stiffener adequacy requirements can be computed from (vii) and (viii) with σ_s substituted for Y_s. If an edge stiffened element forms the web, i.e, bending element, of a beam in bending such that the stiffeners are in compression then the adequacy requirements are as given by (vii) and (viii). For an adequate stiffener in this case only one quarter of the stiffener area should be used in computing the section properties. If the stiffener is inadequate it should be completely discounted and the element treated as unstiffened.

5.5 Intermediate Stiffeners

Requirements for adequacy

If w/t < 50

$$\frac{I_{min}}{t^4} = 0.3\left(\frac{w}{t}\right)^2 \cdot \frac{Y_s}{280} \qquad \text{(xiii)}$$

If w/t > 50

$$\frac{I_{min}}{t^4} = \left[0.15\left(\frac{w}{t}\right)^2 + 375\right] \cdot \frac{Y_s}{280} \qquad \text{(xiv)}$$

Where w is the sub-element width.

Note that if the total element width is less than approximately 30t the addition of an intermediate stiffener will not increase the element efficiency, since a stiffener is not required in this range.

Adequate Stiffeners

If an intermediately stiffened element has adequate rigidity then the effective width of each sub-element at failure, W_e, may be evaluated from

$$\frac{W_e}{W} = \left[1 + 14F_r\left(\sqrt{\frac{Y_s}{\sigma_{CR}}} - 0.35\right)^4\right]^{-0.2} \qquad \text{(xv)}$$

where $F_r = 1 + 0.11\sqrt{\frac{Y_s}{\sigma_{CR}}}$ (xvi)

and $\sigma_{CR} = 185000\ K\left(\frac{t}{w}\right)^2$ (xvii)

with K = 4 for an element of a compression member (xviii)

and $K = 5.4 - \frac{1.4H}{0.6+H} - 0.02H^3$ for a compression element (xix)

of a channel-type beam

H is the ratio of w to the beam web depth.

The effective area of an adequate stiffener may be taken as

$A_e = A_S$ for an element of a compression member (xx)

$A_e = A_S \frac{\sigma_{CR}}{Y_S}$ for a compression element of a beam (xxi)

but $A_e \not> A_S$

Inadequate Stiffeners

The maximum load which can be carried by an inadequately stiffened element is given by the expression

$$P_{ULT} = P_S + (P_{SA} - P_S) \left(\frac{I}{I_{min}}\right)^{1/3} \qquad \text{(xxii)}$$

where P_S is the ultimate load for a stiffened element without an intermediate stiffener and P_{SA} is the ultimate load for a stiffened element with an intermediate stiffener of just adequate rigidity (i.e, $I = I_{min}$).

In terms of the effective widths

$$b_e = b_{es} + (b_{eSA} - b_{es}) \qquad \text{(xxiii)}$$

where b_{es} is the effective width of the complete element with no stiffener a b_{eSA} is the sum of the effective widths of the sub-elements if they are just adequately stiffened.

The effective area of an inadequate stiffener may be determined from

$$A_e = A_S \times \frac{I}{I_{min}} \quad \text{for an element of a compression member} \qquad \text{(xxix)}$$

or $$A_e = A_S \times \frac{I}{I_{min}} \times \frac{\sigma_{ce}}{\gamma_s} \quad \text{for a compression element of a beam} \qquad \text{(xxv)}$$

but $A_e \not> A_S$ and $\frac{I}{I_{min}}$ taken as $\not> 1$

5.6 Beam Analysis Procedure

In derivation of some of the design rules it has been assumed that elasto-plastic behaviour is possible under certain circumstances, as permitted by the European Recommendations. With regard to this type of behaviour it is assumed that the ultimate moment is reached when the maximum compressive stress-attains the value p_c, as given by equation

(iii) of this section. The effective properties of the compression element are calculated on the assumption that this is subjected to the stress p_c, and p_c is used in the relevant effective width formulae (e.g, equation (xv)) in place of Y_S.

At this condition, if the stresses on the tension side of the beam are less than the yield stress, evaluation of the beam moment capacity is made on the basis of elastic analysis. If the tension stresses exceed yield then an elasto-plastic stress distribution is used to evaluate the moment capacity.

6. COMPARISON WITH EUROPEAN RECOMMENDATIONS

In this section the ultimate load predictions of the European Recommendations are compared with the proposed rules and with the experimental results.

6.1 Unstiffened elements

In evaluation of the effective widths of unstiffened elements under stress gradient with compression of the free edge and tension of the supported edge, rules of the European Recommendations are based on the assumption that the tensile portions are fully effective, and that the governing stress f_{ty} occurs at the free edge of the non-reduced element, although this is non effective. The reduced effective section is then analysed using engineers bending theory to find the ultimate moment. This then assumes that f_{ty} acts on the free edge of the effective element. The European Recommendations suggest that sufficient accuracy

will be obtained if the effective widths are evaluated on the basis of a stress distribution obtained using fully effective webs, Figure 106(a), although it is recognised that for correctness an iterative solution should be employed to ensure that the stress distribution upon which the effective section is based should be consistent with that which is assumed by the effective section approximations, Figure 106(b). Figure 107 shows the results of analysing using the first approximation and using the fully iterated solution. Analysis using the first approximation is reasonably accurate, but unfortunately the use of more refinements in the analysis reduces the accuracy substantially.

The effectiveness of the unstiffened elements is dependant upon the degree of tension at the supported edges and upon the degree of fixity supplied by the web. The European Recommendations do not consider the effects of fixity in this case but only that of tension, and this is of less importance than the fixity effects for the problem under examination.

6.2 Edge stiffened elements

The ultimate loads of individual edge stiffened elements obtained using the European Recommendations, the proposed rules and experiments are shown in Figures 108 to 112, and the ultimate loads for channel sections are shown in Figures 113 to 115.

For the individual elements there is a very large difference between the stiffener requirements proposed here and those of the European

Recommendations, and the European Recommendations consistently over-estimate the load capacity except in the case of the thickest element. The 'R" factor used in the proposed rules was the minimum value.

It should be mentioned that the individual elements give the most severe test of stiffener requirements, and provide worse conditions than are likely to occur in practice. Nevertheless the tests on these elements do serve to indicate the necessity to take the effects of restraint from adjacent members into account. In the case of channel sections agreement between the European Recommendations, the proposed rules and the experiments is better. There is still a tendency for the European Recommendations to over-estimate the capacity of inadequately stiffened elements of thin material, but this is not so marked in the case of individual elements. For adequately stiffened elements the European Recommendations agree more closely with the experimental results than the proposed rules, although both are in fairly good, conservative, agreement with experiments.

6.3 Intermediately stiffened elements

The European Recommendations regarding intermediately stiffened elements are based on the work of Desmond, and for the case of intermediate stiffeners in compressed sections the comparison with experiment may be seen from Figure 95. This figure shows that the ultimate loads predicted using the rules of the European Recommendations are reasonably accurate, but err slightly on the non-conservative side.

In the case of compression elements of beams the very scattered comparison with Desmond's analysis shown in Figure 103 does not apply to the European Recommendations, since the European Recommendations permit yield in tension before failure.

In deriving the failure moments for such elements using the European Recommendations some assumptions had to be made. The European Recommendations prescribe an effective width approach for the webs, and also permit the use of tensile yield in the webs. No guidance is given on how the effective web widths are to be evaluated in the presence of tensile yield, which changes the stress and strain distributions in the webs.

In deriving the ultimate loads using the European Recommendations it was decided to base the effective web widths, and positions of the effective parts, on a stress distribution obtained on the assumption that the compression flange stress was f_{ty} and the tension flange stress was obtained as in the European Recommendations without regard to whether or not this was greater than f_{ty}. Having derived the effective web geometry using these considerations, elasto-plastic evaluation of beam capacity could then be carried out. Figure 116 shows the comparison between ultimate moments obtained on this basis and the experimental ultimate moments.

From this figure it can be seen that the extremely conservative results of Figure 103 for elements of low w/t ratios are replaced by reasonably conservative estimates for these elements. However for the three

thinnest materials non conservatism is evident, the degree of non-conservatism increasing as the w/t ratio of the elements increased. Note also that the non-conservatism also increased as the stiffener rigidity increases.

This is largely because the calculation method does not take into account the cross curvature effects, which arise in practice. In the European Recommendations if an intermediate stiffener is of adequate rigidity then the sub-elements of the compression flange behave as stiffened elements and any further increase in stiffener area increases the beam resistance further because of the addition area. However, in practice if the material is thin then the effects of cross-curvature negate any such increases and indeed the experimental results given in Table 10 show that for all material thicknesses tested the ultimate moment reached a maximum and then decreased as stiffener area increased. The effect must be taken into account in design if slender intermediately stiffened elements are to be considered for beam compression elements.

7. SUMMARY

The research carried out in this project concentrated on three main areas: (1) Unstiffened Elements in Bending, (2) Edge Stiffened Elements and (3) Intermediately Stiffened Elements. All three aspects were examined theoretically and experimentally and design rules were drawn up for the elements in question.

In the course of the experimentation a total of 361 tests to failure of elements and sections were carried out together with over 100 tensile tests. A general breakdown of the elements and sections tested is shown in Figure 117.

Comparison of the experimental results with the predictions of the European Recommendations has indicated that good agreement occurs in many instances, but there are areas in which changes are required. The design rules proposed have attempted to take effects not considered in the European Recommendations into account.

The research carried out here has highlighted various aspects of cold formed section behaviour on which further knowledge is needed. Work is now continuing on the examination of some of these problems.

8. REFERENCES

1. Lim Boh Soon, "Buckling behaviour of asymmetric edge stiffened plates" PhD Thesis, University of Strathclyde, 1985.

2. Hoon Kay Hiang, "Buckling behaviour of intermediately stiffened plates", PhD Thesis, University of Strathclyde, 1986.

3. Sim Kok Wah, "The collapse behaviour of thin-walled sections", PhD Thesis, University of Strathclyde, 1986.

4. Fath El Rahman Ahmed Elmahi, "Buckling of beams with unstiffened bending elements", MSc Thesis, University of Strathclyde.

5. European Recommendations for the Design of Light Gauge Steel Members, First Edition, 1987.

6. AISI Specification for the Design of Cold Formed Steel Structural Members, August 1986 Edition.

7. BS 5950 : Part 5. Code of Practice for the design of cold formed sections, British Standards Institution, 1987.

8. J Rhodes, "Post buckling behaviour of bending elements", Proc. Int. Specialty Conf. on Cold Formed Steel Sections, St Louis, USA, 1982

9. K Marguerre, "The apparent width of the plate in compression". NACA TM No 833, 1937, (English Translation).

10. K von Kloppel and E Schiedel, "Beulwerte der dresseitig gelenkig gelagerten, am freien rand verteiften rechteckplatte mit beliebig verteilter randspannung", Der Stahbau 12/1968.

11. Bulson, P S, "The stability of flat plates", Chatto & Window, 1970.

12. Desmond, T P, "The behaviour and strength on thin-walled compression members with longitudinal stiffeners", Dept. Struct. Engr. Report No 369, Cornell University, 1977.

13. Rhodes, J and Walker, J M. "Current problems in the design of cold formed steel sections", Aspects of the Analysis of Plate Structures, Clarendon Press, Oxford 1985.

14. Konig, V. "Transversally loaded thin-walled C-shaped panels with intermediate stiffeners", Document D7:1978, Swedish Council for Building Research 1978.

15. Skaloud, M, "Uberkritisches Verhalten Gedruckter, mit Nachgiebigen Rippen Versterfter Platten, AETA Technica (Prague), Nr.5, 1963.

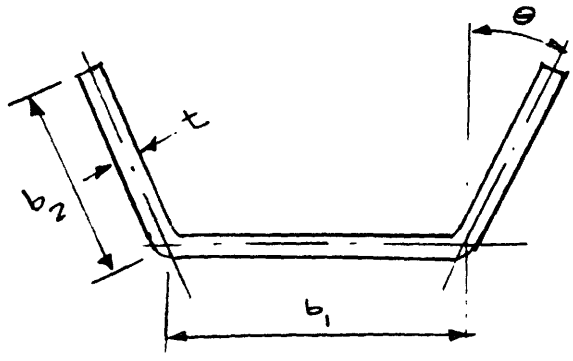

TABLE 1: DIMENSIONS AND EXPERIMENTAL FAILURE MOMENTS OF CHANNEL SECTIONS

Spec No	t mm	b_1 mm	b_2 mm	θ degrees	Span mm	σ_Y N/mm^2	M_{ult} Nm
1	1.55	49.17	12.38	0.0	500	270	73.43
2	1.56	49.97	25.89	0.0	500	270	307.05
3	1.58	49.65	36.80	0.0	500	270	422.75
4	1.56	52.25	51.56	0.0	500	270	525.1
5	1.18	51.03	13.18	0.0	500	270	57.85
6	1.17	50.80	25.03	0.0	500	270	144.63
7	1.17	51.20	38.59	0.0	500	270	201.95
8	1.18	50.73	51.68	0.0	500	270	261.44
9	1.18	51.44	23.86	13.5	500	270	137.51
10	1.18	52.07	23.54	29.0	500	270	125.5
11	1.18	51.44	23.86	46.0	500	270	111.25
12	1.18	52.12	49.53	15.5	500	270	230.51
13	1.18	52.38	49.50	29.0	500	270	209.15
14	1.18	52.39	49.58	47.5	500	270	172.66
15	1.17	51.15	13.90	0.0	700	270	53.4
16	1.15	52.19	25.59	0.0	700	270	151.3

Spec No	t mm	b_1 mm	b_2 mm	θ degrees	Span mm	σ_Y N/mm^2	M_{ult} Nm
17	1.17	49.63	40.10	0.0	700	270	183.34
18	1.17	50.39	52.13	0.0	700	270	240.3
19	1.52	51.19	13.21	0.0	700	270	72.27
20	1.57	53.68	25.26	0.0	700	270	290.14
21	1.57	52.41	38.59	0.0	700	270	427.2
22	1.57	51.14	51.29	0.0	700	270	494.84
23	1.59	50.00	25.40	16.0	700	270	284.8
24	1.62	52.07	24.13	28.0	700	270	243.86
25	1.57	52.07	24.13	46.0	700	270	174.44
26	1.63	51.44	49.53	15.0	700	270	412.96
27	1.62	53.34	48.26	29.0	700	270	441.44
28	1.63	53.34	49.34	45.0	700	270	338.2
29	0.55	51.80	12.50	0.0	700	270	16.73
30	0.55	51.50	25.80	0.0	700	270	34.72
31	0.56	51.50	38.50	0.0	700	270	48.77
32	0.54	52.00	51.00	0.0	700	270	56.96
33	0.55	52.00	23.00	15.0	700	270	30.97
34	0.56	49.50	23.50	29.0	700	270	28.48
35	0.55	50.00	23.50	45.0	700	270	16.91
36	0.54	49.00	40.00	16.0	700	270	47.00
37	0.55	49.50	49.00	30.0	700	270	43.35
38	0.55	50.00	49.00	44.0	700	270	24.92
39	0.703	50.5	51.00	0	305	279	103.6

Spec No	t mm	b_1 mm	b_2 mm	θ degrees	Span mm	σ_Y N/mm^2	M_{ult} Nm
40	0.71	50.5	38.4	0	305	279	80.7
41	0.708	50.8	25.5	0	305	279	55.8
42	0.71	50.8	51.5	0	305	279	112.4
43	0.71	50.3	50.3	0	305	279	76.00
44	0.70	51.00	25.6	0	305	279	53.00
45	0.81	52.00	26.00	0.0	700	184	60.22
46	0.81	52.5	33.2	0.0	700	184	63.82
47	0.81	54.0	41.0	0.0	700	184	77.53
48	0.815	53.5	45.5	0.0	700	184	77.75
49	0.80	53.0	51.0	0.0	700	184	77.53
50	1.20	54.5	26.0	0.0	700	262	173.93
51	1.20	53.0	33.5	0.0	700	262	213.48
52	1.205	53.5	46.0	0.0	700	262	257.08
53	1.21	53.5	41.0	0.0	700	262	238.20
54	1.20	54.0	51.0	0.0	700	262	230.76
55	1.21	54.0	51.0	0.0	700	262	257.08
56	0.81	51.0	40.0	25.0	700	184	67.41
57	0.805	51.0	40.0	35.0	700	184	56.18
58	0.81	50.5	40.5	40.0	700	184	47.19
59	0.80	51.0	40.0	46.0	700	184	45.84
60	0.815	51.0	40.0	49.0	700	184	46.29
61	0.8	50.5	40.0	55.0	700	184	33.71
62	0.81	51.0	40.0	60.0	700	184	31.01

Spec No	t mm	b_1 mm	b_2 mm	θ degrees	Span mm	σ_Y N/mm^2	M_{ult} Nm
63	1.2	51.0	40.0	35.0	700	262	179.8
64	1.21	50.0	40.5	40.0	700	262	160.45
65	1.205	5.1	40.0	46.0	700	262	144.72
66	1.20	5.1	40.0	53.0	700	262	123.6
67	1.21	50.5	40.5	60.0	700	262	106.52
68	1.53	52.0	50.0	51.0	700	227	234.8
69	1.52	52.0	50.0	49.0	700	227	234.8
70	1.52	52.5	50.0	60.0	700	227	171.5
71	1.52	52.0	50.0	59.0	700	227	197.8
72	1.52	52.0	50.0	70.0	700	227	85.8
73	1.52	52.0	50.0	70.0	700	227	93.2
74	1.52	52.0	50.0	80.0	700	227	32.0
75	1.52	52.0	50.0	80.0	700	227	30.6
76	1.20	52.0	50.0	50.0	700	186	138.07
77	1.22	52.0	50.0	50.0	700	186	141.27
78	1.22	52.0	50.0	60.0	700	186	107.8
79	1.23	52.0	50.0	60.0	700	186	100.7
80	1.215	52.0	50.0	71.0	700	186	52.7
81	1.22	52.0	50.0	71.0	700	186	45.2
82	1.20	52.0	50.0	80.0	700	186	14.24
83	1.19	52.0	50.0	80.0	700	186	13.17
84	0.775	52.0	50.0	51.0	700	160	46.3
85	0.775	52.0	50.0	50.0	700	160	48.4

Spec No	t mm	b_1 mm	b_2 mm	θ degrees	Span mm	σ_Y N/mm^2	M_{ult} Nm
86	0.77	52.0	50.0	60.5	700	160	26.7
87	0.775	52.0	50.0	60.0	700	160	33.8
88	0.775	51.5	50.0	69.0	700	160	19.6
89	0.775	52.0	50.0	70.0	700	160	16.7
90	0.775	52.0	50.0	80.0	700	160	5.34
91	0.78	52.0	50.0	79.0	700	160	8.01
92T	0.87	51.5	49.2	80.0	600	286	16.01
93T	0.87	50.5	50.0	75.0	600	286	37.8
94T	0.85	50.5	49.6	70.0	600	286	70.1
95T	0.87	50.5	49.8	65.5	600	286	116.5
96T	0.852	50.5	49.6	60.0	600	286	154.8
97T	0.85	50.8	49.2	55.0	600	286	190.4
98T	0.87	50.0	50.0	50.0	600	286	236.2
99T	0.87	50.0	50.0	45.0	600	286	269.1
100T	1.01	50.25	49.9	80.0	600	332	26.7
101T	1.005	50.25	49.6	75.0	600	332	60.5
102T	1.01	51.0	49.2	70.0	600	332	150.1
103T	1.015	49.5	50.1	65.0	600	332	150.1
104T	1.00	50.0	49.87	60.5	600	332	195.7
105T	1.00	51.5	49.0	55.0	600	332	250.9
106T	1.01	50.0	49.5	50.5	600	332	299.1
107T	1.01	50.0	50.0	45.0	600	332	353.6
108T	1.12	50.0	49.87	80.0	600	256	32.3

Spec No	t mm	b_1 mm	b_2 mm	θ degrees	Span mm	σ_Y N/mm^2	M_{ult} Nm
109T	1.12	50.0	50.0	75.0	600	256	71.2
110T	1.11	50.0	50.0	70.0	600	256	115.2
111T	1.12	50.0	49.75	65.0	600	256	169.0
112T	1.11	50.0	49.75	60.0	600	256	213.96
113T	1.11	50.0	49.87	55.0	600	256	262.9
114T	1.12	50.0	49.8	60.5	600	256	299.1
115T	1.12	50.0	49.8	45.5	600	256	355.9

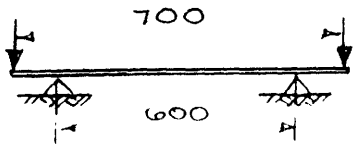

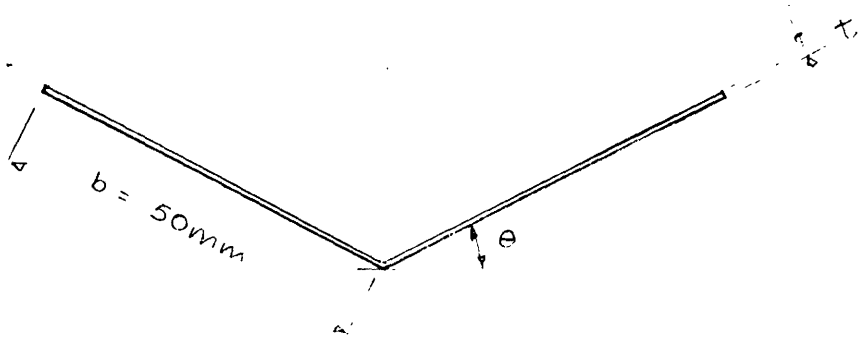

TABLE 2: DIMENSIONS AND FAILURE MOMENTS OF VEE SECTIONS

Spec No.	t mm	θ degrees	σ_Y N/mm^2	M_{ult} Nm
VT1	0.875	5	237	6.67
VT2	0.884	8	237	13.23
VT3	0.881	12	237	30.03
VT4	0.883	16	237	50.71
VT5	0.877	20	237	72.95
VT6	0.875	24	237	94.75
VT7	1.003	5	332	8.90
VT8	1.001	8	332	18.46
VT9	1.002	12	332	42.93
VT10	0.999	16	332	66.72
VT11	1.005	20	332	99.64
VT12	1.003	24	332	137.0
VT13	1.257	5	292.5	12.90

Spec No.	t mm	θ degrees	σ_Y N/mm^2	M_{ult} Nm
VT14	1.256	8	292.5	30.03
VT15	1.253	12	292.5	57.38
VT16	1.254	16	292.5	88.96
VT17	1.258	20	292.5	123.44
VT18	1.257	24	292.5	162.36
VC1	0.873	8	237	7.45
VC2	0.859	12	237	14.46
VC3	0.882	16	237	20.24
VC4	0.869	20	237	22.24
VC5	0.871	24	237	32.47
VC6	0.860	28	237	35.59
VC7	1.002	8	332	10.34
VC8	1.001	12	332	18.90
VC9	1.001	16	332	28.69
VC10	1.002	20	332	35.36
VC11	1.002	24	332	44.48
VC12	1.00	28	332	52.27
VC13	1.249	8	292.5	19.35
VC14	1.253	12	292.5	29.58
VC15	1.255	16	292.5	40.03
VC16	1.255	20	292.5	52.27
VC17	1.258	24	292.5	65.61
VC18	1.252	28	292.5	74.84

TABLE 3i Dimensions of edge stiffened plates

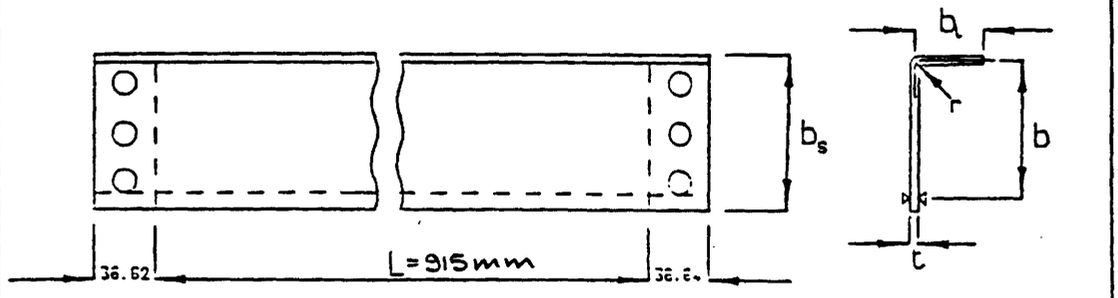

All dimensions in mm

Yield stress = 271·1 N/mm²

Specimen Number	t (mm)	b (mm)	b_1 (mm)	b_s (mm)	r (mm)	L (mm)
1/1.579/0.0	1.579	71.590	0	76.12	0	915.4
2/1.579/0.0	1.579	71.590	0	76.12	0	915.4
3/1.580/0.0	1.580	71.590	0	76.06	0	915.4
4/1.582/.25	1.582	71.591	6.34	77.55	3.65	915.5
5/1.582/.25	1.582	71.591	6.32	77.04	3.64	915.4
6/1.584/.25	1.584	71.592	6.30	77.14	3.65	915.5
7/1.583/.50	1.583	71.592	12.25	76.58	3.64	915.5
8/1.578/.50	1.578	71.589	12.05	76.78	3.64	915.4
9/1.572/.50	1.572	71.586	12.18	76.59	3.64	915.4
10/1.506/.75	1.506	71.553	18.05	77.54	3.64	915.0
11/1.554/.75	1.554	71.577	17.98	77.57	3.64	915.1
12/1.555/.75	1.555	71.578	18.21	77.37	3.64	915.5
13/1.576/1.0	1.576	71.588	24.06	77.85	3.64	915.3
14/1.576/1.0	1.576	71.588	24.02	77.87	3.64	915.3
15/1.575/1.0	1.575	71.588	23.94	77.96	3.64	915.3

3 i

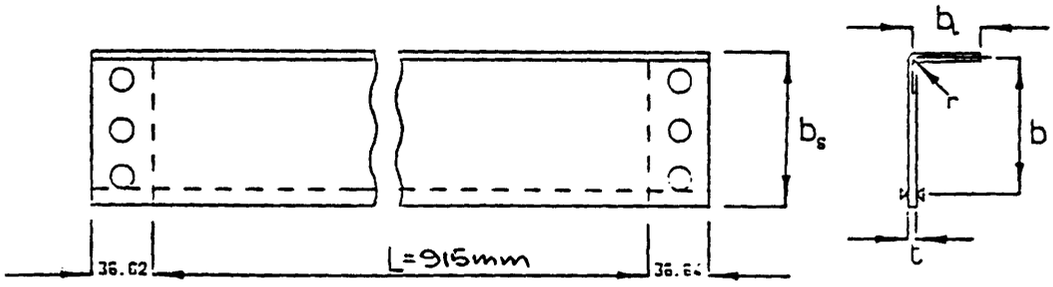

All dimensions in mm Yield stress = 291.9 N/mm^2

Specimen Number	t (mm)	b (mm)	b_1 (mm)	b_s (mm)	r (mm)	L (mm)
1/1.151/0	1.151	71.378	0	74.75	0	915.3
2/1.176/0	1.176	71.388	0	74.99	0	915.2
3/1.162/.25	1.162	71.381	5.12	76.30	3.32	915.3
4/1.182/.25	1.182	71.391	6.23	75.87	3.30	915.3
5/1.164/.50	1.164	71.382	12.53	74.81	3.30	914.9
6/1.181/.50	1.181	71.391	12.73	74.85	3.29	915.2
7/1.168/.75	1.168	71.384	13.67	75.41	3.29	915.2
8/1.182/.75	1.182	71.391	18.56	75.75	3.29	915.3
9/1.172/1.0	1.172	71.386	24.37	76.30	3.30	915.3
10/1.184/1.0	1.184	71.392	24.25	76.36	3.29	915.3
1A/1.170/0	1.170	71.385	0	75.24	3.30	915.8
2A/1.160/.25	1.160	71.380	5.42	76.10	3.33	915.3
3A/1.170/.50	1.170	71.385	12.22	76.13	3.32	914.8
4A/1.180/.75	1.180	71.390	18.87	75.95	3.29	915.8
5A/1.180/1.0	1.180	71.390	24.01	75.75	3.30	915.8

3i

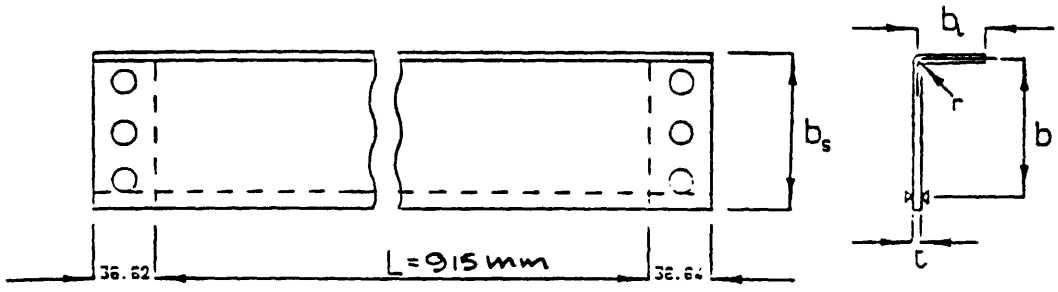

All dimensions in mm Yield stress = 276.9 N/mm^2

Specimen Number	t (mm)	b (mm)	b_1 (mm)	b_s (mm)	r (mm)	L (mm)
1/.963/0.0	0.963	71.282	0	74.87	0	915.5
2/.963/0.0	0.963	71.282	0	75.00	0	914.6
3/.969/0.0	0.969	71.284	0	75.18	0	914.3
4/.957/0.25	0.957	71.278	5.48	75.83	2.71	916.1
5/.956/0.25	0.956	71.278	5.54	75.94	2.71	916.4
6/.955/0.25	0.955	71.278	5.56	75.95	2.71	916.2
7/.960/0.50	0.960	71.280	12.24	74.85	2.70	915.5
8/.957/0.50	0.957	71.278	12.26	74.85	2.70	915.5
9/.960/0.50	0.960	71.280	12.24	74.86	2.70	915.5
10/.955/0.75	0.955	71.278	18.28	75.74	2.70	915.5
11/.957/0.75	0.957	71.278	18.25	75.75	2.70	915.4
12/.959/0.75	0.959	71.280	18.69	75.36	2.70	915.0
13/.957/1.0	0.957	71.278	24.53	75.52	2.70	915.4
14/.957/1.0	0.957	71.278	24.54	75.50	2.70	915.6
15/.958/1.0	0.958	71.279	24.32	75.73	2.71	915.0

3.1

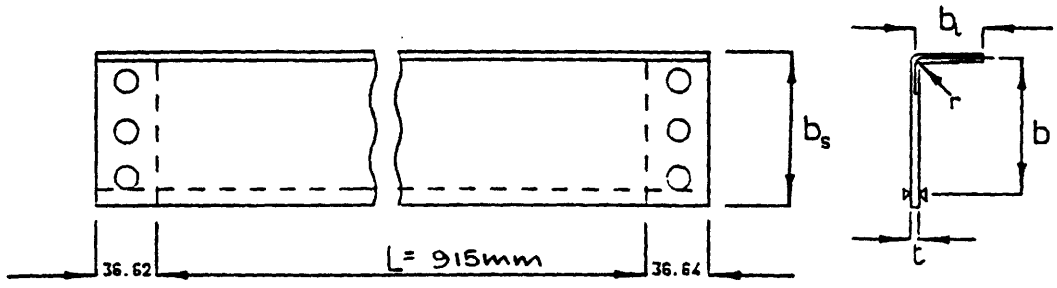

All dimensions in mm Yield stress = 313.9 N/mm^2

Specimen Number	t (mm)	b (mm)	b_1 (mm)	b_s (mm)	r (mm)	L (mm)
1/.754/0	0.754	71.177	0	74.88	0	915.5
2/.764/0	0.764	71.182	0	75.12	0	915.2
3/.765/0	0.765	71.182	0	75.13	0	915.1
4/.764/.25	0.764	71.182	6.39	75.74	2.13	915.3
5/.766/.25	0.766	71.183	6.33	75.61	2.13	915.2
6/.766/.25	0.766	71.183	6.35	75.50	2.13	915.3
7/.756/.50	0.756	71.178	12.22	74.85	2.13	914.9
8/.759/.50	0.759	71.180	12.45	74.60	2.13	914.9
9/.758/.50	0.758	71.179	12.40	74.70	2.13	914.8
10/.759/.75	0.759	71.180	18.46	75.25	2.13	914.9
11/.755/.75	0.755	71.178	18.34	75.40	2.13	914.7
12/.767/.75	0.767	71.184	18.30	75.58	2.13	915.3
13/.752/1	0.752	71.176	24.34	75.74	2.13	914.7
14/.768/1	0.768	71.184	24.33	75.84	2.13	915.3
15/.767/1	0.767	71.184	24.26	75.86	2.13	915.3

3 i

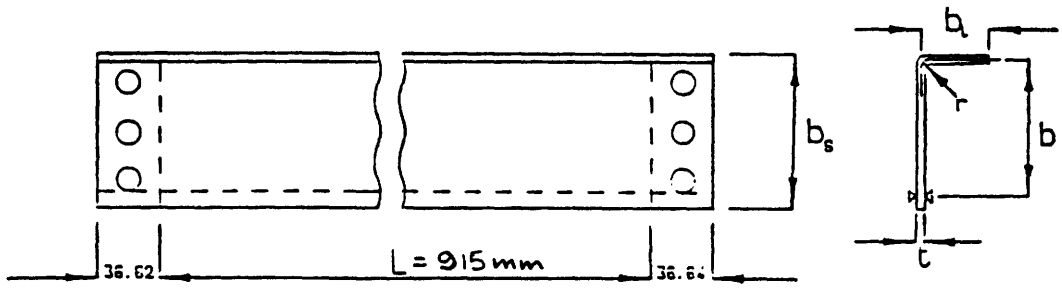

All dimensions in mm Yield stress = 174 N/mm^2

Specimen Number	t (mm)	b (mm)	b_1 (mm)	b_s (mm)	r (mm)	L (mm)
1/.652/0.0	0.652	71.126	0	74.78	0	915.4
2/.656/0.0	0.656	71.128	0	74.82	0	915.2
3/.662/0.0	0.662	71.131	0	75.07	0	914.7
4/.657/0.25	0.657	71.128	6.17	75.55	2.09	915.0
5/.656/0.25	0.656	71.128	6.13	75.72	2.09	915.1
6/.661/0.25	0.661	71.131	6.16	75.54	2.09	915.2
7/.662/0.50	0.662	71.131	12.19	74.91	2.09	915.0
8/.661/0.50	0.661	71.131	12.40	74.70	2.09	914.9
9/.662/0.50	0.662	71.131	12.25	74.84	2.09	914.9
10/.662/0.75	0.662	71.131	18.25	75.39	2.09	914.8
11/.661/0.75	0.661	71.131	18.25	75.49	2.09	914.8
12/.663/0.75	0.663	71.132	18.26	75.54	2.09	914.9
13/.644/1.0	0.644	71.122	24.11	75.81	2.09	914.7
14/.659/1.0	0.659	71.130	24.23	75.86	2.10	914.7
15/.661/1.0	0.661	71.131	24.21	75.93	2.09	914.7

TABLE 3.ii

ANGLED ASYMMETRIC EDGE-STIFFENED PLATE'S GEOMETRICAL DIMENSIONS AND TEST RESULTS

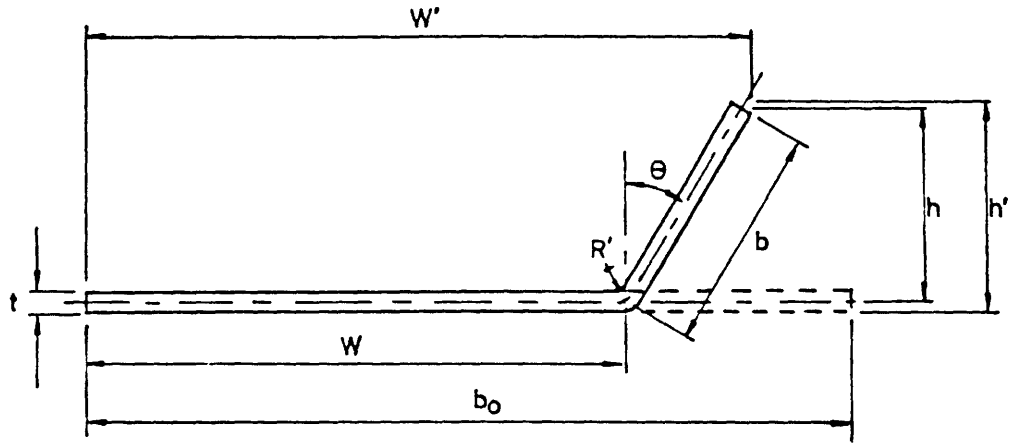

Cross-Sectional Dimensions

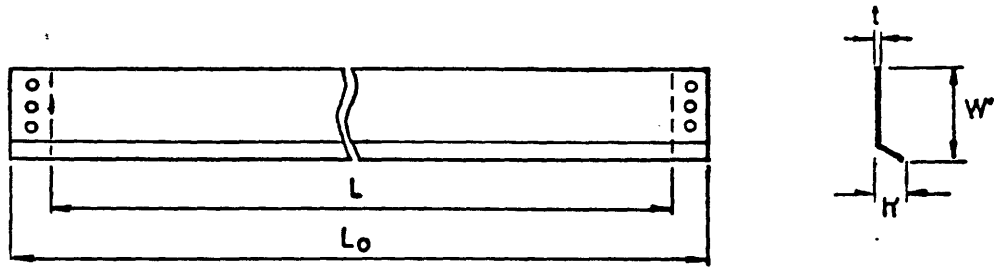

Dimensions of Specimen

NOTE

Since R is small, the effect of radius is neglected.

Radius $R = R' + \frac{1}{2}t$ where R is the centre-line radius

Lip size $b = h/\cos\theta$ where $h = h' - \frac{1}{2}t(1+\sin\theta)$

Flange width $W = W' - b\sin\theta - \frac{1}{2}t\cos\theta$

Effective length L = 898.0 mm

TABLE OF GEOMETRICAL DIMENSIONS AND ULTIMATE LOADS

Specimen Number	Angle (Deg.)	L_o (mm)	b_o (mm)	W'(mm)	h'(mm)	t(mm)	R'(mm)	b(mm)	W(mm)	P_{ult} (N)
1	14.2	959.5	86.0	77.495	14.32	1.158	3.175	13.96	73.843	15588
2	42.2	961.0	86.0	82.588	10.77	1.162	6.085	12.47	74.454	13071
3	29.5	961.0	86.0	80.874	12.19	1.168	4.762	12.69	74.684	14697
4	15.0	959.5	99.0	80.891	26.20	1.160	3.175	25.49	74.378	20487
5	29.5	959.5	99.0	86.222	23.16	1.163	5.750	24.95	74.549	20665
6	44.75	960.5	99.0	92.280	18.80	1.160	6.220	23.39	76.717	21734

NOTE

P_{ult} is the ultimate load obtained from the test specimen

Material Yield Stress, σ_y = 264.3 N/mm²

The experiments were carried out in the L-Compression Rig (LCR), as used in Chapter (6.0).
Special angled-inserts of various angular inclinations were manufactured to be used in conjunction with the existing Clamp-Units (LCR-1, LCR-2, LCR-3).
This was to accomodate the A symmetric A ngled Edge Stiffener.

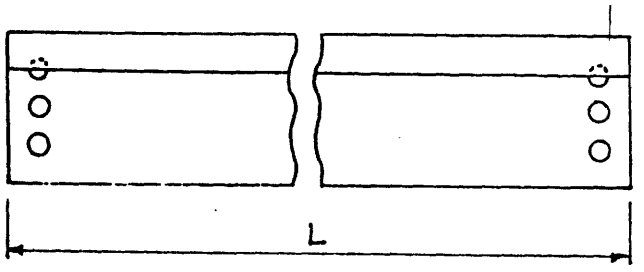

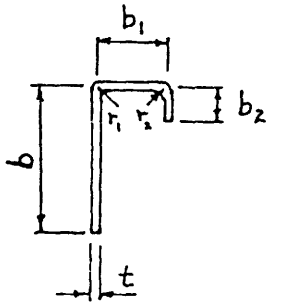

TABLE 3iii Dimensions of compound lip edge stiffened plates

Specimen No.	b	b_1	b_2	r_1	r_2	t	L	σ_y (N/mm^2)
1/0.8/1	75.54	20.58	9.16	2.34	2.34	0.877	980.5	233.46
1/0.8/2	77.29	19.17	9.35	2.34	2.34	0.874	980.0	233.46
2/0.8/1	76.55	15.08	8.48	2.04	2.20	0.876	980.5	233.46
2/0.8/2	76.43	15.58	8.19	2.12	2.68	0.877	979.5	233.46
1/1.0/1	76.62	21.22	10.99	2.94	2.94	1.014	979.5	315.95
1/1.0/2	77.25	20.66	10.86	2.83	2.75	1.012	979.0	315.95
2/1.0/1	76.47	14.14	7.89	2.12	2.04	1.006	980.5	330.16
2/1.0/2	76.22	14.29	7.90	2.68	2.83	1.006	980.5	330.16
1/1.1/1	75.90	18.77	10.40	3.03	2.95	1.081	981.5	265.12
1/1.1/2	76.11	18.36	10.23	2.79	2.73	1.102	981.5	265.12
2/1.2/1	75.60	15.41	7.87	2.78	2.95	1.261	980.5	323.95
2/1.2/2	75.83	15.19	8.07	2.79	2.70	1.262	981.0	323.95

All dimension in mm and taken from centre line

GEOMETRICAL DIMENSIONS OF SIZE 3 SPECIMENS

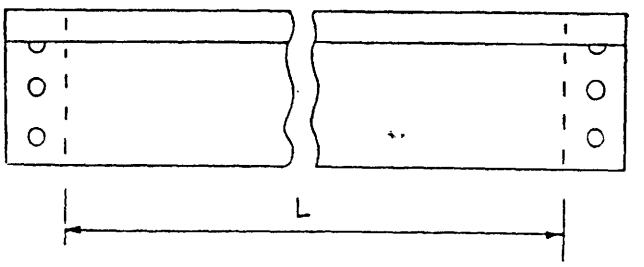

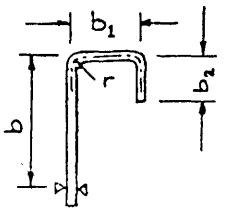

All dimensions in mm

SPECIMEN	t	b	b_1	b_2	r	L
3/0.85/1	0.884	71.44	8.38	8.42	2.03	907.7
3/0.85/2	0.882	71.44	8.81	8.16	2.03	908.2
3/1.0 /1	1.011	71.51	7.90	7.92	2.09	907.2
3/0.1 /2	1.020	71.51	8.63	8.12	2.10	907.2
3/1.1 /1	1.087	71.54	7.97	8.08	2.13	907.7
3/1.1 /2	1.082	71.54	8.27	8.45	2.13	907.7

$t = 0.85$ mm $\sigma_Y = 313\ N/mm^2$
$t = 1$ mm $\sigma_Y = 330\ N/mm^2$
$t = 1.1$ mm $\sigma_Y = 265\ N/mm^2$

TABLE 3i(a) - TEST FAILURE LOADS FOR SPECIMENS OF TABLE 3.i

Specimen Number	P_{EX}(N)	Specimen Number	P_{EX}(N)
3/1.580/0.0	16817	2/.764/0	4391
6/1.584/.25	21311	3/.765/0	4538
9/1.572/.50	23535	4/.764/.25	5944
12/1.555/.75	30565	5/.766/.25	5507
15/1.575/1.0	39151	6/.766/.25	5784
2/1.176/0	9009	7/.756/.5	5784
1A/1.17/0	8297	8/.759/.5	7092
4/1.182/.25	11567	9/.758/.5	6940
2A/1.160/.25	11679	11/.755/.75	8987
6/1.182/.50	13925	12/.767/.75	9654
3A/1.179/.50	13903	13/.752/1	9877
7/1.168/.75	17929	14/.768/1	10544
8/1.168/.75	18953	15/.767/1	10224
4A/1.180/.75	18063	3/.662/0.0	2500
9/1.172/1.0	20065	4/.657/0.25	3181
10/1.184/1.0	21177	5/.656/0.25	2981
5A/1.180/1.0	19620	7/.656/0.50	3684
1/.963/0.0	6140	8/.661/0.75	4316
3/.969/0.0	6264	9/.662/0.75	4689
4/.957/0.25	7452	10/.662/0.75	4956
5/.956/0.25	7643	11/.661/0.75	5285
6/.955/0.25	7830	13/.644/1.0	4774

Specimen Number	P_{EX}(N)	Specimen Number	P_{EX}(N)
7/.960/0.50	9521	14/.659/1.0	5570
8/.957/0.50	9810		
9/.960/0.75	9699		
10/.955/0.75	13347		
11/.957/0.75	12457		
12/.959/0.75	13881		
13/.957/1.0	14059		
14/.957/1.0	14548		

TABLES 3iii(a) - TEST FAILURE LOADS FOR SPECIMENS OF TABLE 3iii

SPECIMEN NUMBER	P_{EX} (N)
1/0.8/1	16331
1/0.8/2	17576
2/0.8/1	16108
2/0.8/2	15129
1/1.0/1	22115
1/1.0/2	21225
2/1.0/1	17309
2/1.0/2	17532
1/1.1/1	20825
1/1.1/2	21030
2/1.2/1	25141
2/1.2/2	24874
3/0.85/1	9210
3/0.85/2	9167
3/1.0/1	11312
3/1.0/2	11570
3/1.1/1	13751
3/1.1/2	13573
4/0.85/1	16243
4/0.85/2	16243
4/1.0/1	25098
4/1.0/2	19580
4/1.1/1	22828
4/1.1/2	21850

TABLE 4. Dimensions of channel sections.

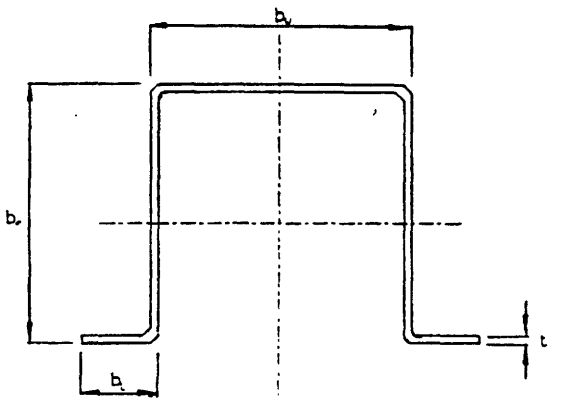

Specimen Number	t (mm)	b_w (mm)	b_f (mm)	b_1 (mm)	L (mm)
A1	0.6276	77.6970	76.8715	0.0000	610.00
A2	0.6214	77.7810	77.8098	7.5792	609.00
A3	0.6256	77.4034	77.7693	13.0511	605.50
A4	0.6246	77.6124	77.5492	20.4763	610.80
A5	0.6220	77.7486	78.2059	26.1453	610.00
A6	0.6250	78.6228	76.8280	32.9045	606.50
B1	1.2437	79.2820	77.3893	0.0000	609.00
B2	1.2358	78.9910	78.3772	8.0854	610.20
B3	1.2381	79.4200	78.6047	13.9927	610.00
B4	1.2328	79.8900	78.5924	20.6996	609.50
B5	1.2349	79.9602	78.8134	26.7713	607.00
B6	1.2426	79.4848	78.8374	33.0797	609.50
C1	0.8962	78.2867	75.9938	0.0000	457.50
C2	0.8900	78.3822	77.9225	7.2162	458.00
C3	0.8938	79.6933	78.0712	13.4662	458.00
C4	0.8931	79.3128	77.5175	19.8912	459.00
C5	0.8888	79.3128	77.5175	26.2962	458.00
C6	0.8925	79.5367	78.0712	31.9512	458.00

TABLE 41 Dimensions of top hat sections with compound lips

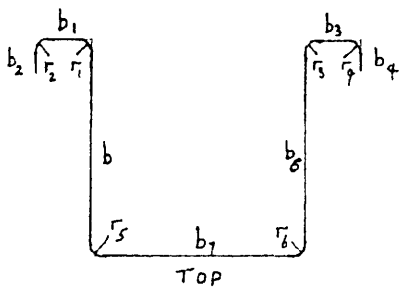

Specimen No.	1H/1.1/1	1H/1.2/1	2H/1.1/1	2H/1.2/1
b_1	19.50	18.27	13.42	14.83
b_2	9.21	9.18	8.71	7.59
b_3	19.18	18.19	13.77	13.48
b_4	9.25	9.17	8.84	8.28
b_5	76.01	77.29	75.16	75.85
b_6	76.02	76.19	75.06	76.87
b_7	77.36	77.32	78.63	77.05
r_1	2.63	2.63	2.39	2.70
r_2	3.02	2.18	2.63	2.62
r_3	3.02	2.18	2.23	2.55
r_4	3.02	2.63	2.23	2.55
r_5	3.02	2.18	3.03	3.18
r_6	3.02	2.18	3.03	2.86
r_m	2.96	2.33	2.27	2.74
thickness	1.12	1.26	1.09	1.26
length	610	610	610	608
σ_y	265.12	293.13	265.12	293.13
P_{Ex} (N)	50616	70640	40048	67859

TABLE 5. TEST FAILURE LOADS FOR SPECIMENS OF TABLE 4.

Specimen Number	h	P_{EX}(N)
A1	0.0	10121.48
A2	0.0917	11856.56
A3	0.1651	17640.28
A4	0.2621	18685.80
A5	0.3330	19575.00
A6	0.4277	18552.33
B1	0.0	27606.04
B2	0.0968	48494.10
B3	0.1729	63175.80
B4	0.2596	66735.00
B5	0.3371	68959.50
B6	0.4183	66067.65
C1	0.0	18107.43
C2	0.0879	23837.74
C3	0.1687	33078.32
C4	0.2533	37816.50
C5	0.3340	37371.60
C6	0.4082	40953.04

P_{EX} - Ultimate Strength obtained from experiment

TABLE 6

GEOMETRICAL DIMENSIONS OF TOP HAT CHANNEL SECTION.

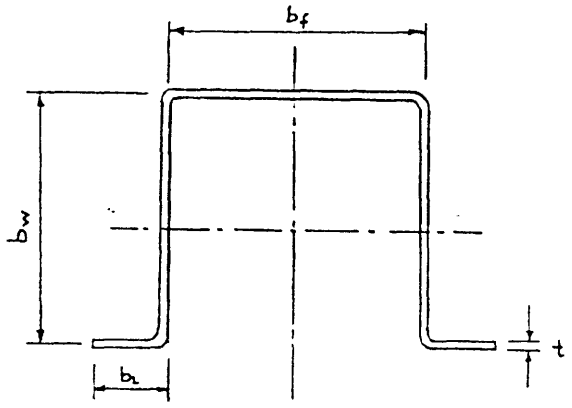

All dimensions in mm $\sigma_y = 290\ N/mm^2$

SPECIMEN	t	b_f	b_w	b_L	L
0/0.85/1	0.880	52.38	51.42	0	915
1/4 /0.85/1	0.870	52.81	52.24	8.038	915
3/8 /0.85/1	0.878	53.12	52.62	10.765	915
1/2 /0.85/1	0.865	52.70	53.64	13.800	915
5/8 /0.85/1	0.888	53.36	52.42	16.975	915
3/4 /0.85/1	0.842	54.06	52.14	20.360	915
7/8 /0.85/1	0.874	53.08	52.50	23.430	915
1/0.85/1	0.865	54.17	52.45	26.605	915

TABLE 7. - FAILURE MOMENTS FOR SPECIMENS OF TABLE 6

SPECIMEN NUMBER	M_{EX} (Nm)
0/0.85/1	144.1
1/4/0.85/1	337 *
3/8/0.85/1	193
1/2/0.85/1	440.8
5/8/0.85/1	337.8 *
3/4/0.85/1	452.1
7/8/0.85/1	526.7
1/0.85/1	531.2

* Denotes that specimen failed by web crushing at supports.

TABLE 8i - DIMENSIONS OF STIFFENED PLATES

Spec. No.	a	w/t	b_s	b_{sb}	d	t	B_t
SP1/0.4	949	188.3	5.5	7.5	2.944	0.405	169.0
SP2/0.4	950	187.6	6.0	8.5	5.678	0.4038	167.1
SP3/0.4	950.5	181.7	6.0	8.0	10.5	0.4183	164.4
SP4/0.4	950.5	180.8	6.0	8.5	12.54	0.4190	168.0
SP1/0.57	950	132.9	5.5	8.5	3.43	0.5700	167.5
SP2/0.57	950	133.3	6.0	8.2	5.208	0.5691	168.5
SP3/0.57	952	135.0	6.8	6.8	6.233	0.5673	167.0
SP4/0.57	950	134.5	6.5	7.0	9.30	0.5668	168.0
SP5/0.57	950	133.7	6.25	8.0	12.26	0.5683	169.3
SP1/0.63	948	118.7	5.5	9.5	3.1	0.634	166.0
SP2/0.63	948	120.6	7.0	8.0	6.07	0.63	165.5
SP3/0.63	948	120.5	7.0	7.0	9.1	0.635	165.6
SP4/0.63	948	120.3	7.0	7.0	12.15	0.636	167.0
SP5/0.63	948	117.8	6.5	11.5	23.5	0.63	168.0
SP1/0.81	948	92.1	6.5	10.0	2.9	0.814	167.3
SP2/0.81	948	96.1	7.0	7.0	5.92	0.796	164.4
SP3/0.81	948	94.5	7.0	7.0	8.9	0.809	167.1
SP4/0.81	948	91.3	7.0	7.0	11.5	0.838	170.0
SP5/0.81	948	96.6	7.0	7.0	25.2	0.792	170.0
SP1A/0.81	947	92.1	6.5	10.0	3.25	0.8143	169.0
SP2A/0.81	947.3	93.4	7.0	7.0	6.15	0.8189	169.0

Spec. No.	a	w/t	b_s	b_{sb}	d	t	B_t
SP3A/0.81	948	93.5	7.0	7.0	9.671	0.8178	168.0
SP4A/0.81	948	95.6	7.0	7.0	12.675	0.8001	169.5
SP5A/0.81	948	98.0	7.5	7.6	25.63	0.7782	171.3
SP6A/0.81	949	93.5	7.5	7.5	25.3	0.8148	172.7
SP1/1.2	948.5	64.1	6.5	10.0	5.235	1.17	167.5
SP2/1.2	948	65.1	7.0	7.0	8.928	1.1703	164.7
SP3/1.2	948.7	63.7	7.5	7.5	9.471	1.1975	169.0
SP4/1.2	948	63.7	7.5	7.5	12.585	1.1975	170.0
SP5/1.2	948.5	63.7	7.5	7.5	25.25	1.1975	170.5
SP1/1.6	948	48.1	7.5	7.5	4.357	1.5846	169.7
SP2/1.6	948.5	47.6	7.65	7.65	9.343	1.6011	164.5
SP3/1.6	948	47.4	7.65	7.65	11.8	1.6079	165.5
SP4/1.6	948	47.4	8.0	8.0	16.186	1.6033	164.7
SP5/1.6	947.3	47.3	7.9	7.9	25.0	1.6003	172.0

Symbols refer to Fig 65.

TABLE 8i(a) - FAILURE LOADS FOR STIFFENED PLATES

Spec.No.	σ_Y (N/mm^2)	P_E (N)
SP1/0.4	270	3694
SP2/0.4	270	4637
SP3/0.4	270	6595
SP4/0.4	270	7850
SP1/0.57	314.5	7521
SP2/0.57	314.5	9634
SP3/0.57	314.5	9456
SP4/0.57	314.5	12327
SP5/0.57	314.5	12816
SP1/0.63	270	8455
SP2/0.63	270	10680
SP3/0.63	270	13261
SP4/0.63	270	17222
SP5/0.63	270	20470
SP1/0.81	343	14182
SP2/0.81	343	16243
SP3/0.81	343	21360
SP4/0.81	343	28035
SP5/0.81	343	35244
SP1A/0.81	343	14997
SP2A/0.81	343	18957

Spec.No.	$\sigma_Y (N/mm^2)$	$P_E (N)$
SP3A/0.81	343	22784
SP4A/0.81	343	28258
SP5A/0.81	343	31239
SP6A/0.81	343	37825
SP1/1.2	262	31150
SP2/1.2	262	38493
SP3/1.2	262	42275
SP4/1.2	262	46814
SP5/1.2	262	56293
SP1/1.6	181.5*	33375
SP2/1.6	181.5*	45835
SP3/1.6	181.5*	53400
SP4/1.6	181.5*	56960
SP5/1.6	181.5*	70310

* - 0.2% Proof Stress

TABLE 8ii - DIMENSIONS OF FLAT PLATES

Spec.No.	B/t	a	t	B_t	B	σ_y (N/mm^2)
FP1	157.3	950	0.966	160	152	300
FP2	157.3	949	0.966	160	152	297
FP3	158.6	954	0.958	160	152	291
FP4	158.1	954	0.961	160	152	292
FP5	156.6	954	0.9705	160	152	273
FP6	199.1	951	0.8033	165.5	160	285
FP7	198.7	950	0.805	167	160	285

Symbolts refer to Fig 65.

TABLE 8ii(a) - FAILURE LOADS FOR FLAT PLATES

Spec.No.	$\sigma_Y (N/mm^2)$	$P_E (N)$
FP1	300	14859
FP2	297	14240
FP3	291	13688
FP4	292	13662
FP5	273	13795
FP6	285	9750
FP7	285	10057

TABLE 9. **Dimensions of lipped channel beams**

Sp. No.	w/t	b_s	b_{sb}	d	t	b_f	b_w	b_l
LC0	49.0	0.00	0.00	0.00	1.57	153.9	78.5	15.00
A0	186.8	0.00	0.00	0.00	0.41	153.2	77.1	15.1
A1	176.8	5.25	11.25	2.95	0.405	154.2	76.4	17.3
A2	178.2	6.5	8.1	5.5	0.410	154.3	77.4	17.5
A3	179.4	6.65	7.1	9.0	0.410	154.2	76.8	16.6
A4	177.4	6.8	7.25	11.77	0.415	154.5	76.9	18.0
A5	181.2	6.6	8.0	18.2	0.405	154.7	76.9	17.1
B1	103.5	4.75	13.25	4.35	0.682	154.3	76.9	17.6
B2	105.2	6.5	8.8	5.5	0.691	154.2	76.7	17.4
B3	104.7	6.5	7.8	7.75	0.698	154.0	77.1	18.5
B4	105.3	6.75	8.0	10.75	0.695	154.4	77.0	18.9
C0	94.0	0.0	0.0	0.0	0.818	153.8	77.4	15.3
C1	86.4	4.5	12.75	3.9	0.818	154.2	77.0	17.2
C2	88.5	5.75	9.5	5.15	0.821	154.8	76.7	17.7
C3	90.7	6.9	7.35	8.75	0.814	155.0	77.4	17.1
C4	90.3	7.0	7.4	11.75	0.815	154.6	77.0	18.5
C5	90.6	6.9	7.6	18.25	0.810	154.3	77.5	18.2
D1	93.9	5.5	9.5	4.1	0.759	152.0	76.5	16.2
D2	95.2	6.5	8.0	8.9	0.761	153.0	76.4	25.5
D3	94.6	6.25	8.25	11.3	0.762	152.5	76.2	16.8
D4	94.8	6.25	8.25	15.1	0.763	153.0	76.9	9.0
E1	59.1	7.0	11.0	4.4	1.213	154.3	76.3	17.0
E2	59.9	7.0	10.0	4.94	1.207	154.6	77.8	17.0
E3	60.9	7.0	7.0	8.25	1.207	154.1	79.0	18.0
E4	61.0	7.05	8.15	9.0	1.2	154.5	77.2	14.5
E5	61.0	7.75	7.75	12.0	1.209	155.3	76.7	17.0
E6	61.2	7.5	7.5	18.8	1.202	154.5	78.7	17.5
F1	46.2	5.25	13.0	3.3	1.519	153.5	76.0	17.7
F2	46.4	5.5	12.0	5.0	1.528	153.8	75.5	17.8
F3	46.9	6.25	10.0	9.5	1.528	153.5	76.3	17.0
F4	47.2	6.5	10.5	12.4	1.514	153.5	76.3	15.5
F5	47.0	7.0	9.75	18.25	1.525	153.0	77.6	18.5

All dimensions are in mm.

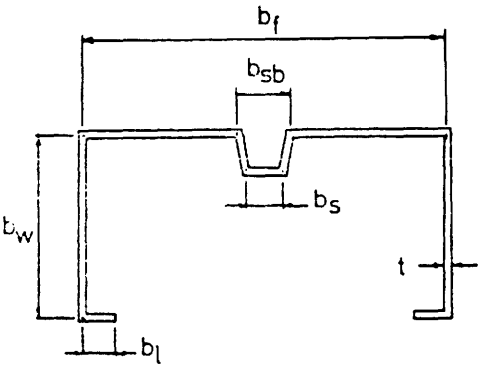

TABLE 10 - EXPERIMENTAL ULTIMATE MOMENTS

Test Series		σ_Y (N/mm^2)	M_E (Nm)
	LC0		3223.1
w/t=180	A0	275	339.0
	A1	275	350.8
	A2	275	375.7
	A3	275	349.6
	A4	275	318.9
	A5	272	306.4
w/t=105	B1	374	1177.8
	B2	374	1250.0
	B3	374	1291.4
	B4	374	1273.7
w/t=90	C0	285	1097.7
	C1	285	1395.0
	C2	285	1489.6
	C3	285	1463.0
	C4	285	1380.2
	C5	285	1377.2
w/t=94	D1	147.4*	889.2
	D2	147.4*	1023.4
	D3	147.4*	924.2
	D4	147.4*	877.3

Test Series		σ_Y (N/mm^2)	$\bar{M}_E$ (Nm)
w/t=60	E1	176.5*	1909.0
	E2	176.5*	1904.9
	E3	176.5*	2045.1
	E4	176.5*	1930.3
	E5	176.5*	1980.8
	E6	176.5*	1980.8
w/t=47	F1	214.5*	2717.1
	F2	214.5*	2918.3
	F3	214.5*	2924.2
	F4	214.5*	2687.6
	F5	214.5*	2829.5

* 0.2% Proof Stress.

Table 11. Desmond's Tests

DIMENSIONS OF INTERMEDIATELY STIFFENED BEAMS

Test Series	w/t	b (in)	web (in)	bp (in)	bl (in)	L (in)	LS (in)	t (in)	t_{bp} (in)	r_s (in)	d_s (in)	$\frac{I_s}{t^4}$	$\frac{A_s}{t^2}$
(1)	(2)	(3)	(4)	(5)	(6)	(7)	(8)	(9)	(10)	(11)	(12)	(13)	(14)
I-47	48.0	6.10	5.00	9.35	1.50	88.	24.	.0565	.0575	.210	.145	60.0	16.3
	47.0	6.11	5.00	9.33	1.55	88.	24.	.0575	.0580	.213	.223	110.0	19.4
	47.4	6.10	5.00	9.35	1.55	88.	24.	.0570	.0588	.217	.259	142.	20.8
	47.0	6.10	5.00	9.38	1.54	88.	24.	.0578	.0572	.209	.350	217.	23.5
	46.8	6.00	5.00	9.38	1.50	88.	24.	.0577	.0590	.215	.535	499.	30.2
I-70	71.8	8.89	4.08	12.0	1.50	88.	24.	.0564	.0585	.192	.108	40.5	14.5
	70.4	8.83	4.09	12.0	1.50	88.	24.	.0571	.0585	.213	.230	118.	19.8
	70.1	8.80	4.00	12.0	1.50	88.	24.	.0571	.0593	.213	.230	118.	19.8
	69.5	8.95	4.10	12.0	1.30	112.	37.3	.0590	.0593	.217	.367	232.	24.0
	69.5	8.95	4.08	12.0	1.31	112.	37.3	.0587	.0592	.224	.458	367.	27.6
	69.8	8.95	4.10	12.0	1.34	112.	37.3	.0587	.0592	.224	.532	488.	30.1
	69.3	8.93	4.00	12.0	1.35	112.	37.3	.0590	.0598	.230	1.150	2650.	51.2
I-97	96.4	11.7	5.50	15.0	1.56	88.	24.	.0570	.0690	.219	.226	115.	19.6
	97.5	11.8	5.45	15.0	1.58	88.	24.	.0564	.0690	.214	.263	150.	21.2
	79.3	11.7	5.50	15.0	1.30	88.	24.	.0694	.0698	.236	.359	153.	21.0
	79.5	11.7	5.50	15.0	1.50	88.	24.	.0692	.0697	.224	.545	313.	25.9
	80.7	11.7	5.50	15.0	1.55	88.	24.	.0681	.0695	.228	.681	527.	30.5
I-156	155.	18.6	5.50	21.9	1.55	88.	14.	.0580	.0595	.217	.218	107.	19.3
	156.	18.6	5.49	21.9	1.50	88.	14.	.0580	.0573	.218	.268	147.	21.0
	159.	18.7	5.50	21.8	1.54	88.	14.	.0572	.0575	.218	.350	235.	24.1
	157.	18.6	5.50	21.8	1.57	88.	14.	.0573	.0575	.217	.514	477.	29.8
	157.	18.6	5.50	21.9	1.58	88.	14.	.0572	.0571	.218	1.130	2670.	51.3

Table 11(a) Desmond's Tests

MATERIAL PROPERTIES AND TEST RESULTS

Test Series	I_s/t^4	MATERIAL PROPERTIES: Yield Stress (ksi)	MATERIAL PROPERTIES: Ultimate Stress (ksi)	TEST RESULTS: M_{ult} (kip-in)	TEST RESULTS: k_b
(1)	(2)	(3)	(4)	(5)	(6)
I-47	60.	45.9	51.4	92.4	10.2[a]
	110.	43.2	50.6	109.	10.2[a]
	142.	43.6	51.2	98.4	10.3[a]
	217.	43.0	50.2	102.	*
	499.	44.9	56.6	119.	10.3[a]
I-70	40.5	43.9	51.4	64.6	12.3
	118.	42.1	50.7	77.5	16.4
	118.	43.0	50.7	69.6	14.9
	232.	43.6	50.7	82.1	18.4
	367.	43.8	50.8	80.6	16.0
	488.	44.9	52.1	89.6	16.8
	2650.	42.6	50.3	87.7	16.7
I-97	115.	42.9	51.3	103.	12.3
	150.	44.5	51.5	108.	16.8
	153.	44.9	50.7	150.	15.3
	313.	44.0	57.2	159.	16.7
	527.	44.9	56.1	168.	18.4
I-156	107.	42.4	50.9	104.	10.6
	147.	42.5	49.6	104.	12.8
	235.	42.5	50.2	106.	11.2
	477.	42.2	51.2	123.	15.1
	2670.	40.0	50.4	127.	17.2

*No observed stiffener or local plate buckling

[a]Inelastic buckling stress coefficient

1 ksi = 6.9 mN/m^2 ; 1 kip-in. = 111 Nm

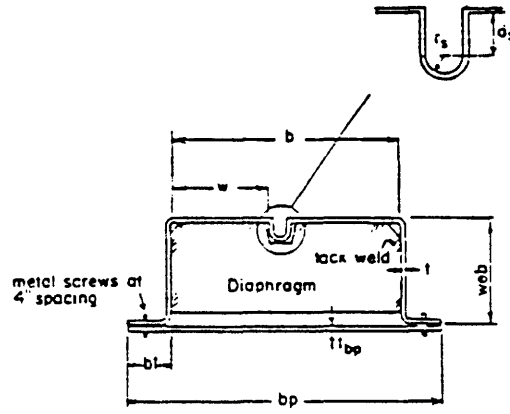

Cross-Sectional Geometry of Desmond's Test Specimens

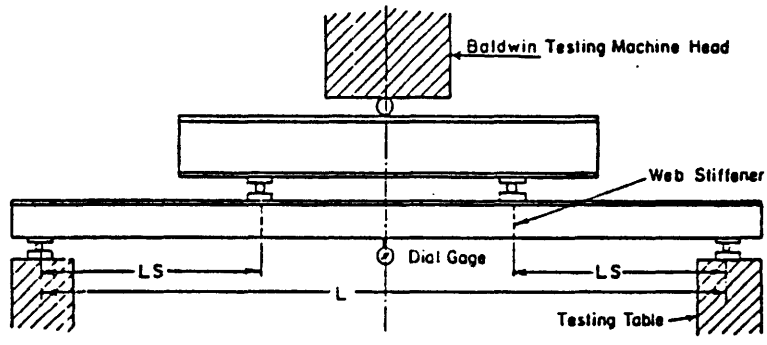

Desmond's Beam Test Set-up

Section dimensions and test results of skaloud's beam tests

w/t	I_s/t^4	M_{ult}^{test} (kip-in)	σ_y (ksi)	b (in)	h_v (in)	b_v (in)	t (in)
40.2	5.86	48.6	27.3	7.52	.236	.394	.0787
40.6	2.76	49.1	29.9	7.52	.181	.335	.0787
39.3	6.24	50.9	28.5	7.56	.224	.571	.0787
38.7	7.49	50.0	31.3	7.48	.240	.591	.0787
37.5	22.0	51.0	29.6	7.56	.343	.858	.0787
37.6	18.9	50.9	28.5	7.56	.323	.847	.0787
54.0	7.15	31.3	31.7	7.60	.185	.433	.0610
55.7	7.69	35.6	35.1	7.60	.185	.413	.0591
54.4	19.1	26.0	26.0	7.60	.248	.583	.0591
54.1	15.5	38.2	31.6	7.56	.224	.575	.0591
50.0	27.9	27.6	23.0	7.60	.291	.748	.0622
51.7	42.7	39.8	33.1	7.56	.315	.858	.0591
89.4	31.5	16.5	27.7	7.64	.193	.413	.0382
89.0	29.0	19.1	29.3	7.64	.193	.374	.0386
82.5	99.1	20.8	29.3	7.68	.307	.575	.0406
84.1	64.3	20.5	28.9	7.60	.248	.583	.0394
83.5	133.	20.8	24.5	7.72	.313	.748	.0394
83.5	167.	20.8	29.2	7.72	.347	.748	.0394

Table 12

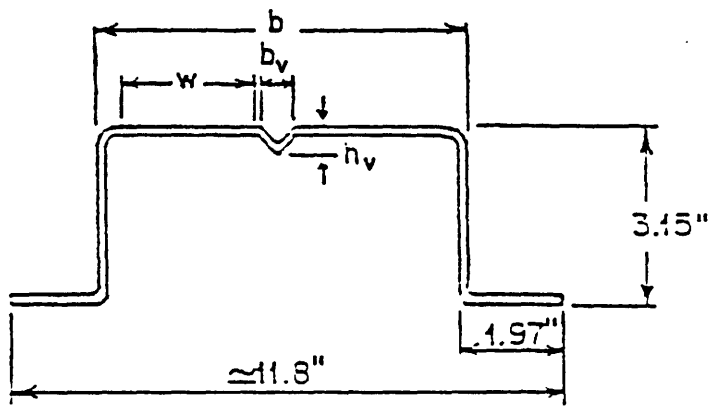

Skaloud's beam tests

CROSS-SECTIONAL GEOMETRY OF
SKALOUD'S BEAM SPECIMENS.

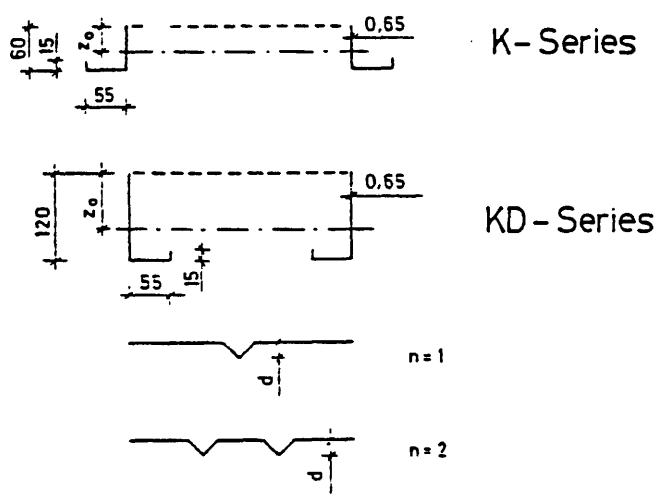

Basic Cross Section of
Konig's Specimens

Table 13. Konig's Test Tables

Specimen	t (mm)	σ_y (N/mm^2)	d (mm)	b_f (mm)	$\bar{M}_E$ (Nm)
K1	0.65	407	0.0	299	814
K2	0.64	398	0.0	299	814
K3	0.66	395	7.55	298	964
K4	0.66	395	7.55	298	994
K5	0.65	412	8.95	298	964
K6	0.65	409	8.95	299	934
K7	0.66	406	11.00	298	994
K8	0.66	417	10.70	298	1024
K9	0.67	403	17.30	297	1084
KD1	0.67	385	8.1	299	2457
KD2	0.68	390	17.24	299	2524

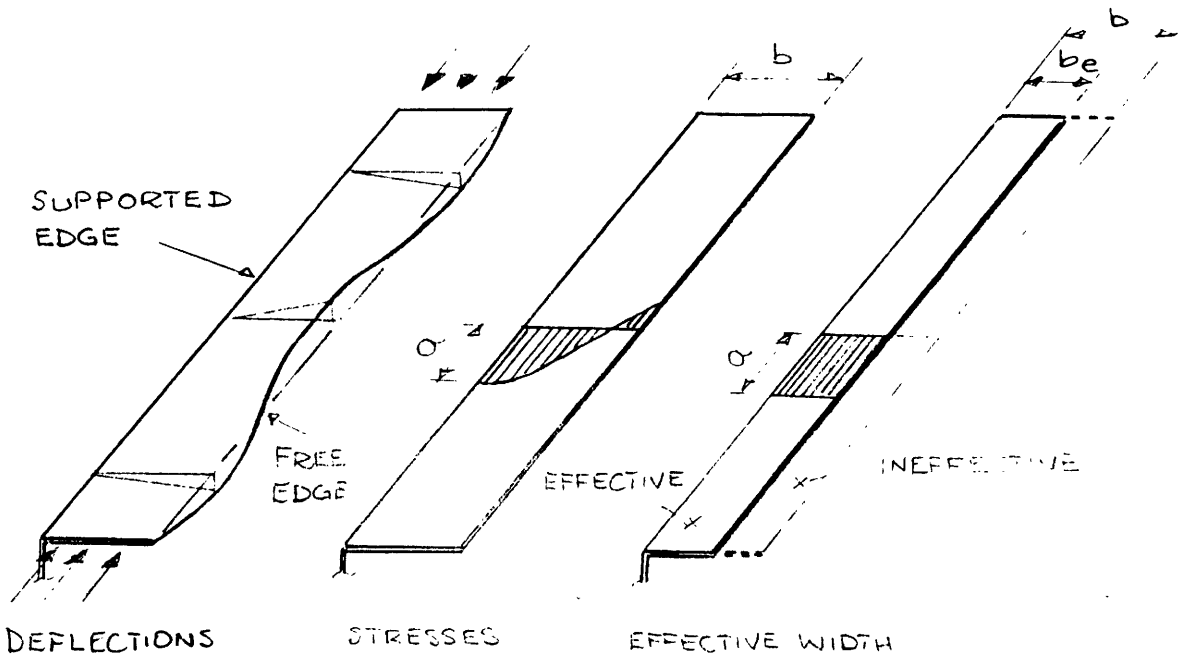

FIGURE 1. UNSTIFFENED ELEMENTS IN COMPRESSION

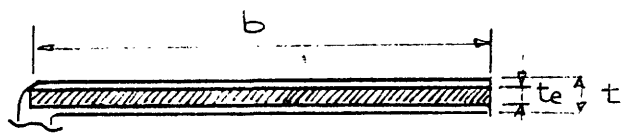

FIGURE 2. EFFECTIVE THICKNESS

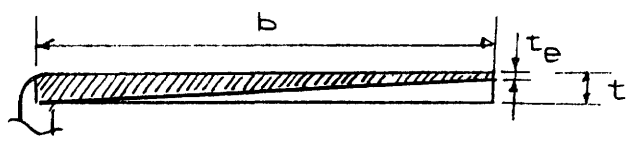

FIGURE 3. LINEARLY VARYING EFFECTIVE THICKNESS

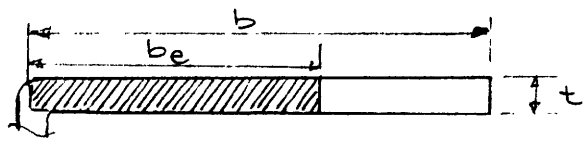

FIGURE 4 EFFECTIVE WIDTH

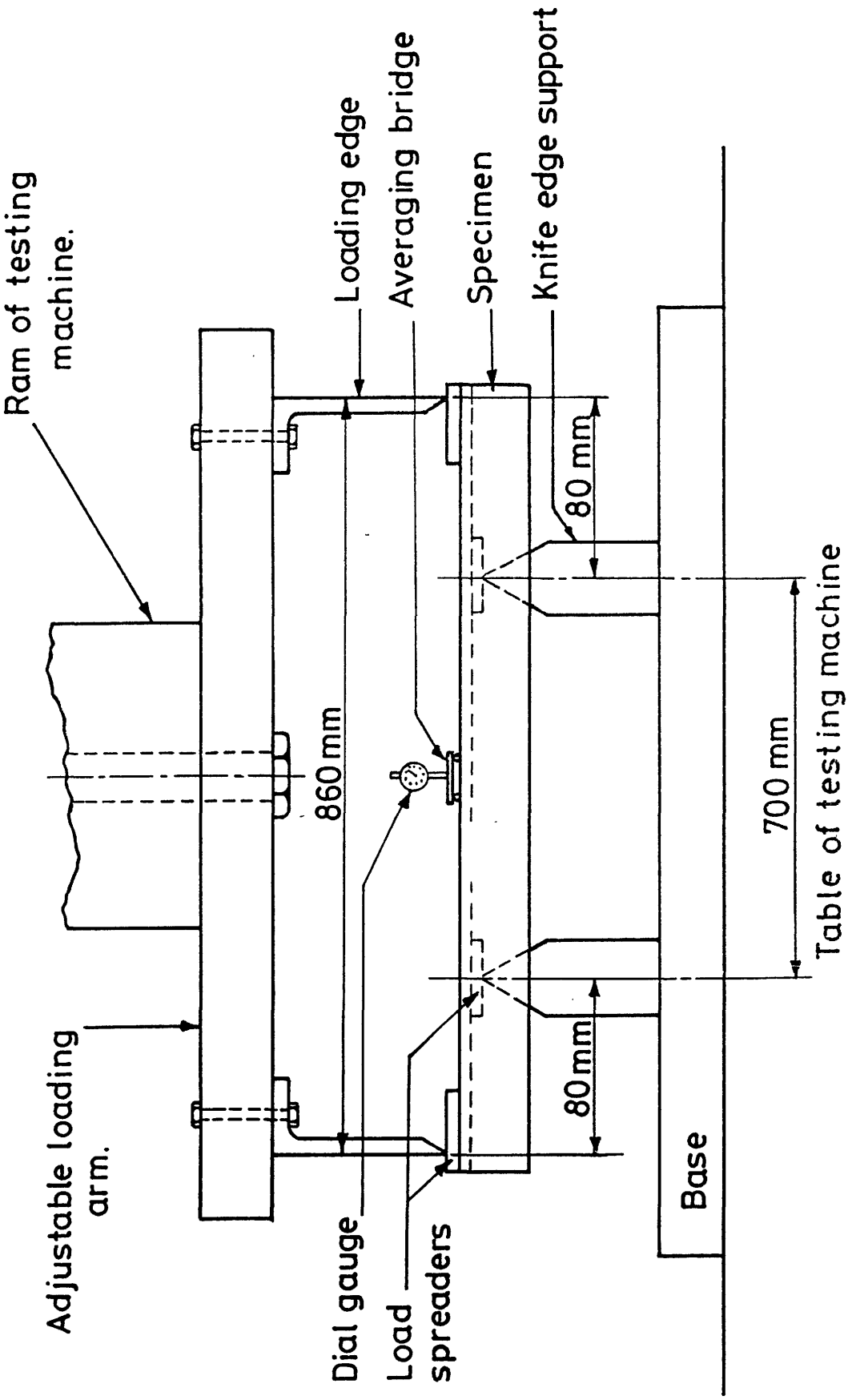

FIGURE 5. SET-UP FOR BENDING TESTS ON MEMBERS WITH UNSTIFFENED ELEMENTS

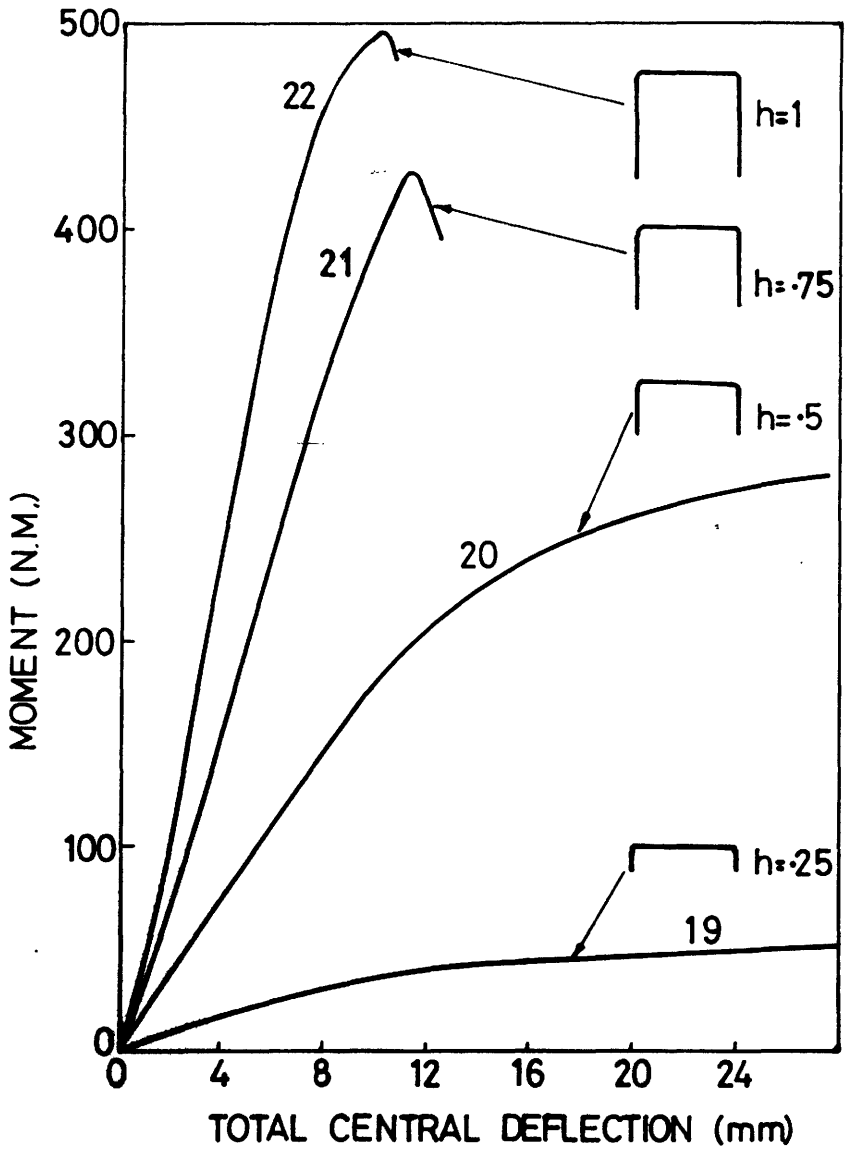

FIGURE 6. MOMENT-DEFLECTION CURVES FOR CHANNELS OF 1.56mm MATERIAL

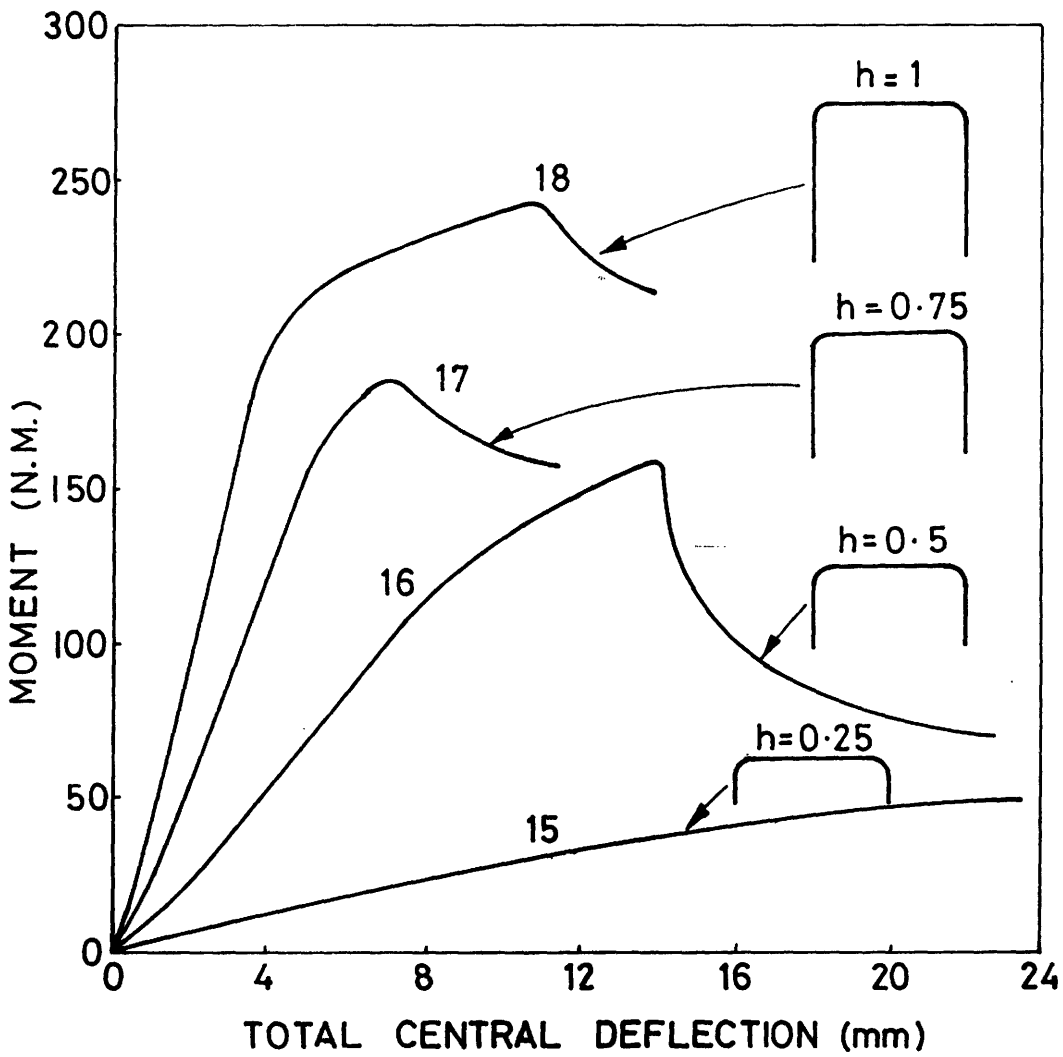

FIGURE 7. MOMENT-DEFLECTION CURVES FOR CHANNELS OF 1.17mm MATERIAL

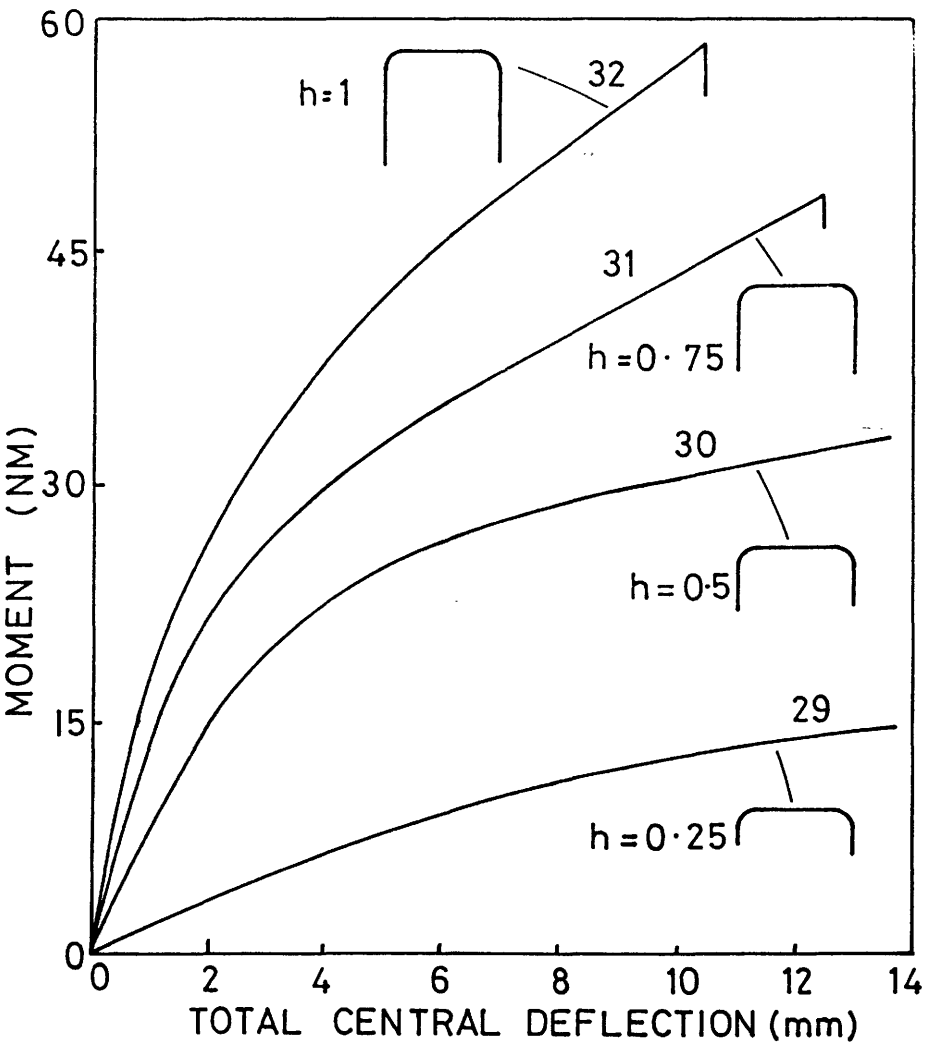

FIGURE 8. MOMENT-DEFLECTION CURVES FOR CHANNELS OF 0.55mm MATERIAL

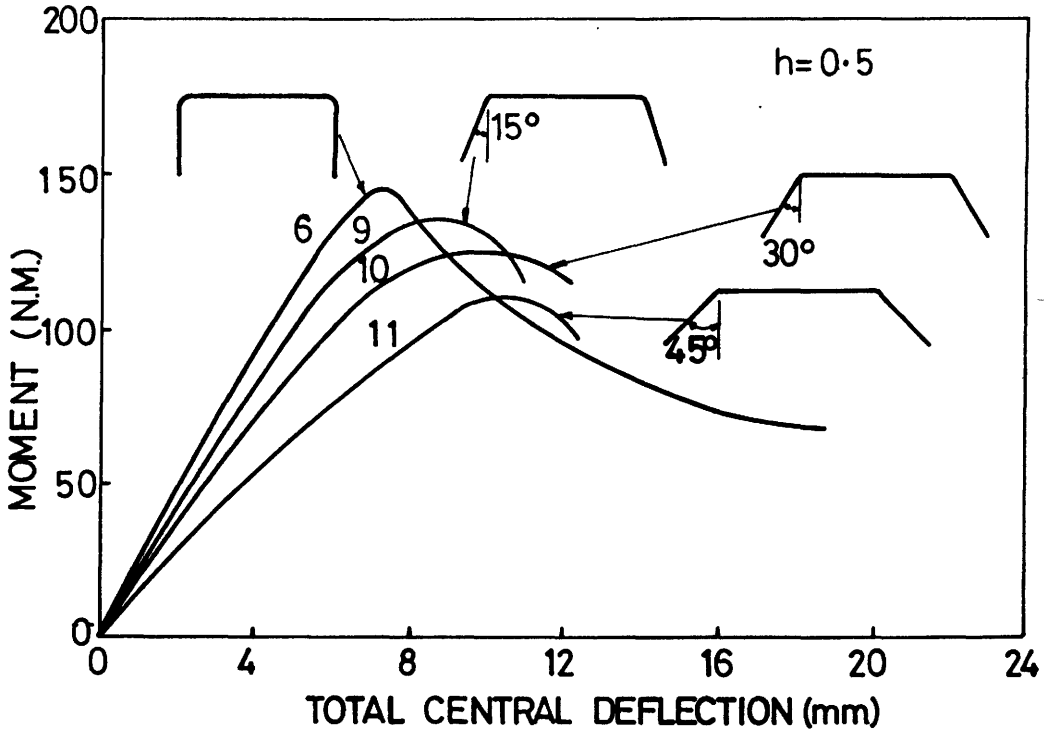

FIGURE 9. EFFECTS OF FLANGE ANGLE ON CHANNEL BEHAVIOUR

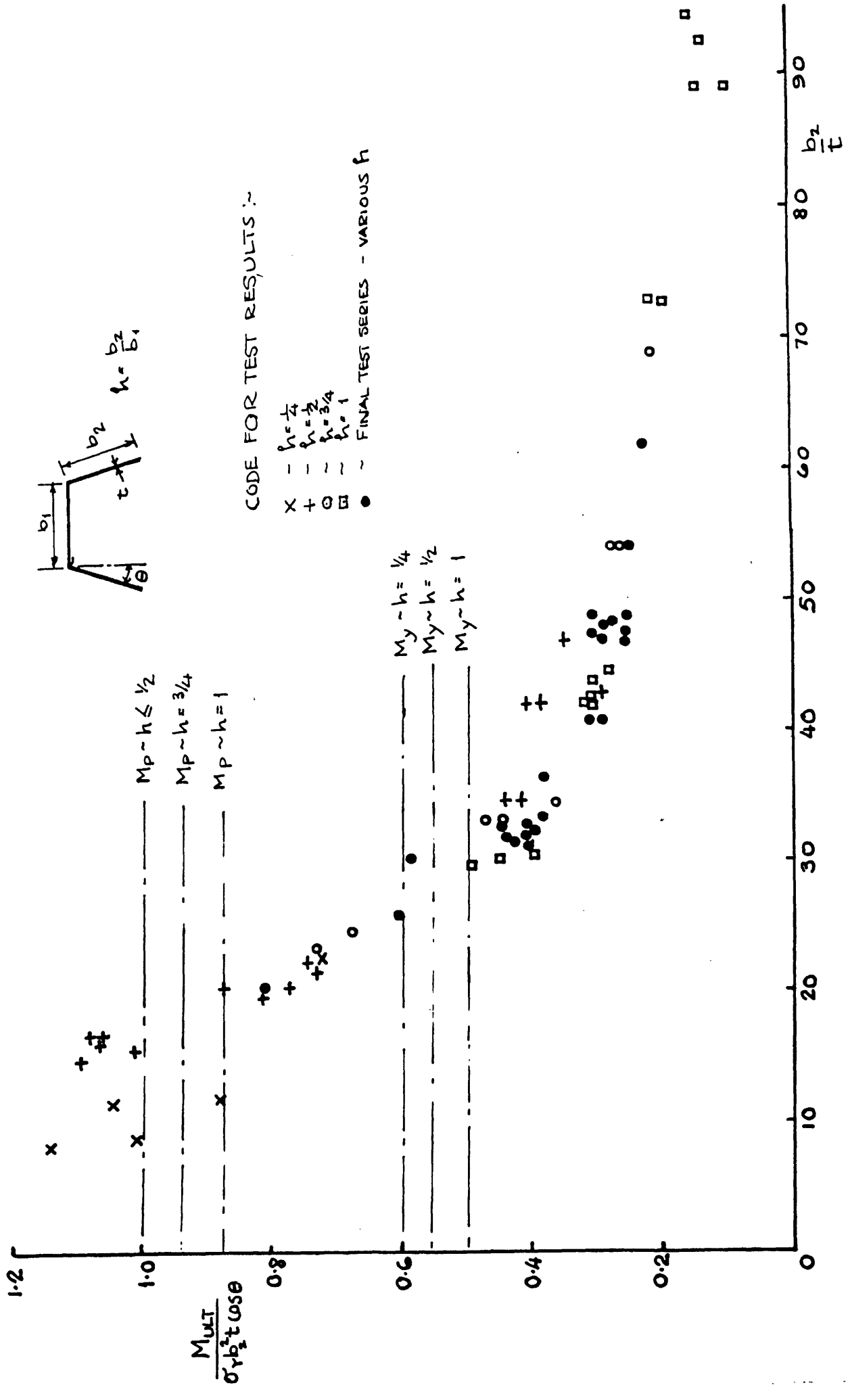

FIGURE 10. FAILURE MOMENTS FOR PLAIN CHANNELS

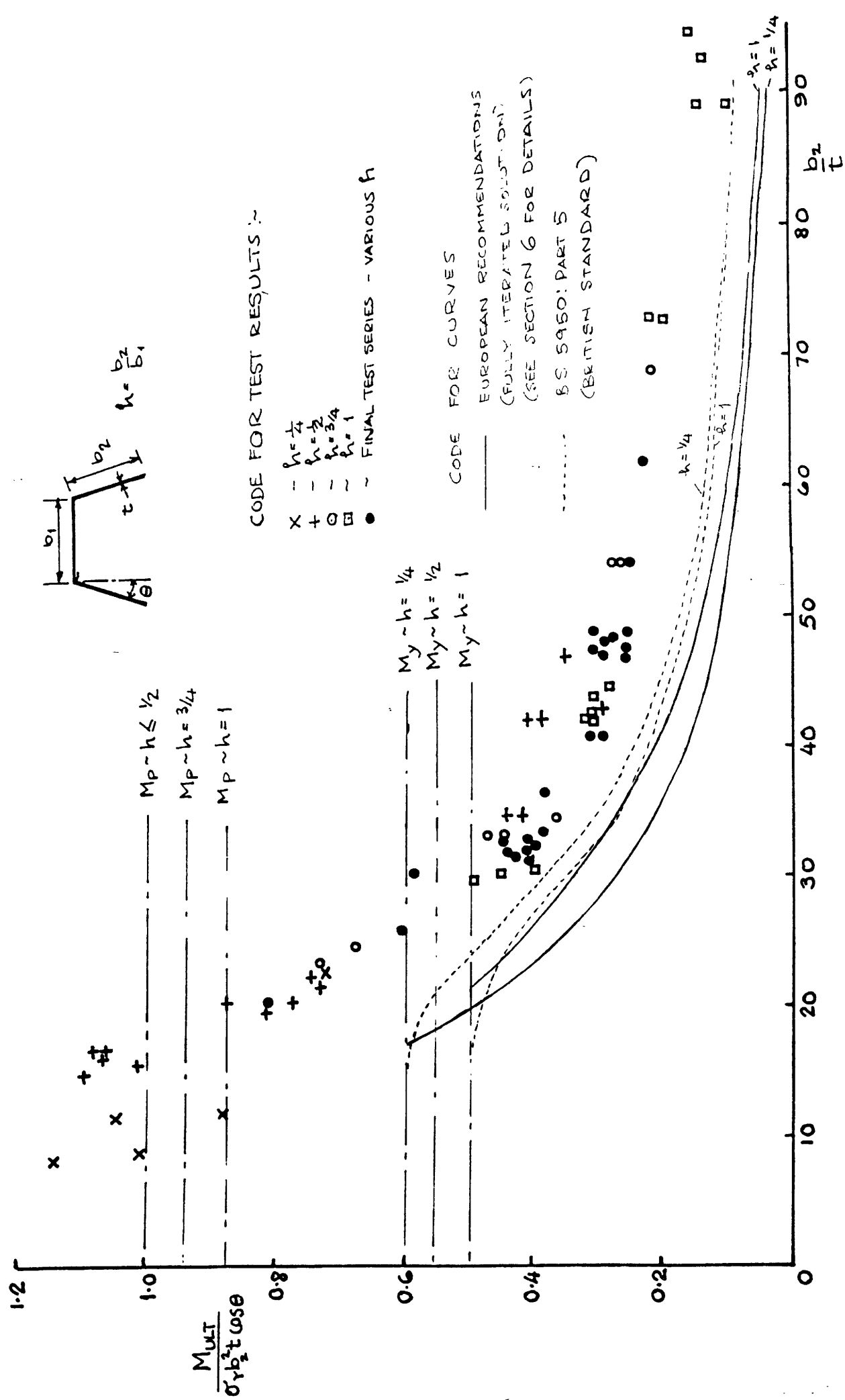

FIGURE 11. COMPARISON WITH EUROPEAN RECOMMENDATIONS AND BRITISH STANDARD

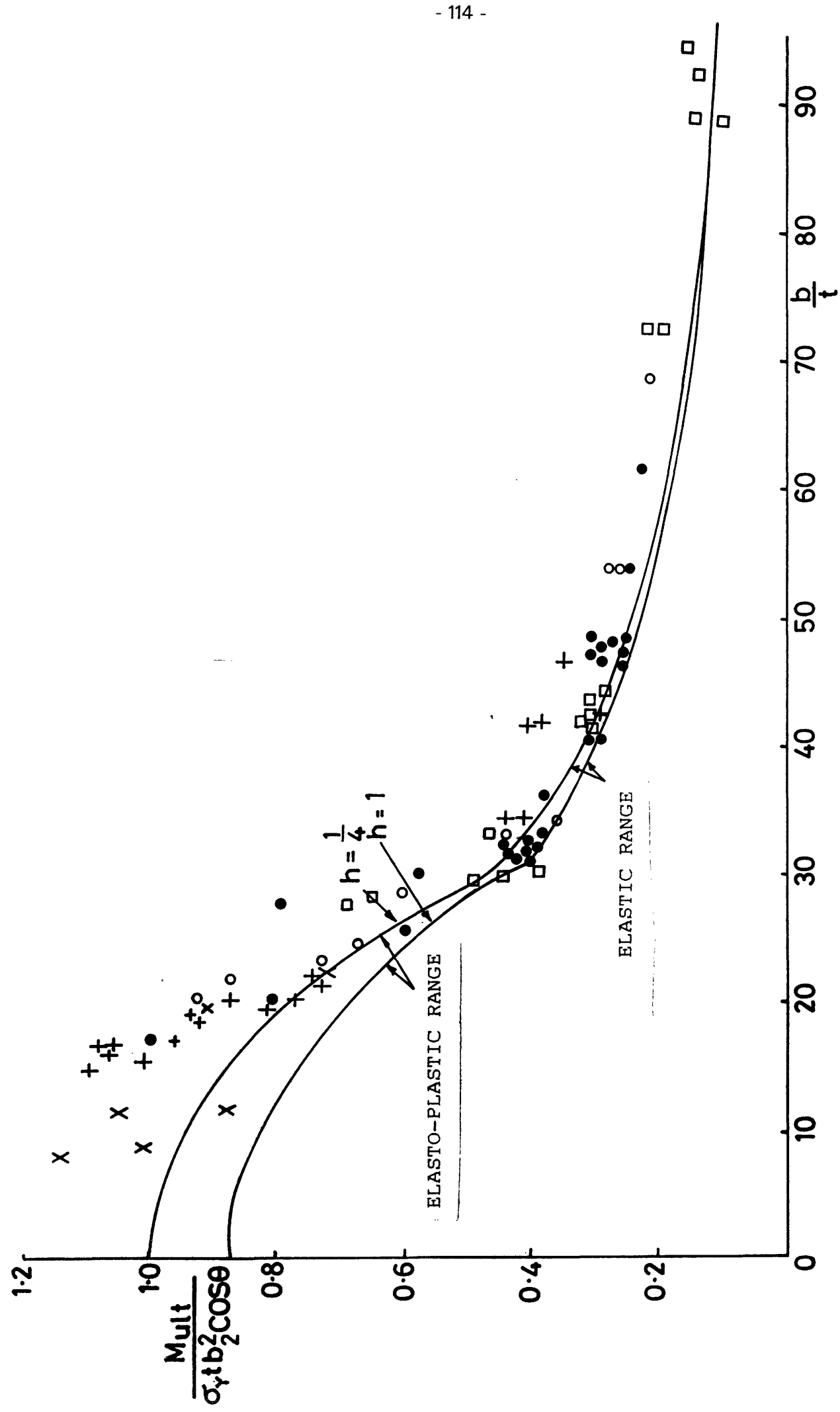

FIGURE 12. COMPARISON WITH PROPOSED DESIGN RULES

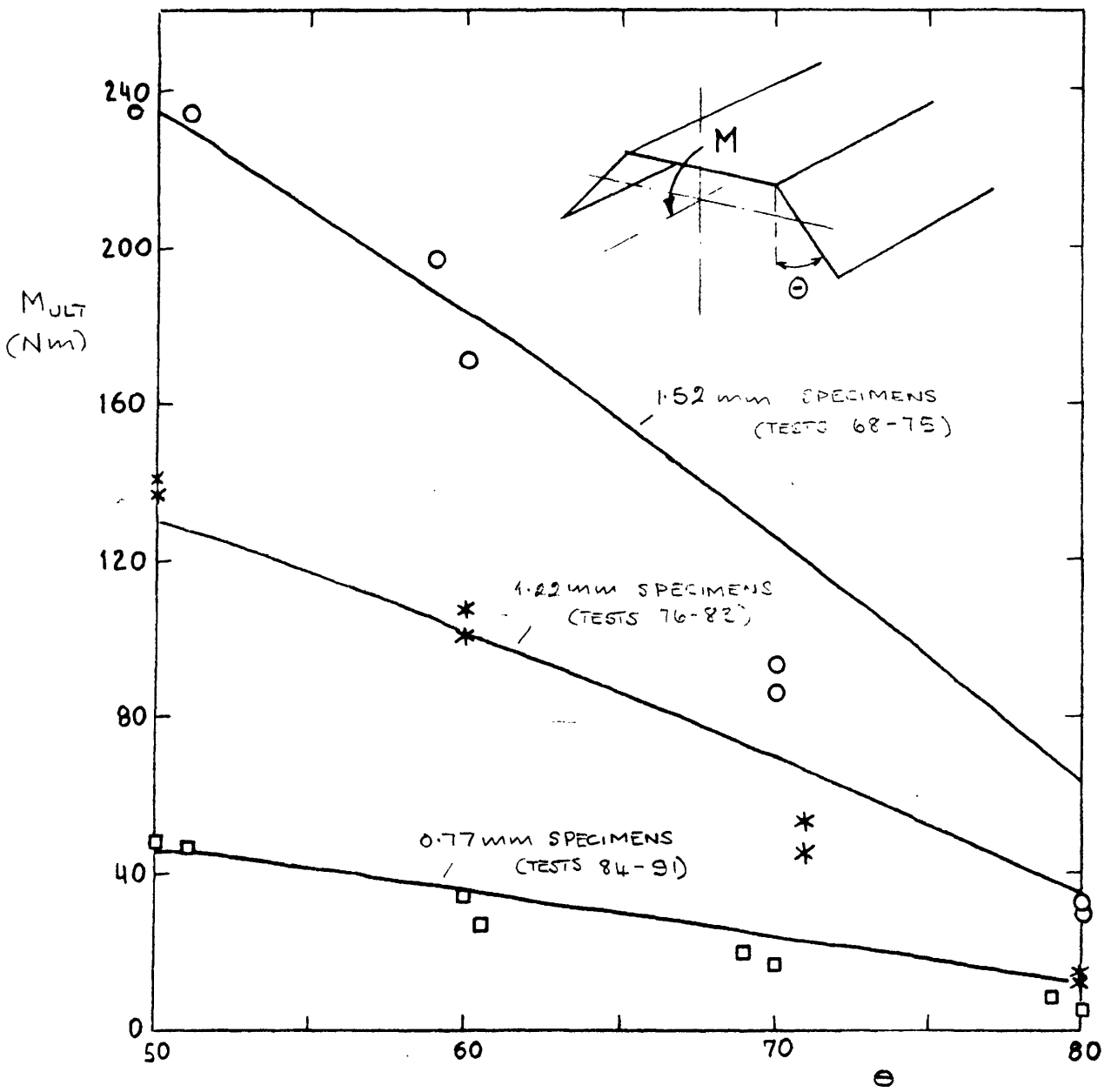

FIGURE 13. FAILURE MOMENTS FOR CHANNELS WITH LARGE CORNER ANGLES

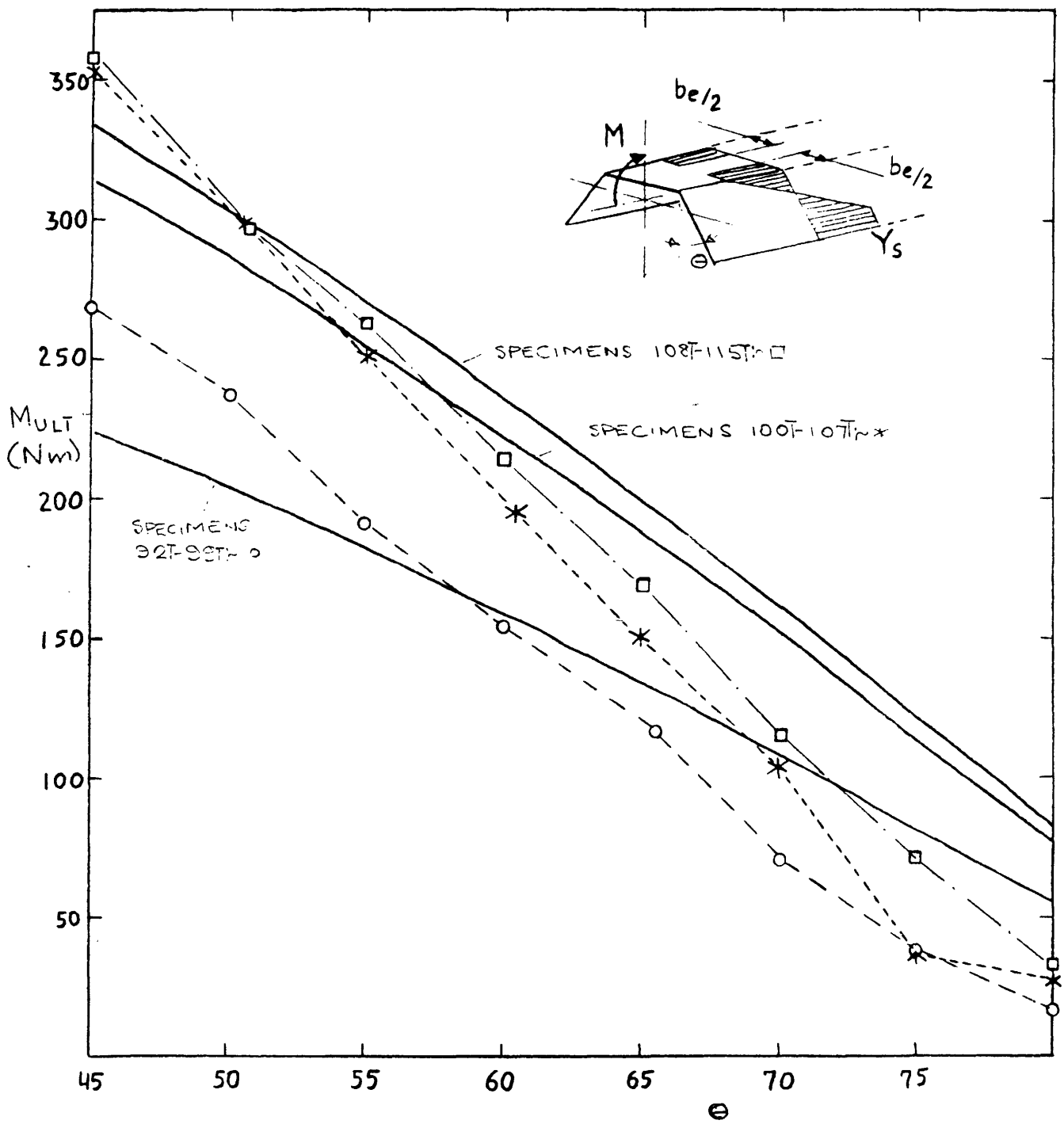

FIGURE 14. FALURE MOMENTS FOR CHANNELS BENT TO CAUSE WEB COMPRESSION

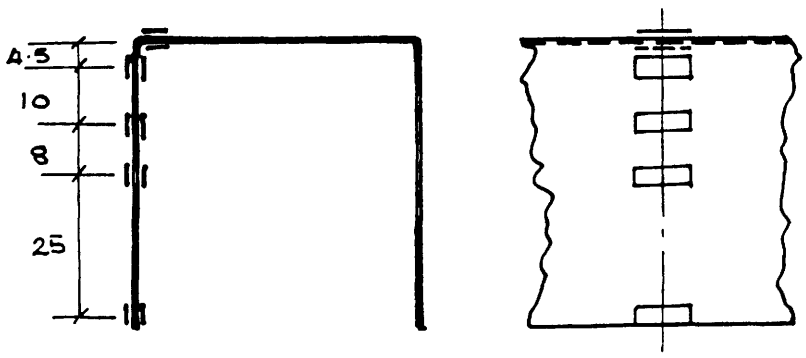

FIGURE 15 TYPICAL STRAIN GAUGE LAYOUT

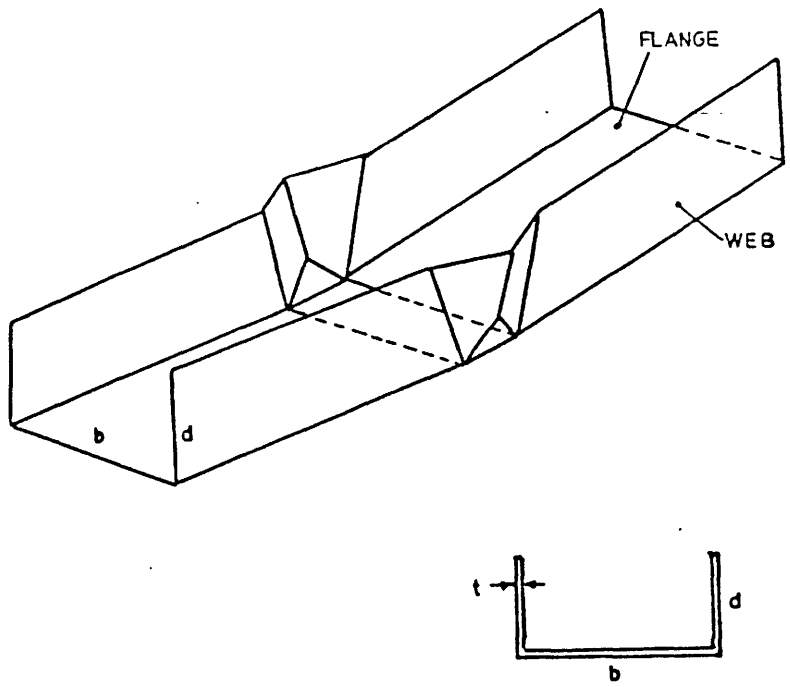

Plain C-Channel

FIGURE 18. PLASTIC FAILURE MECHANISM

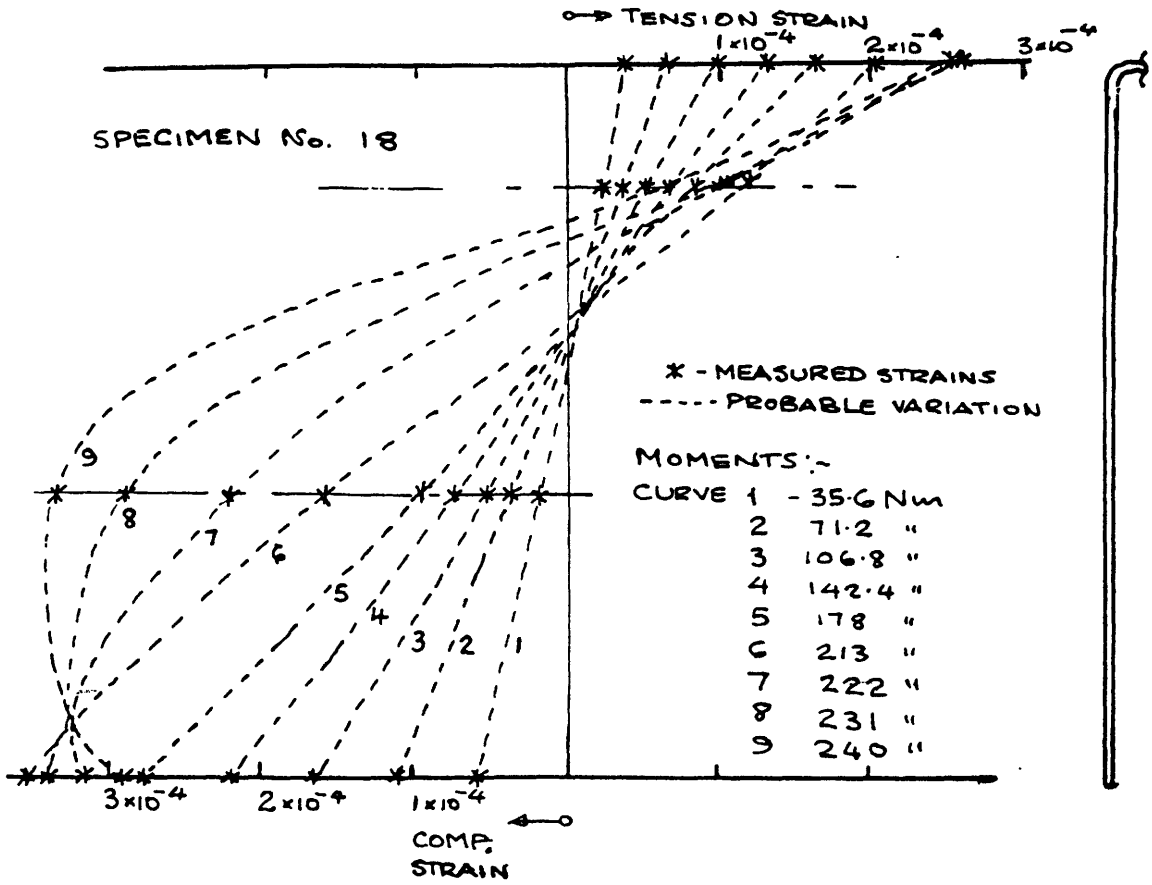

FIGURE 16. STRAIN DISTIBUTIONS - SPECIMEN No. 18.

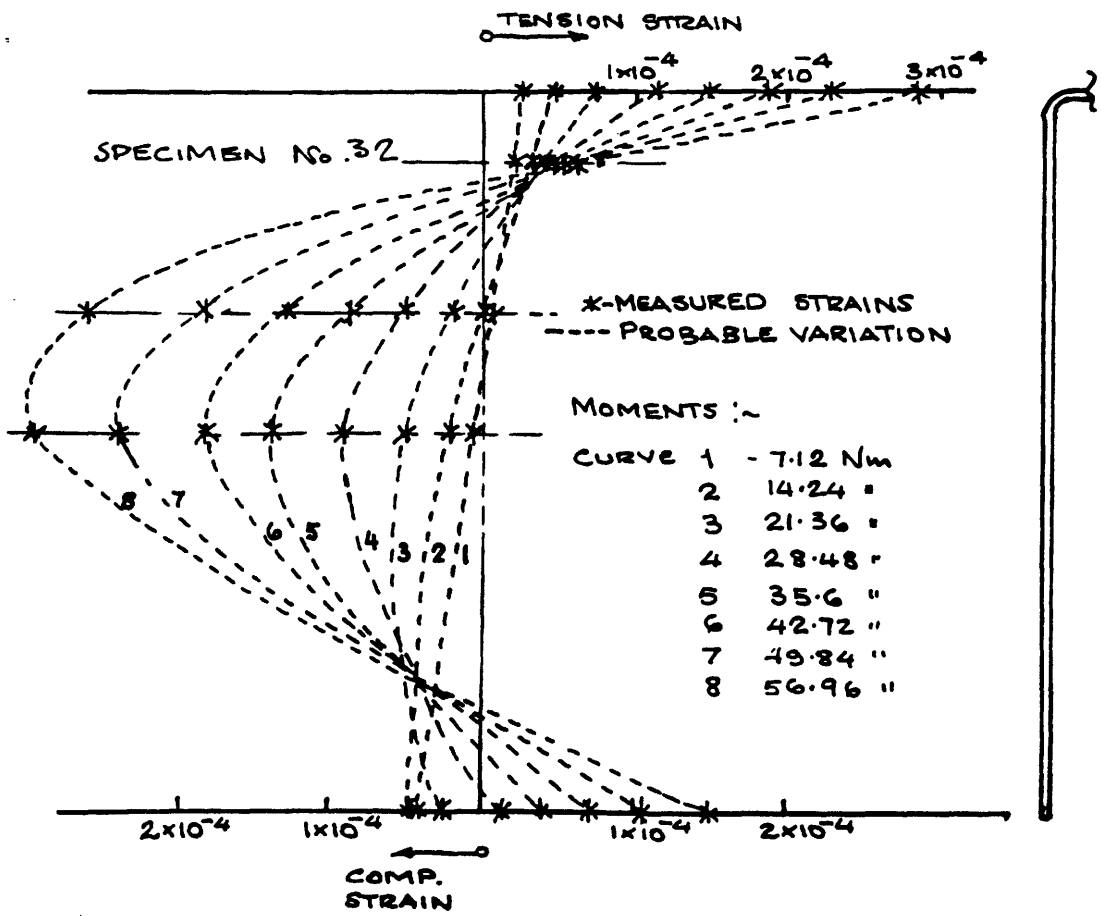

FIGURE 17. STRAIN DISTRIBUTIONS - SPECIMEN No. 32

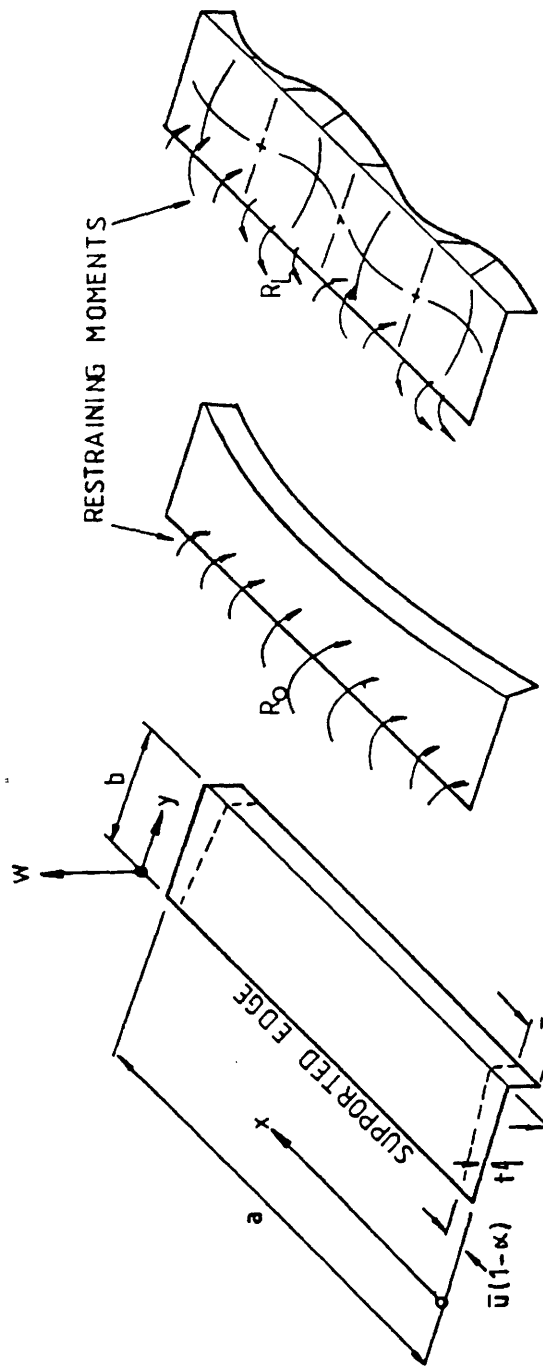

NOMENCLATURE (a)

TORSIONAL MODE (b)

LOCAL MODE (c)

FIGURE 19

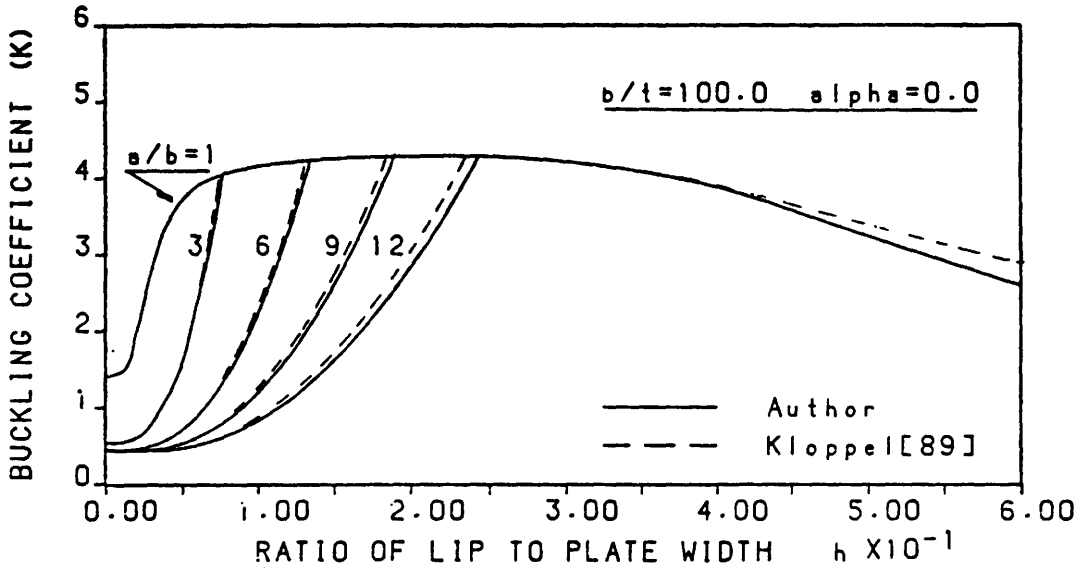

FIGURE 20

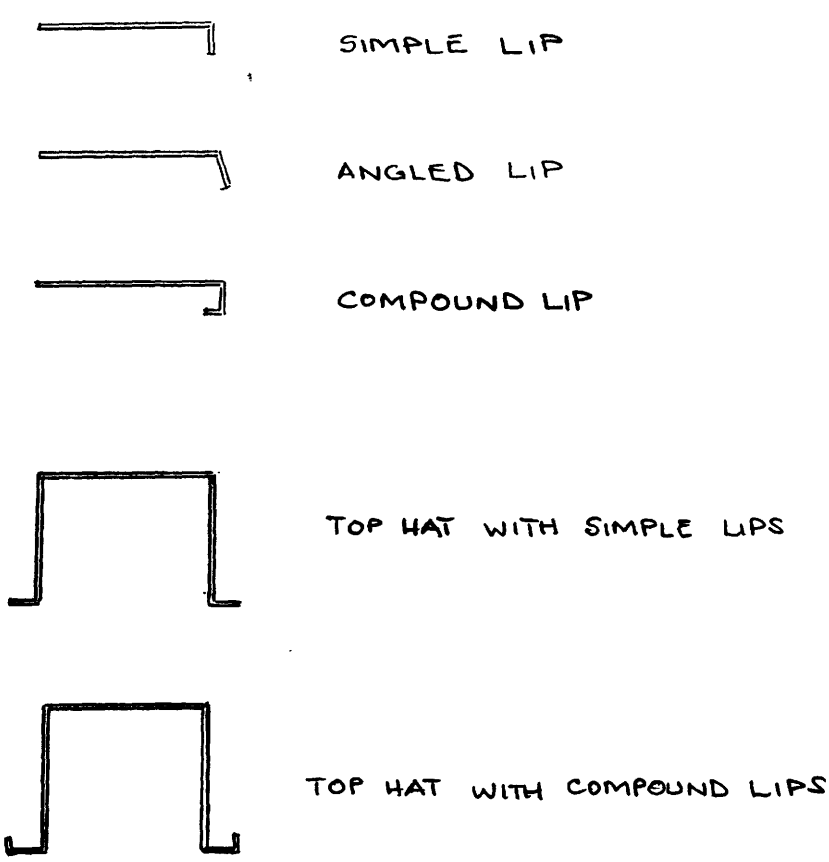

FIGURE 21. TYPES OF SPECIMEN TESTED

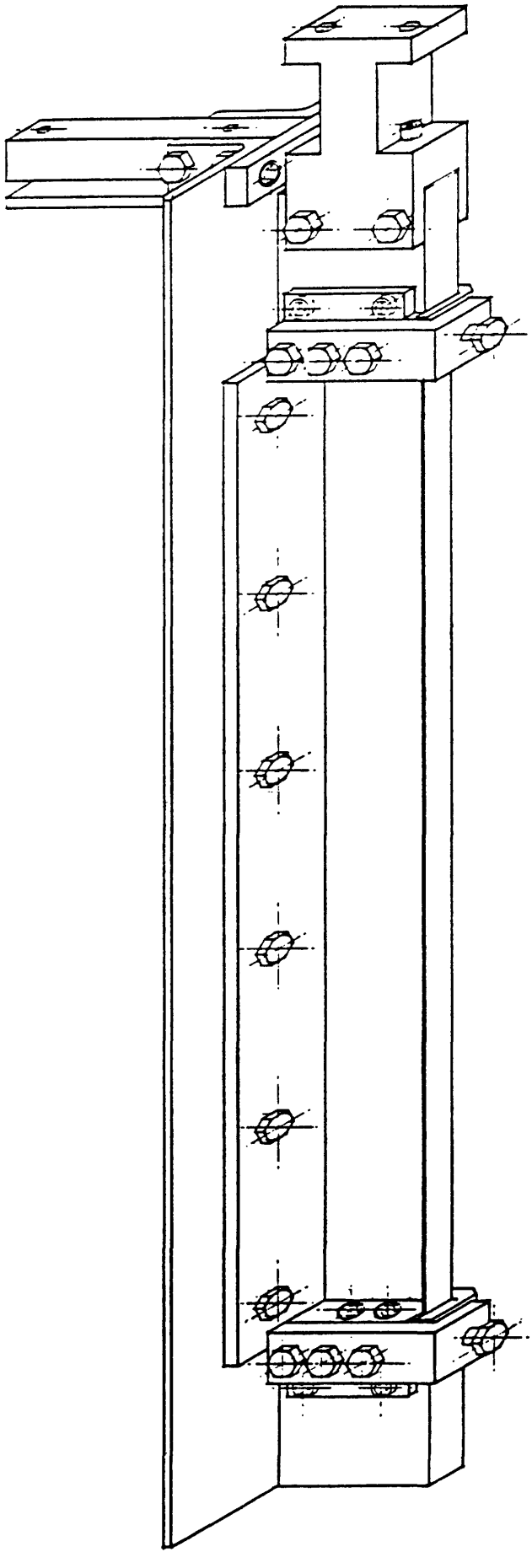

LCR
(L-COMPRESSION RIG)

FIGURE 22

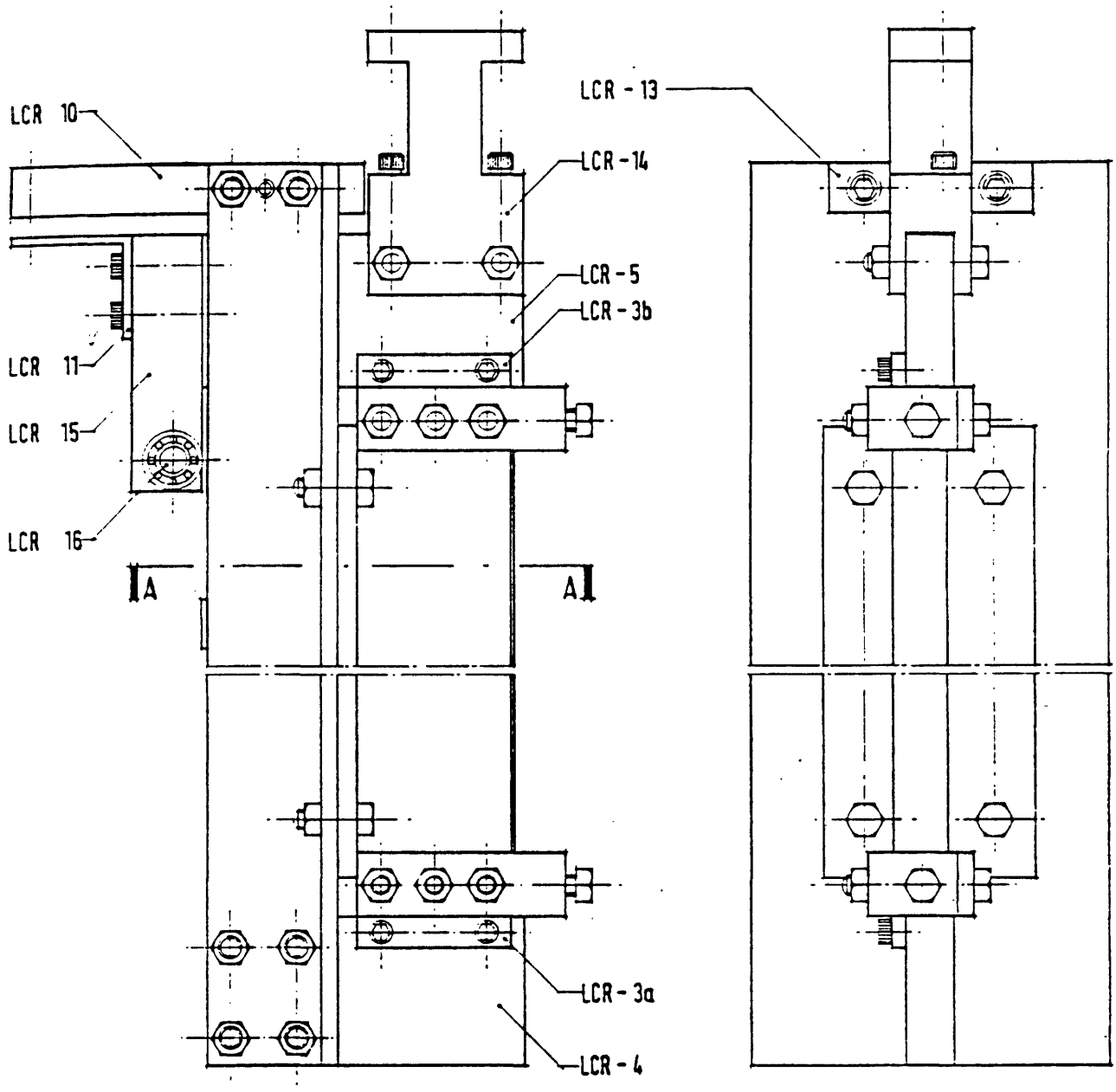

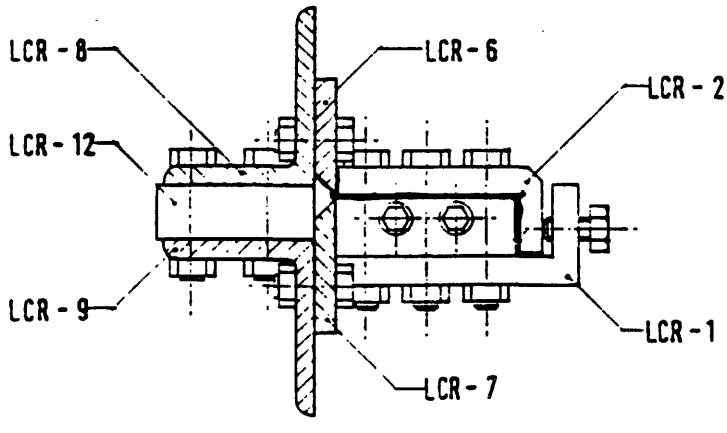

SECTION A - A

LCR
(L-COMPRESSION RIG)

1ST ANGLE PROJECTION

ALL DIMENSIONS IN THE DETAILED DRAWINGS THAT FOLLOW ARE IN MILLIMETRES UNLESS OTHERWISE STATED.

ALL MATERIALS ARE MADE OF MILD STEEL UNLESS OTHERWISE STATED.

FIGURE 23

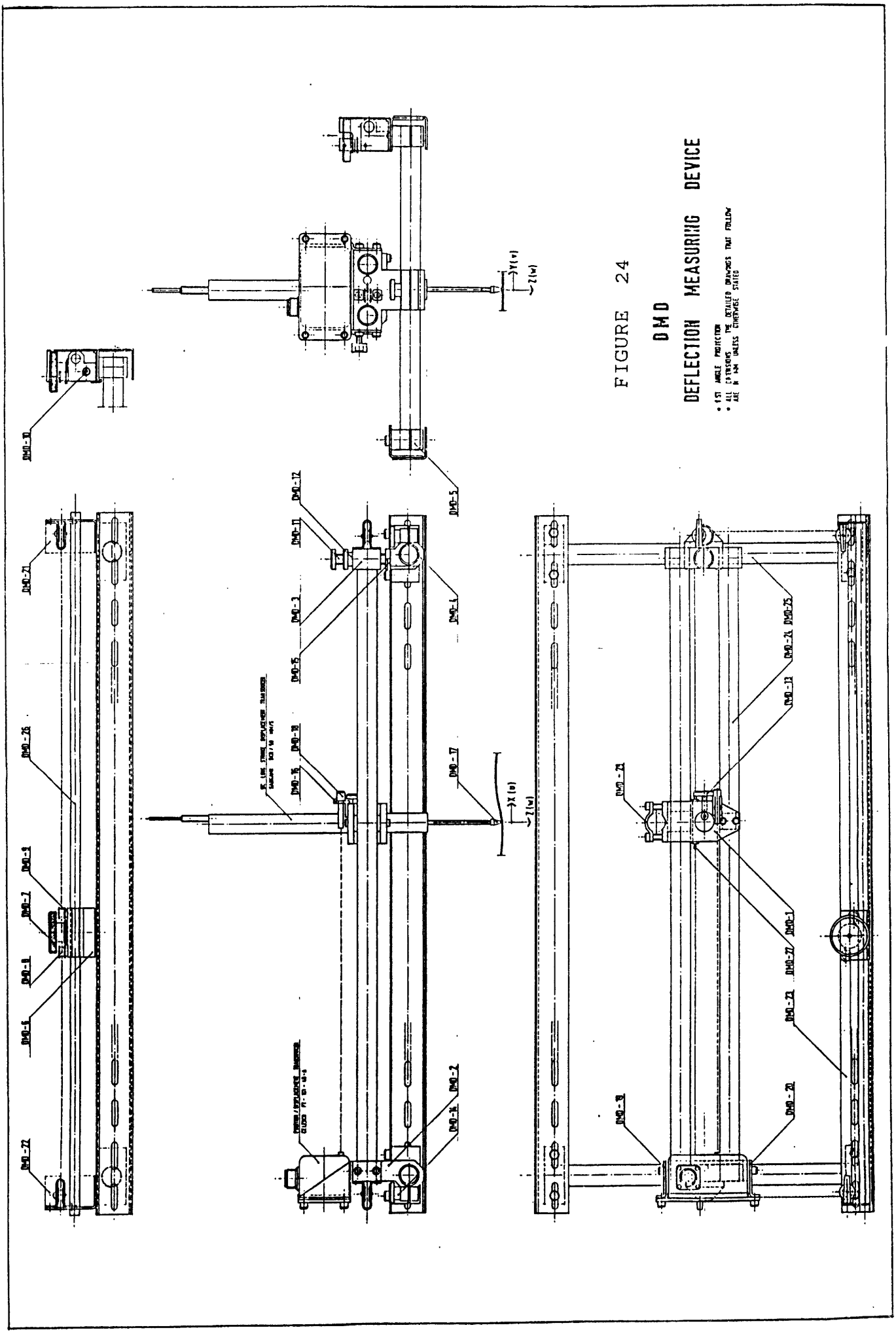

FIGURE 24

DMD

DEFLECTION MEASURING DEVICE

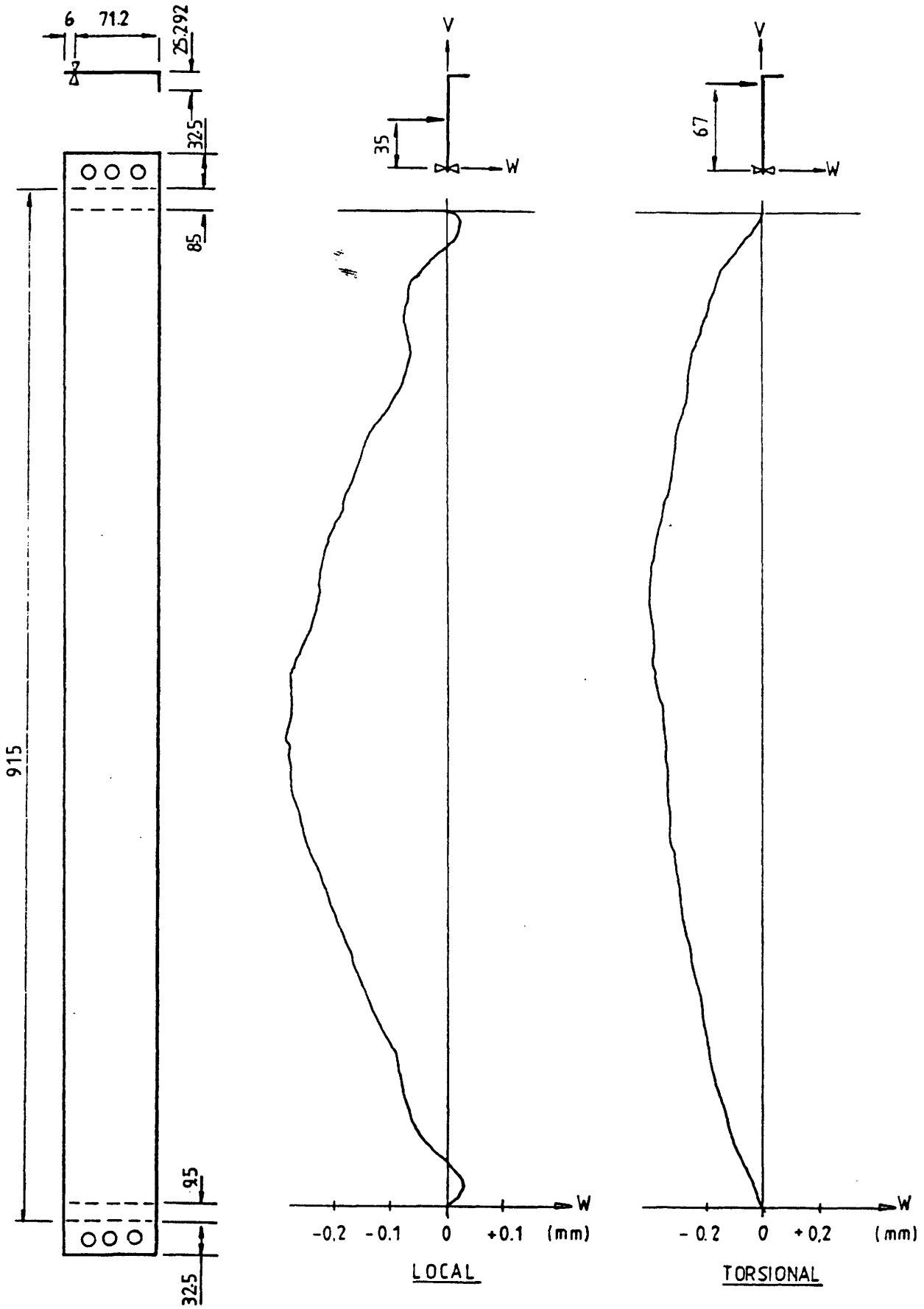

SPECIMEN No.- SGT/0.8/1.0 (Strain gauged specimen) INITIAL IMPERFECTIONS

ALL DIMENSIONS IN M.M

FIGURE 25

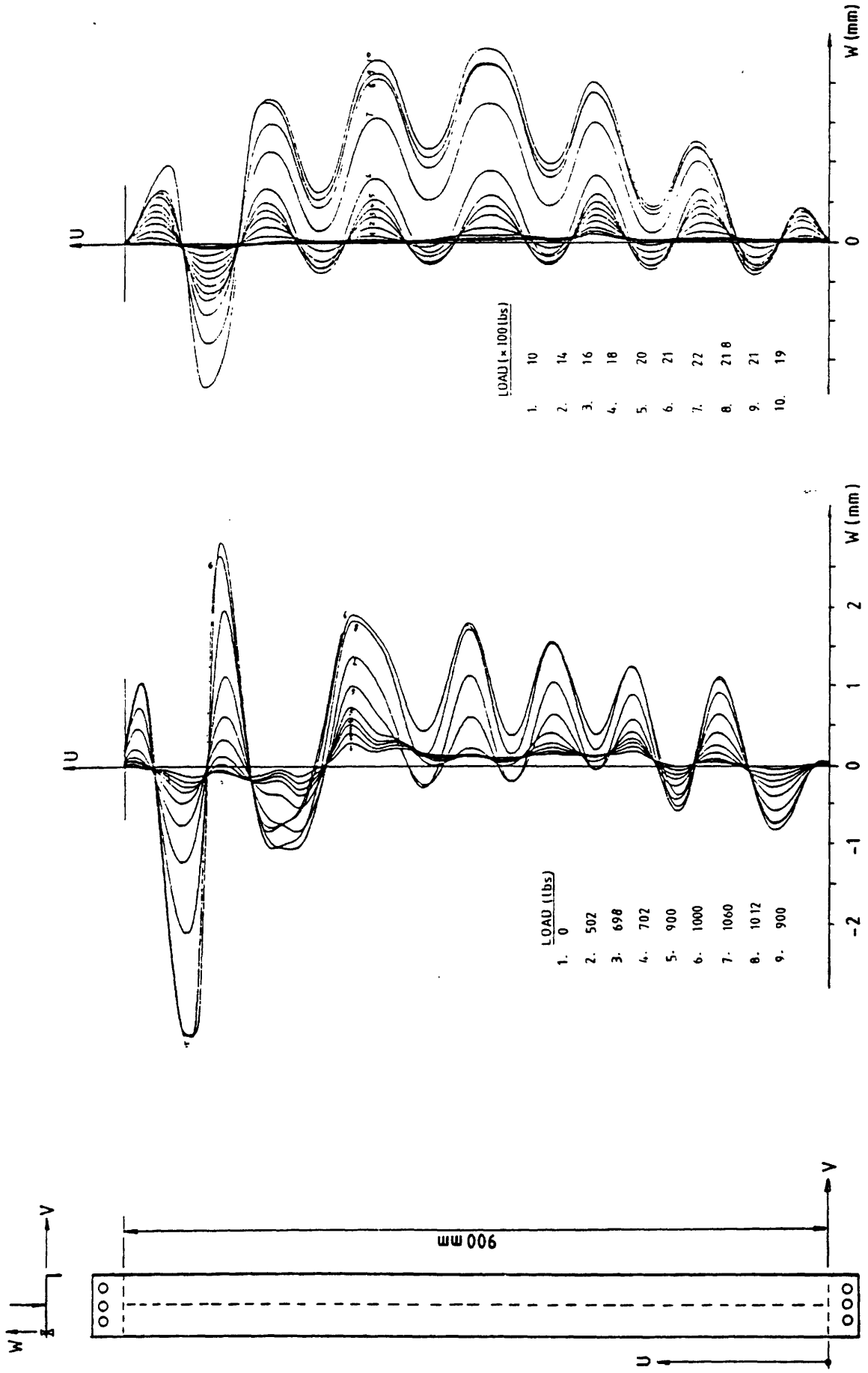
W (mm)
U
LOAD (× 100 lbs)
1. 10
2. 14
3. 16
4. 18
5. 20
6. 21
7. 22
8. 21 8
9. 21
10. 19
Specimen No:- 13/0.752/1
W (mm)
U
LOAD (lbs)
1. 0
2. 502
3. 698
4. 702
5. 900
6. 1000
7. 1060
8. 1012
9. 900
Specimen No:- 13/0.644/1
V
900 mm
U
W
V

FIGURE 26

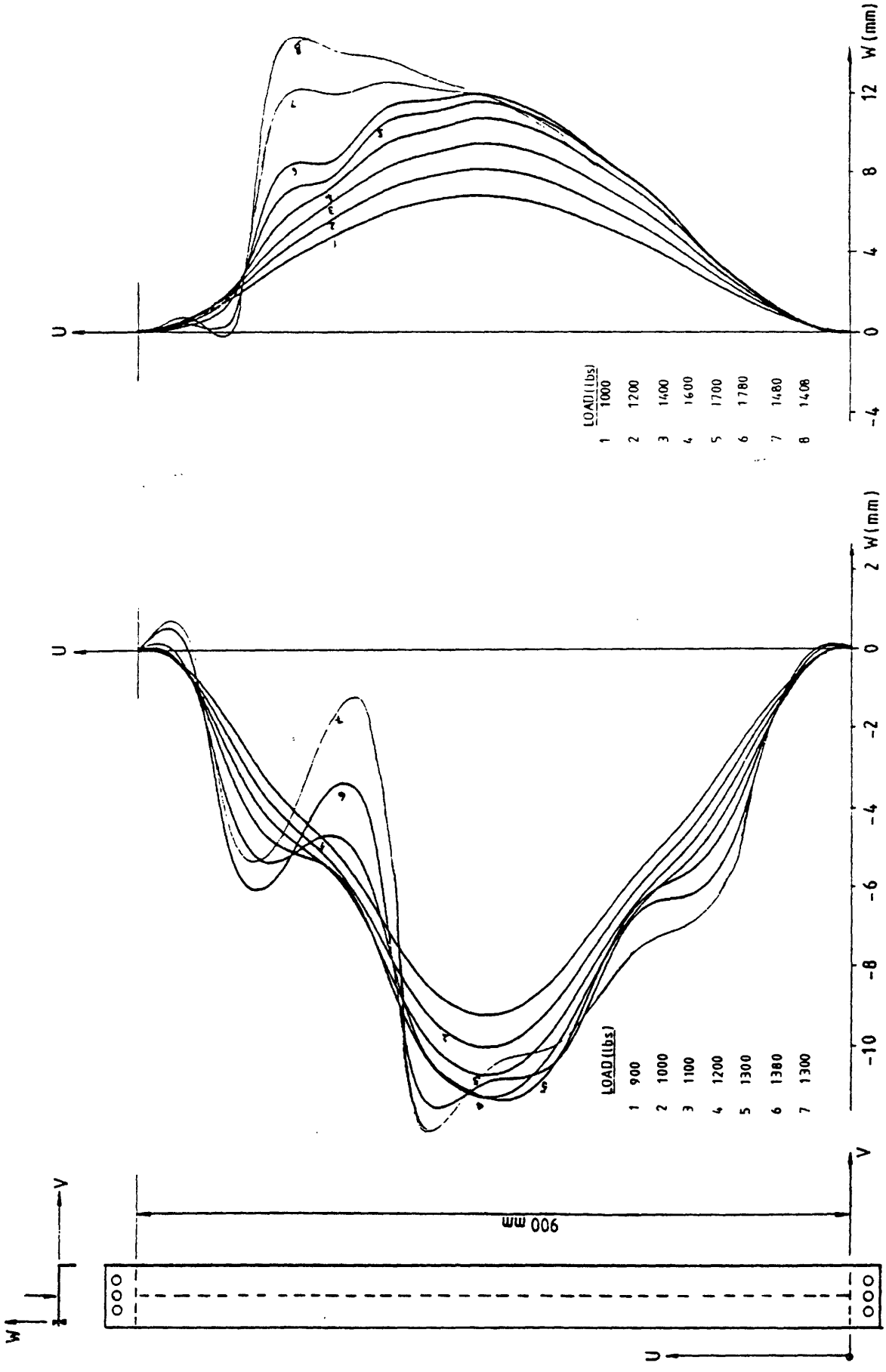
W
V
U
900 mm
LOAD (lbs)
1 900
2 1000
3 1100
4 1200
5 1300
6 1380
7 1300
2 W (mm)
0
-2
-4
-6
-8
-10
Specimen No:- 1/0.963/0
LOAD (lbs)
1000
1 1000
2 1200
3 1400
4 1600
5 1700
6 1780
7 1480
8 1408
12 W (mm)
8
4
0
-4
Specimen No:-5/0.956/0.25

FIGURE 27

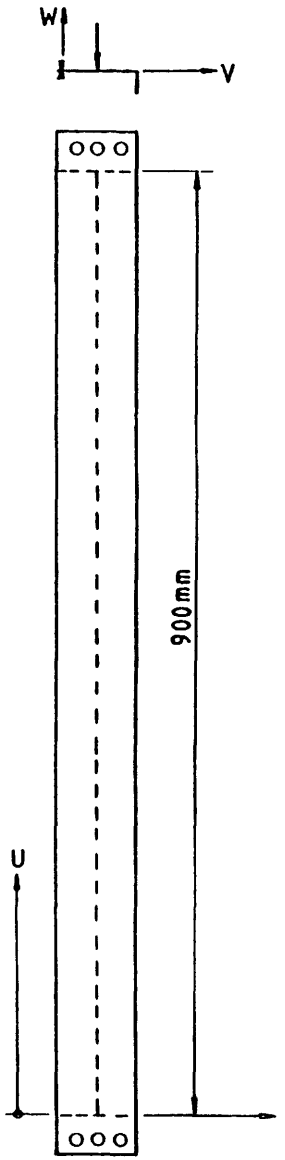

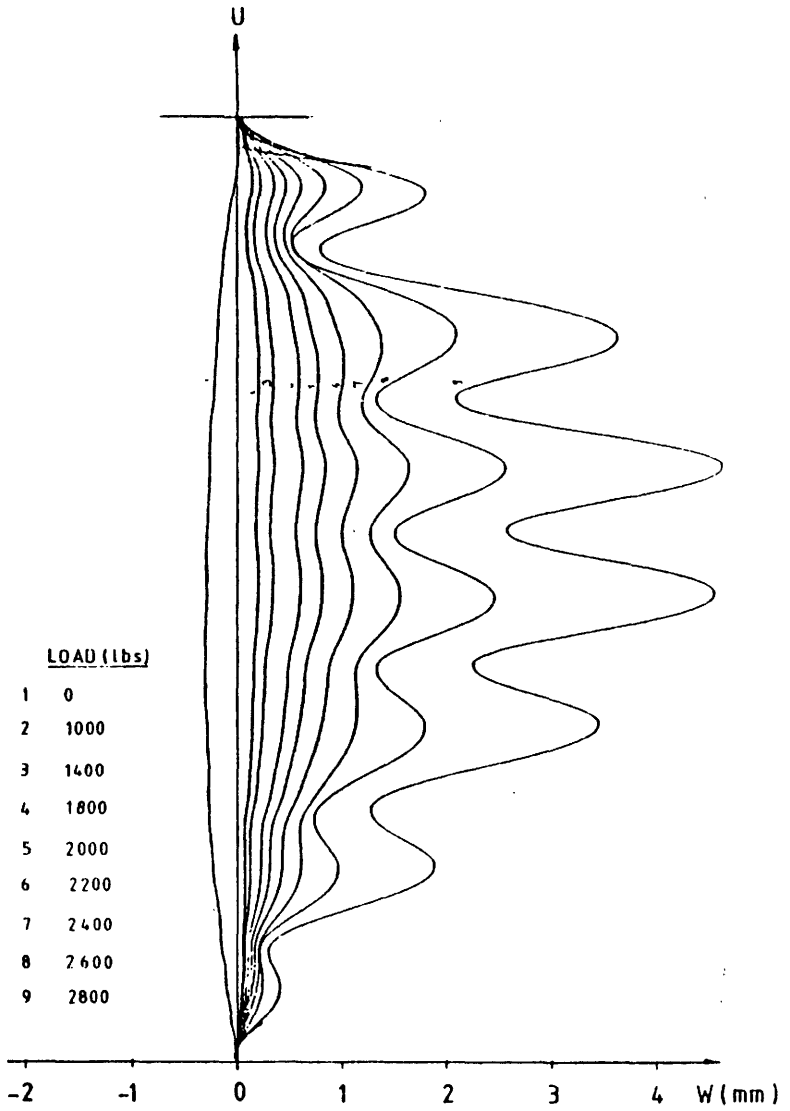

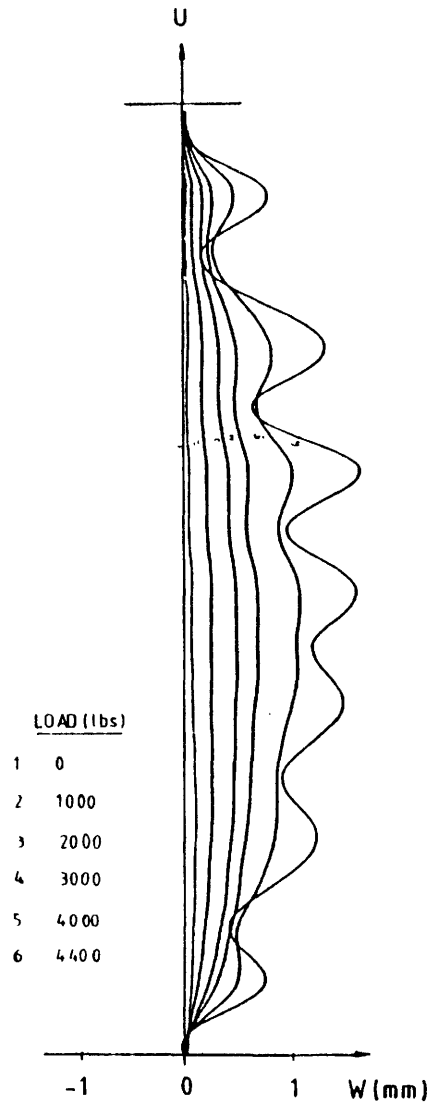

FIGURE 28

Specimen No.:- 11/0.957/0.75

Specimen No.:- 9/1.172/1

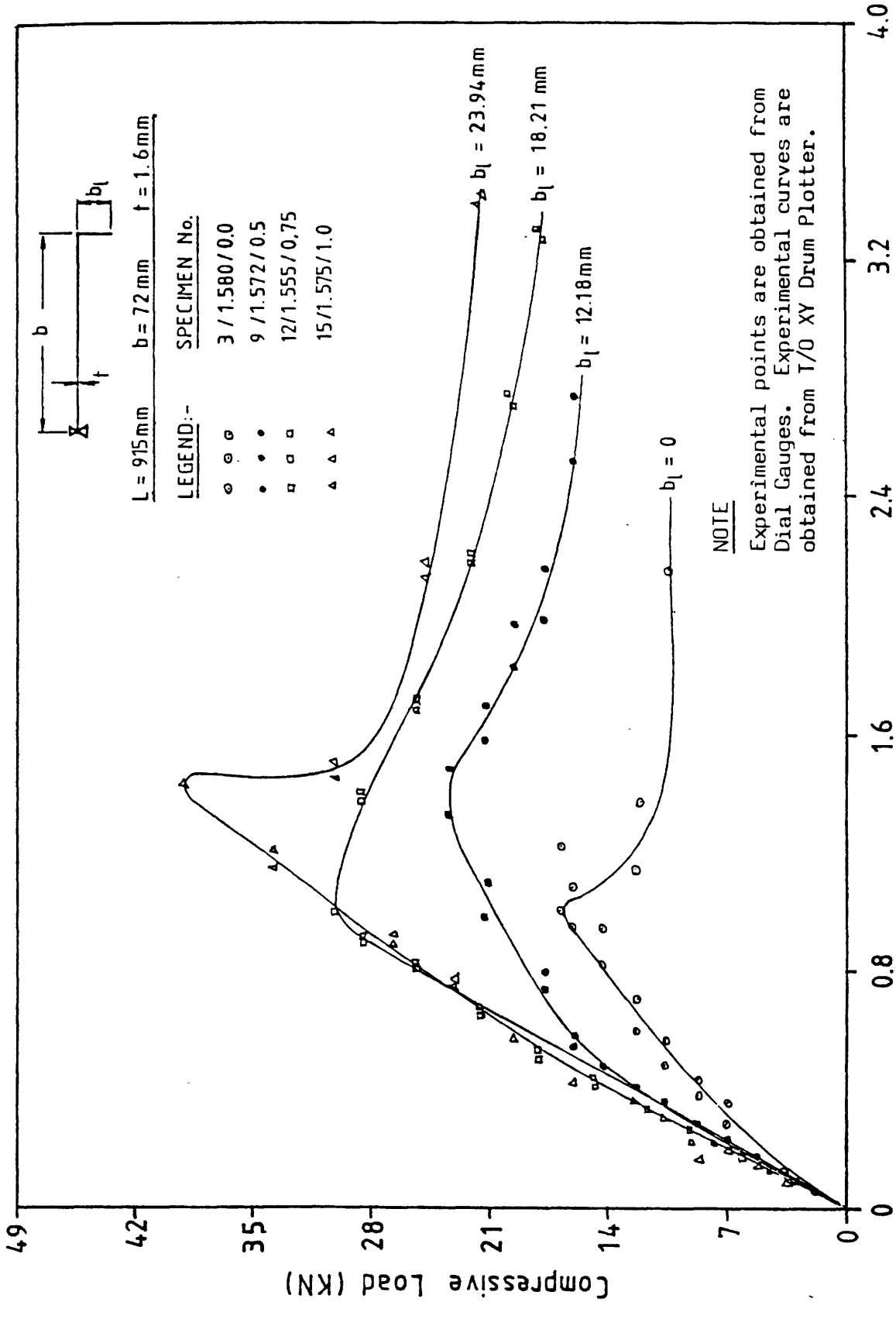
L = 915mm
b = 72mm
t = 1.6mm
LEGEND:-
SPECIMEN No.
3 / 1.580 / 0.0
9 / 1.572 / 0.5
12/1.555 / 0,75
15/1.575/1.0
b
t
b_l
b_l = 23.94mm
b_l = 18.21 mm
b_l = 12.18mm
b_l = 0
NOTE
Experimental points are obtained from Dial Gauges. Experimental curves are obtained from T/O XY Drum Plotter.
Compressive Load (KN)
Applied End-Displacement (mm)
0
7
14
21
28
35
42
49
0
0.8
1.6
2.4
3.2
4.0

FIGURE 29

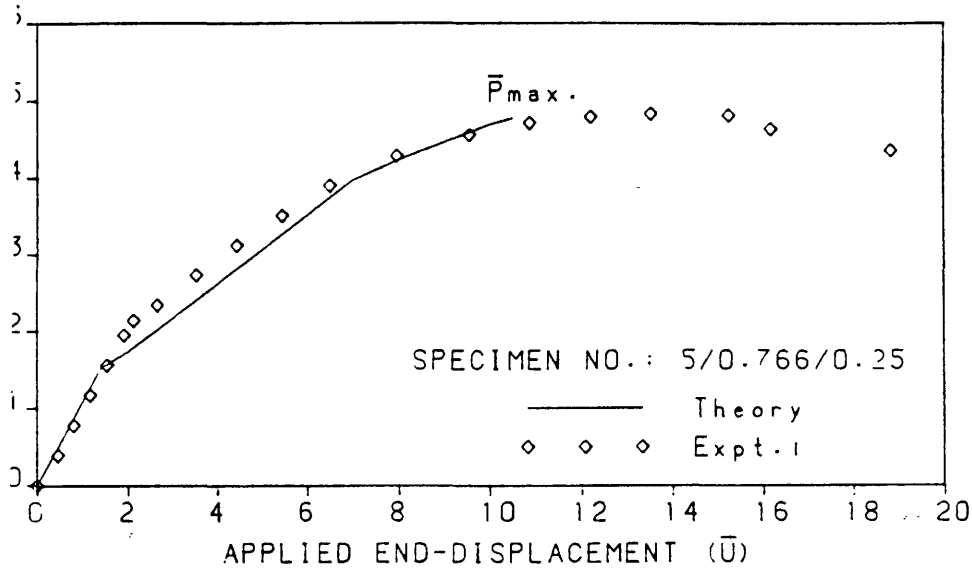

FIGURE 30

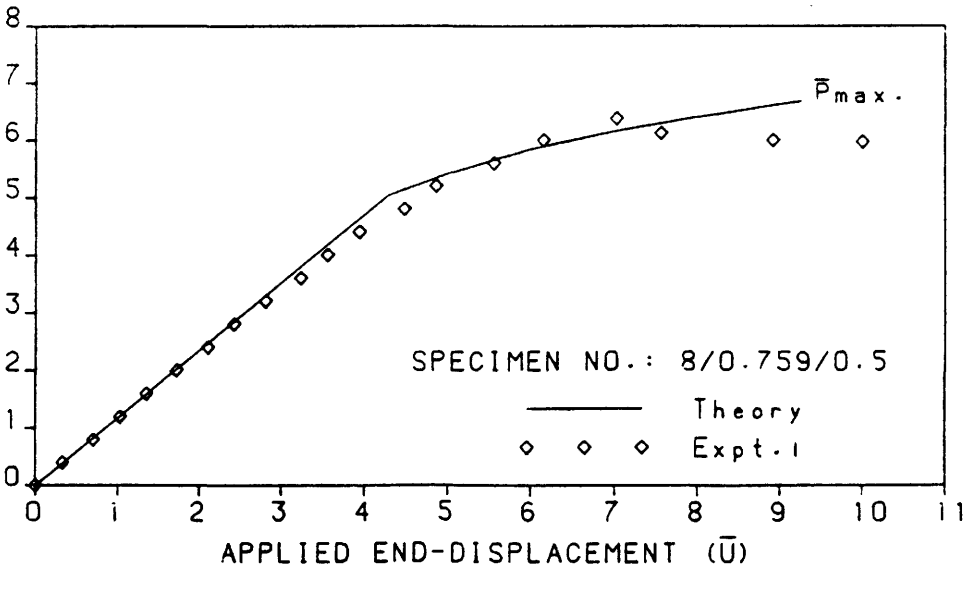

FIGURE 31

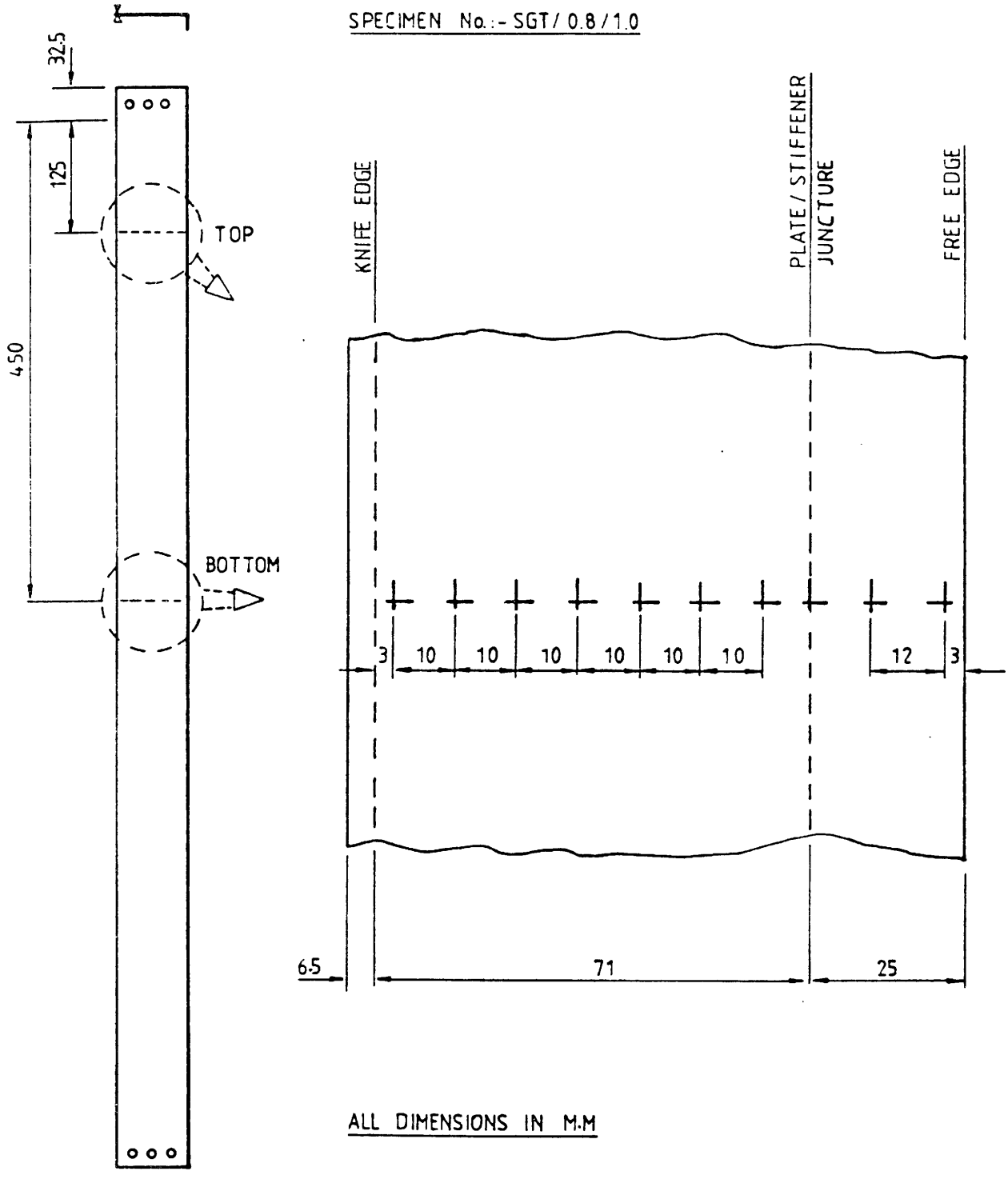

STRAIN GAUGE POSITIONS

FIGURE 32

SPECIMEN NUMBER :- SGT / 0.8 / 1.0

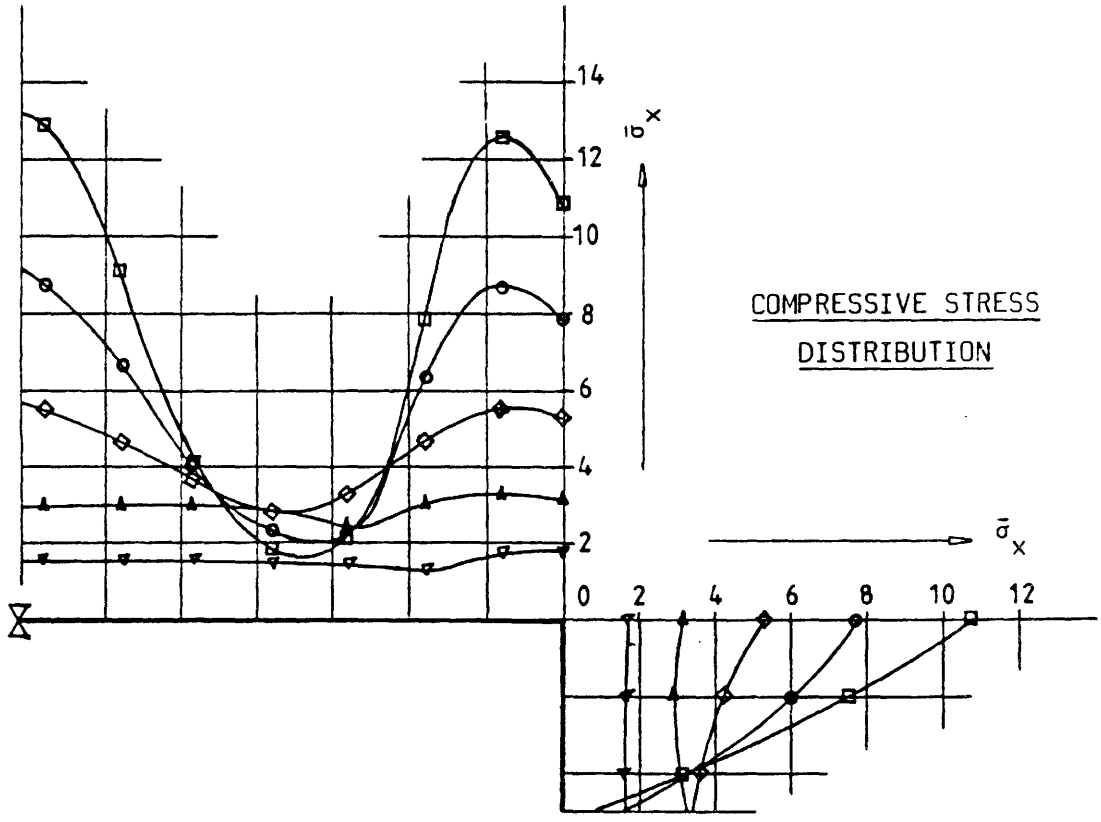

LONGITUDINAL STRESS DISTRIBUTION AT POSITION OF MAXIMUM INITIAL IMPERFECTIONS

LEGEND :-

Load P = 600 lbs

Load P = 1200 lbs

Load P = 1800 lbs

Load P = 2400 lbs

Load P = 3000 lbs

FIGURE 33

SPECIMEN NUMBER :- SGT / 0.8 / 1.0

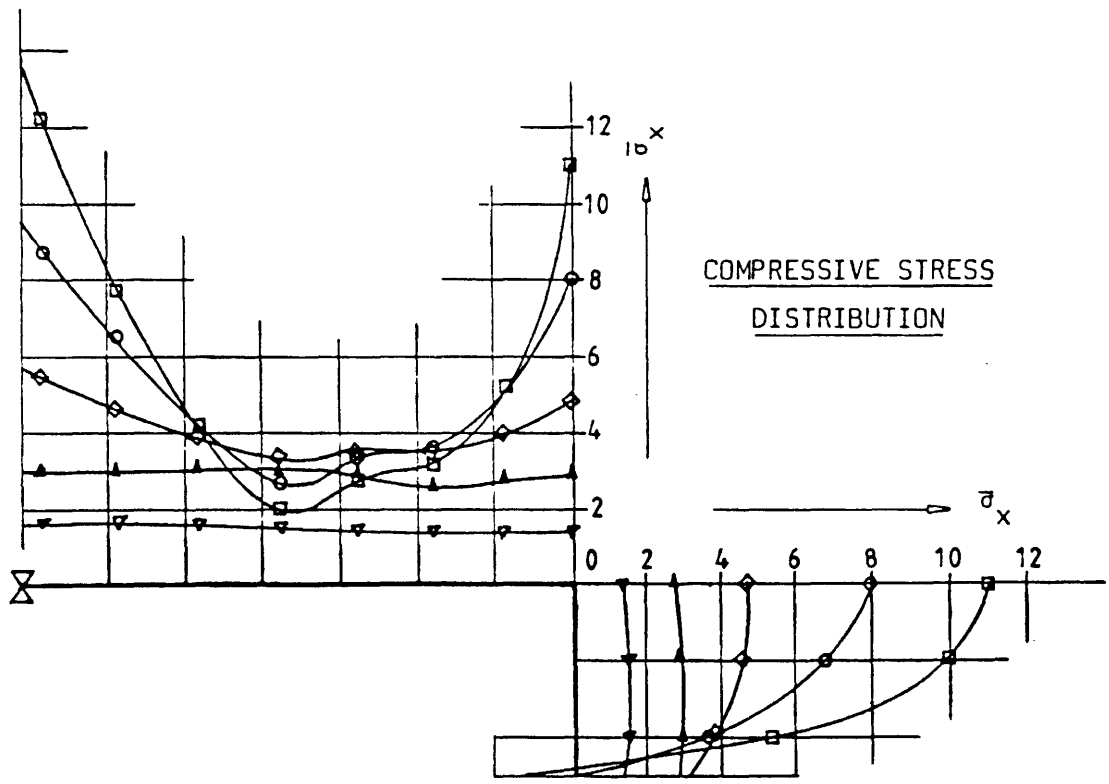

LONGITUDINAL STRESS DISTRIBUTION AT TEST SPECIMEN MID-LENGTH POSITION

LEGEND :-

Load P = 600 lbs

Load P = 1200 lbs

Load P = 1800 lbs

Load P = 2400 lbs

Load P = 3000 lbs

FIGURE 34

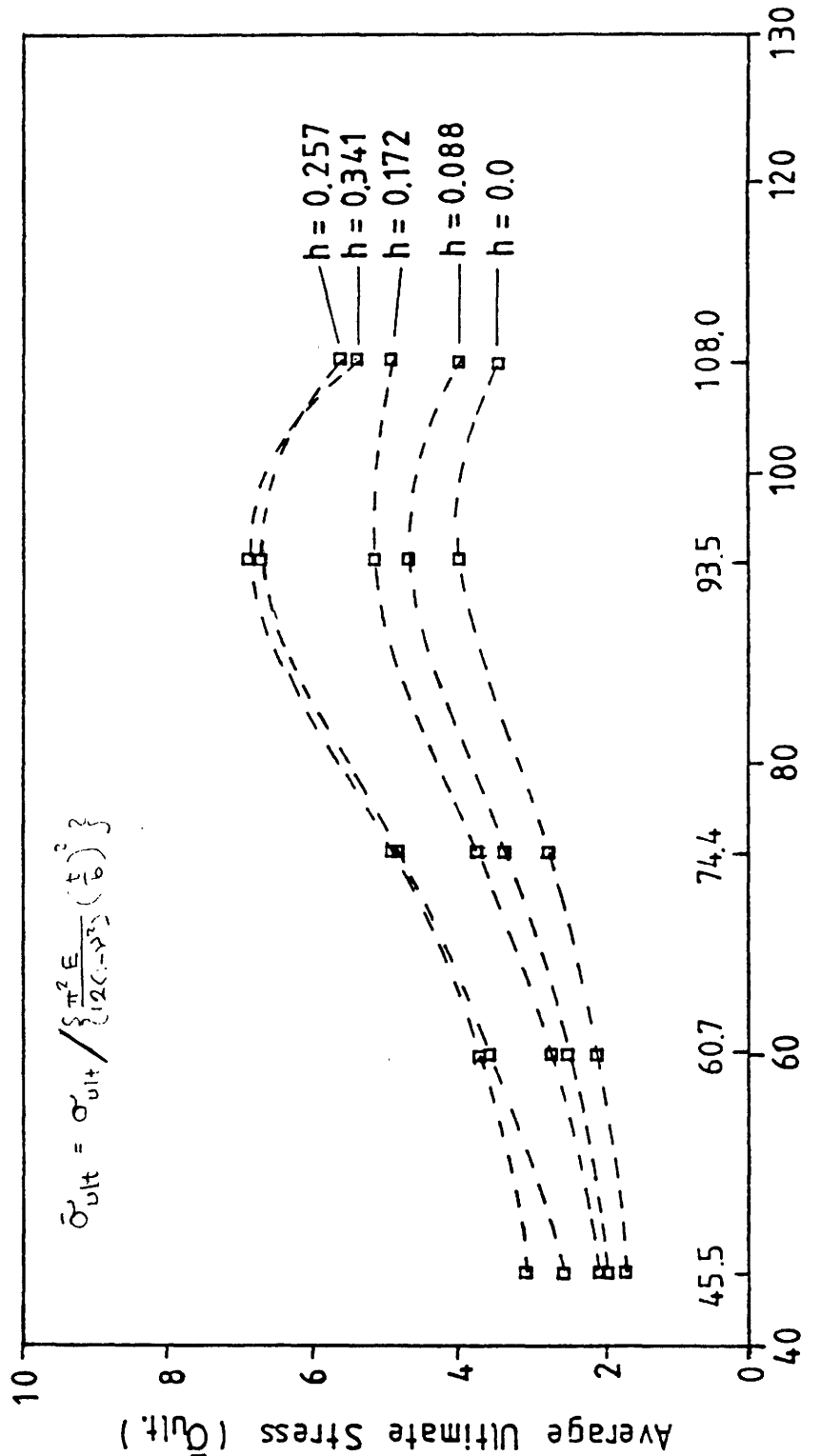
Average Ultimate Stress ($\bar{\sigma}_{ult.}$)
Average Plate Width To Thickness Ratio (b/t)
$\bar{\sigma}_{ult} = \sigma_{ult} / \left\{ \frac{\pi^2 E}{12(1-\nu^2)} \left(\frac{t}{b}\right)^2 \right\}$
h = 0.257
h = 0.341
h = 0.172
h = 0.088
h = 0.0
0
2
4
6
8
10
40
60
80
100
120
130
45.5
60.7
74.4
93.5
108.0

FIGURE 35

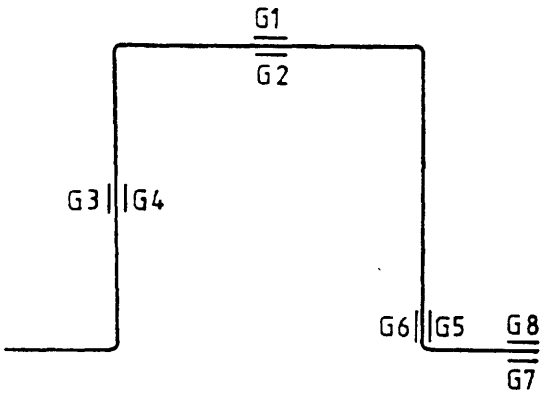

Position of Strain Gauges across mid-length of Top-Hat Section

FIGURE 37

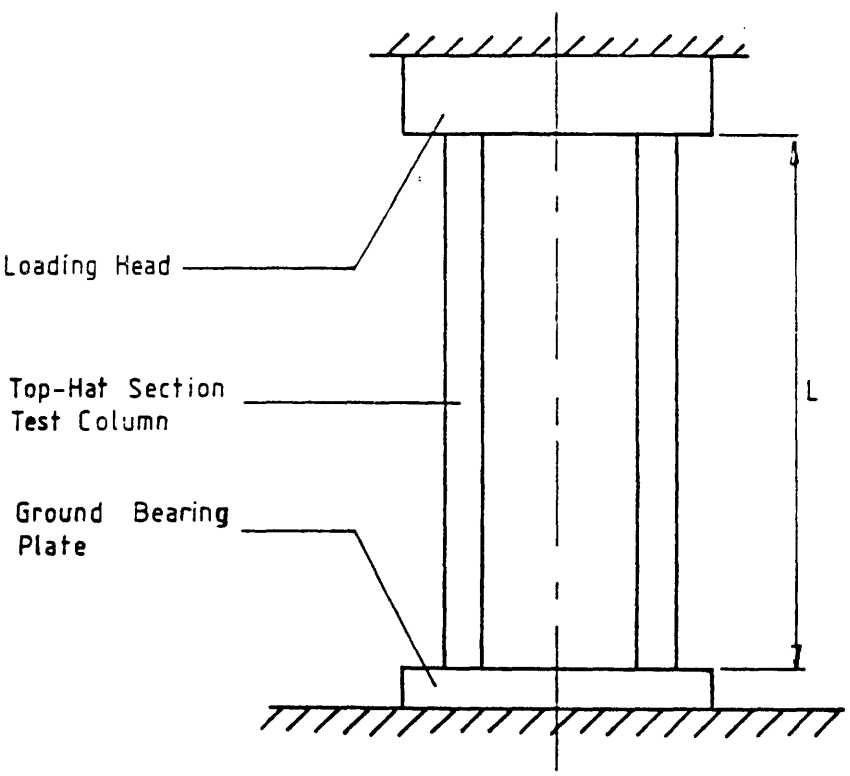

FIGURE 36

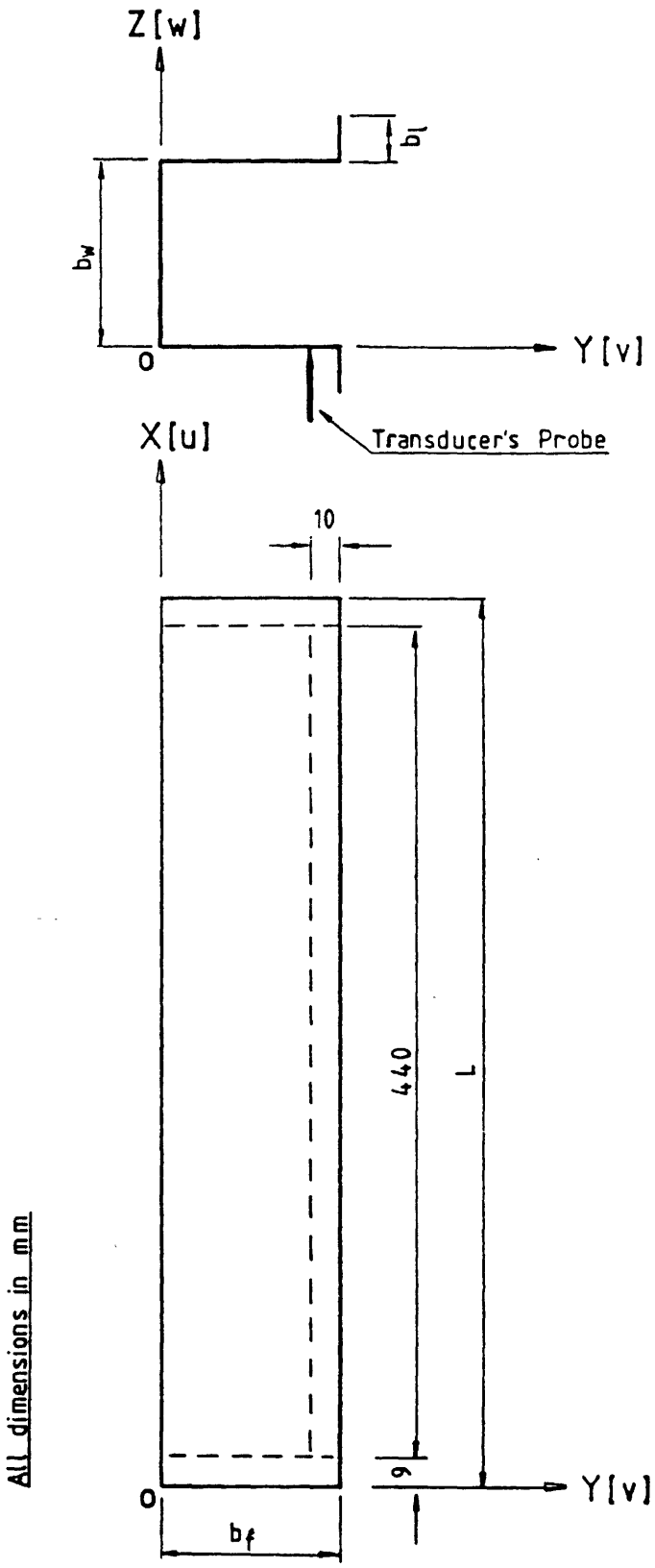
Z[w]
b_1
b_w
0
Y[v]
Transducer's Probe
X[u]
10
440
L
9
0
Y[v]
b_f
All dimensions in mm

FIGURE 38

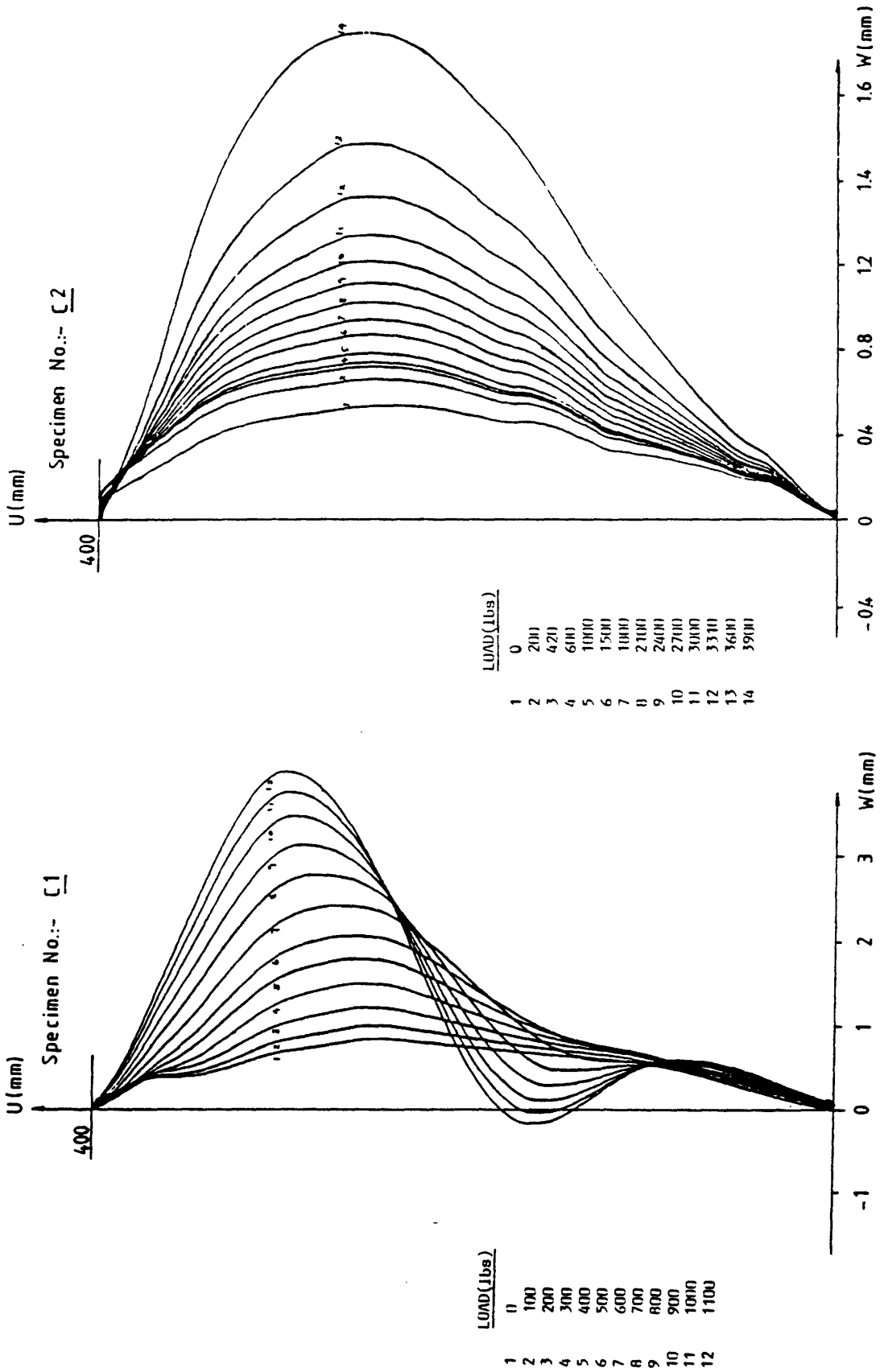
Specimen No.:- C1
U(mm)
400
-1
0
1
2
3
W(mm)
LOAD(lbs)
1 0
2 100
3 200
4 300
5 400
6 500
7 600
8 700
9 800
10 900
11 1000
12 1100
Specimen No.:- C2
U(mm)
400
-04
0
04
0.8
12
1.4
1.6 W(mm)
LOAD(lbs)
1 0
2 200
3 420
4 600
5 1000
6 1500
7 1800
8 2100
9 2400
10 2700
11 3000
12 3300
13 3600
14 3900

FIGURE 39

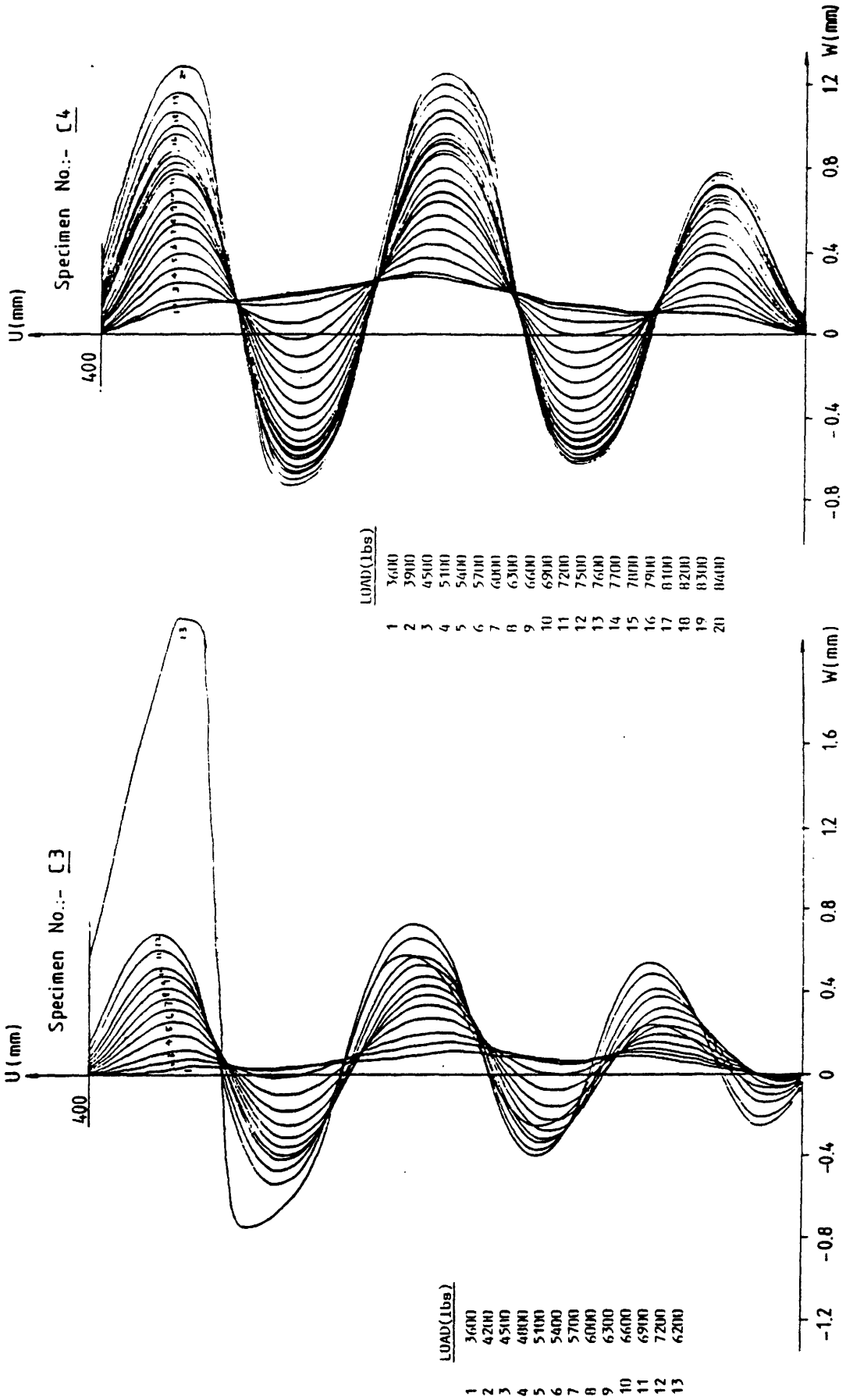
Specimen No.:- C4
U(mm)
400
W(mm)
LOAD(lbs)
1 3600
2 3900
3 4500
4 5100
5 5400
6 5700
7 6000
8 6300
9 6600
10 6900
11 7200
12 7500
13 7600
14 7700
15 7800
16 7900
17 8100
18 8200
19 8300
20 8400
Specimen No.:- C3
U(mm)
400
W(mm)
LOAD(lbs)
1 3600
2 4200
3 4500
4 4800
5 5100
6 5400
7 5700
8 6000
9 6300
10 6600
11 6900
12 7200
13 6200

FIGURE 40

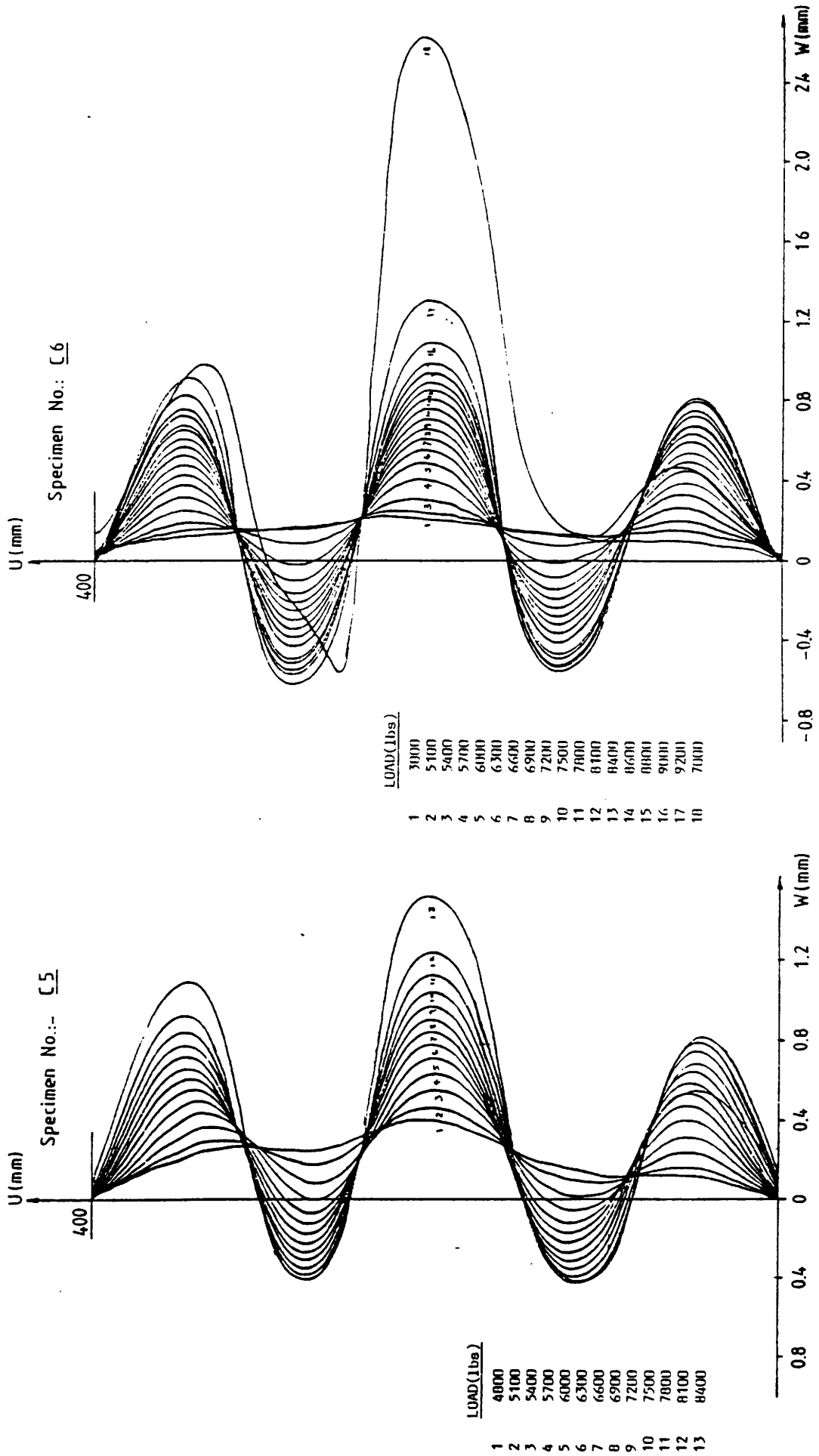
Specimen No.:- C5
U(mm)
400
0.8
0.4
0
0.4
0.8
1.2
W(mm)
LOAD(lbs)
1 4000
2 5100
3 5400
4 5700
5 6000
6 6300
7 6600
8 6900
9 7200
10 7500
11 7800
12 8100
13 8400
Specimen No.: C6
U(mm)
400
0
0.4
0.8
1.2
1.6
2.0
2.4
W(mm)
-0.4
-0.8
LOAD(lbs)
1 3000
2 5100
3 5400
4 5700
5 6000
6 6300
7 6600
8 6900
9 7200
10 7500
11 7800
12 8100
13 8400
14 8600
15 8800
16 9000
17 9200
18 7000

FIGURE 41

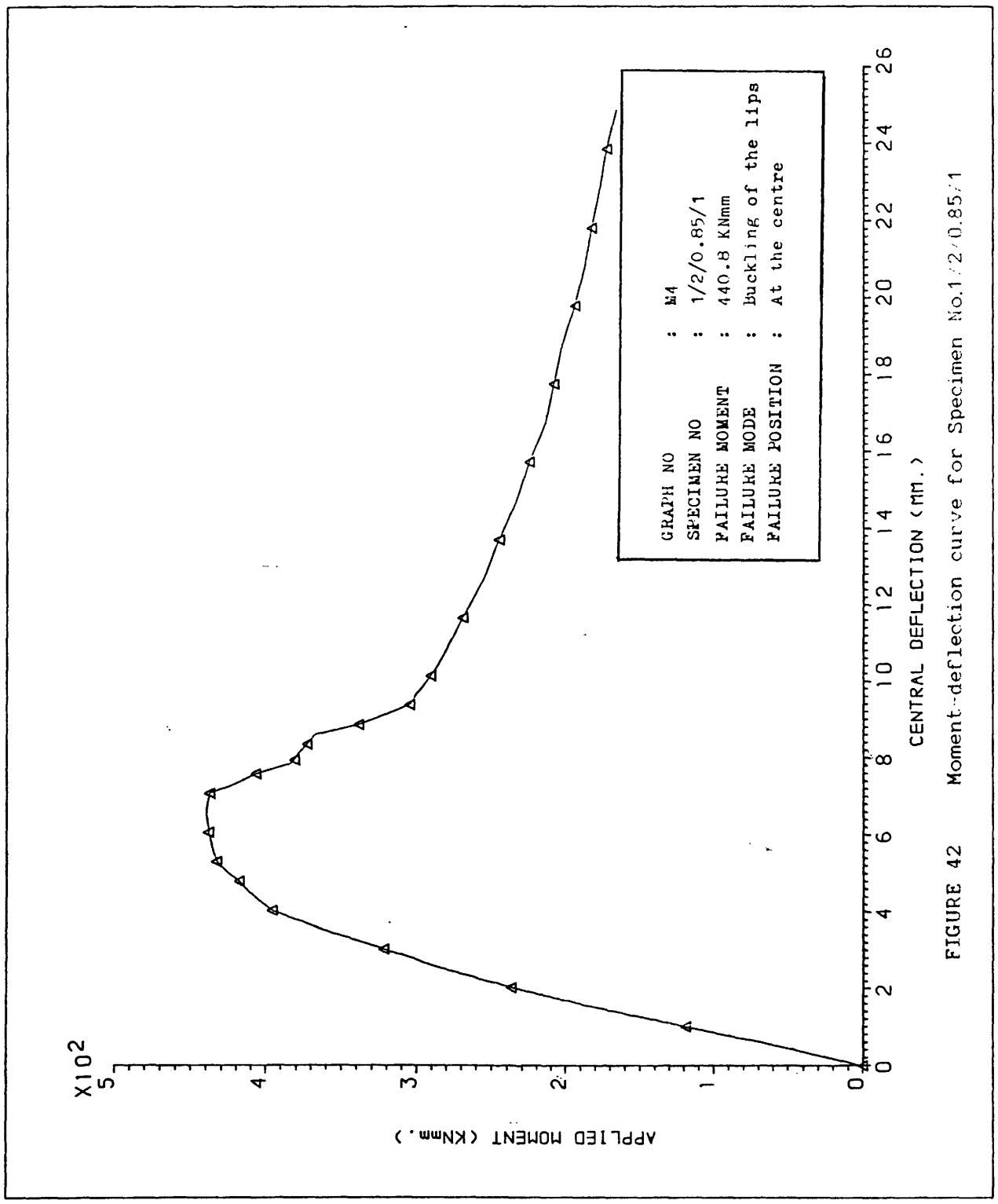

FIGURE 42 Moment-deflection curve for Specimen No.1/2/0.85/1

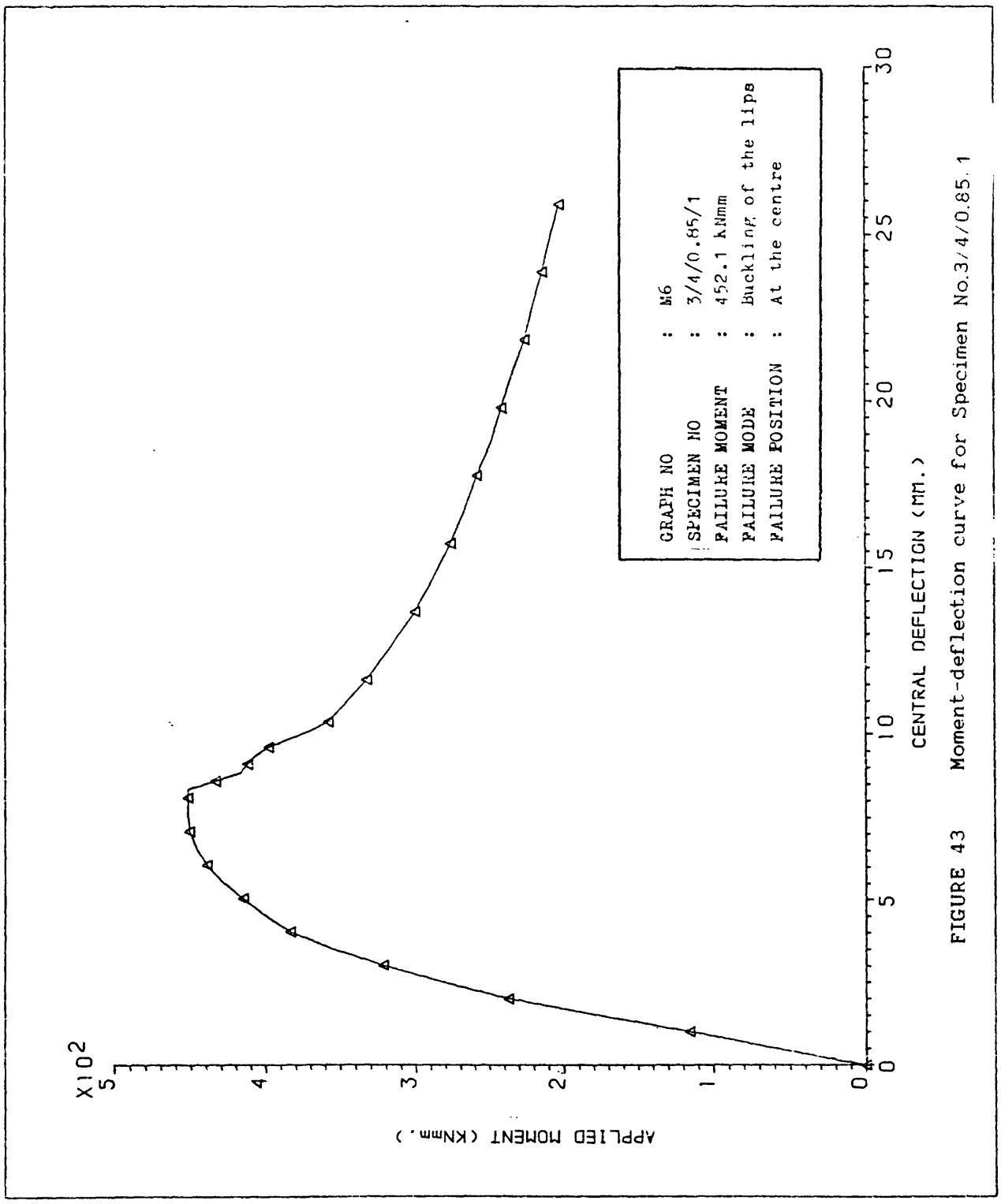

FIGURE 43 Moment-deflection curve for Specimen No.3/4/0.85.1

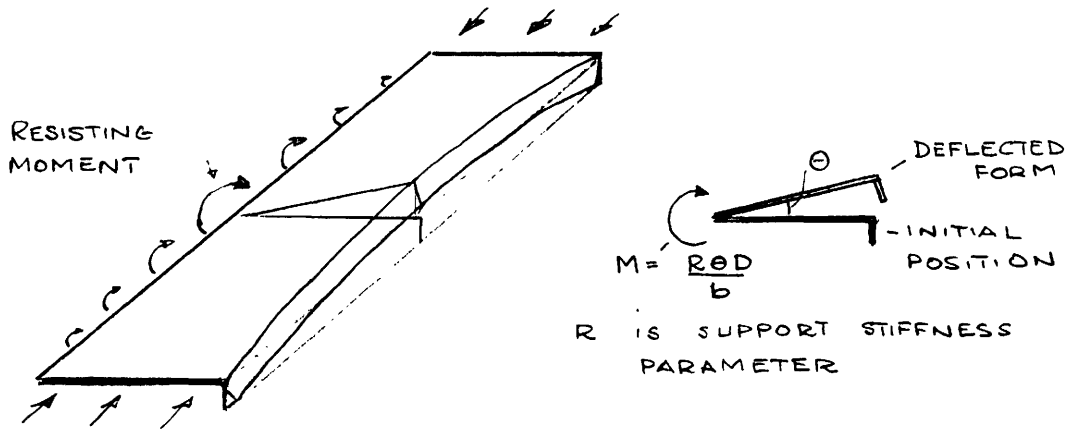

FIGURE 44. TORSIONAL BUCKLING OF AN EDGE STIFFENED ELEMENT

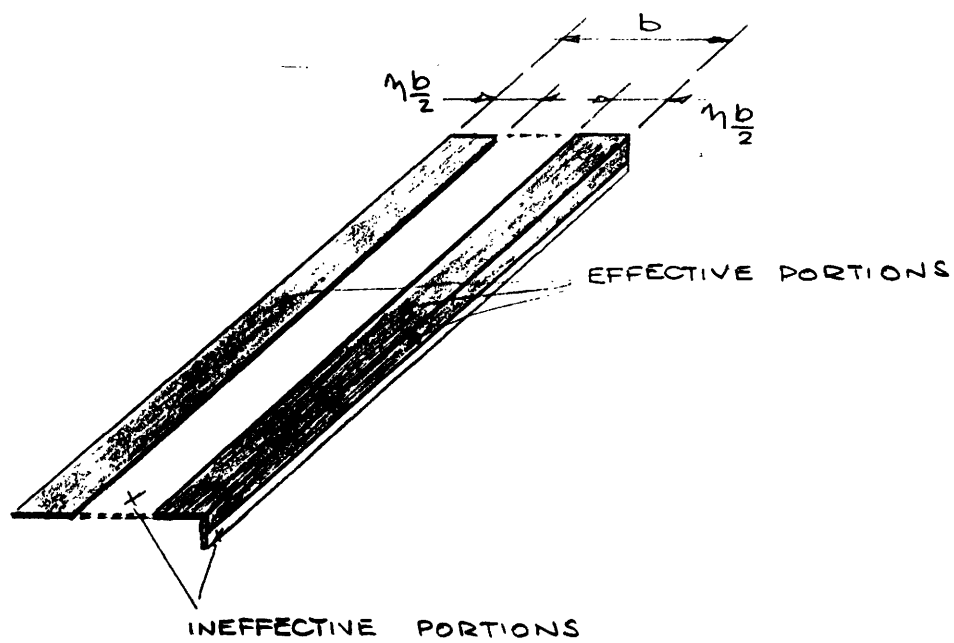

FIGURE 45. PLATE LOSSES IN EFFECTIVENESS DUE TO LOCAL BUCKLING

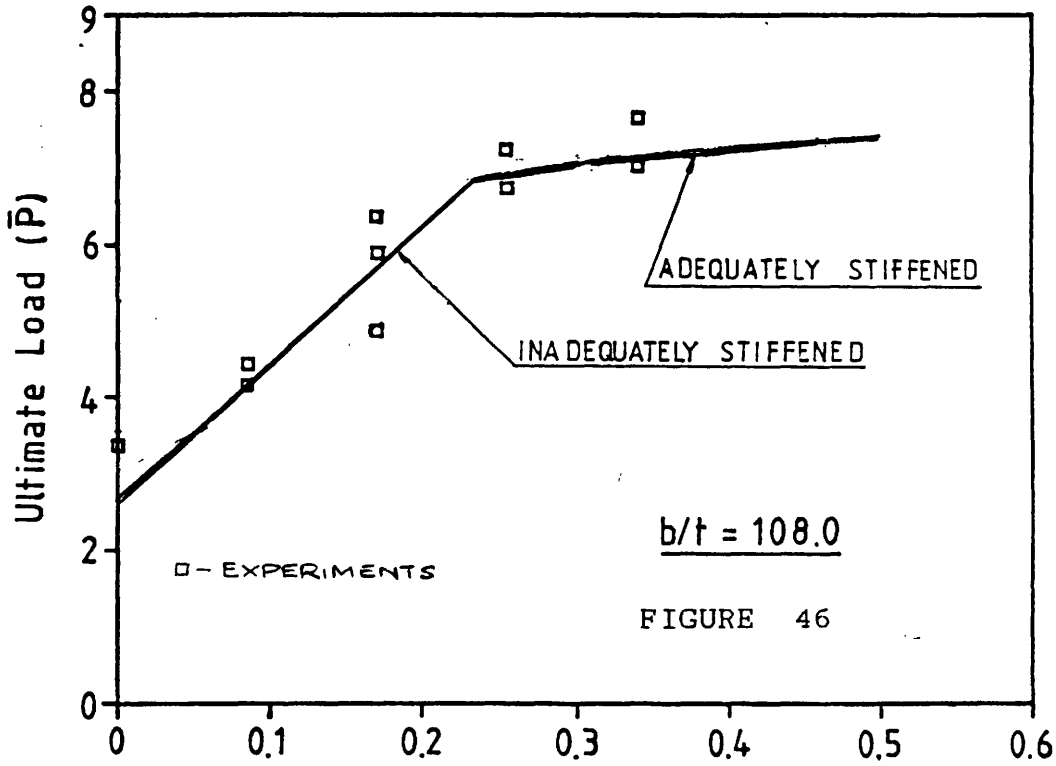

FIGURE 46

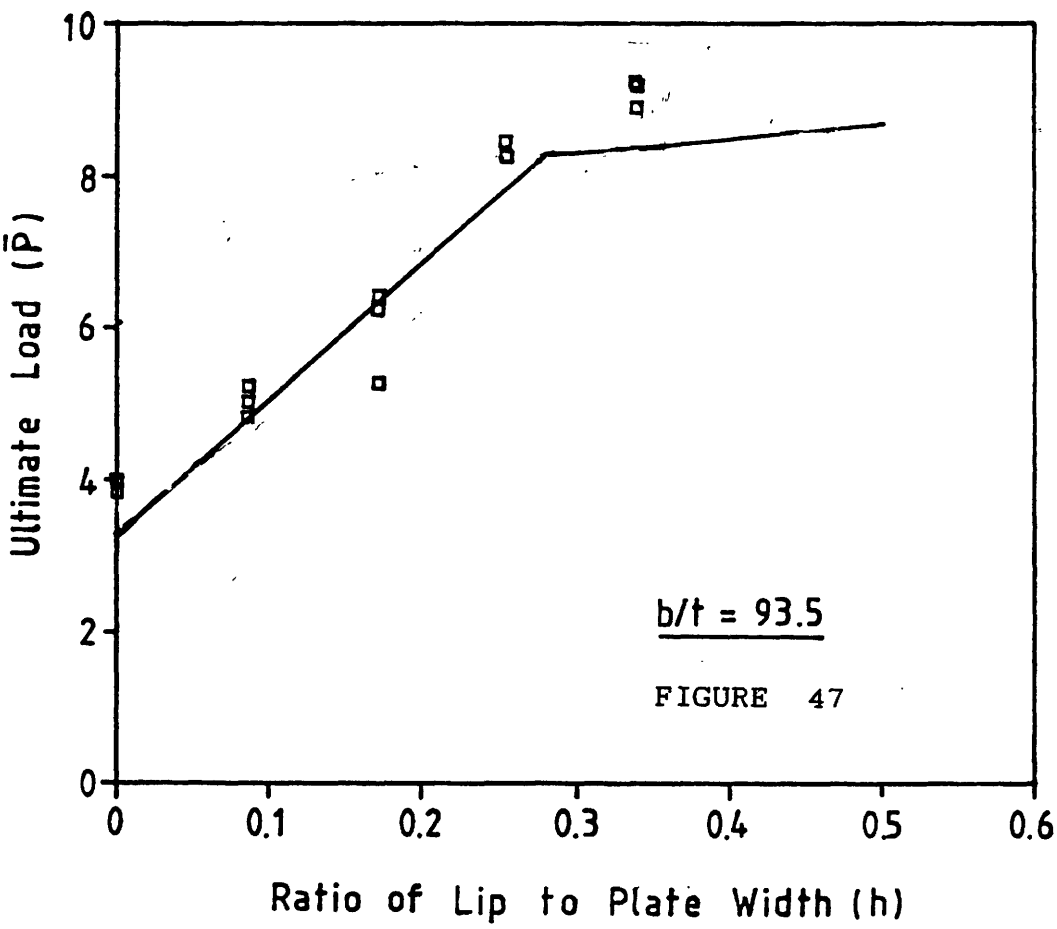

FIGURE 47

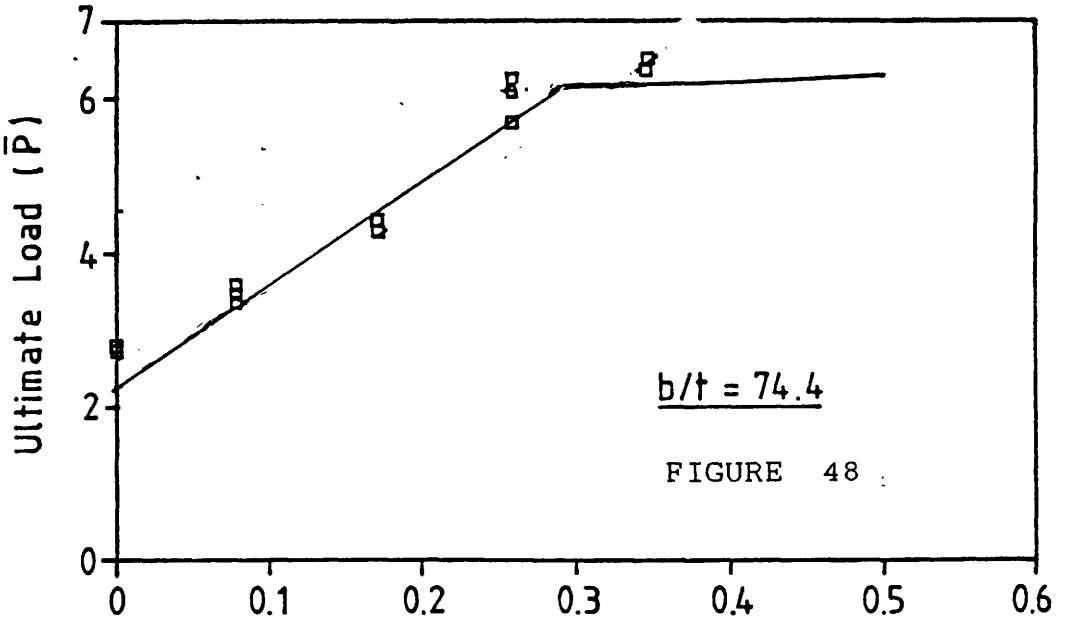

FIGURE 48

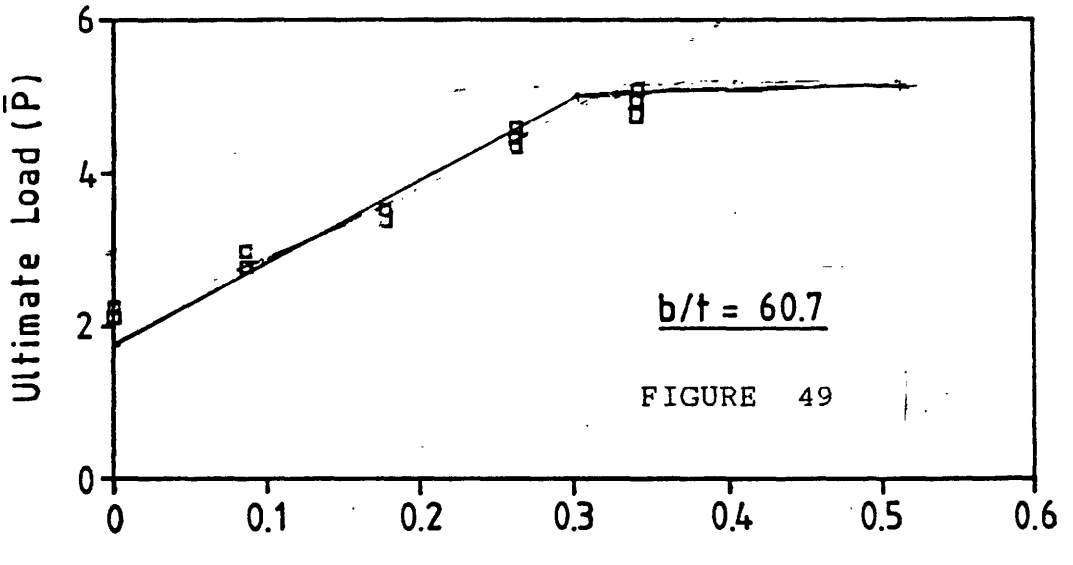

FIGURE 49

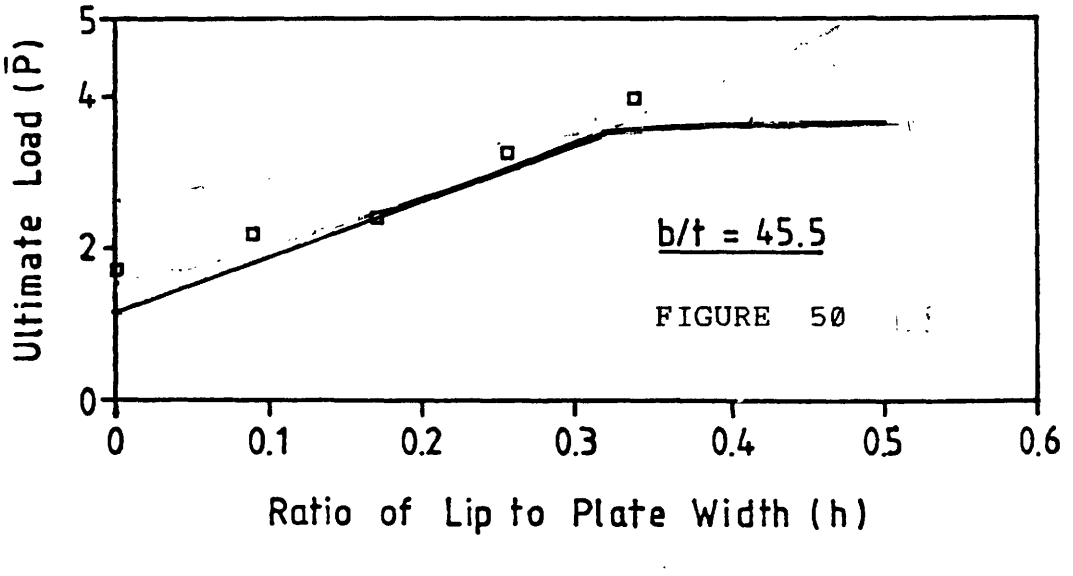

FIGURE 50

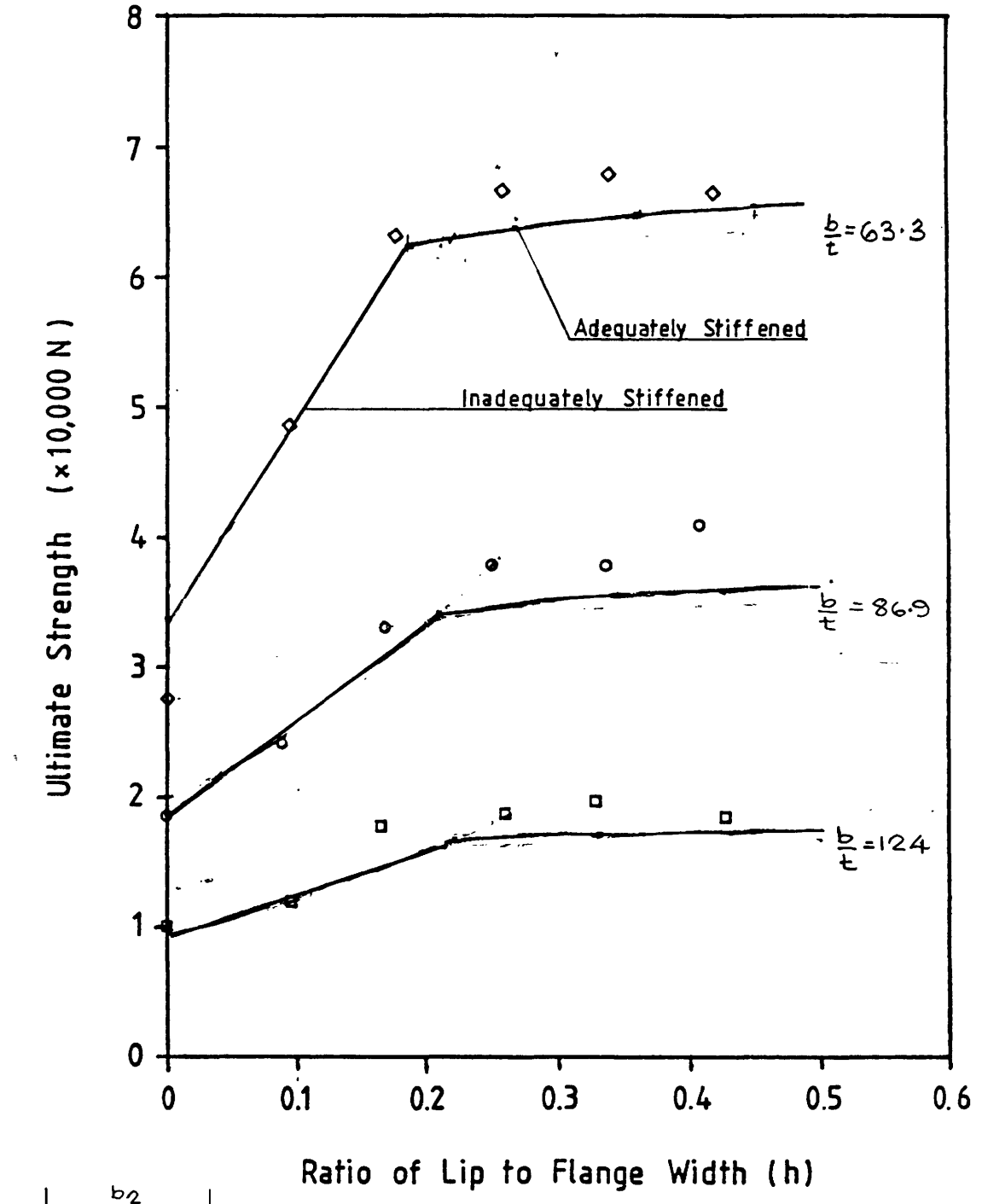
Ultimate Strength (×10,000 N)
Ratio of Lip to Flange Width (h)
0
1
2
3
4
5
6
7
8
0
0.1
0.2
0.3
0.4
0.5
0.6
b/t = 63·3
b/t = 86·9
b/t = 124
Adequately Stiffened
Inadequately Stiffened

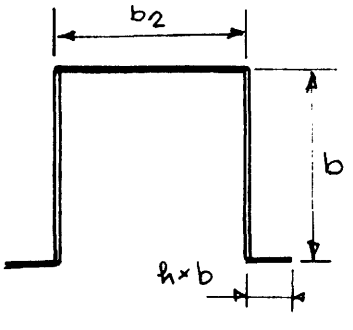
b2
b
h×b

FIGURE 51

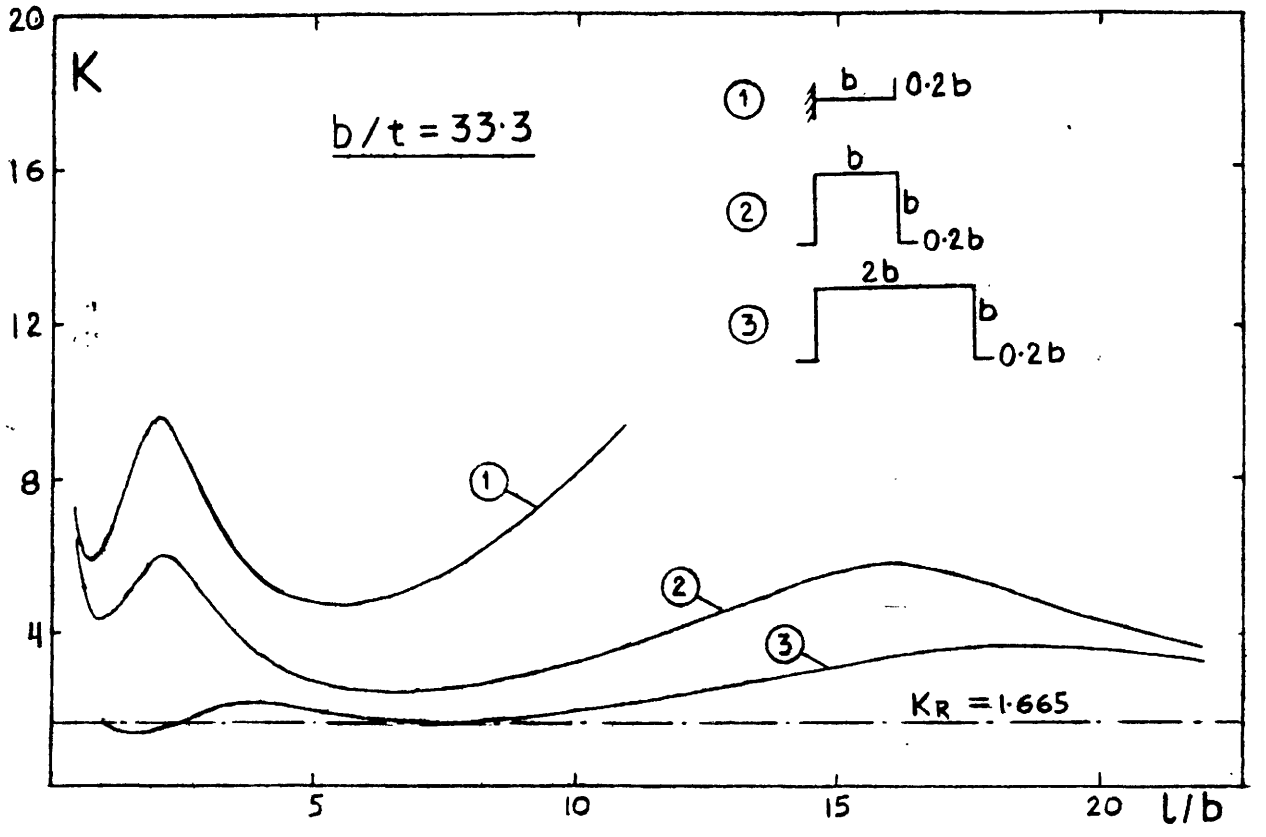

FIGURE 52. FINITE STRIP BUCKLING COEFFICIENTS - b/t=33.3

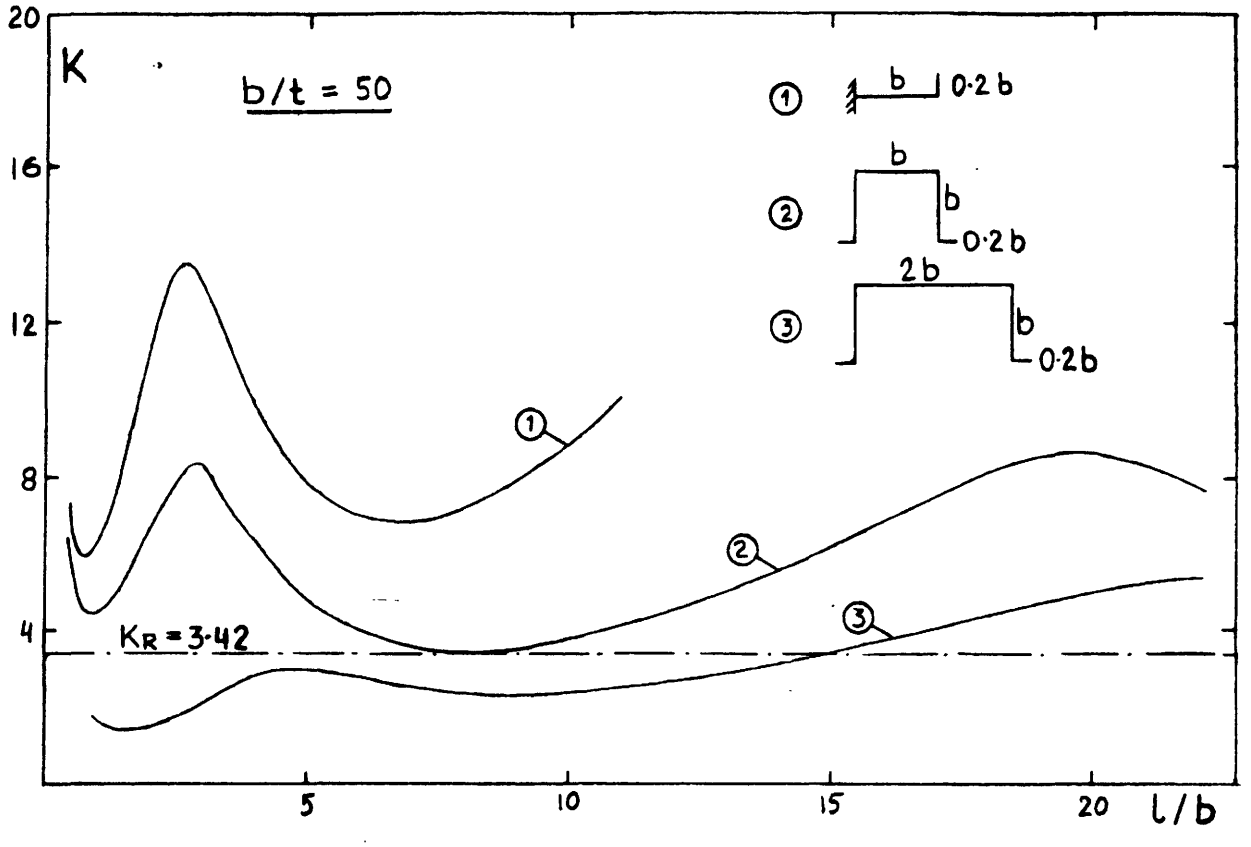

FIGURE 53. FINITE STRIP BUCKLING COEFFICIENTS - b/t=50

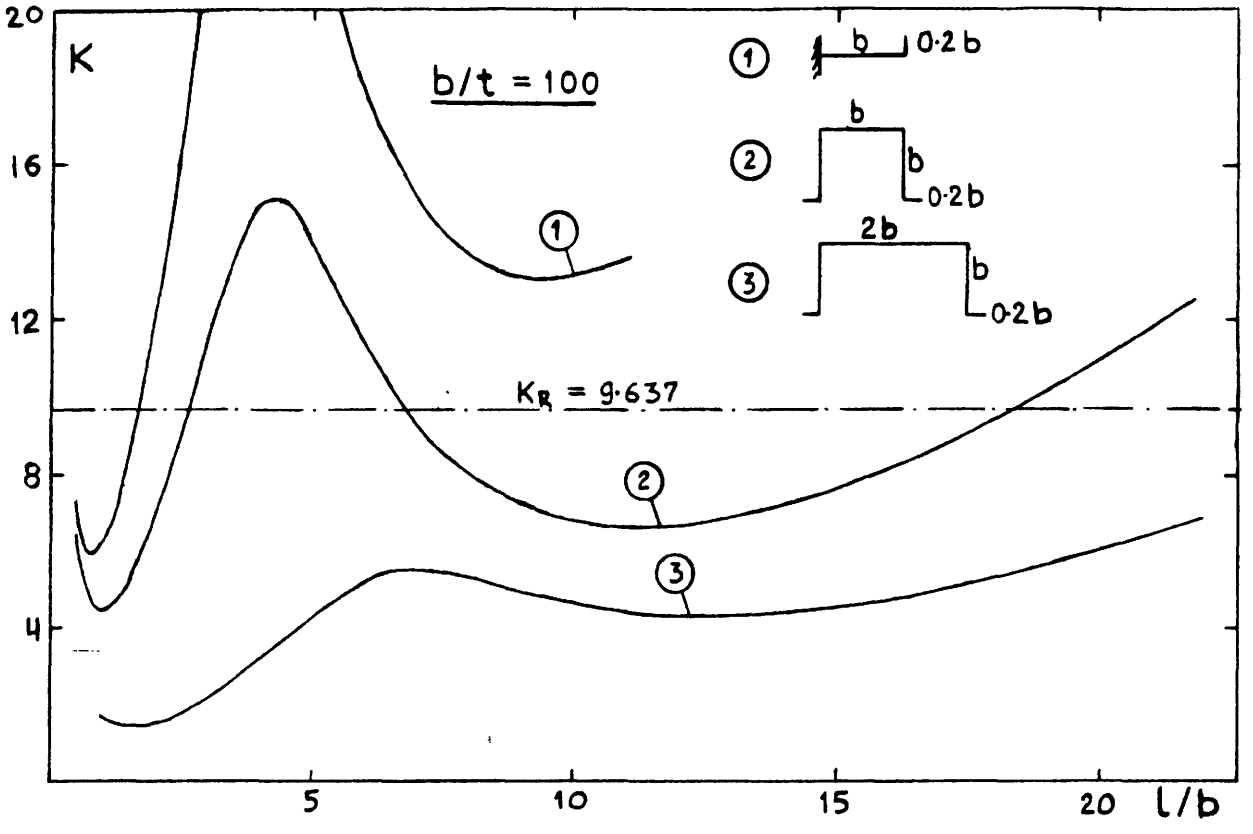

FIGURE 54. FINITE STRIP BUCKLING COEFFICIENTS - b/t=100

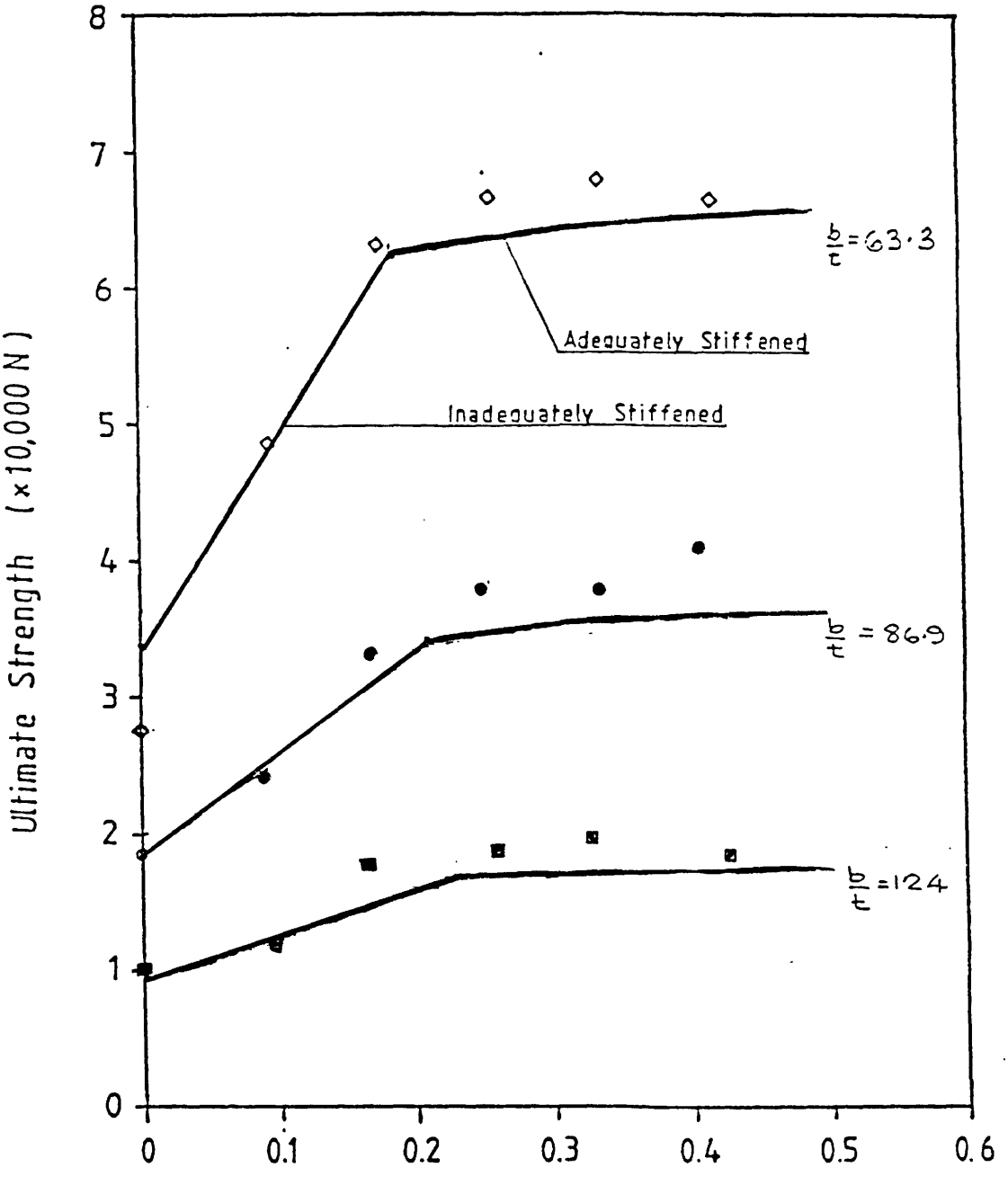
Ultimate Strength (×10,000 N)
Ratio of Lip to Flange Width (h)
0
1
2
3
4
5
6
7
8
0
0.1
0.2
0.3
0.4
0.5
0.6
b/t = 63·3
Adequately Stiffened
Inadequately Stiffened
b/t = 86·9
b/t = 124

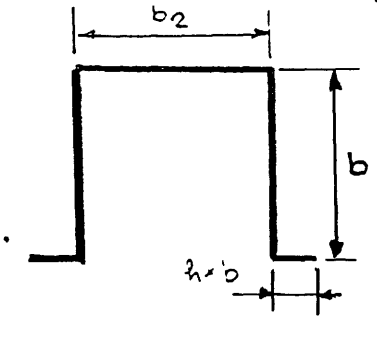
b2
b
h×b

FIGURE 55

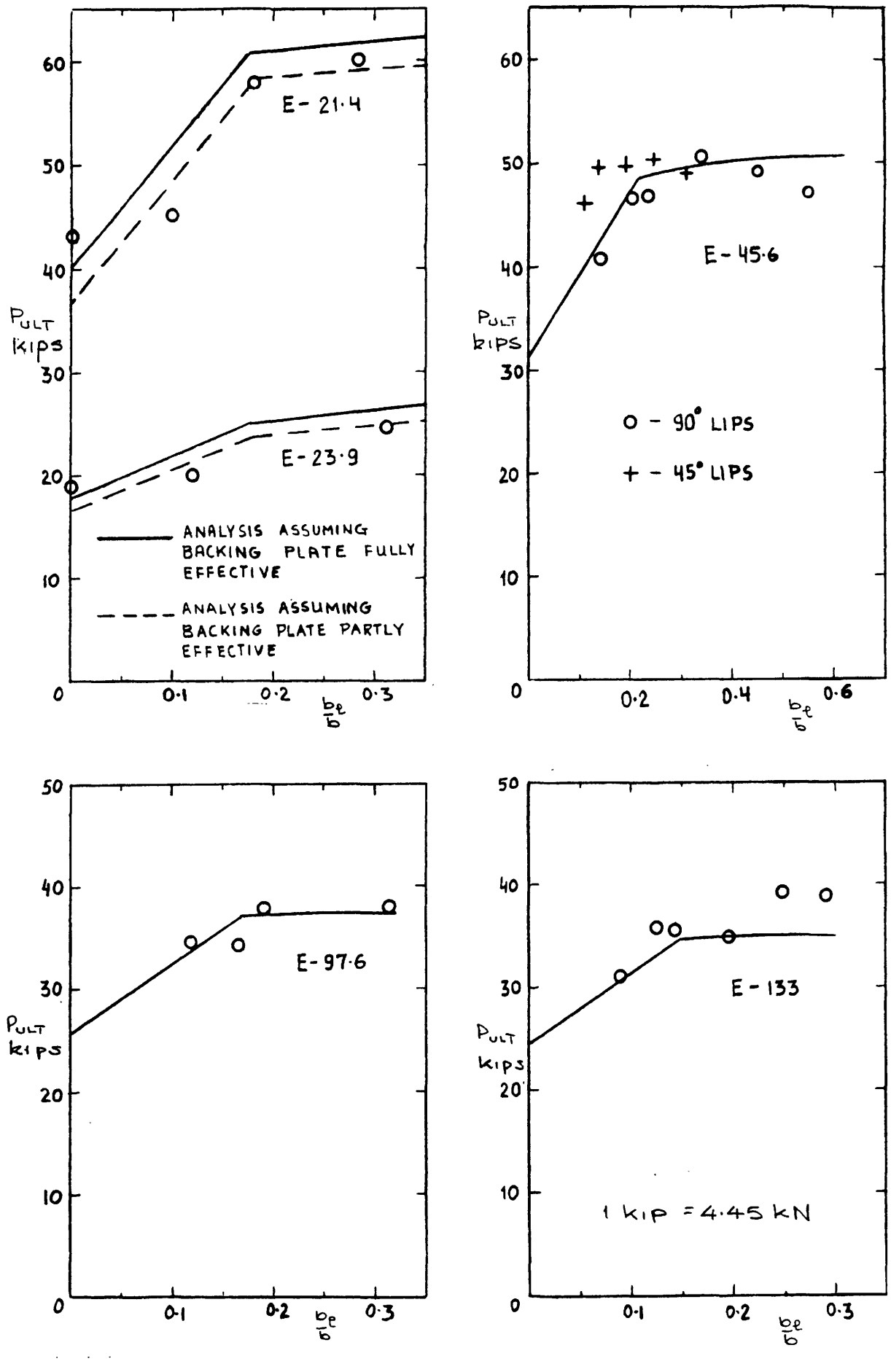

FIGURE 56. COMPARISON OF DESIGN RULES WITH DESMOND'S TESTS

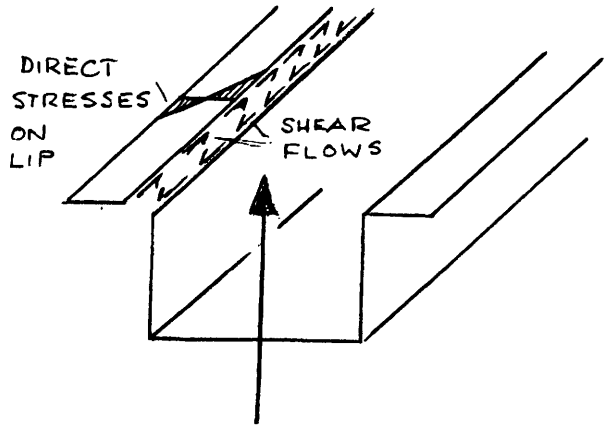

FIGURE 57. BEAM IN BENDING TO COMPRESS EDGE STIFFENER

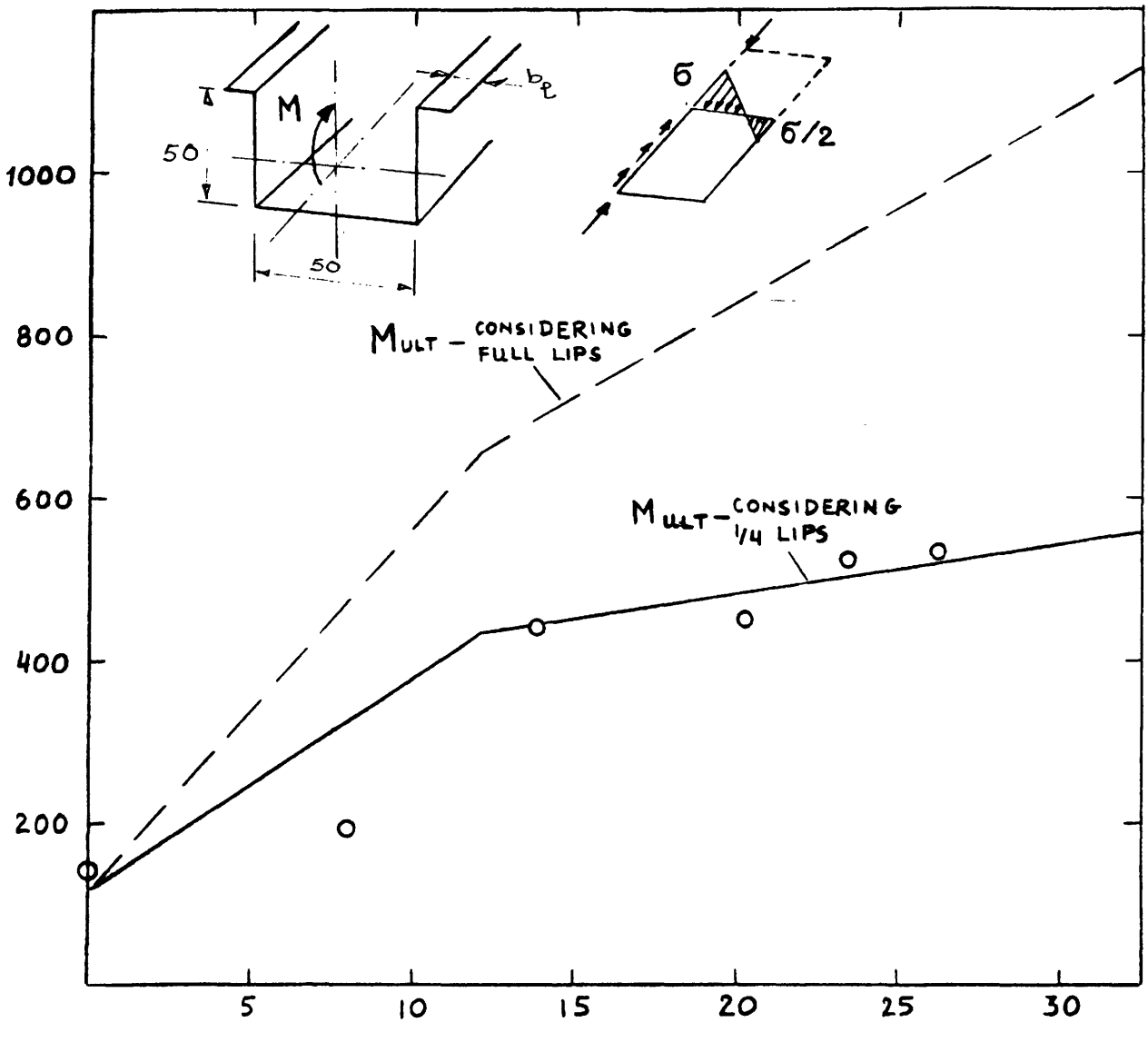

FIGURE 58. FAILURE MOMENTS FOR BEAMS BENT TO COMPRESS EDGE STIFFENERS

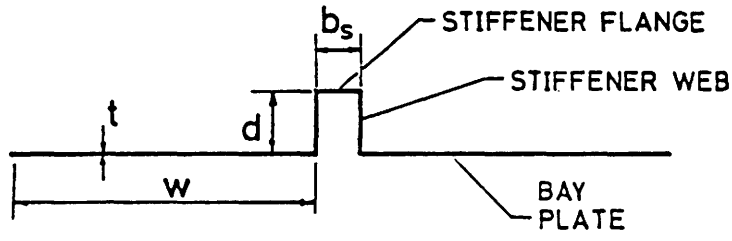

FIGURE 59. INTERMEDIATE STIFFENER

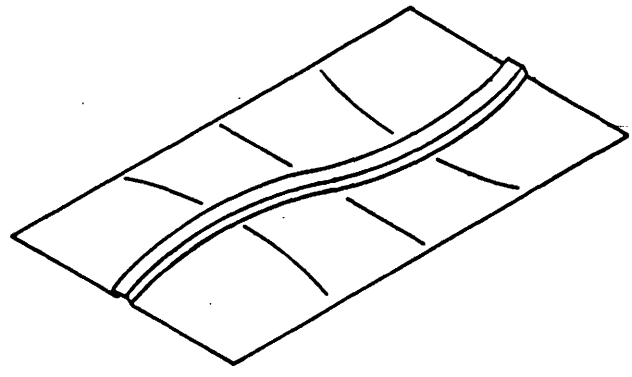

FIGURE 60(a).STIFFENER BUCKLING MODE

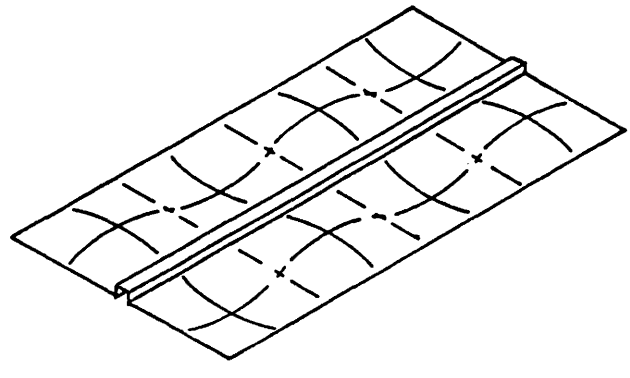

FIGURE 60(B). LOCAL BUCKLING MODE

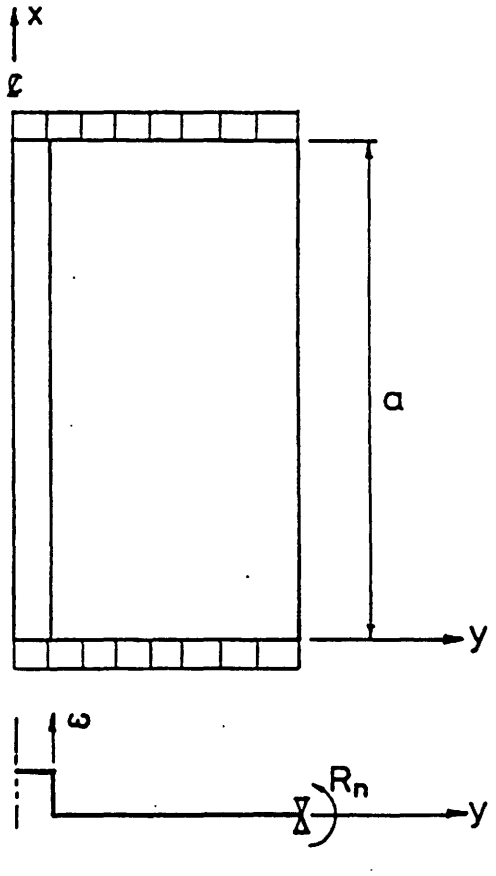

(a) Co-ordinate System

(b) Stiffener Buckling Mode

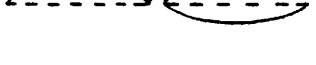

(c) Local Plate Buckling Mode

FIGURE 61

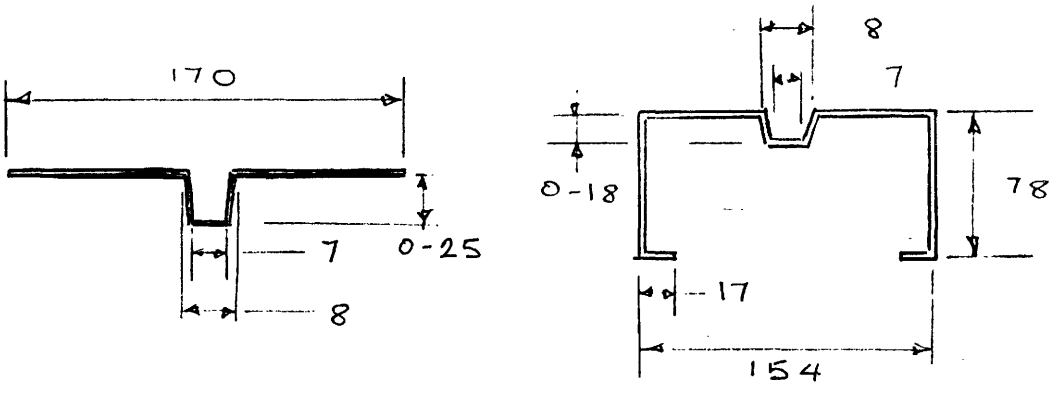

FIGURE 62. TYPES OF INTERMEDIATELY STIFFENED ELEMENTS TESTED

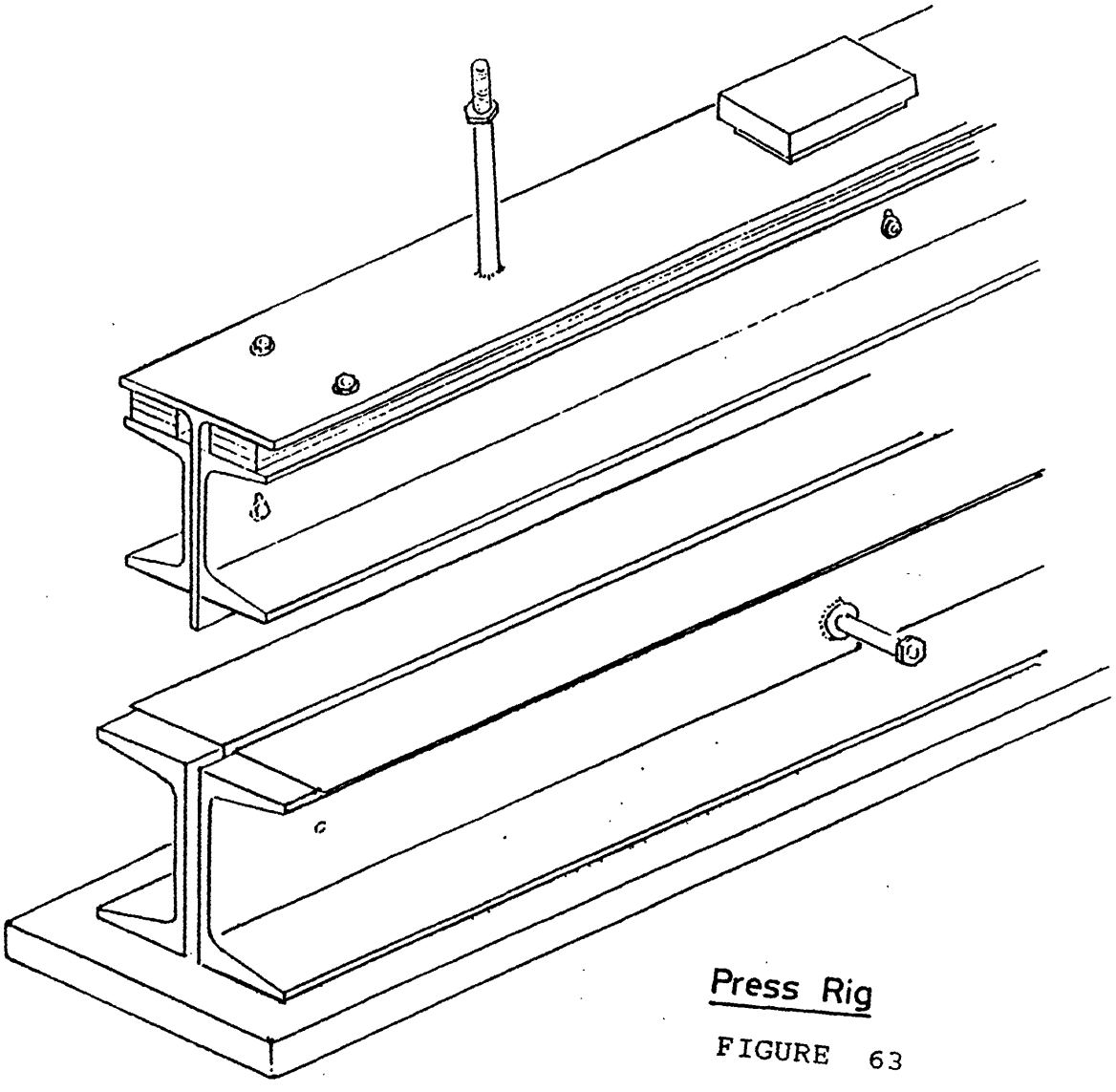

Press Rig

FIGURE 63

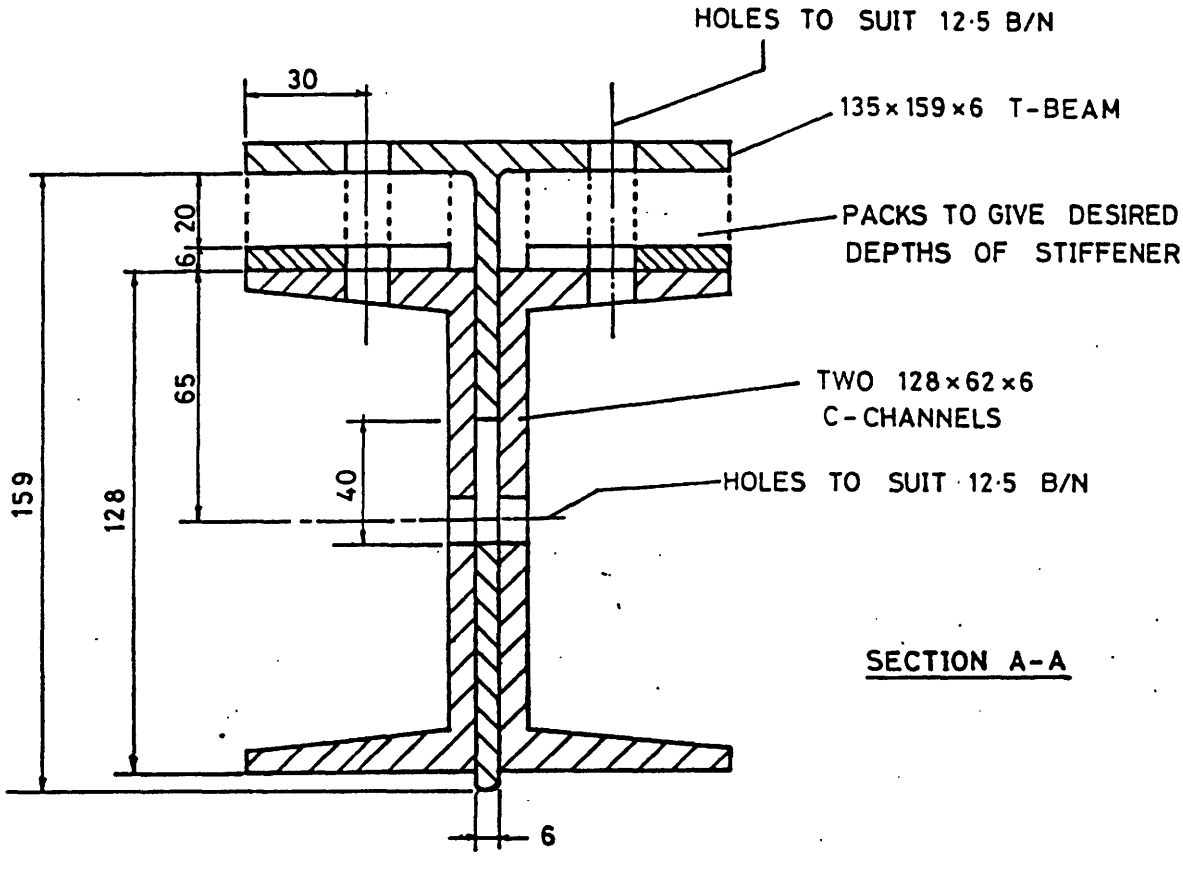
HOLES TO SUIT 12·5 B/N
30
135×159×6 T-BEAM
PACKS TO GIVE DESIRED DEPTHS OF STIFFENER
20
65
TWO 128×62×6 C-CHANNELS
159
128
40
HOLES TO SUIT 12·5 B/N
6
SECTION A-A

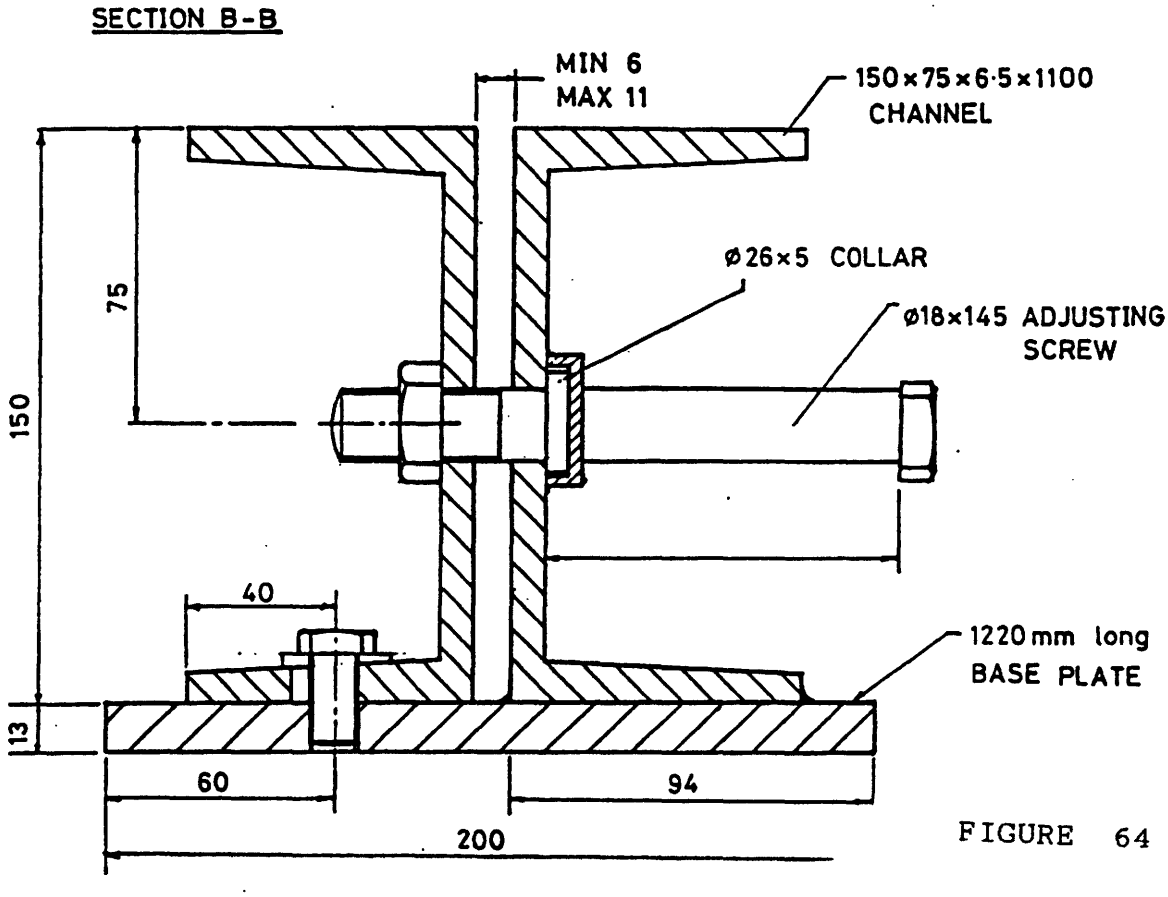
SECTION B-B
MIN 6
MAX 11
150×75×6·5×1100 CHANNEL
ø26×5 COLLAR
ø18×145 ADJUSTING SCREW
75
150
40
1220 mm long BASE PLATE
13
60
94
200

FIGURE 64

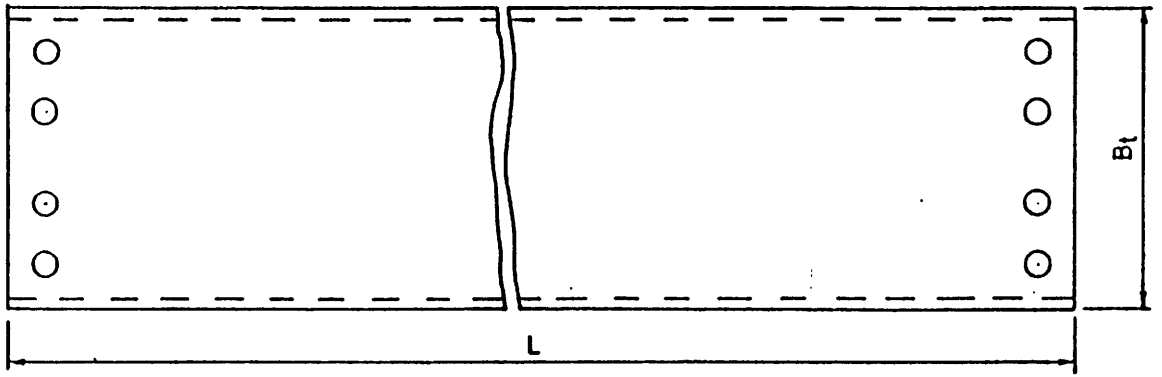

Geometry of Flat Specimens

Fig. 5.2.2.1

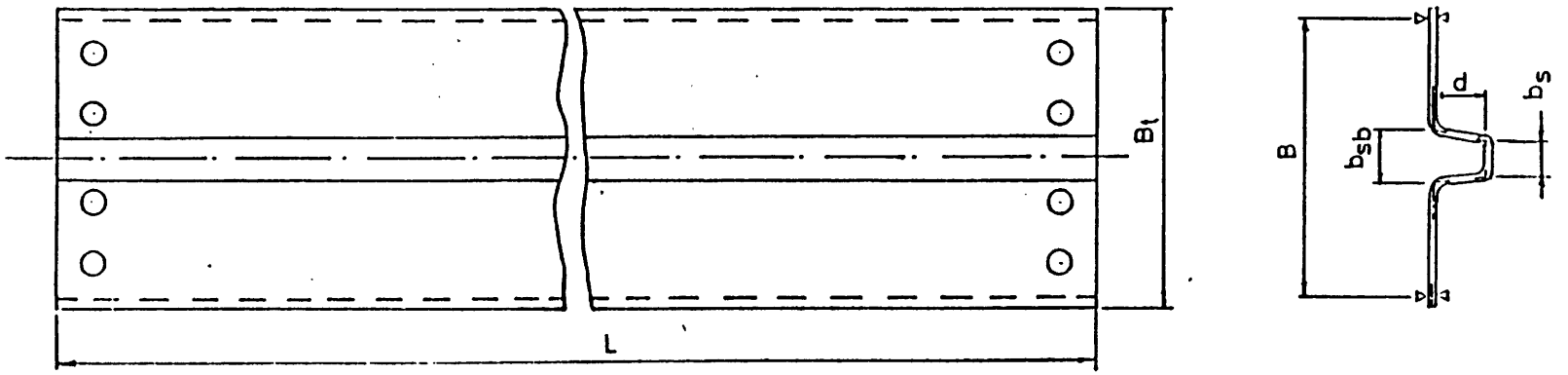

Geometry of Stiffened Specimens

FIGURE 65

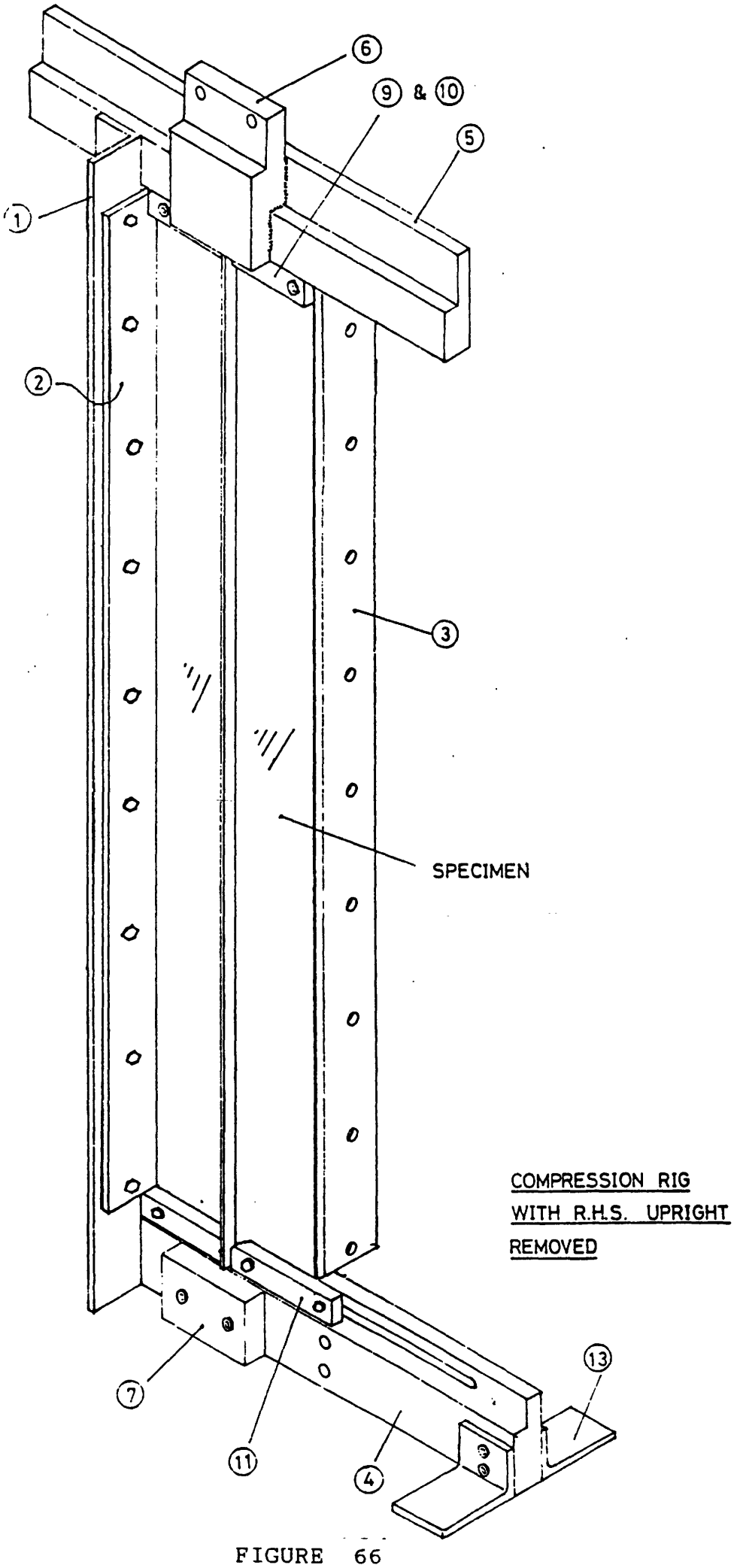
6
9 & 10
5
1
2
3
SPECIMEN
7
11
4
13
COMPRESSION RIG
WITH R.H.S. UPRIGHT
REMOVED

FIGURE 66

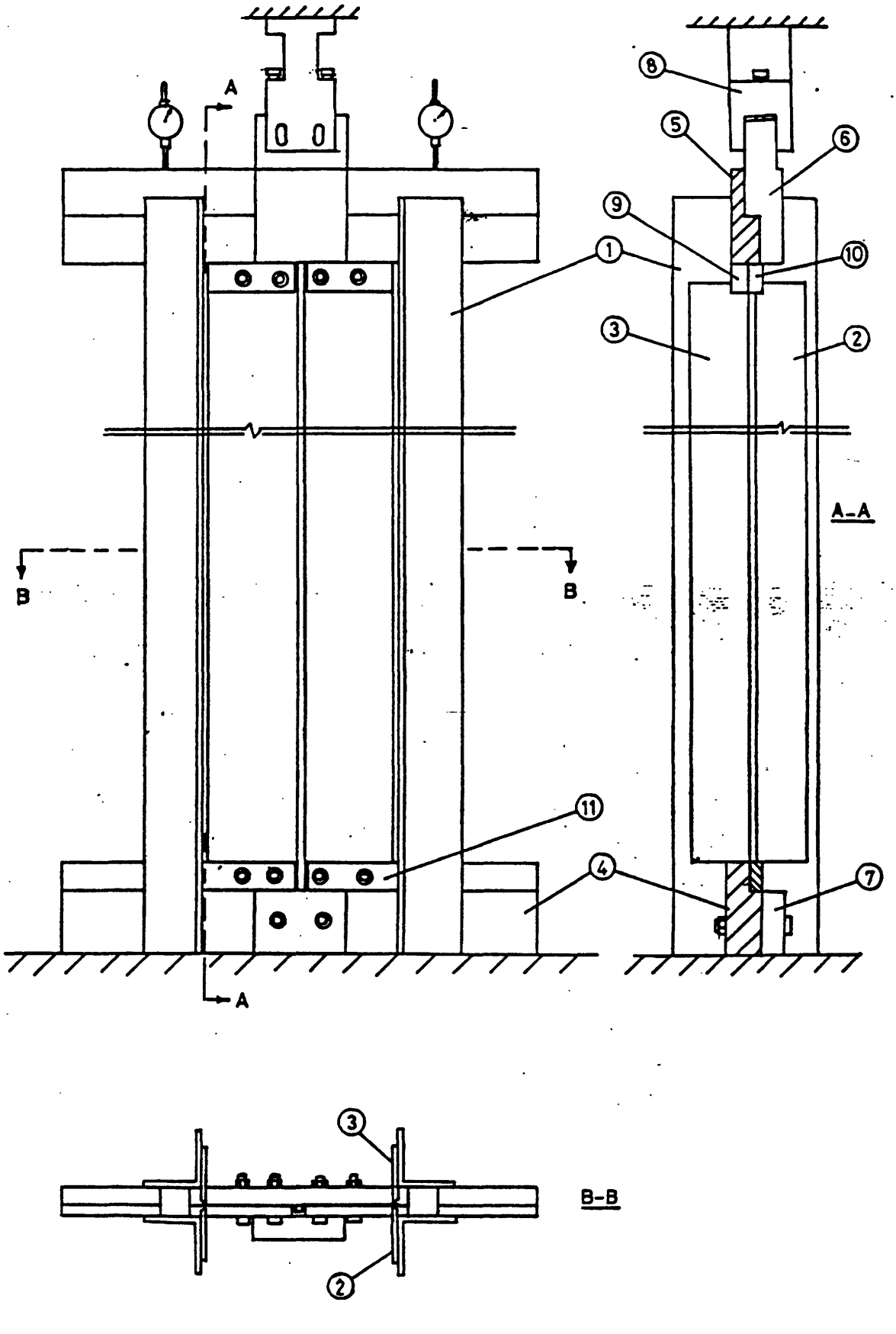

FIGURE 67

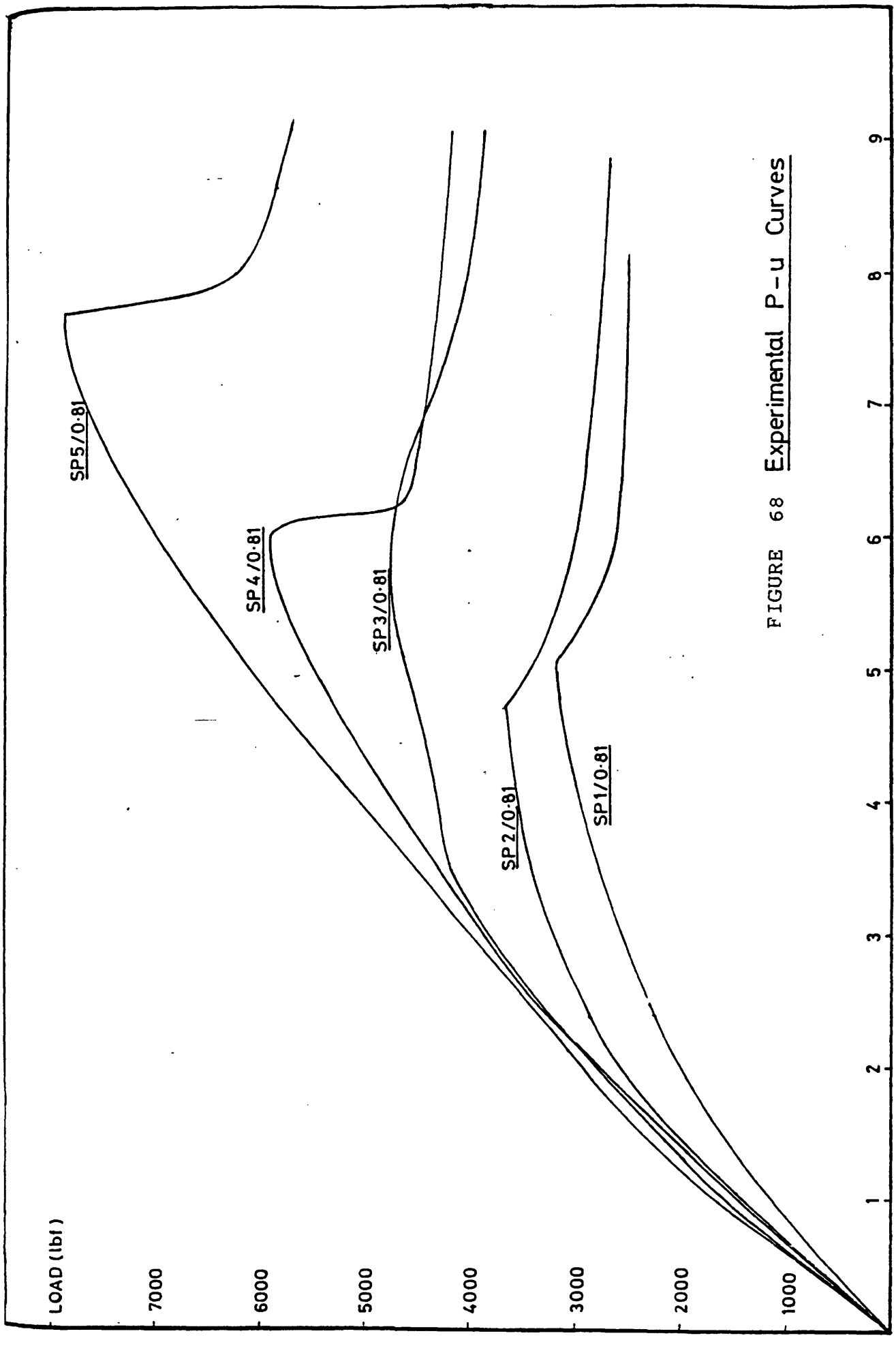

FIGURE 68 Experimental P-u Curves

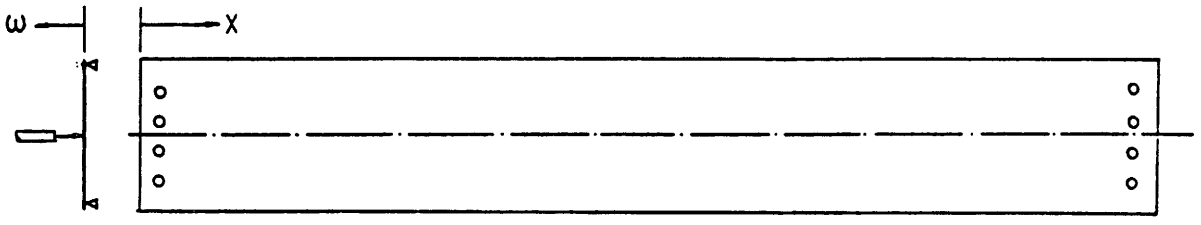
ω
X

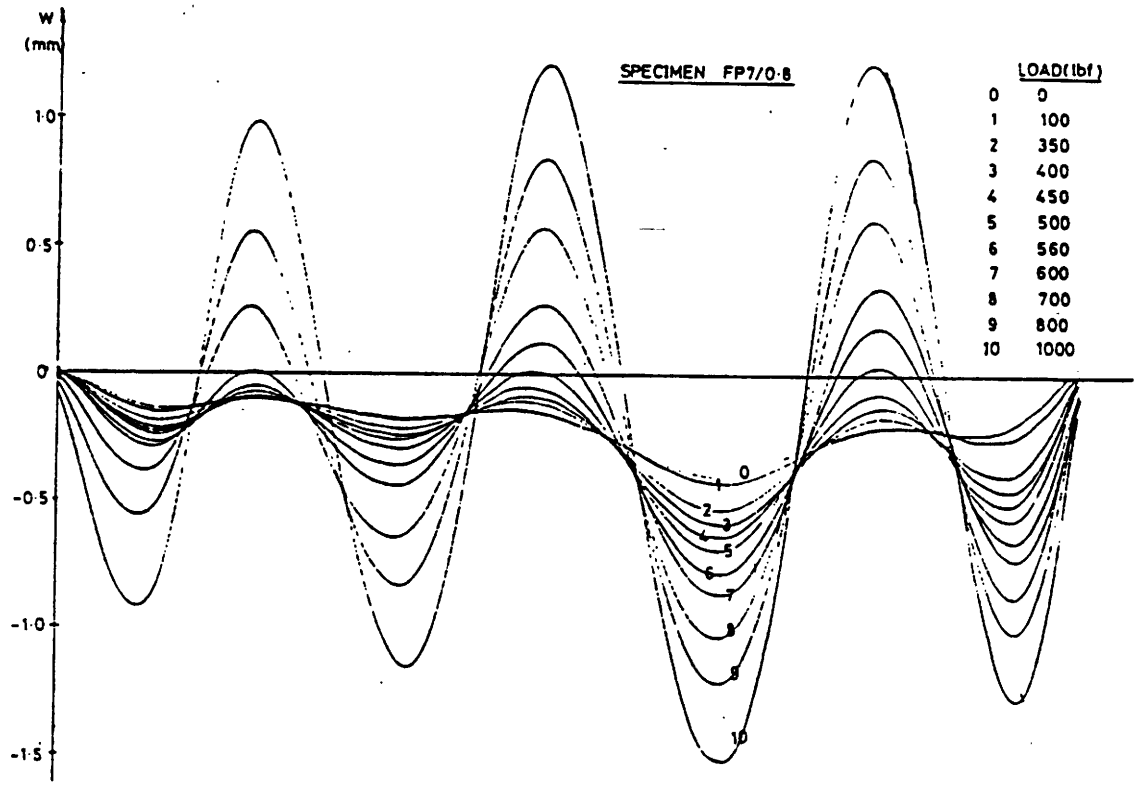
w
(mm)
1·0
0·5
0
-0·5
-1·0
-1·5
SPECIMEN FP7/0·8
LOAD(lbf)
0 0
1 100
2 350
3 400
4 450
5 500
6 560
7 600
8 700
9 800
10 1000

FIGURE 69

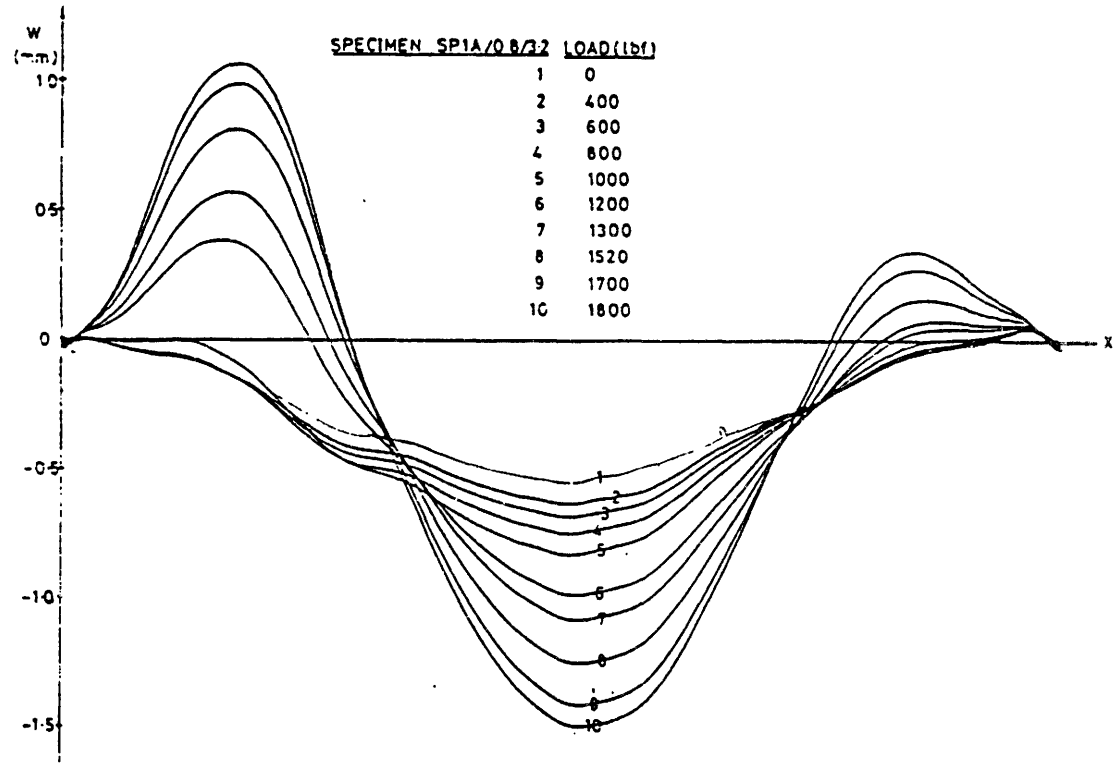
W
(mm)
SPECIMEN SP1A/0·8/3·2
LOAD (lbf)
1 0
2 400
3 600
4 800
5 1000
6 1200
7 1300
8 1520
9 1700
10 1800
X

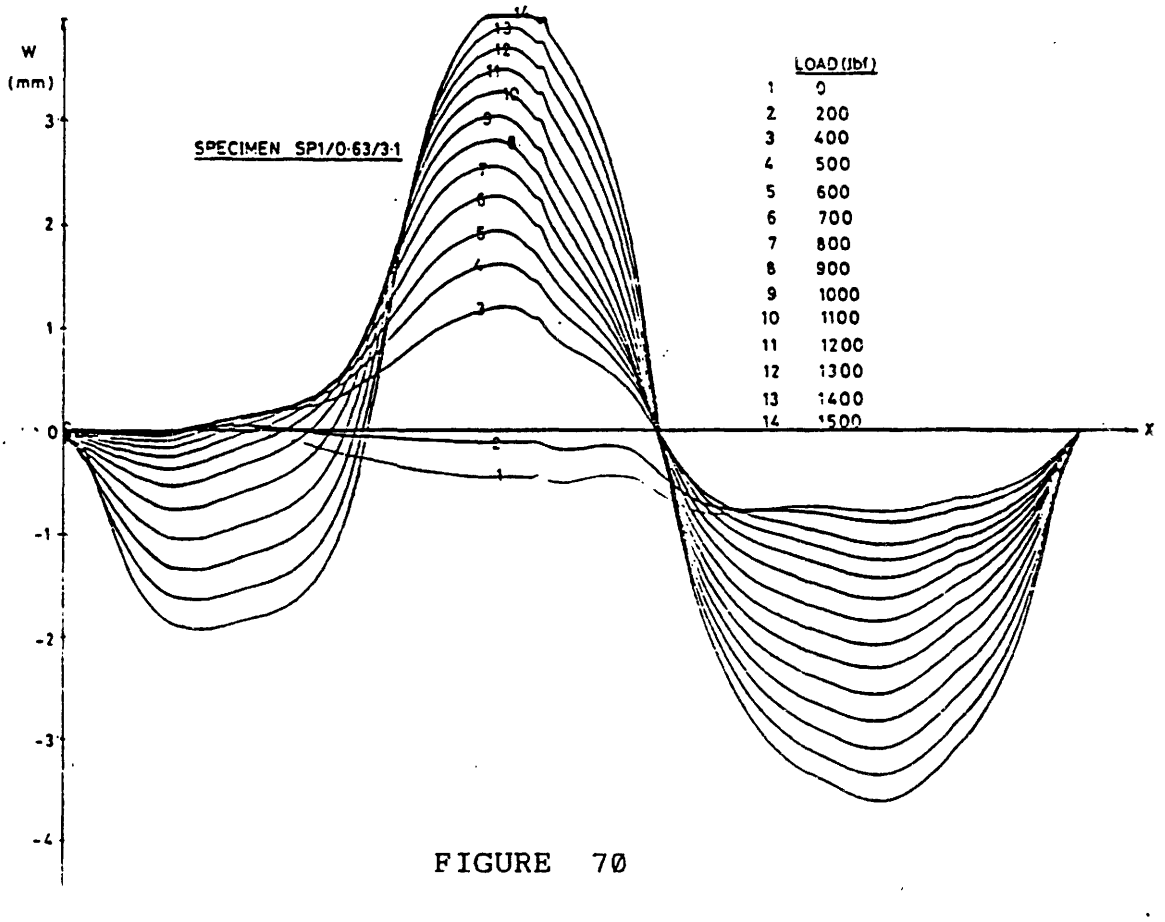
W
(mm)
SPECIMEN SP1/0·63/3·1
LOAD (lbf)
1 0
2 200
3 400
4 500
5 600
6 700
7 800
8 900
9 1000
10 1100
11 1200
12 1300
13 1400
14 1500
X

FIGURE 70

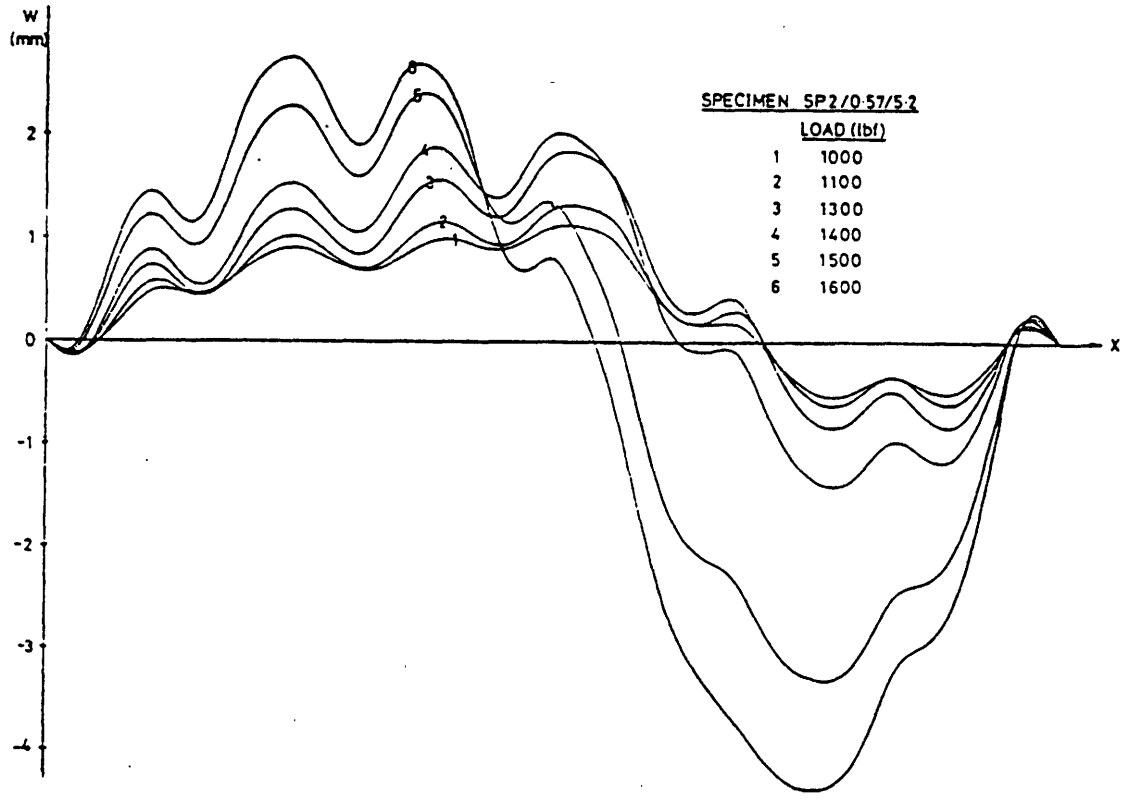
w
(mm)
2
1
0
-1
-2
-3
-4
x
SPECIMEN SP2/0·57/5·2
LOAD (lbf)
1 1000
2 1100
3 1300
4 1400
5 1500
6 1600

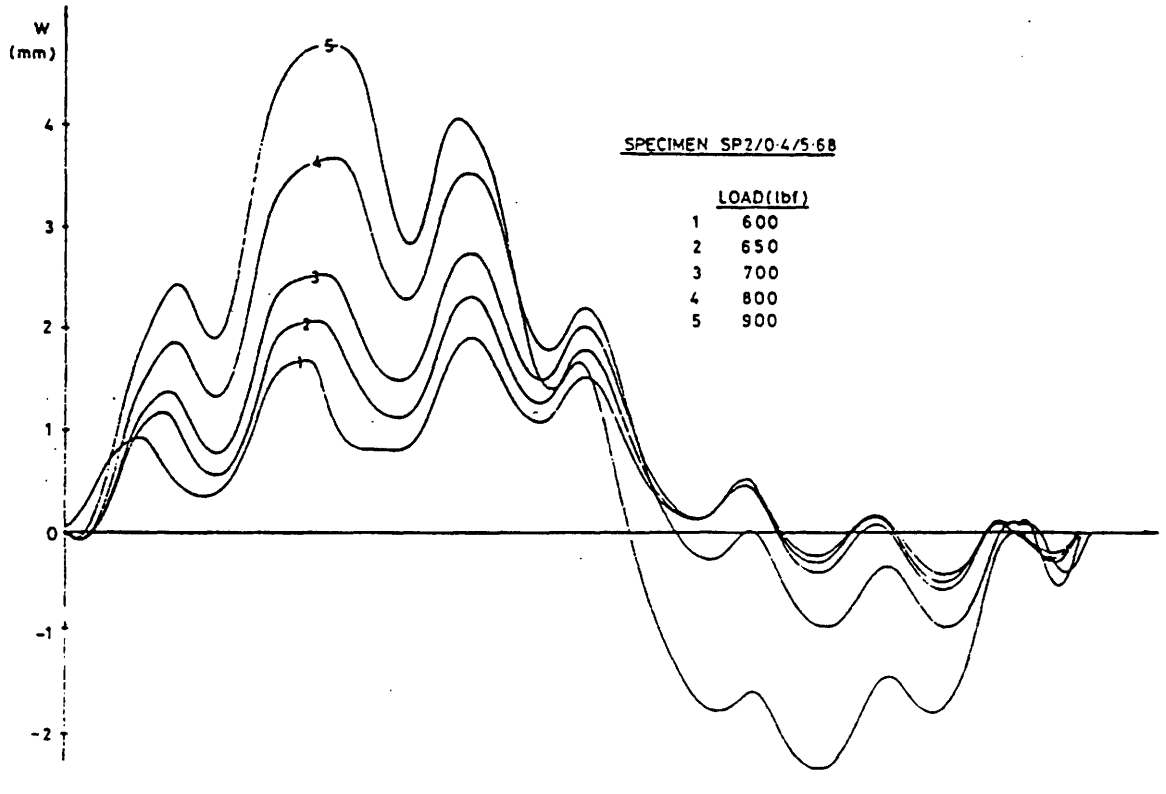
w
(mm)
4
3
2
1
0
-1
-2
SPECIMEN SP2/0·4/5·68
LOAD(lbf)
1 600
2 650
3 700
4 800
5 900

FIGURE 71

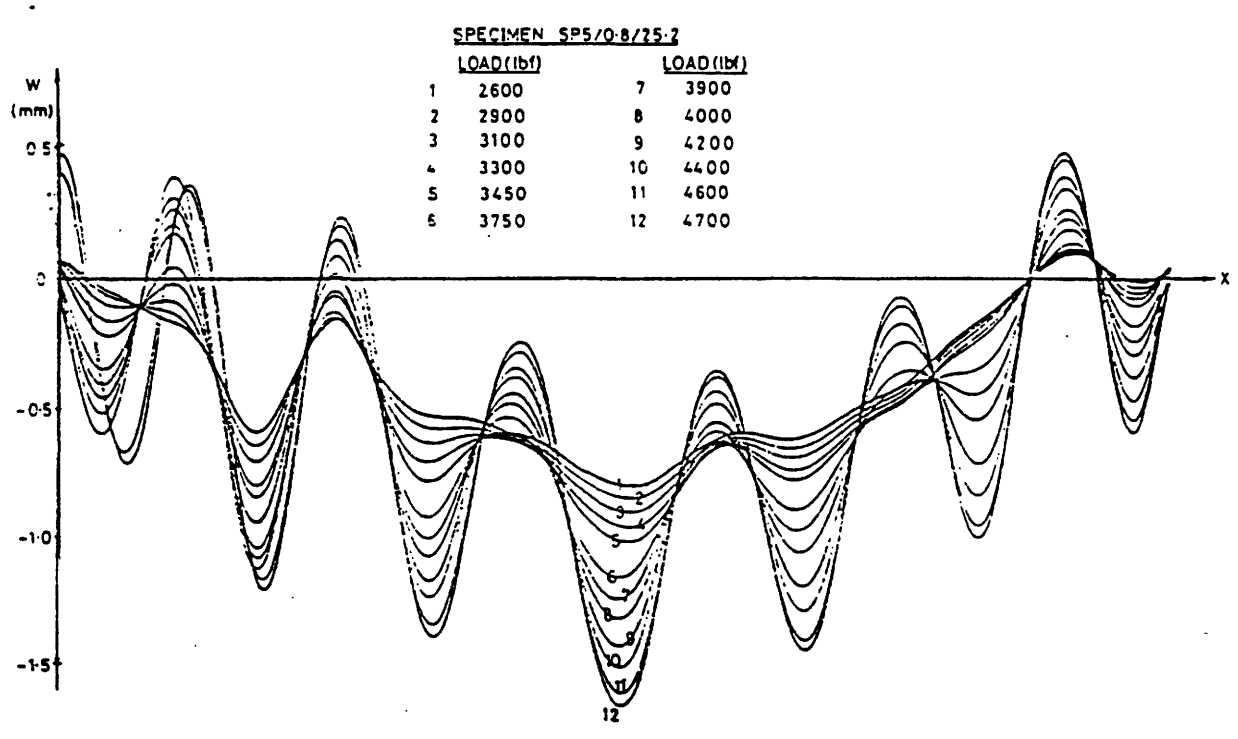
SPECIMEN SP5/0·8/25·2
LOAD (lbf)
1 2600
2 2900
3 3100
4 3300
5 3450
6 3750
7 3900
8 4000
9 4200
10 4400
11 4600
12 4700
w (mm)
0·5
0
-0·5
-1·0
-1·5
x

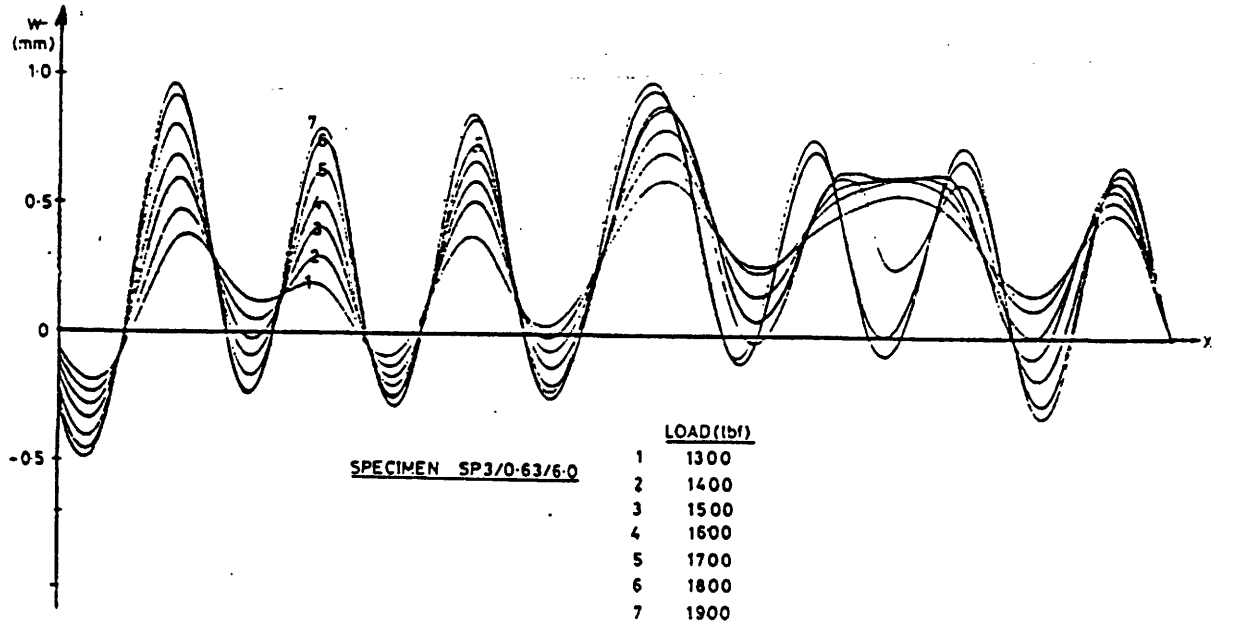
w (mm)
1·0
0·5
0
-0·5
x
SPECIMEN SP3/0·63/6·0
LOAD (lbf)
1 1300
2 1400
3 1500
4 1600
5 1700
6 1800
7 1900

FIGURE 72

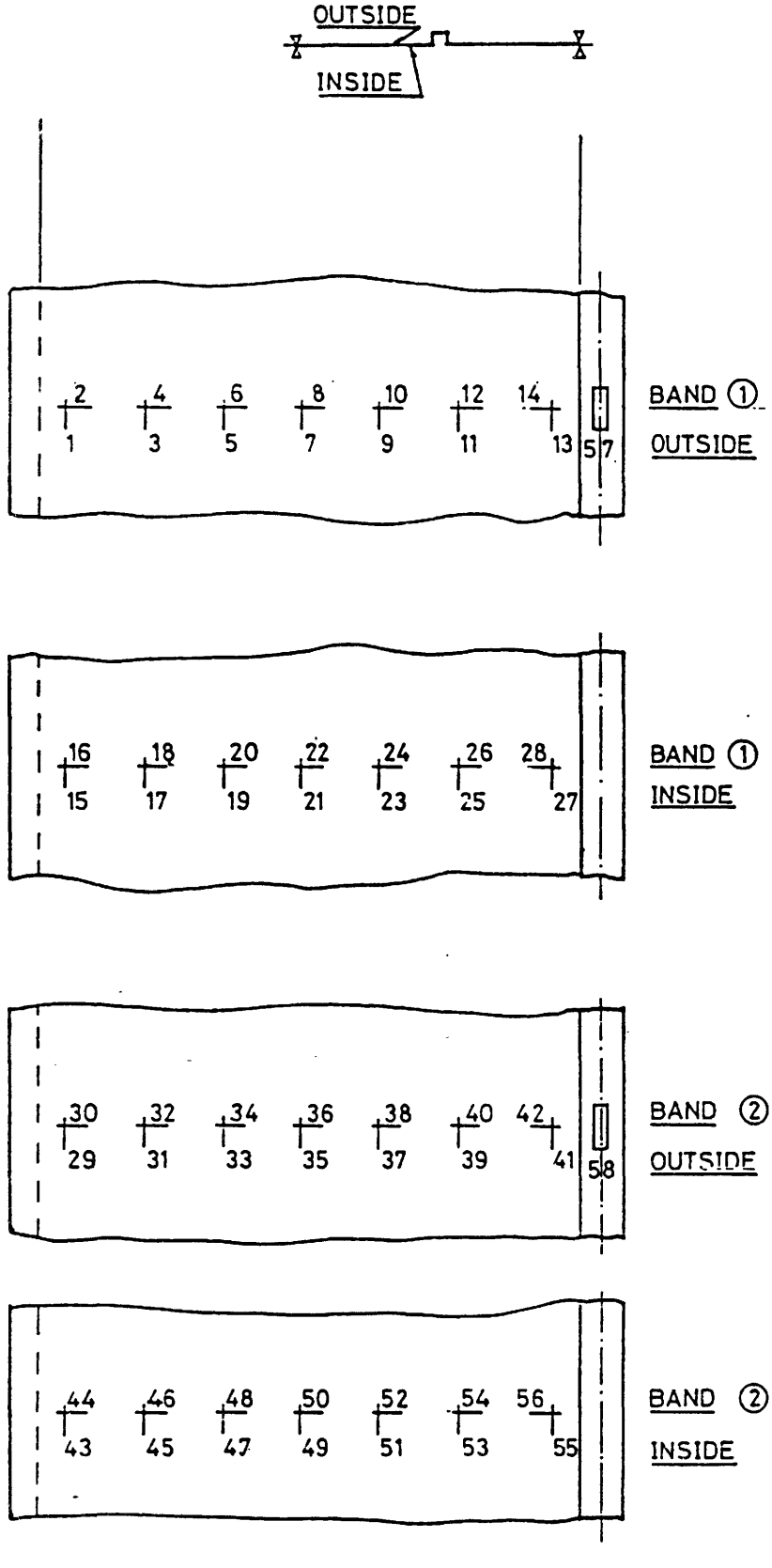

LAYOUT OF STRAIN GAUGES

FIGURE 73

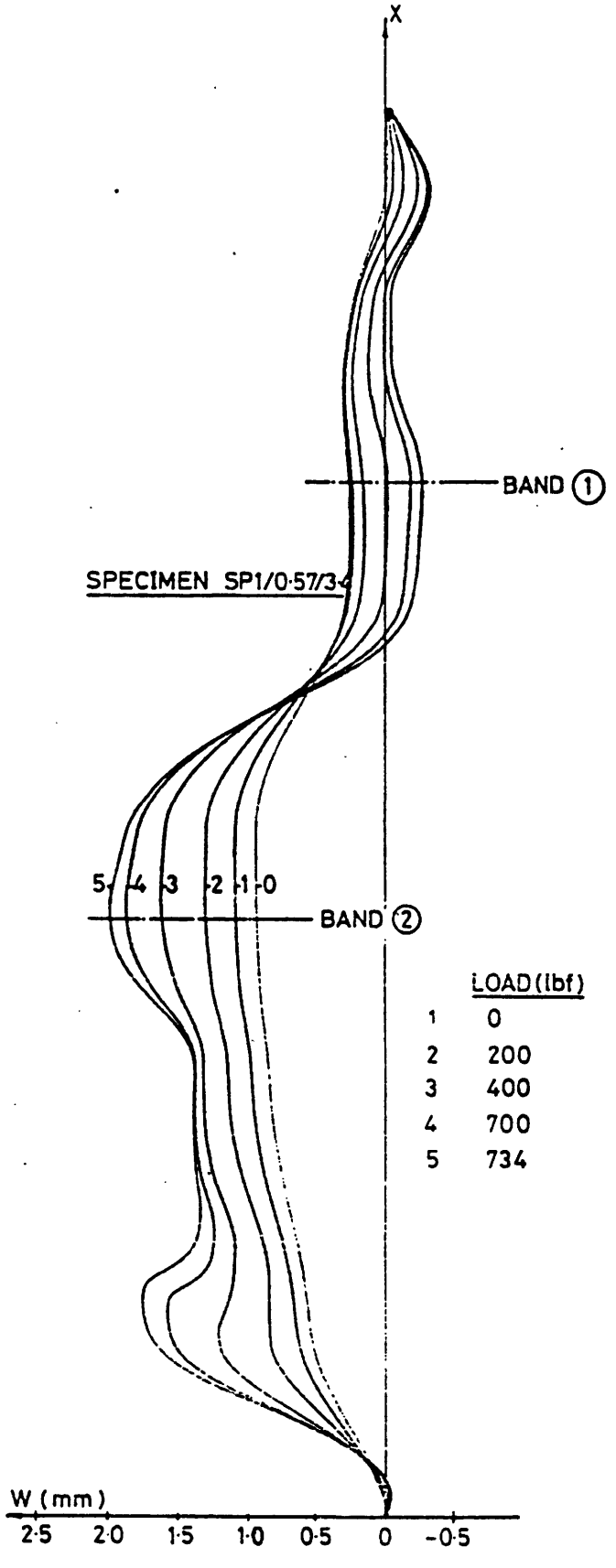

FIGURE 74. DEFLECTIONS ALONG STRAIN GAUGED SPECIMEN

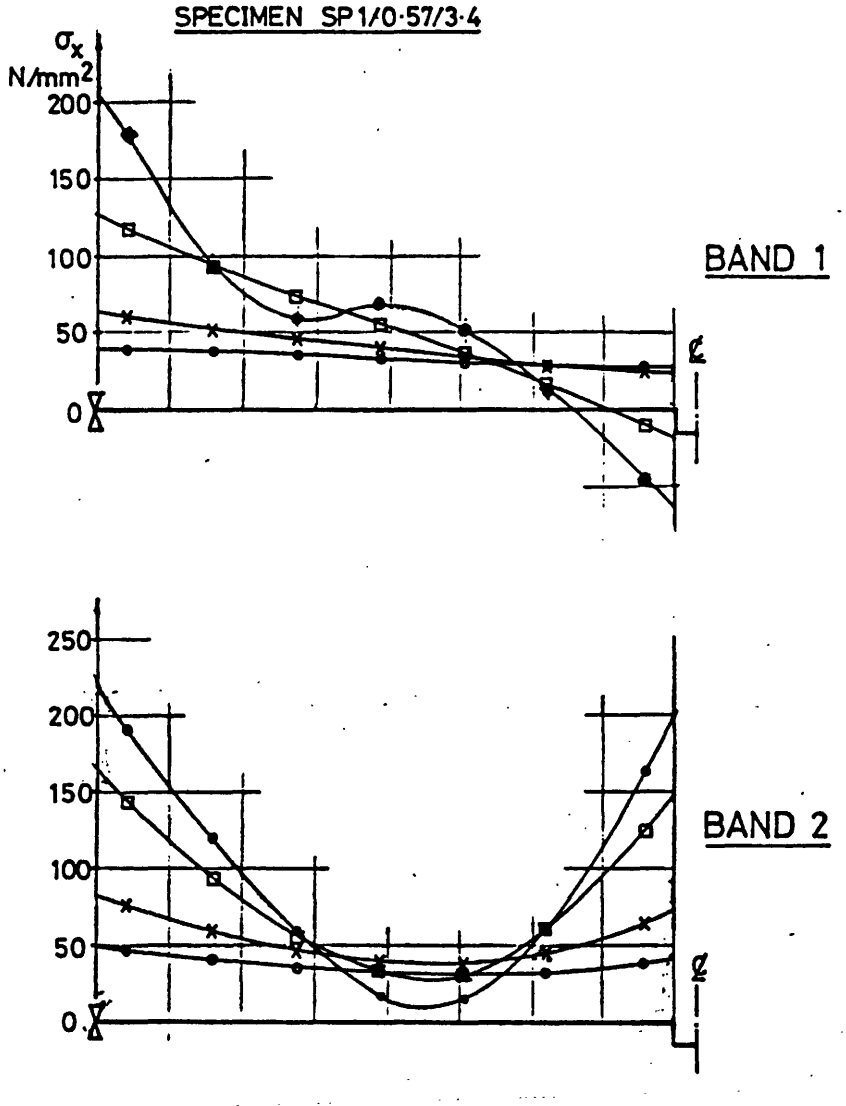

LONGITUDINAL MEMBRANE STRESS DISTRIBUTION

FIGURE 75

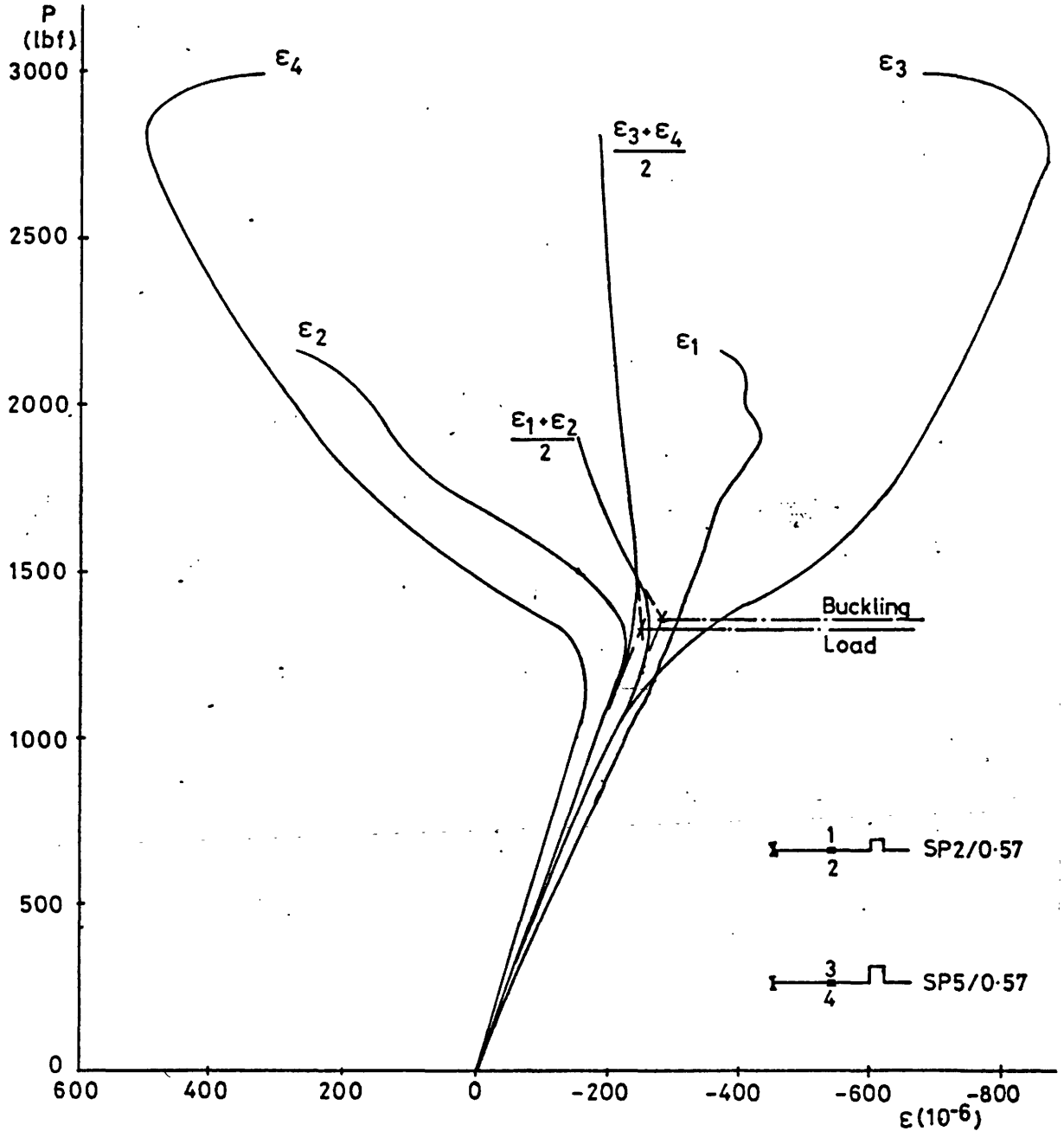
P
(lbf)
3000
2500
2000
1500
1000
500
0
600
400
200
0
-200
-400
-600
-800
ε(10⁻⁶)
ε4
ε3
ε3+ε4
2
ε2
ε1
ε1+ε2
2
Buckling
Load
1
2
SP2/0·57
3
4
SP5/0·57

FIGURE 76

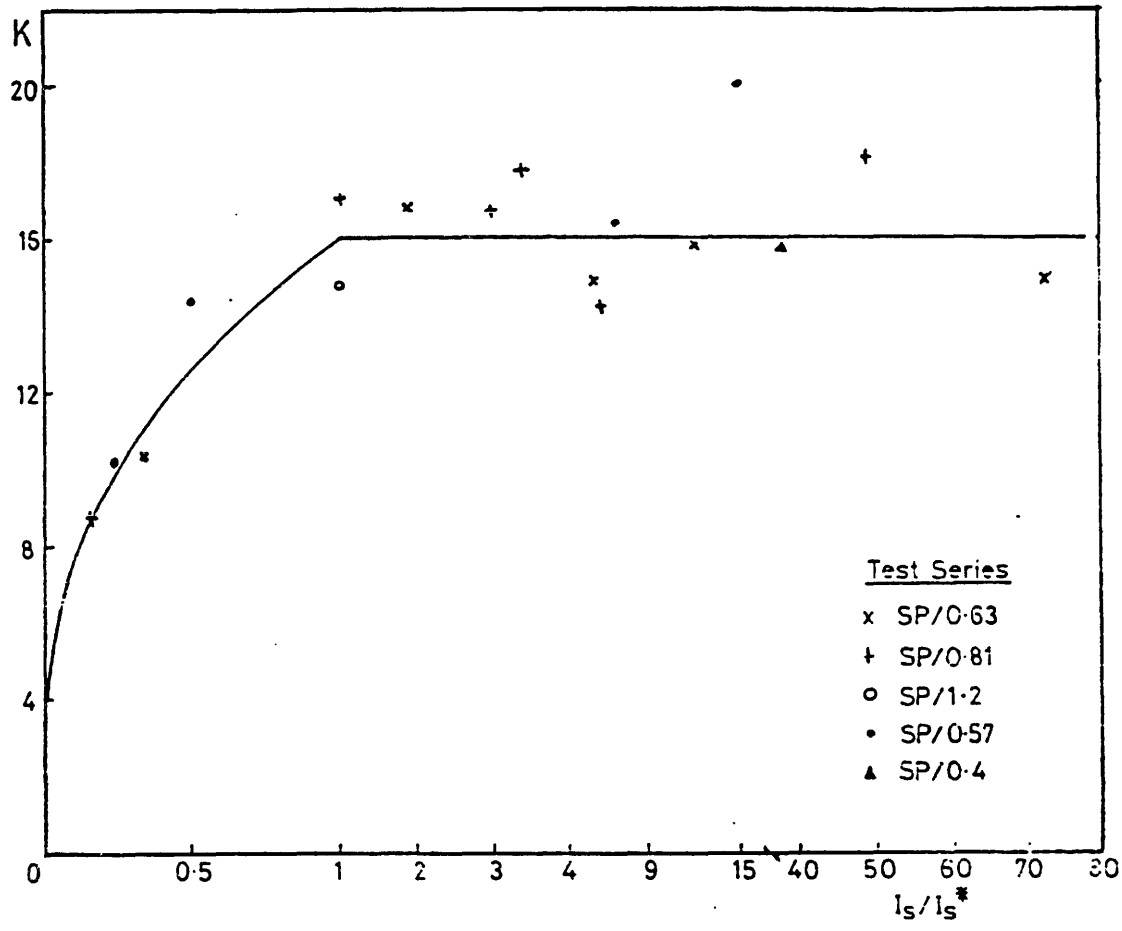

FIGURE 77

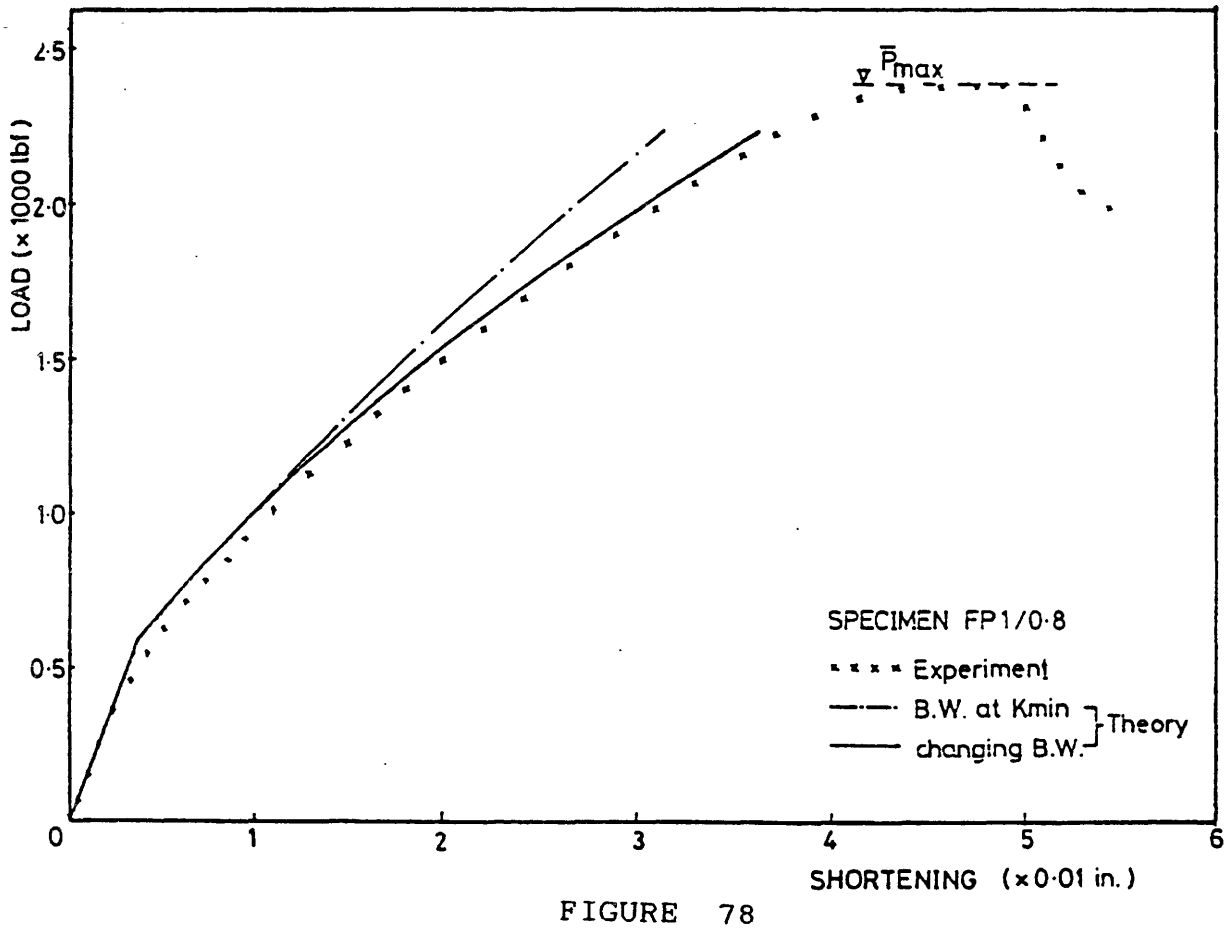

FIGURE 78

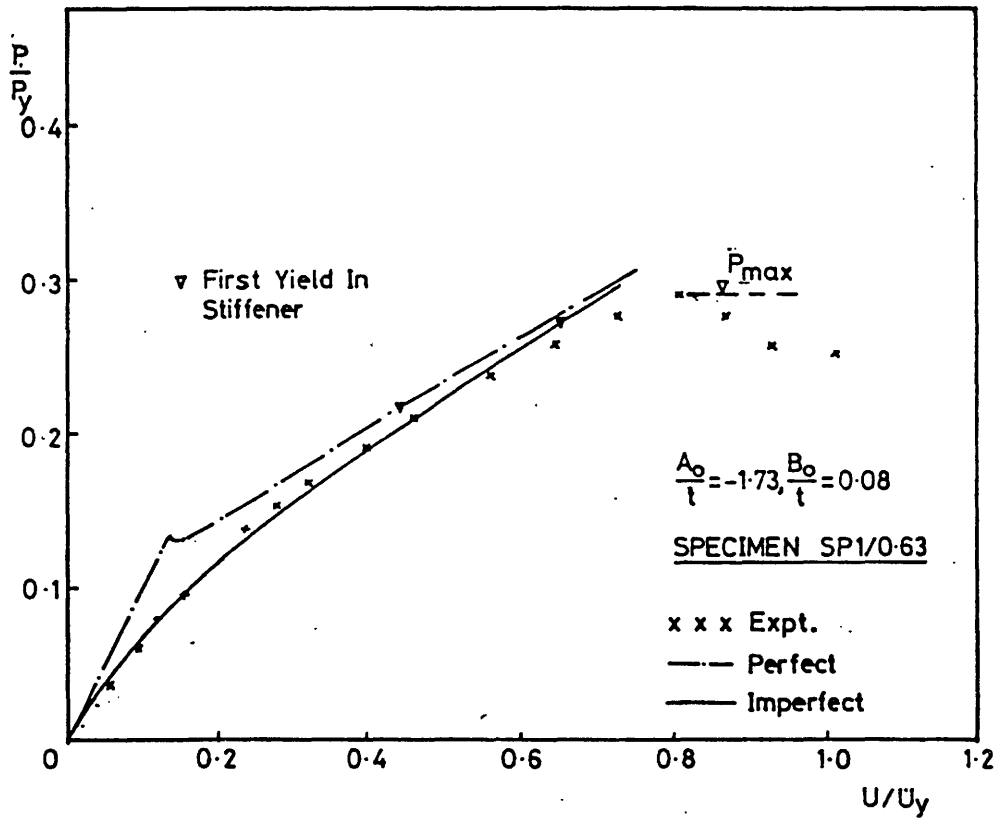

FIGURE 79

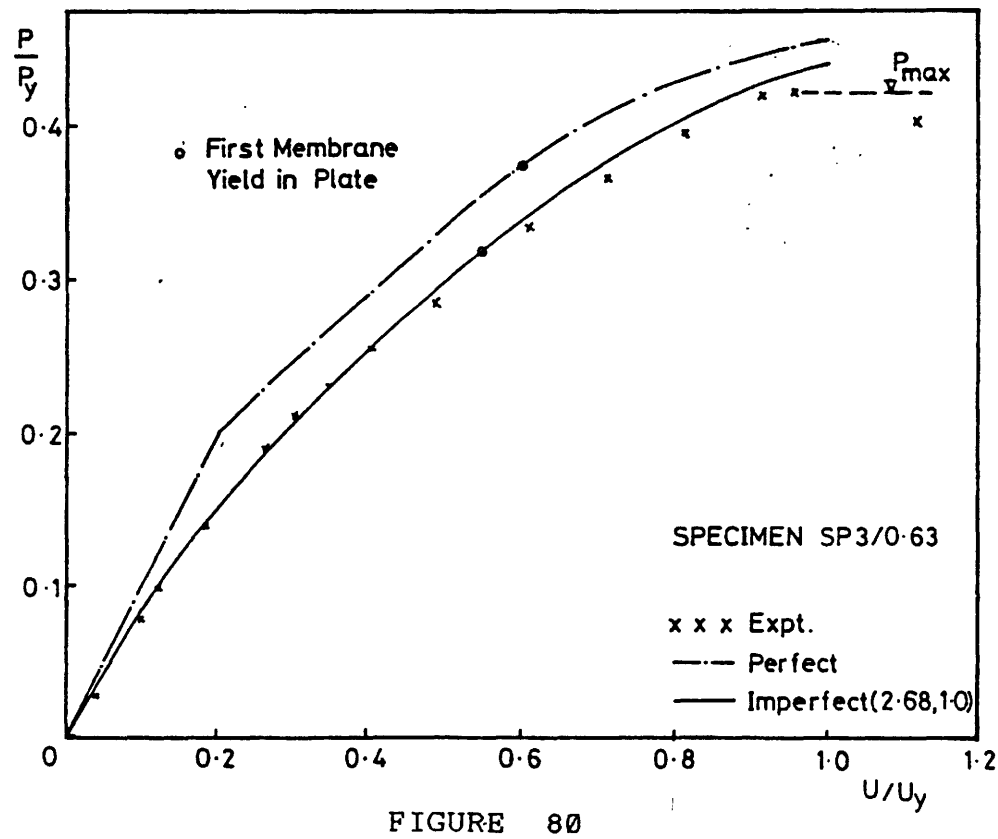

FIGURE 80

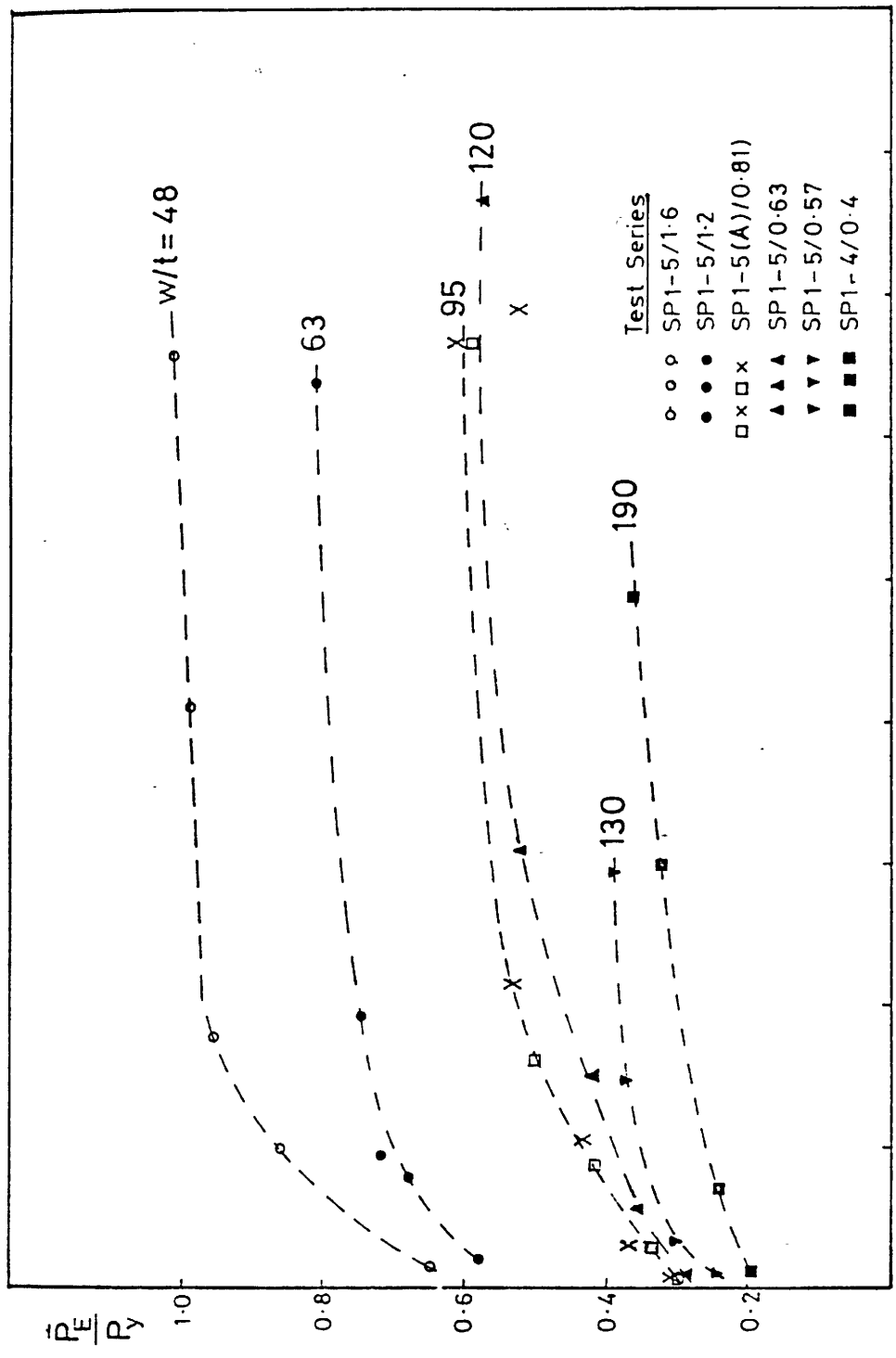
$\frac{\tilde{P}_E}{P_y}$
1·0
0·8
0·6
0·4
0·2
0
1·0
2·0
3·0
4·0
5·0
10·0
15·0
20·0
$I_p / I_{padequate}$
w/t = 48
63
95
120
130
190
Test Series
SP1-5/1·6
SP1-5/1·2
SP1-5(A)/0·81)
SP1-5/0·63
SP1-5/0·57
SP1-4/0·4

Fig. 81

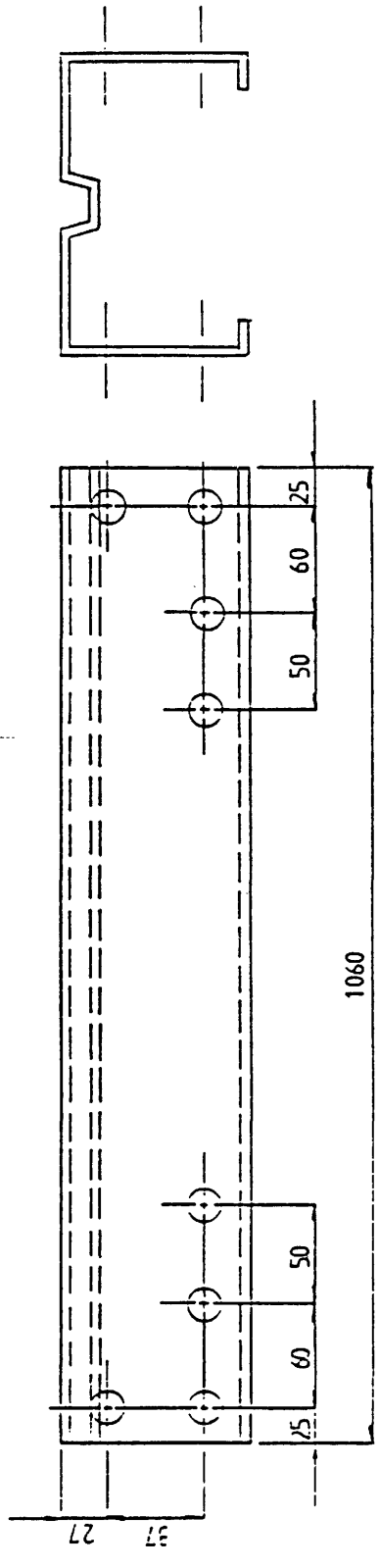

FIGURE 82 BEAM SPECIMEN.

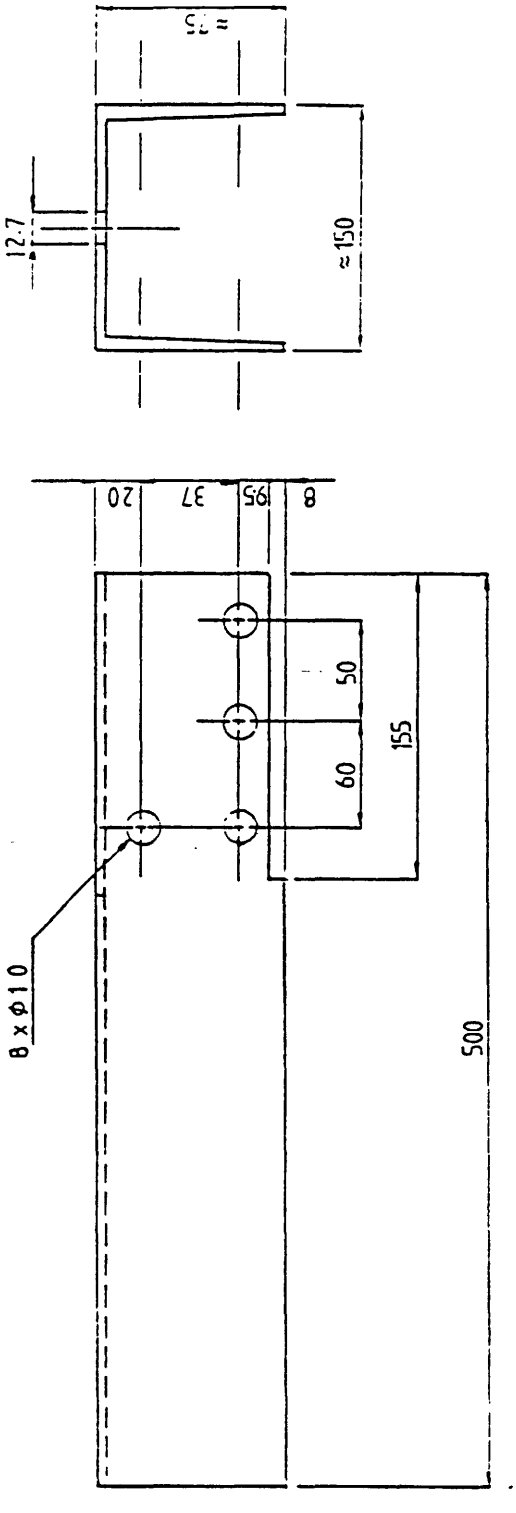

FIGURE 83 END EXTENSION.

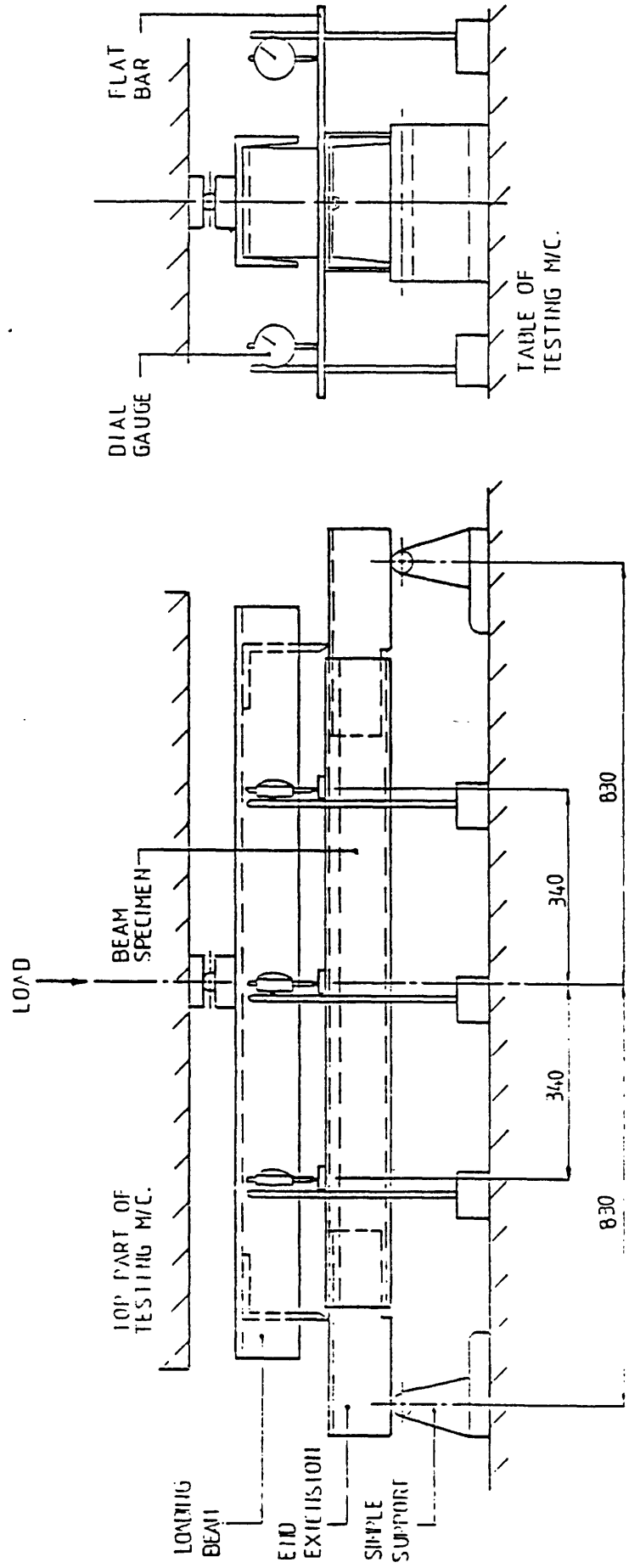

FIGURE 84 GENERAL SET-UP OF TEST RIG.

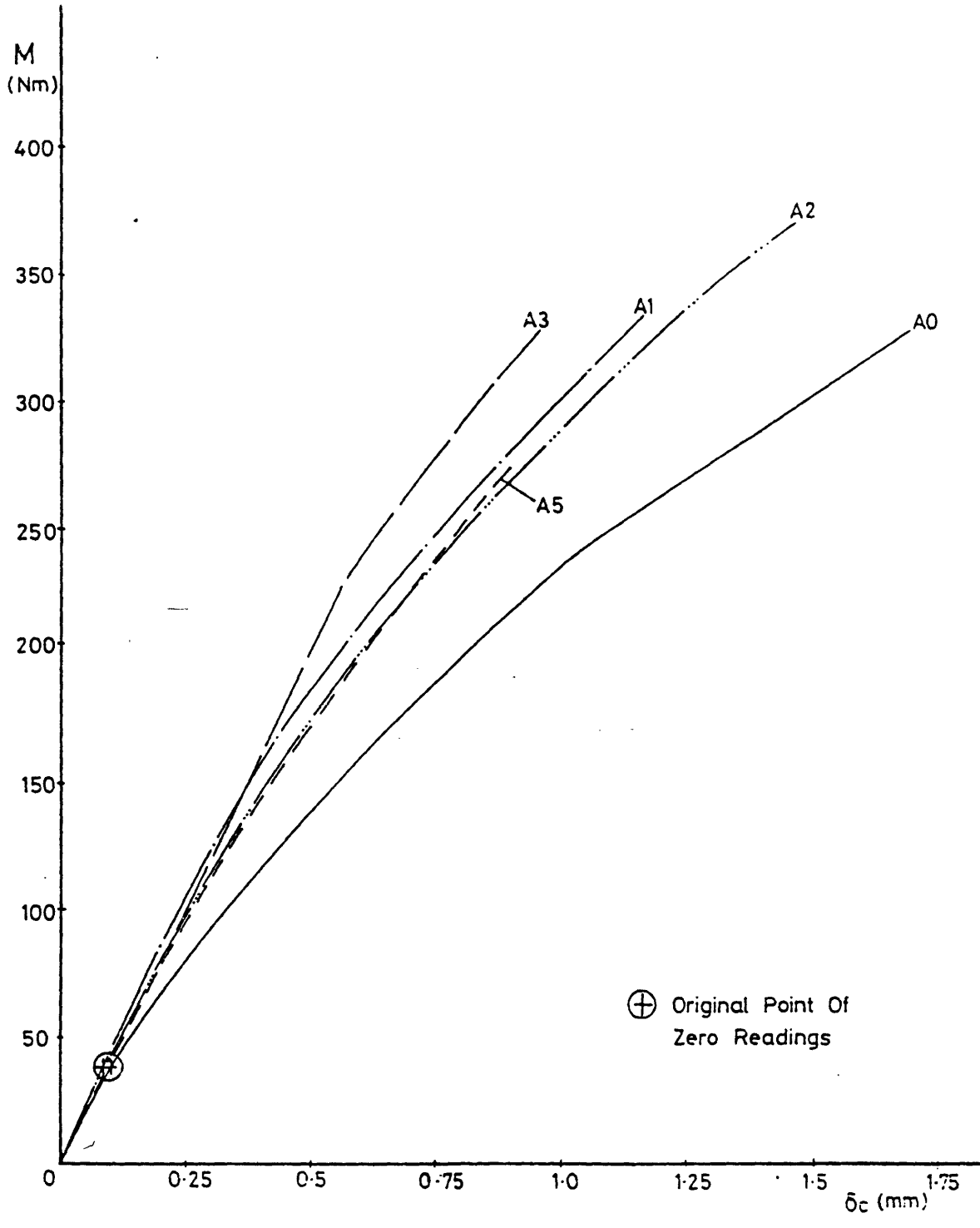

FIGURE 85 Experimental M–δ_c Curves

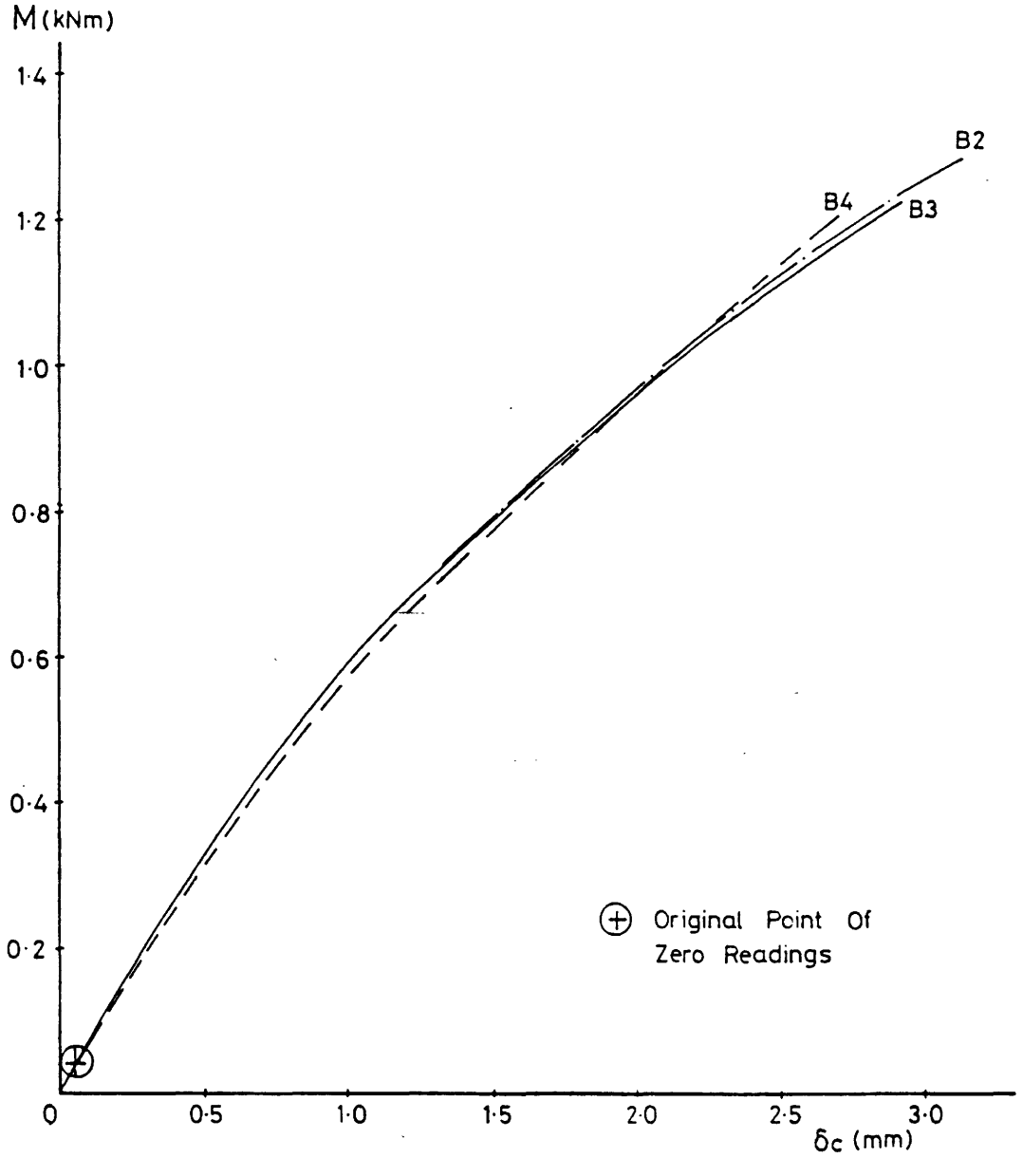

FIGURE 86 Experimental M–δ_c Curves

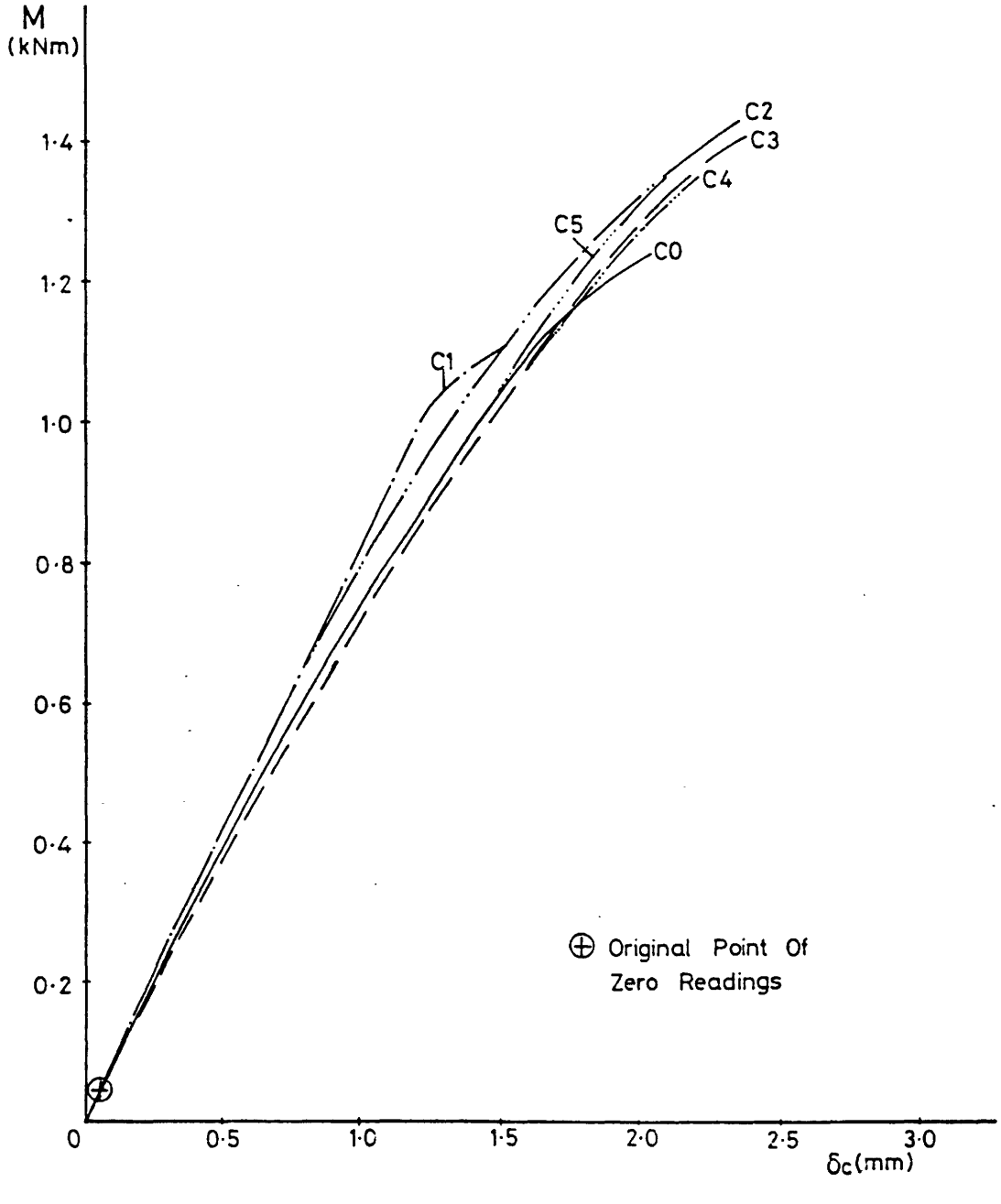

FIGURE 87 Experimental M–δc Curves

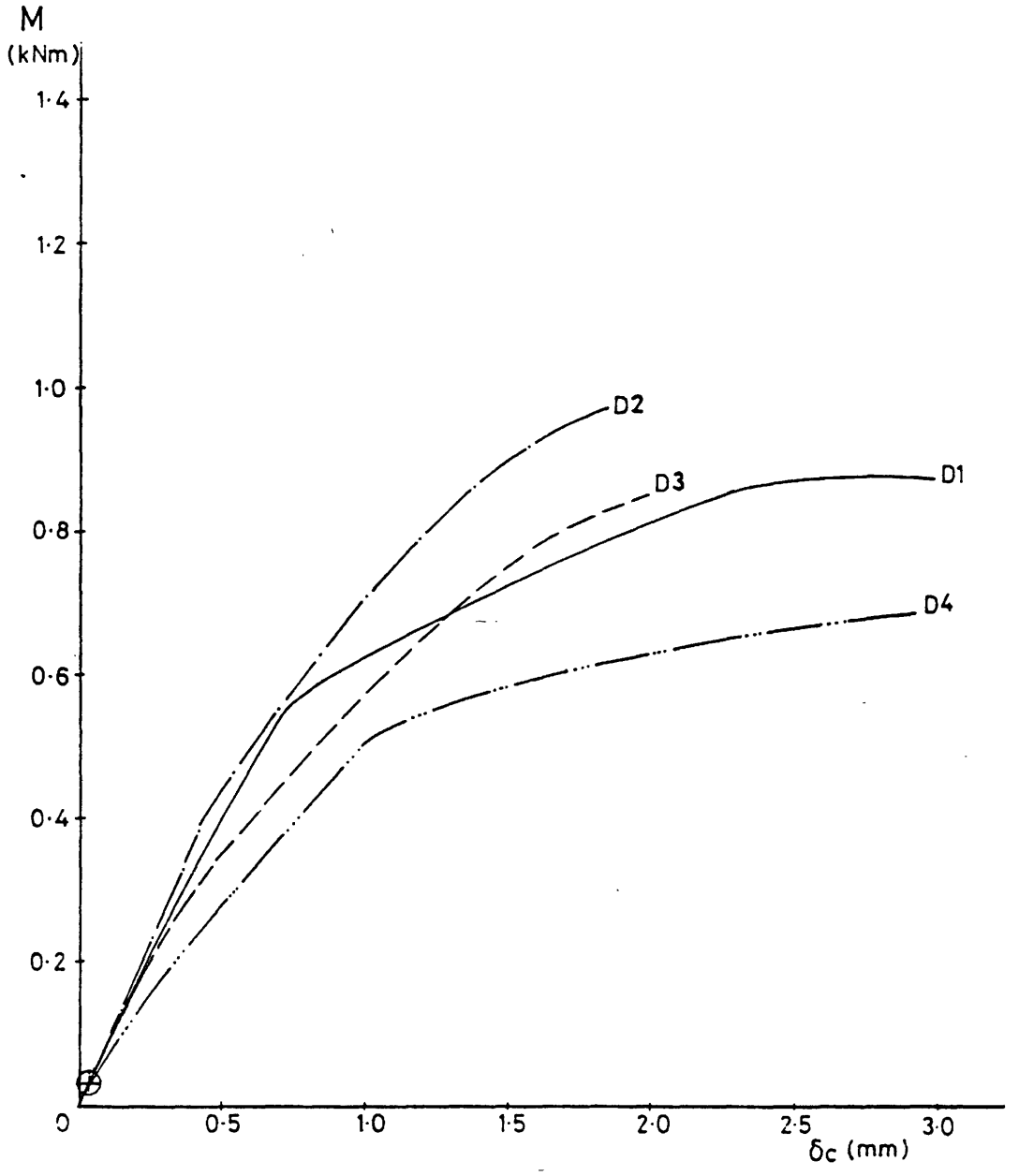

FIGURE 88 Experimental M–δ_c Curves

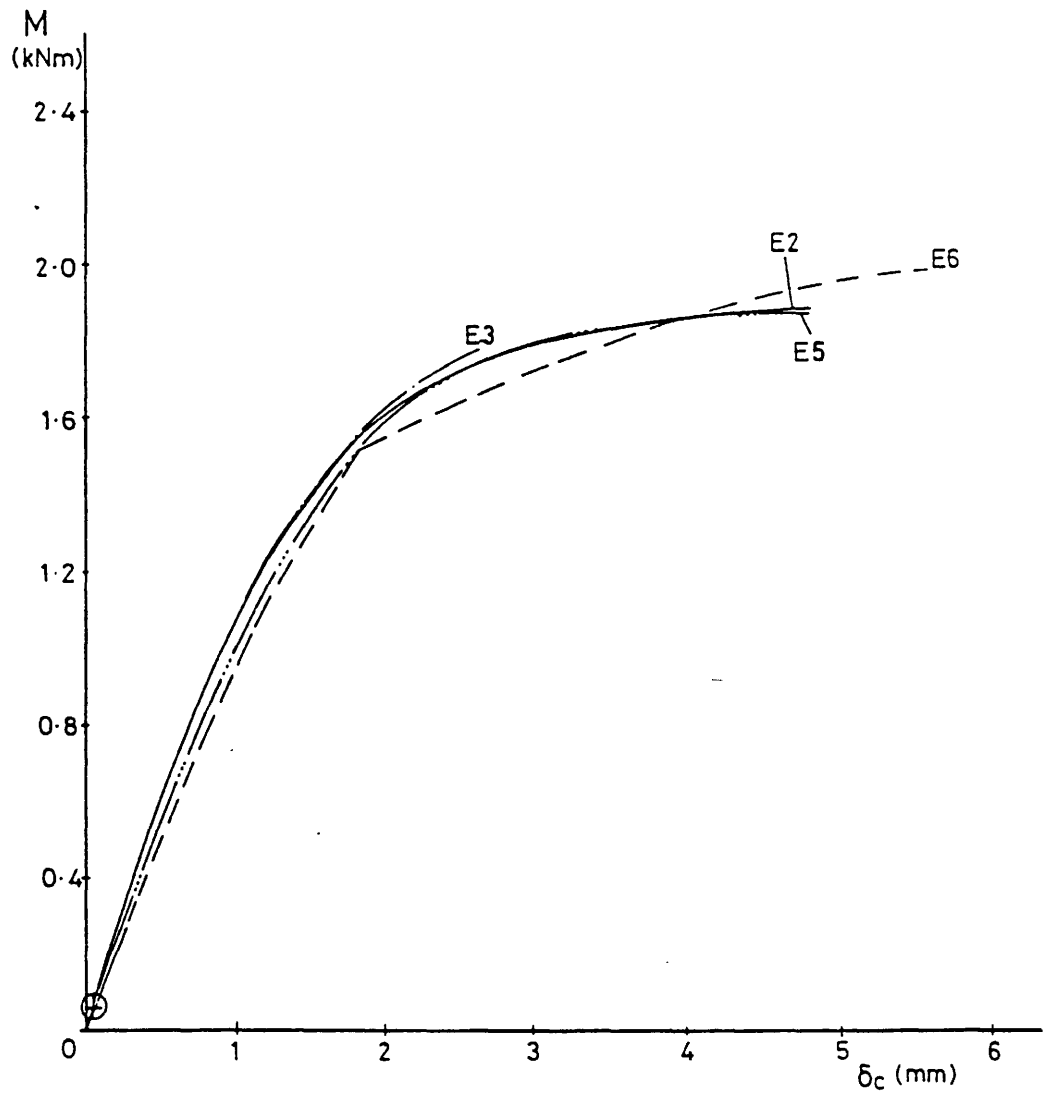

FIGURE 89 Experimental M–δ_c Curves

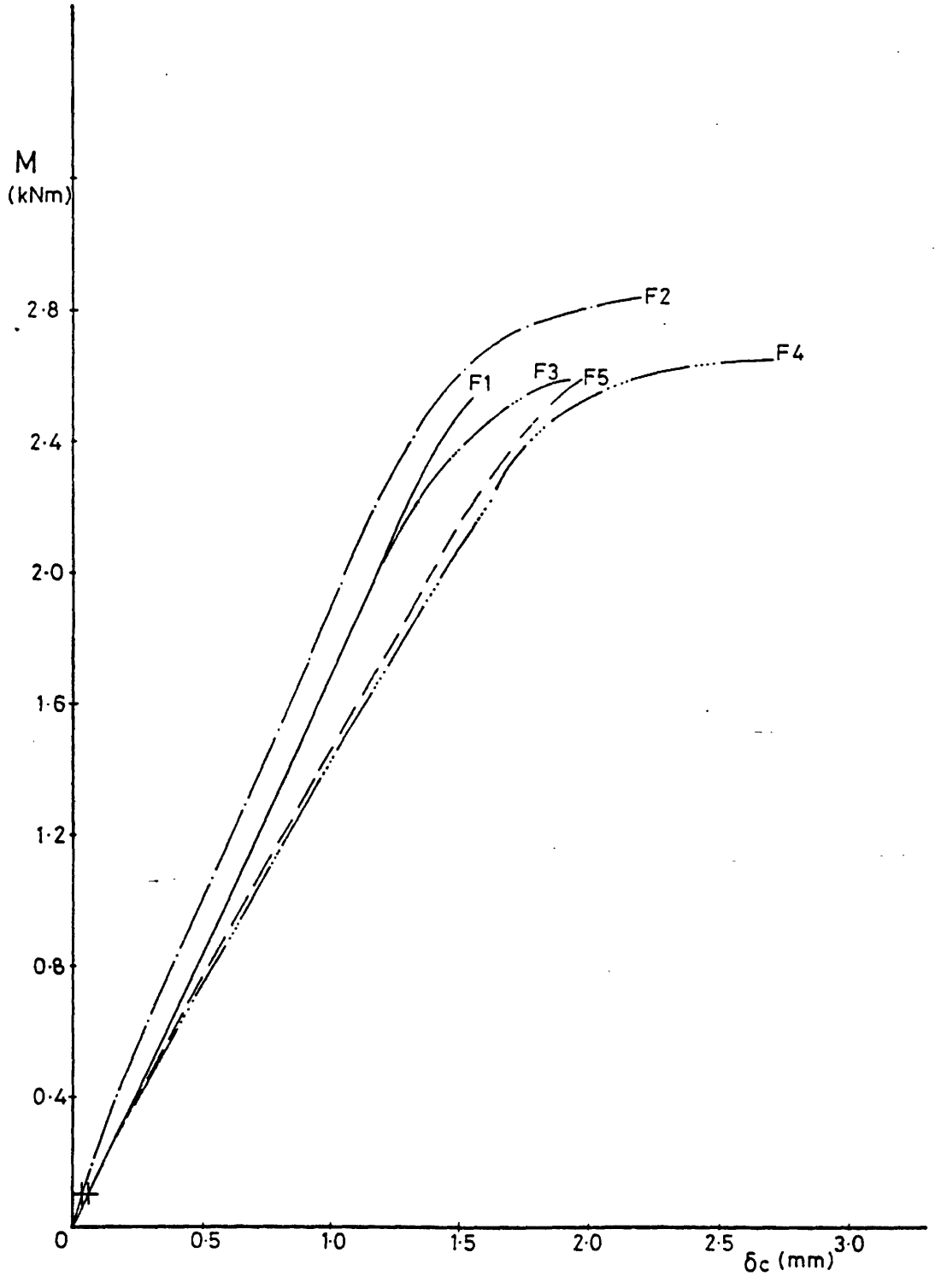

FIGURE 90 Experimental M–δ_c Curves

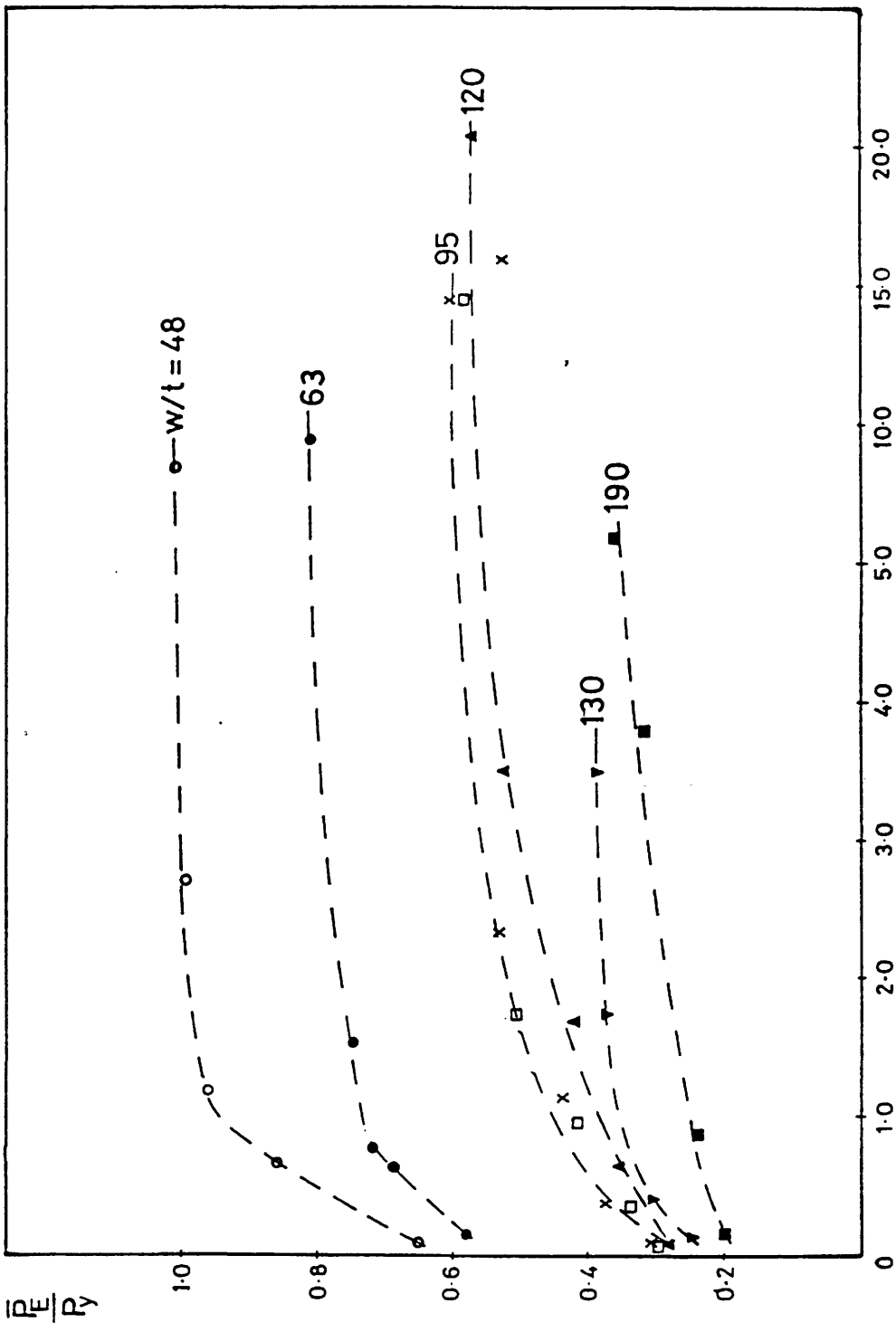
W/t = 48
63
95
120
130
190
$\frac{P_E}{P_y}$
I_p / I_{padeq}
0
1·0
2·0
3·0
4·0
5·0
10·0
15·0
20·0
0·2
0·4
0·6
0·8
1·0

FIGURE 91

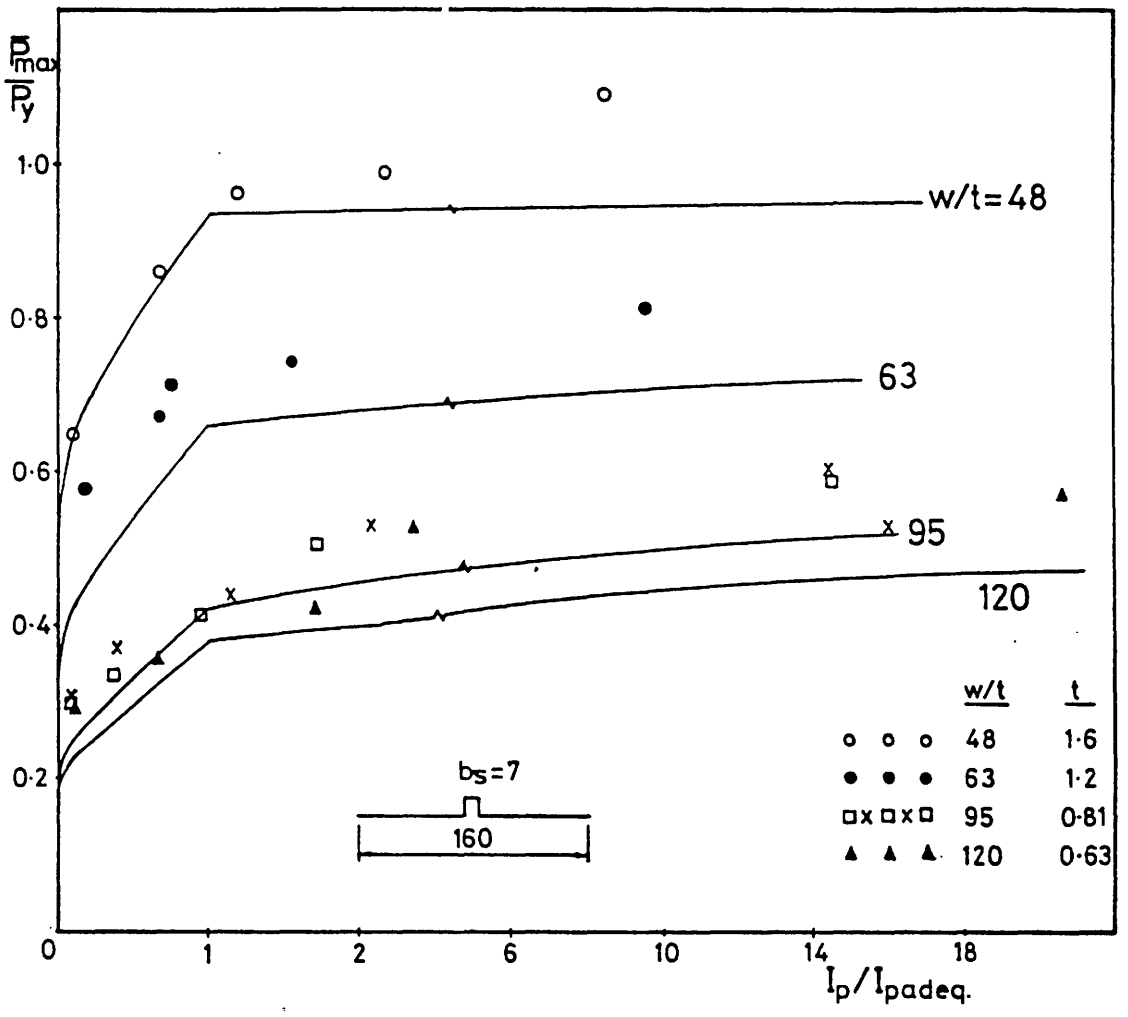

FIGURE 92

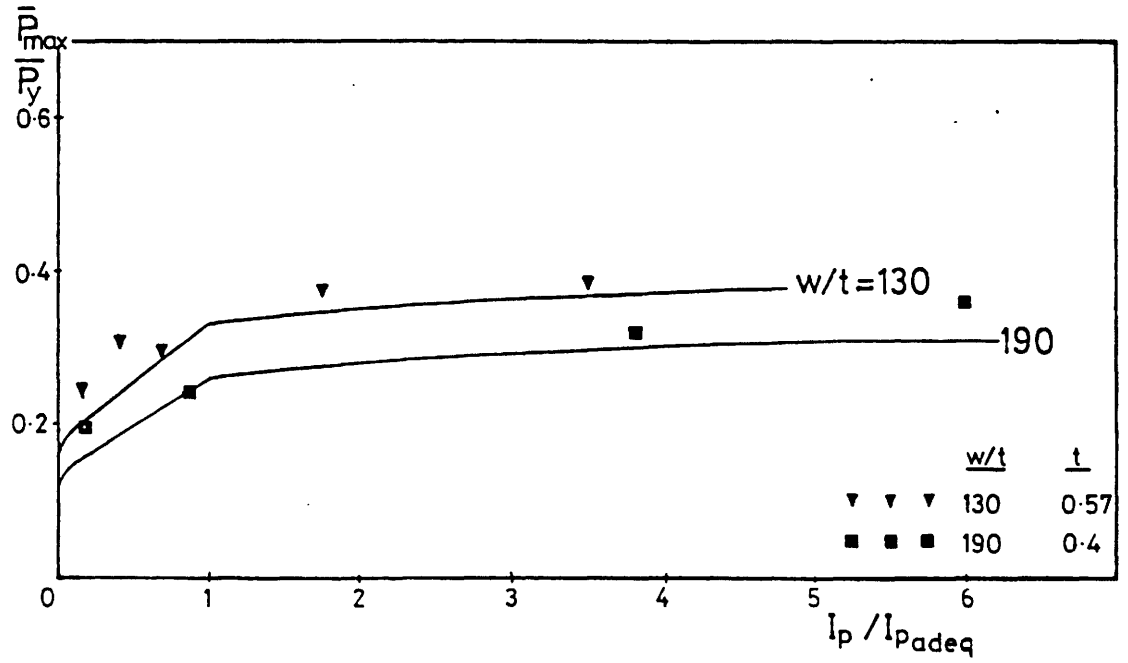

FIGURE 93

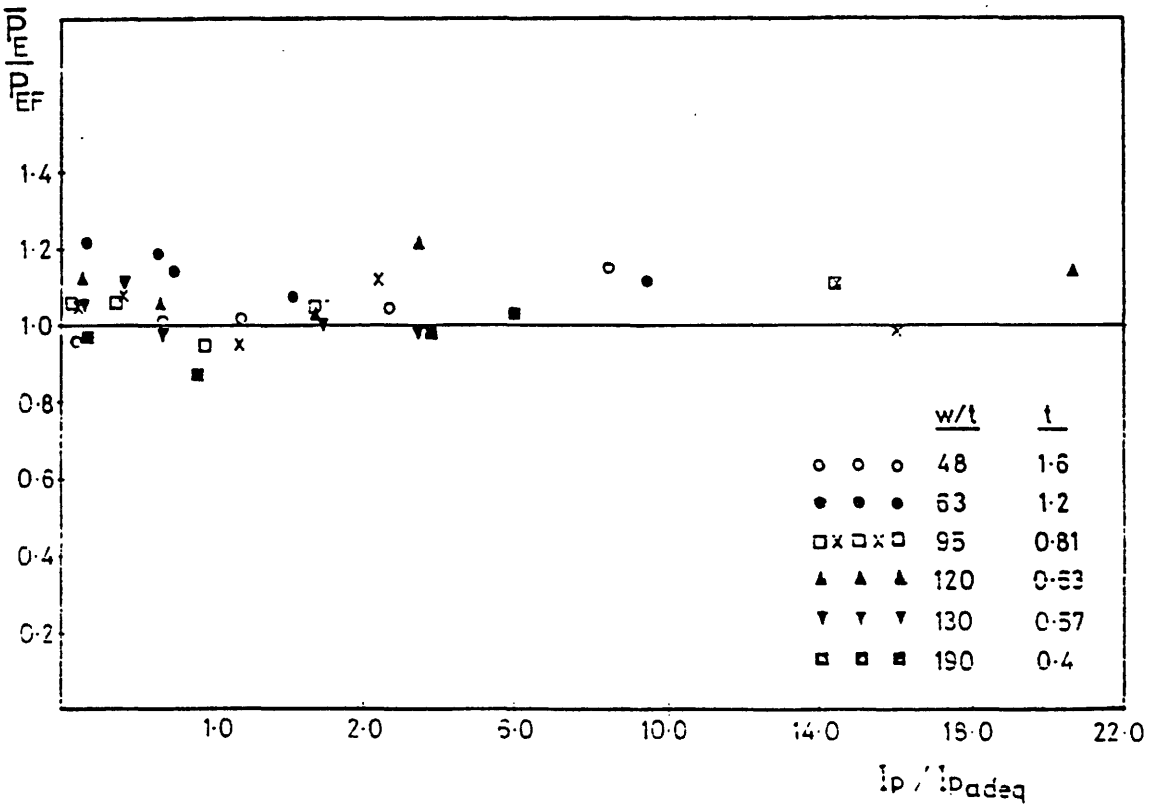

FIGURE 94 Comparison with Present Analysis

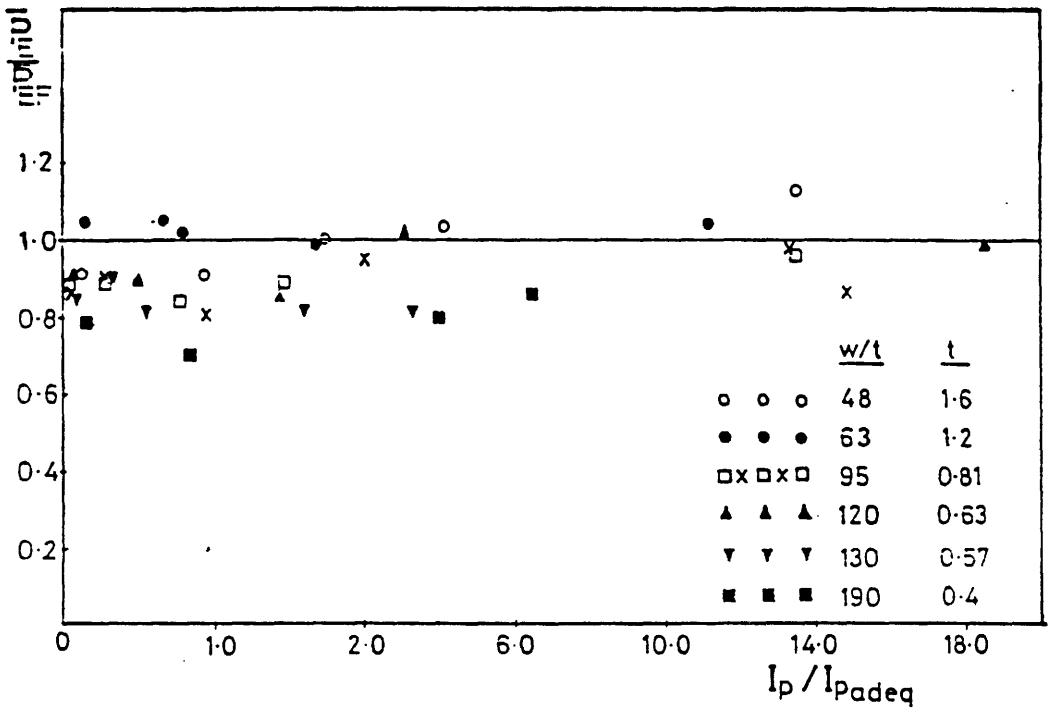

FIGURE 95 Comparison with Desmond's Analysis

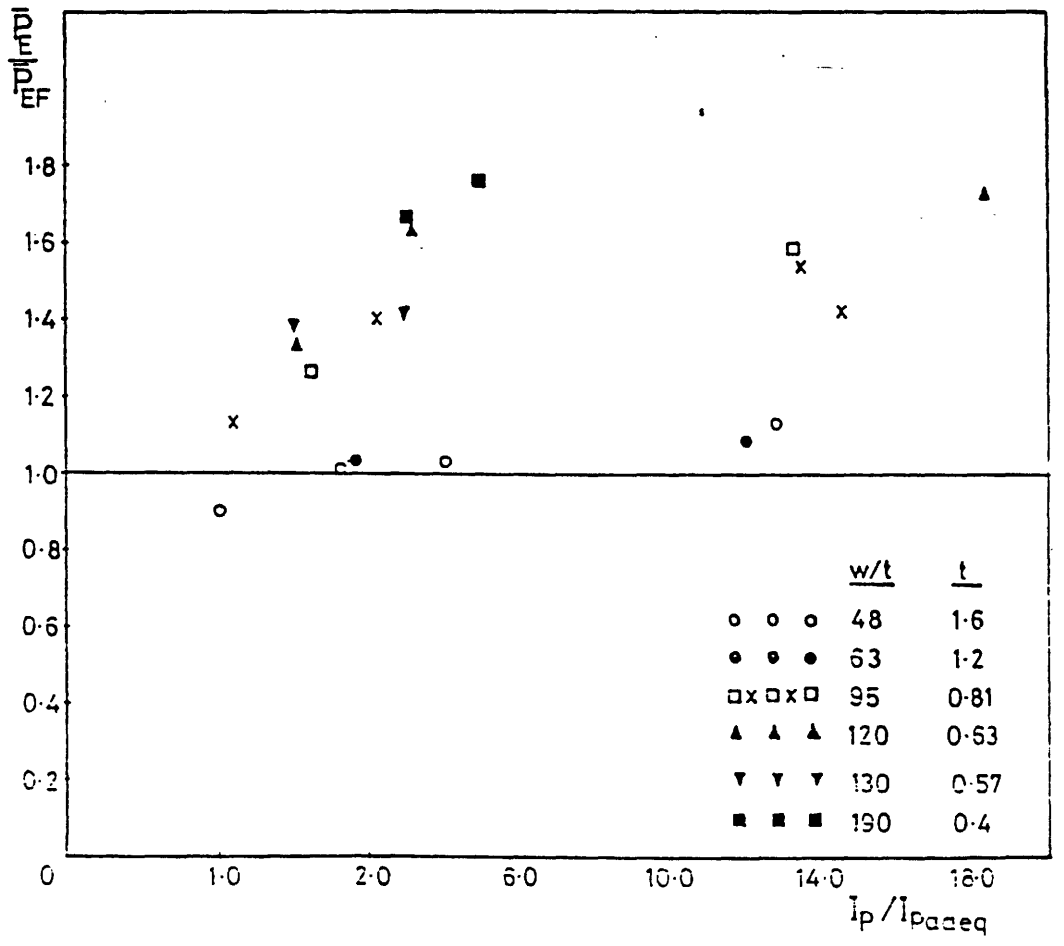

FIGURE 96 Comparison with BS 5950 Pt. 5

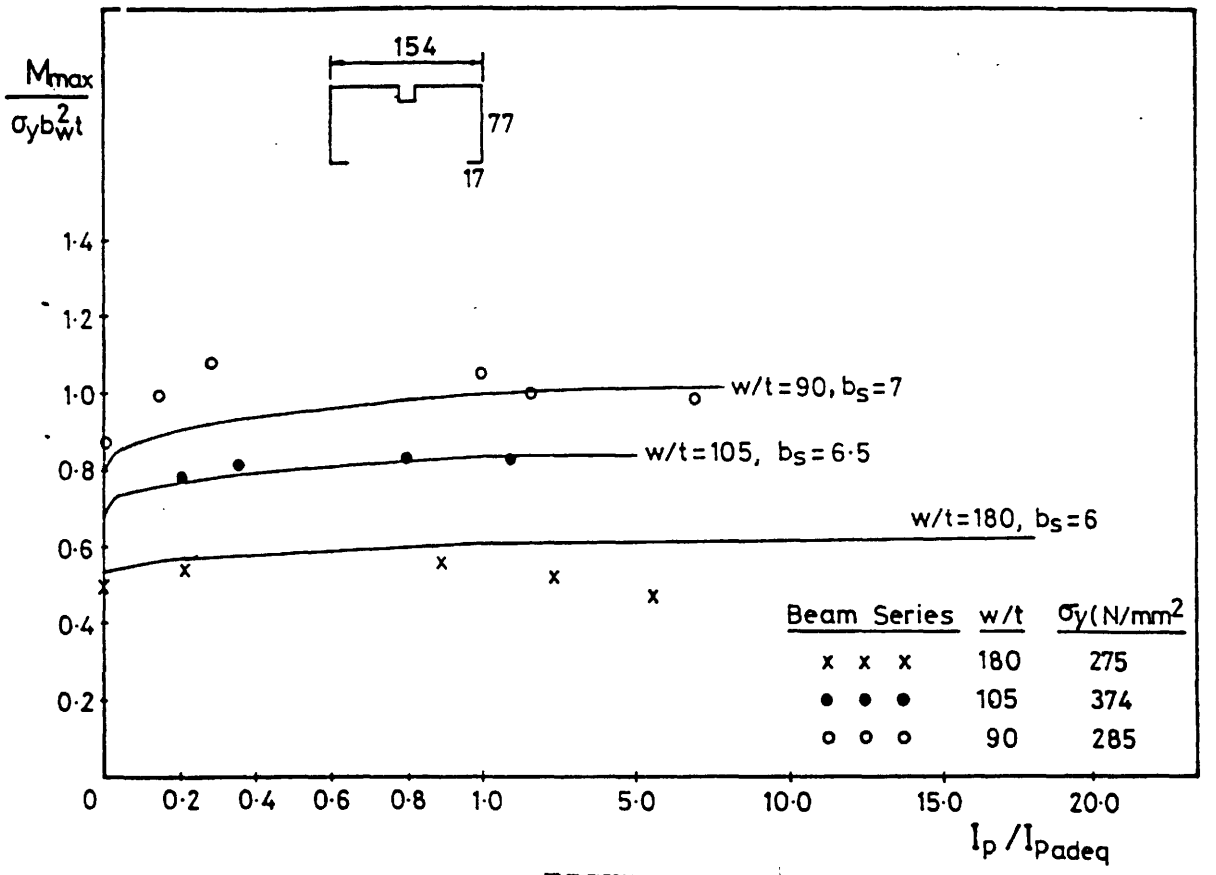

FIGURE 97

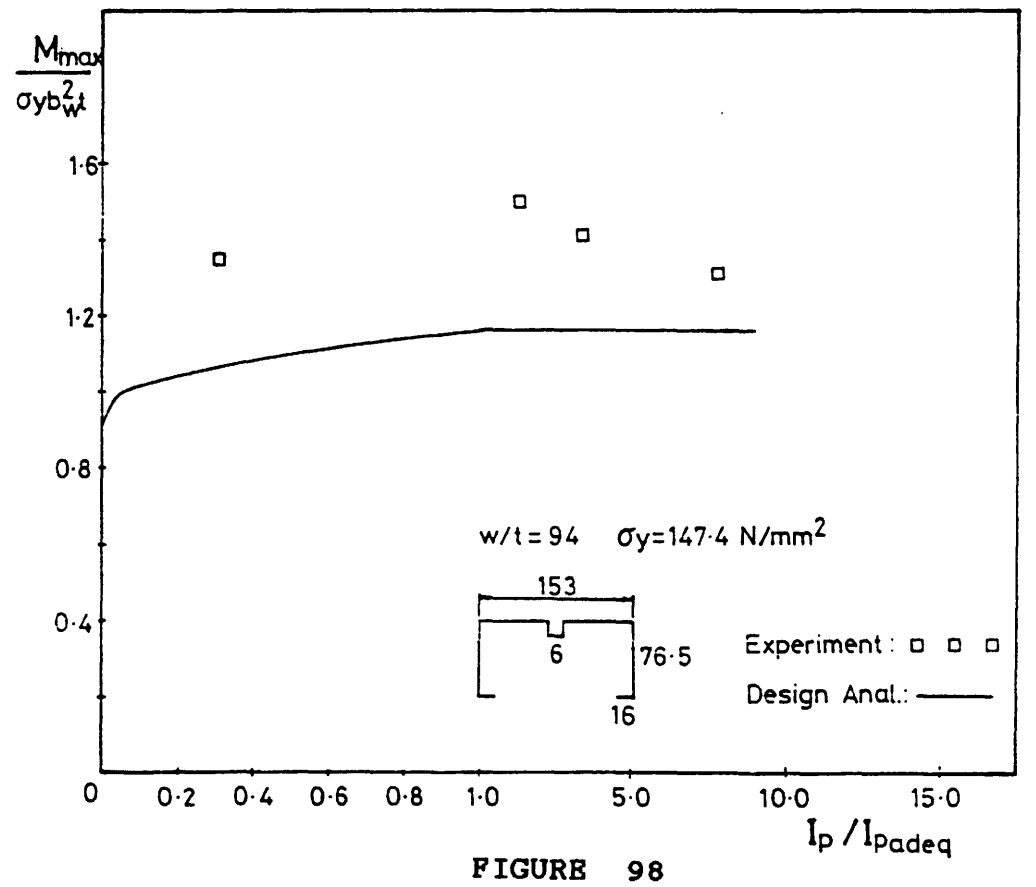

FIGURE 98

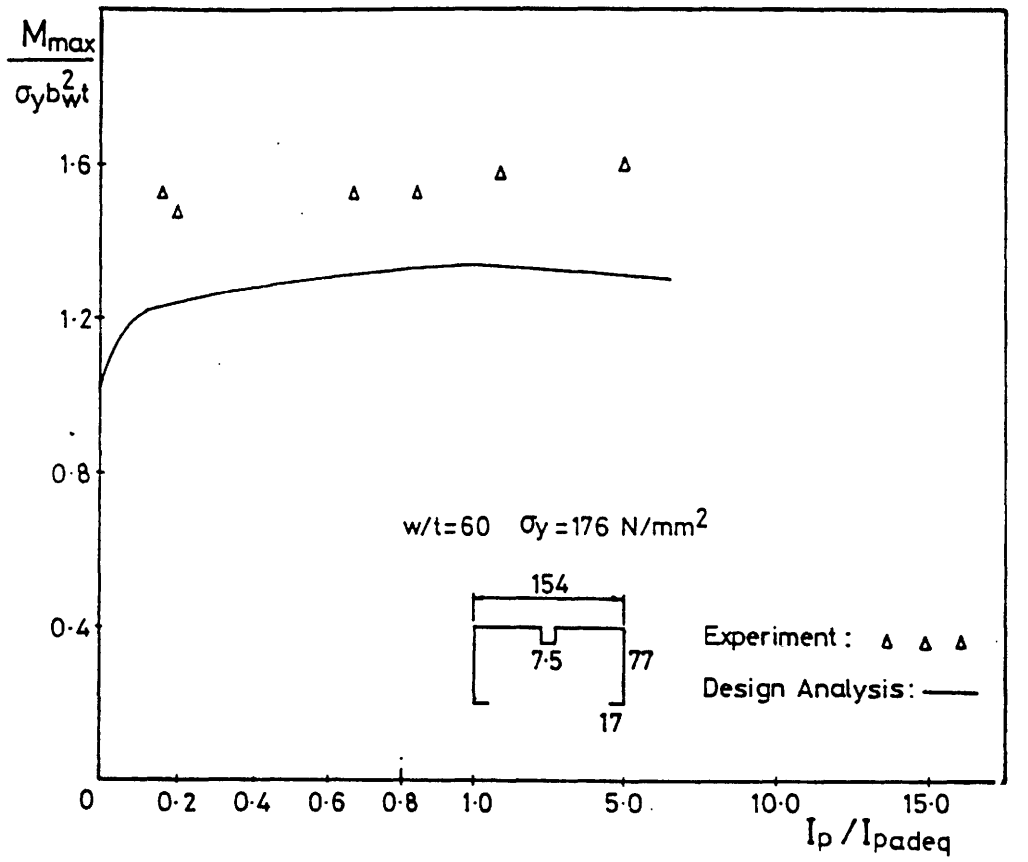

FIGURE 99

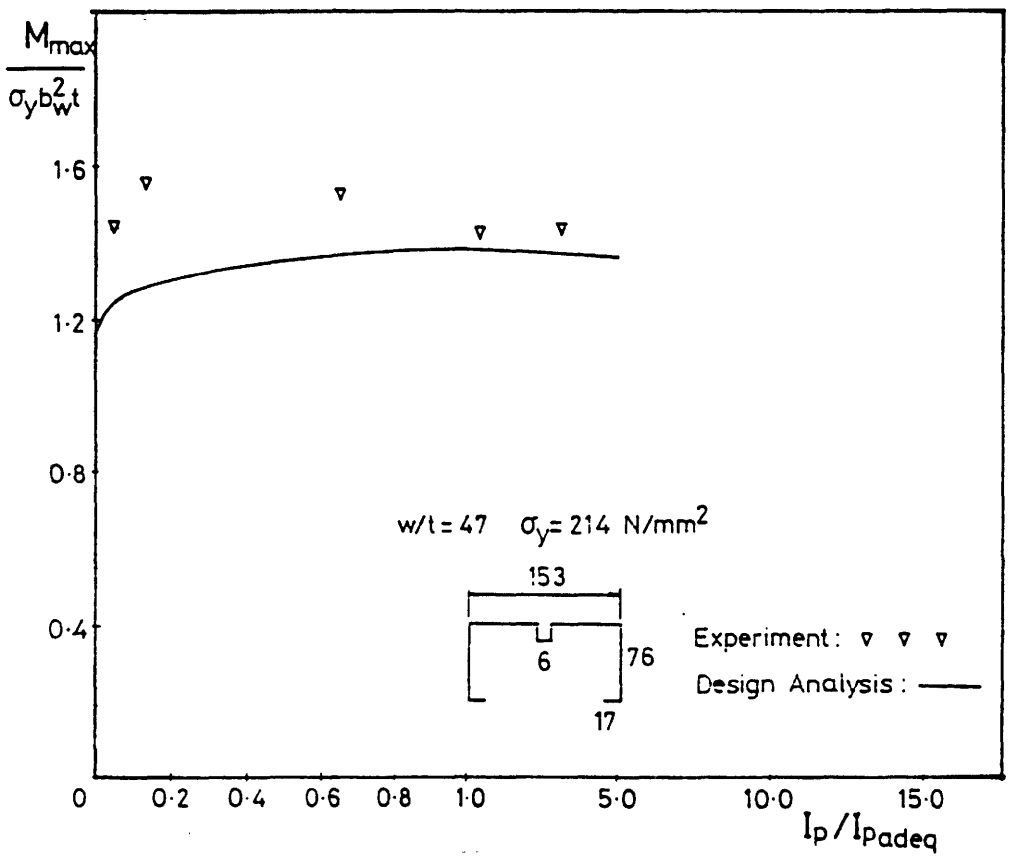

FIGURE 100

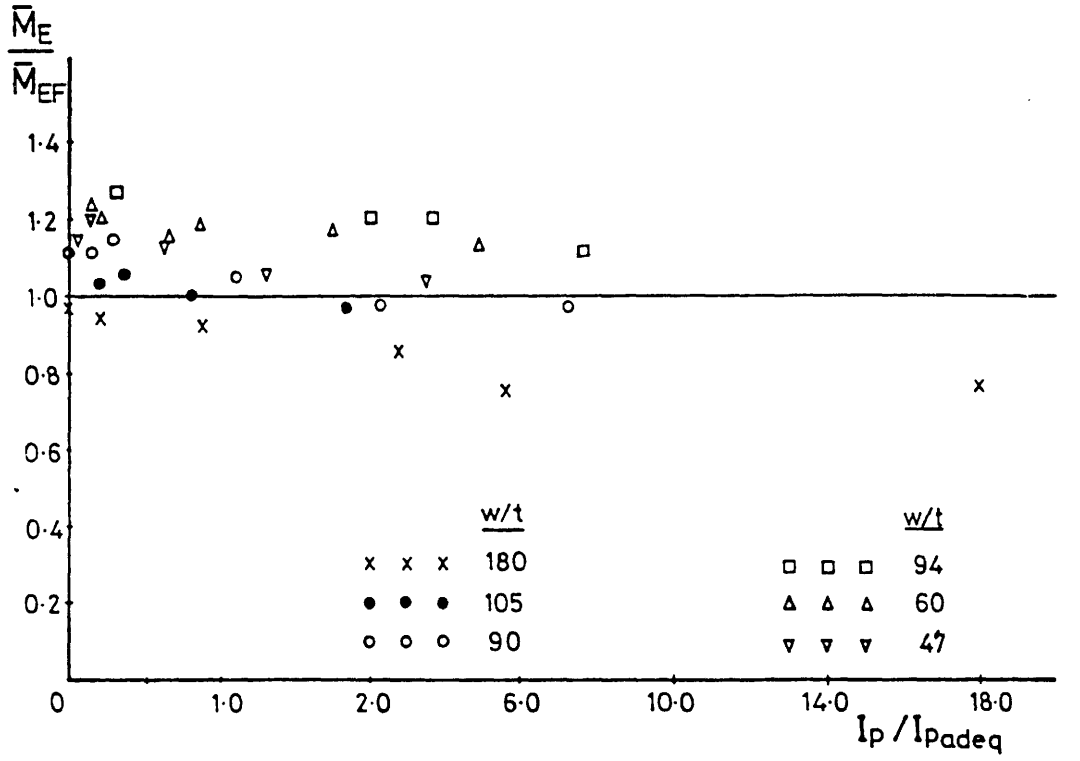

FIGURE 101 Comparison with Present Analysis

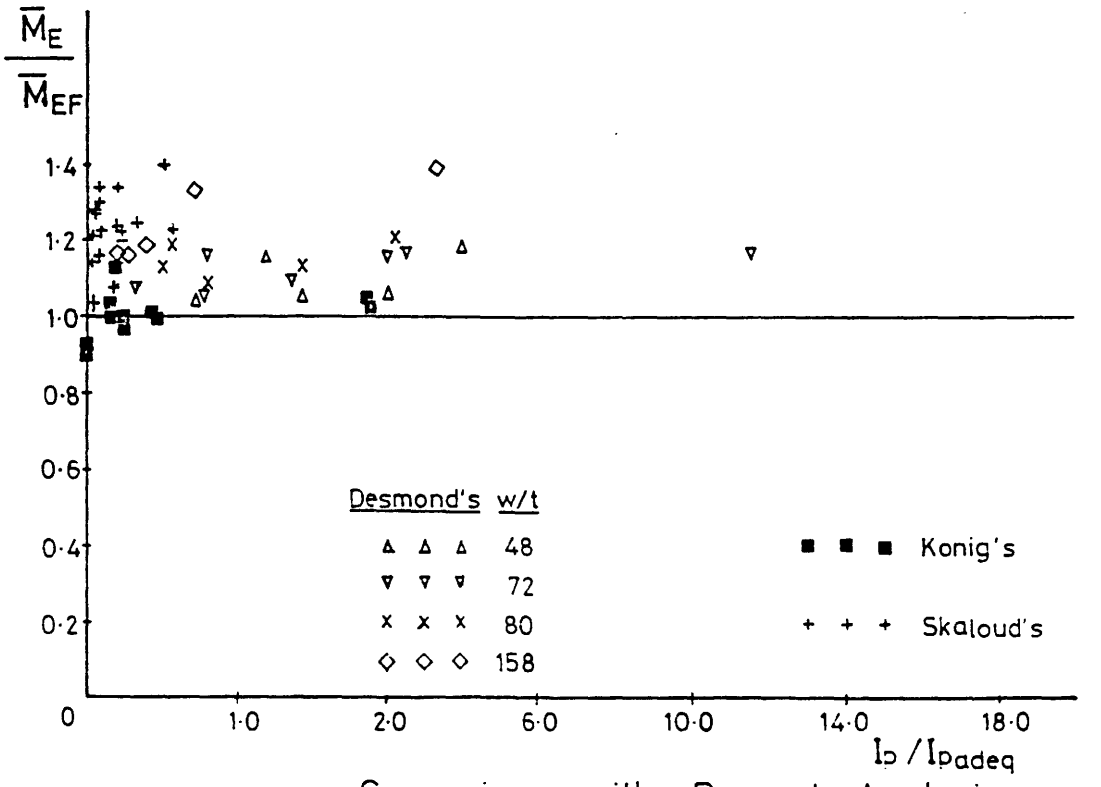

FIGURE 102 Comparison with Present Analysis

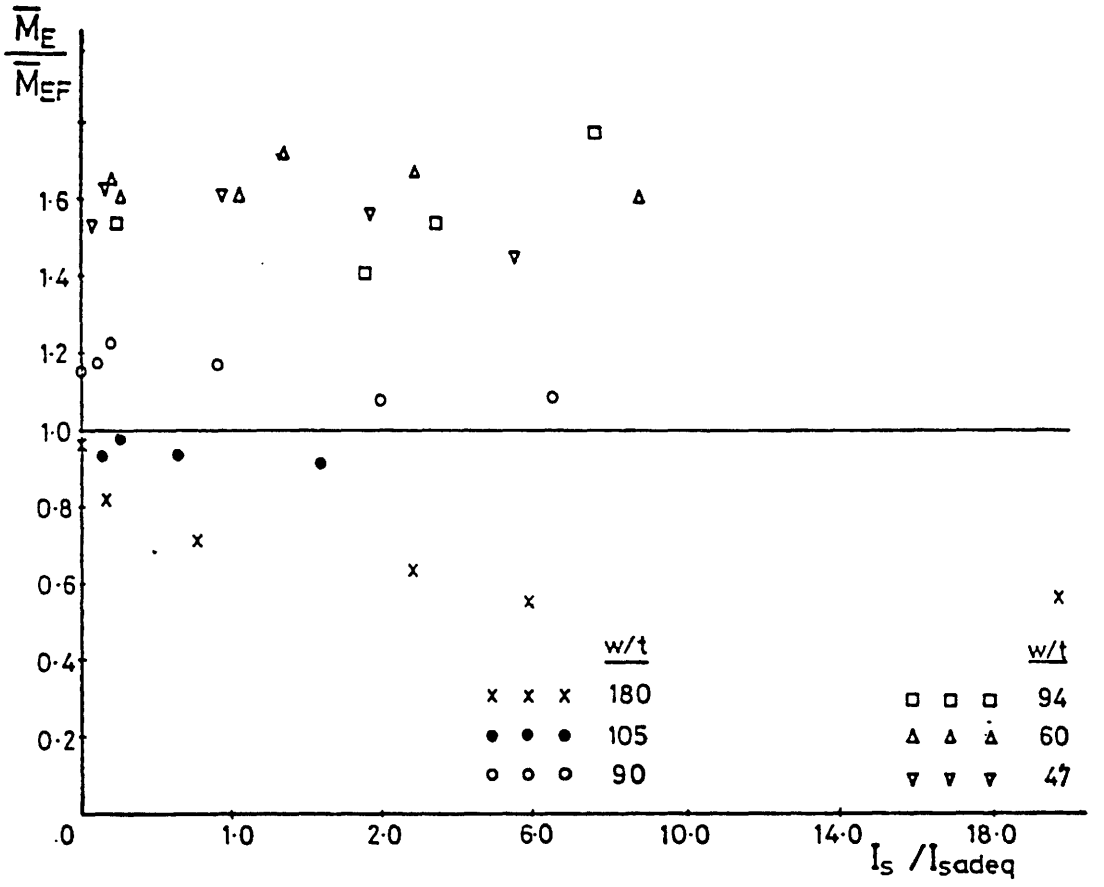

FIGURE 103 Comparison with Desmond's Analysis

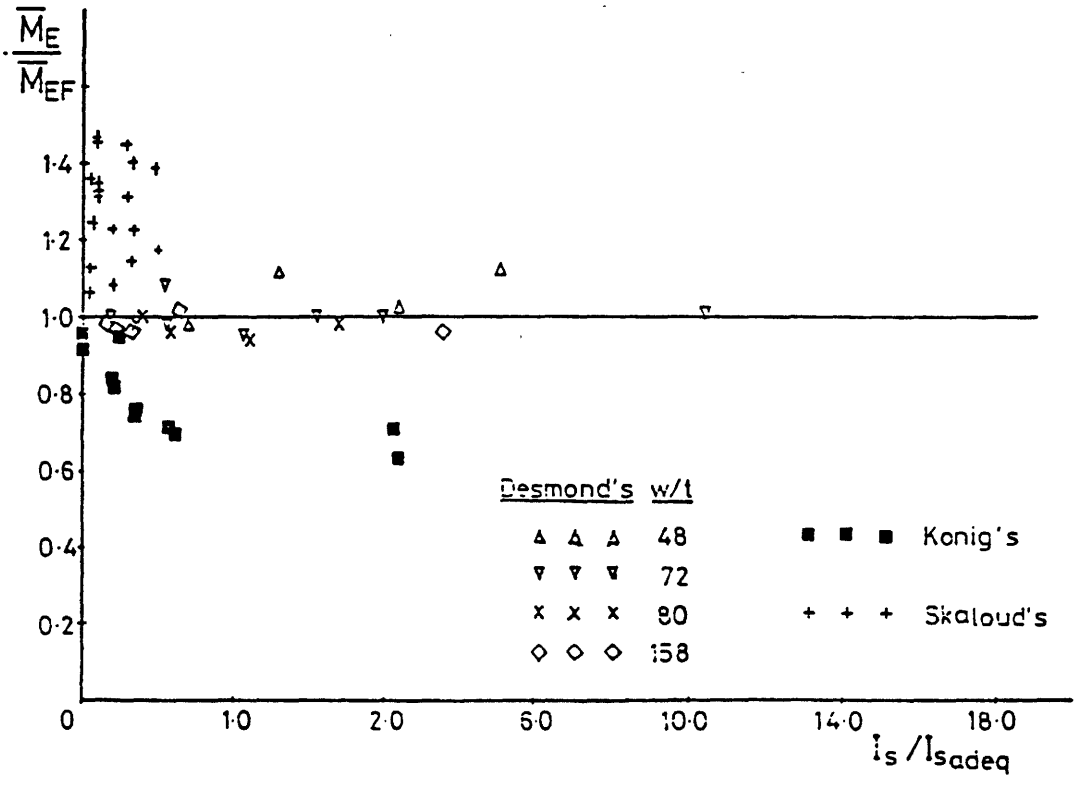

FIGURE 104 Comparison with Desmond's Analysis

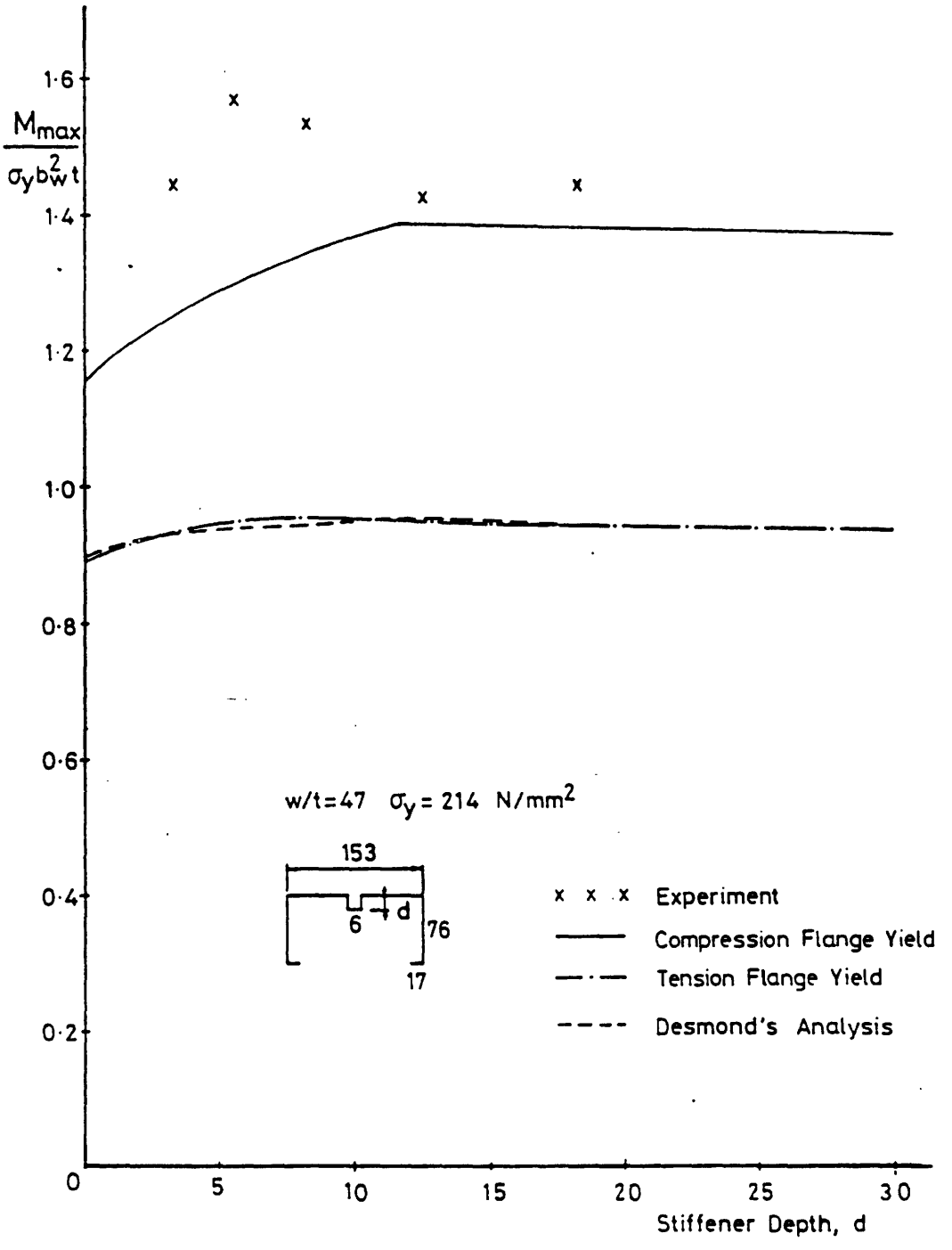

FIGURE 105 Failure Criteria

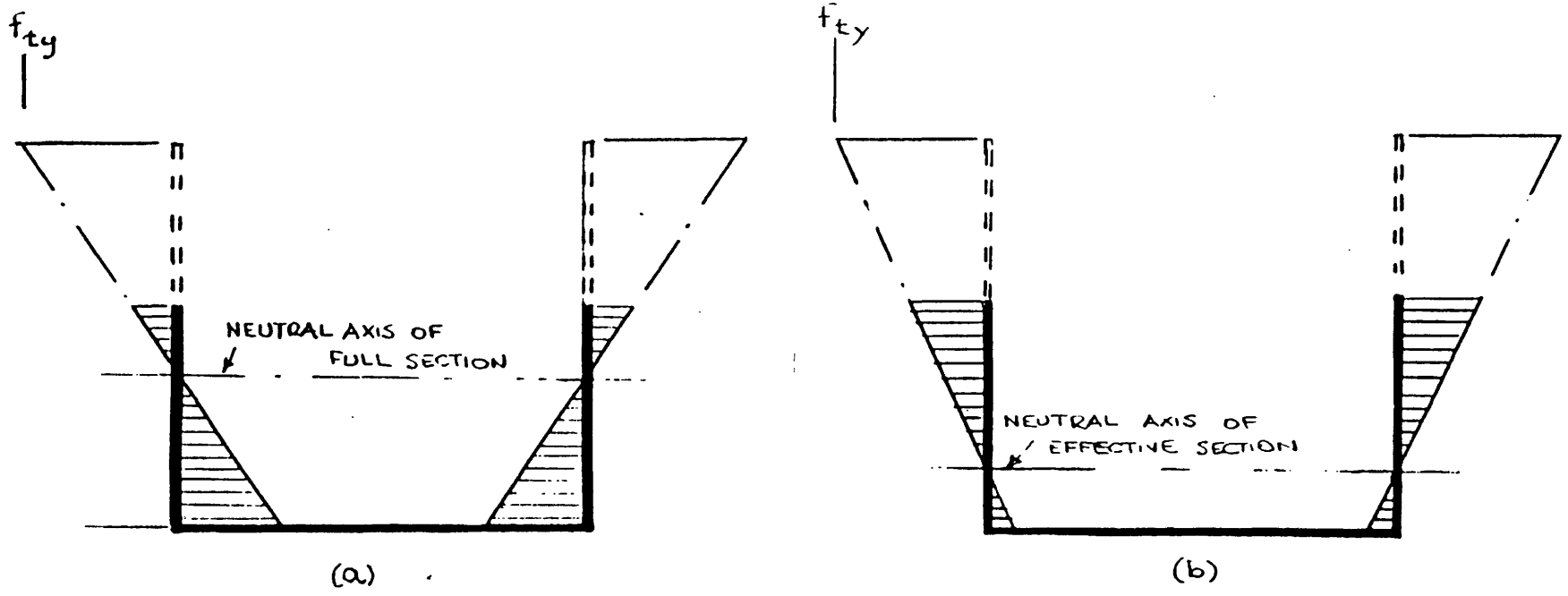

Initial Approximation to Stress Distribution on Unstiffened Elements

Fully Iterated Approximation to Stress Distribution on Unstiffened Elements

FIGURE 106. Stress Distributions used to obtain Effective Width of Unstiffened Bending Elements in European Recommendations

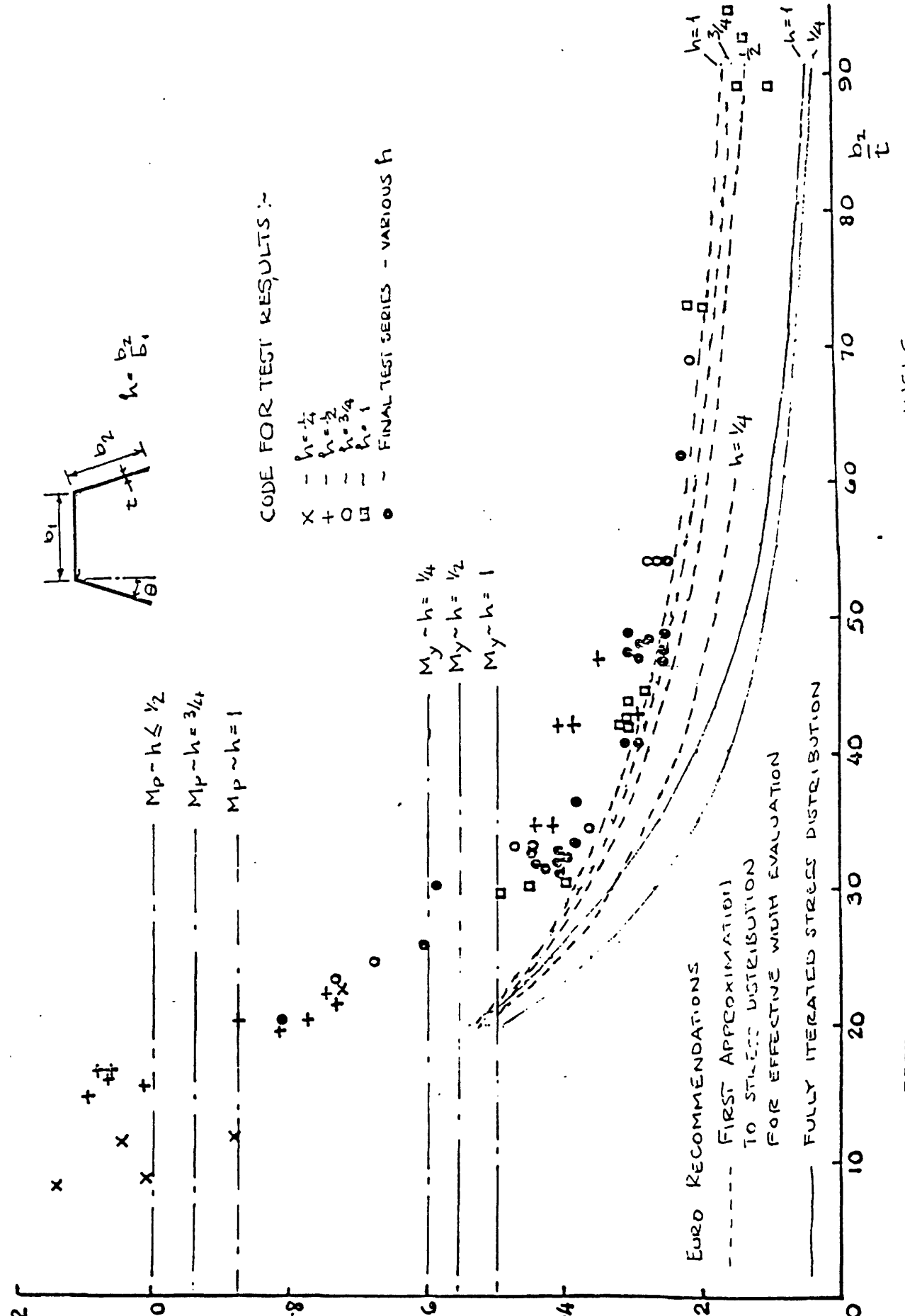

FIGURE 107 FAILURE MOMENTS FOR PLAIN CHANNELS

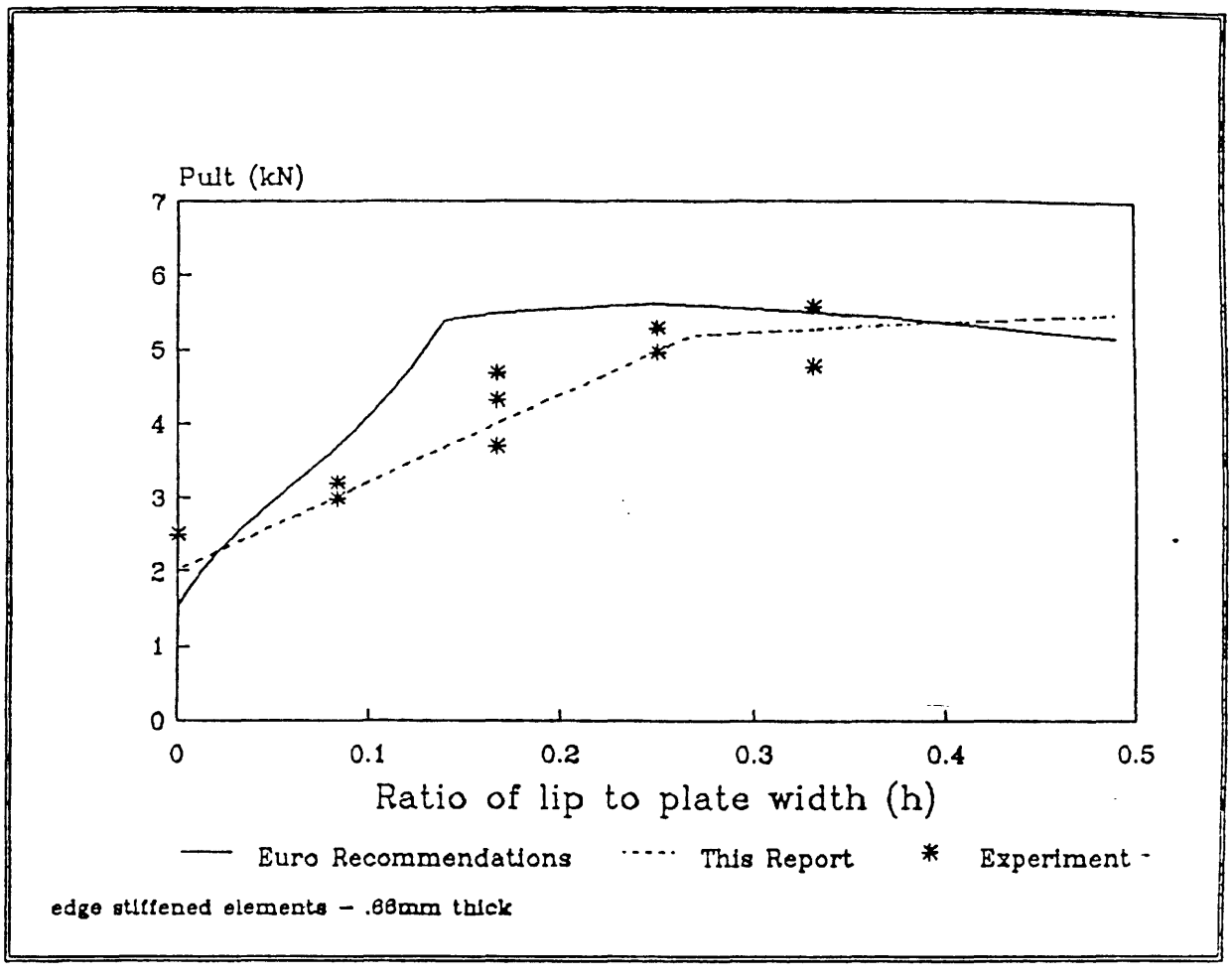
Pult (kN)
7
6
5
4
3
2
1
0
0
0.1
0.2
0.3
0.4
0.5
Ratio of lip to plate width (h)
Euro Recommendations
This Report
Experiment
edge stiffened elements – .88mm thick

FIGURE 108

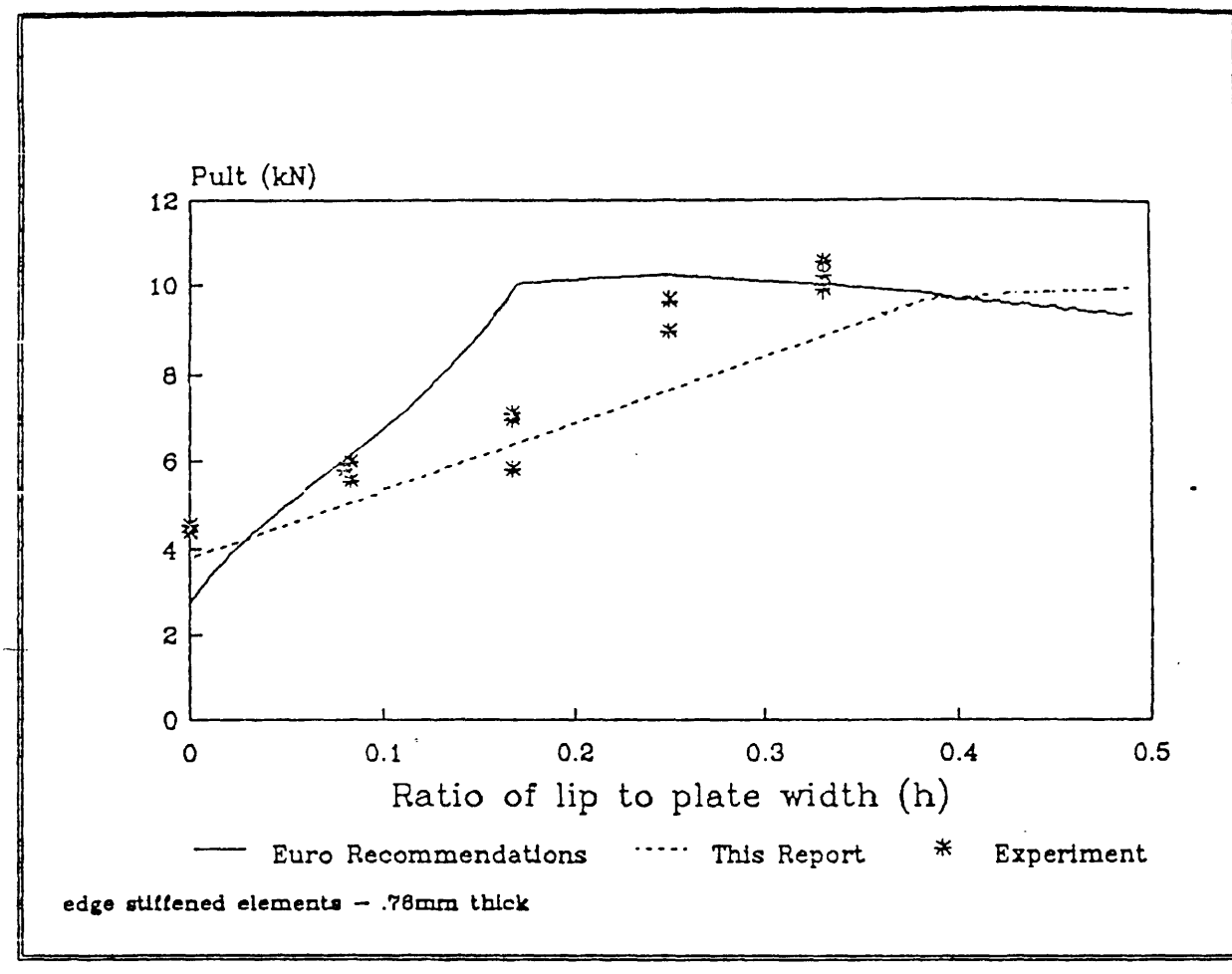
Pult (kN)
12
10
8
6
4
2
0
0
0.1
0.2
0.3
0.4
0.5
Ratio of lip to plate width (h)
Euro Recommendations
This Report
Experiment
edge stiffened elements – .76mm thick

FIGURE 109

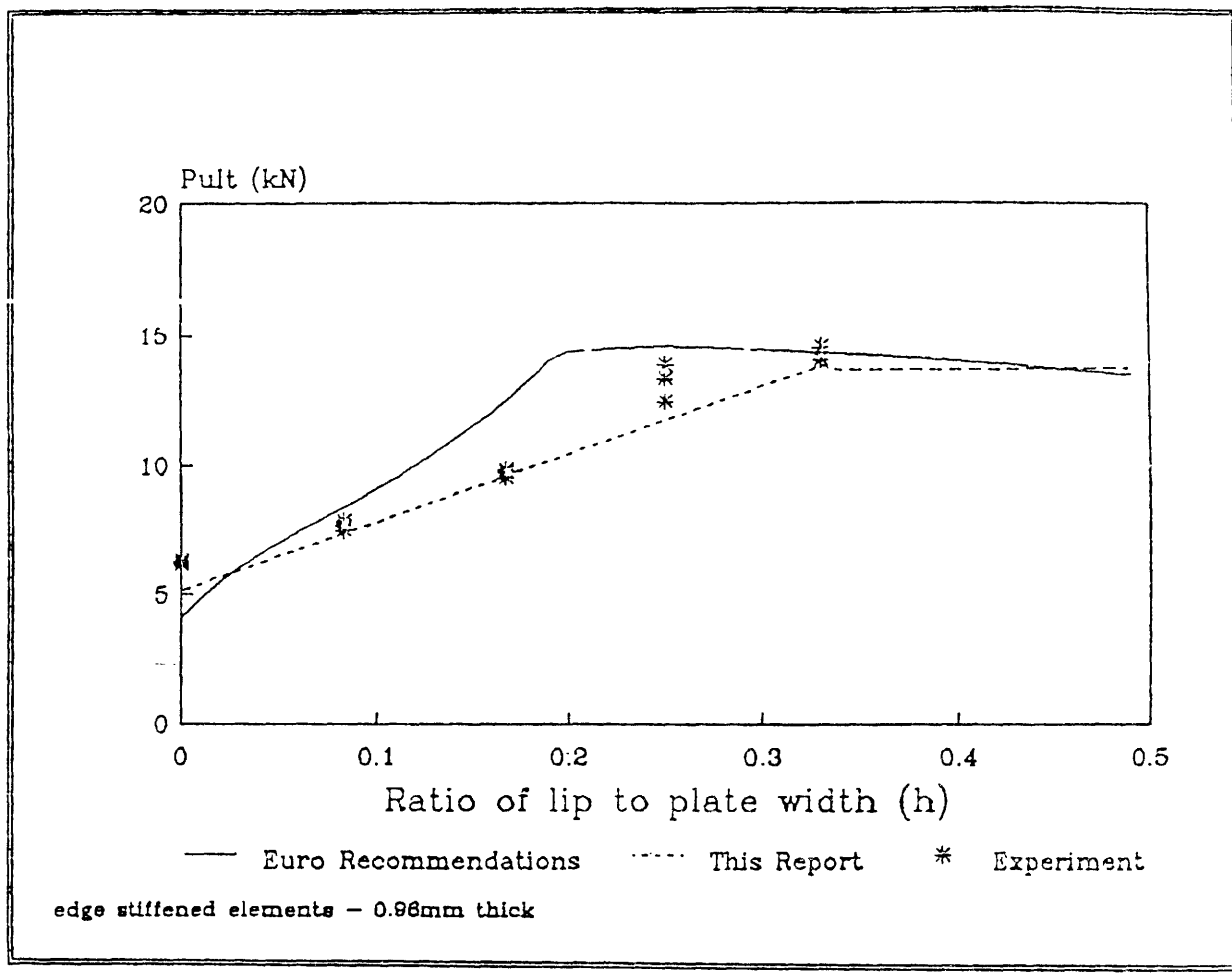
Pult (kN)
20
15
10
5
0
0
0.1
0.2
0.3
0.4
0.5
Ratio of lip to plate width (h)
Euro Recommendations
This Report
Experiment
edge stiffened elements – 0.96mm thick

FIGURE 110

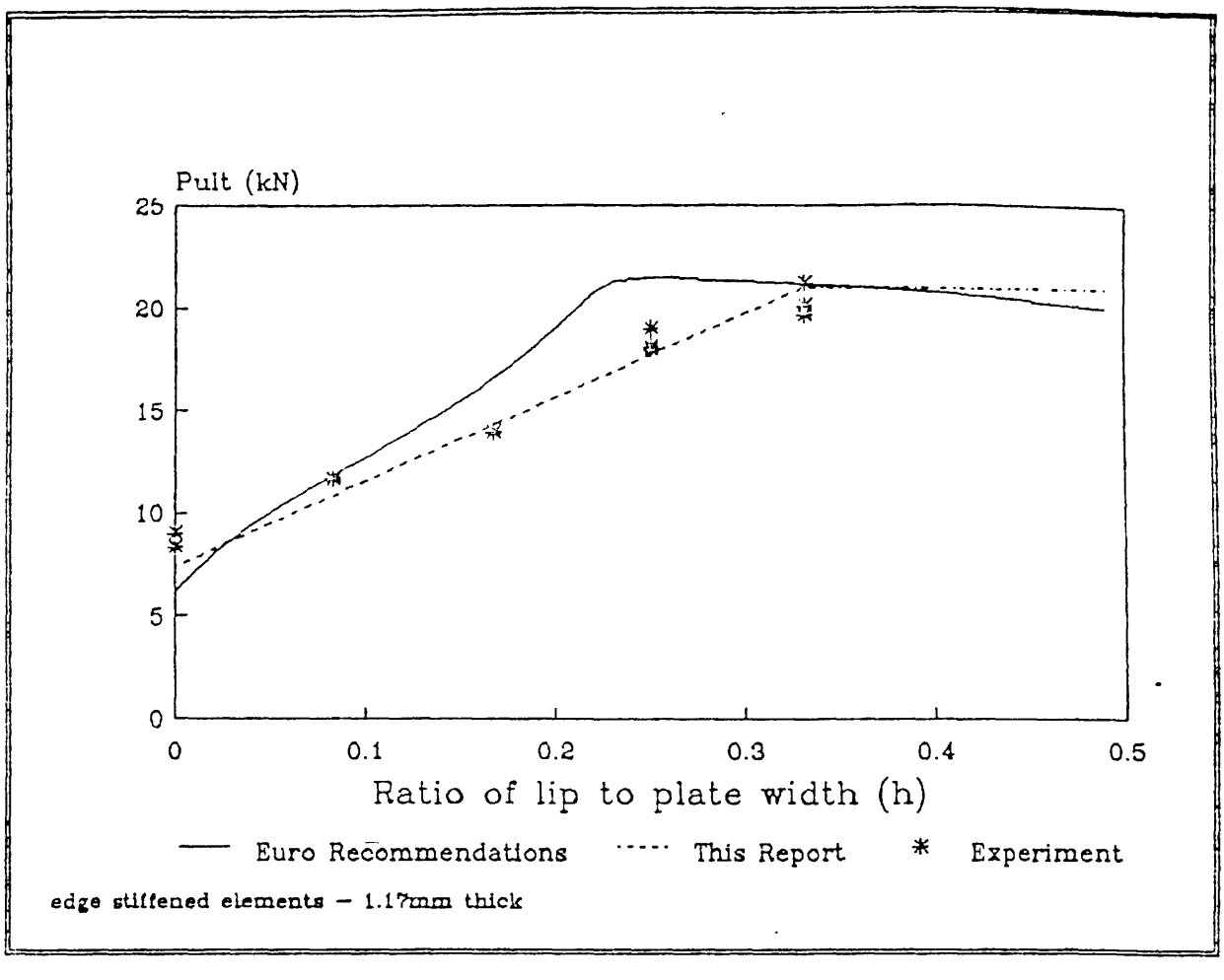
Pult (kN)
25
20
15
10
5
0
0
0.1
0.2
0.3
0.4
0.5
Ratio of lip to plate width (h)
Euro Recommendations
This Report
Experiment
edge stiffened elements – 1.17mm thick

FIGURE 111

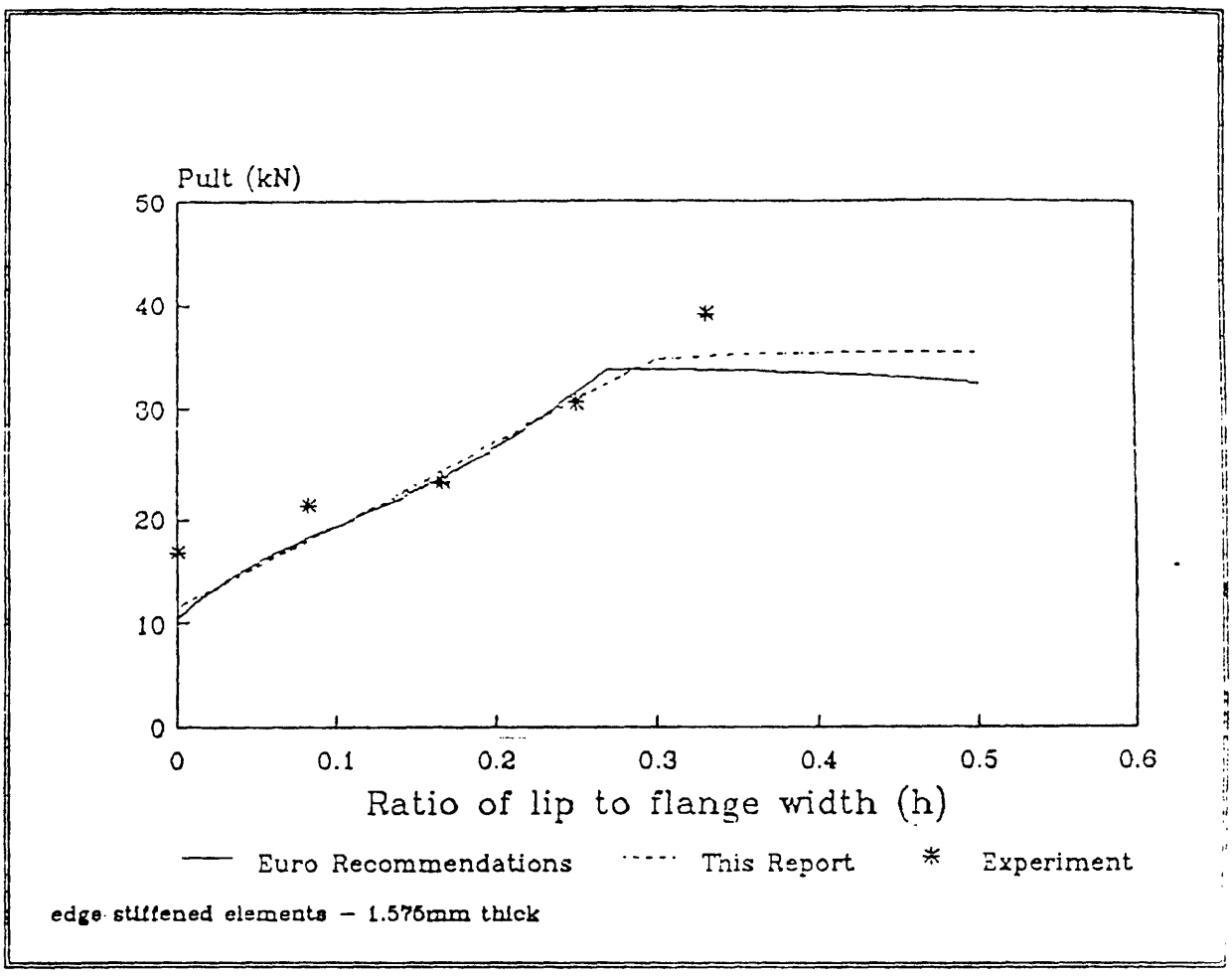
Pult (kN)
50
40
30
20
10
0
0
0.1
0.2
0.3
0.4
0.5
0.6
Ratio of lip to flange width (h)
Euro Recommendations
This Report
Experiment
edge stiffened elements – 1.575mm thick

FIGURE 112

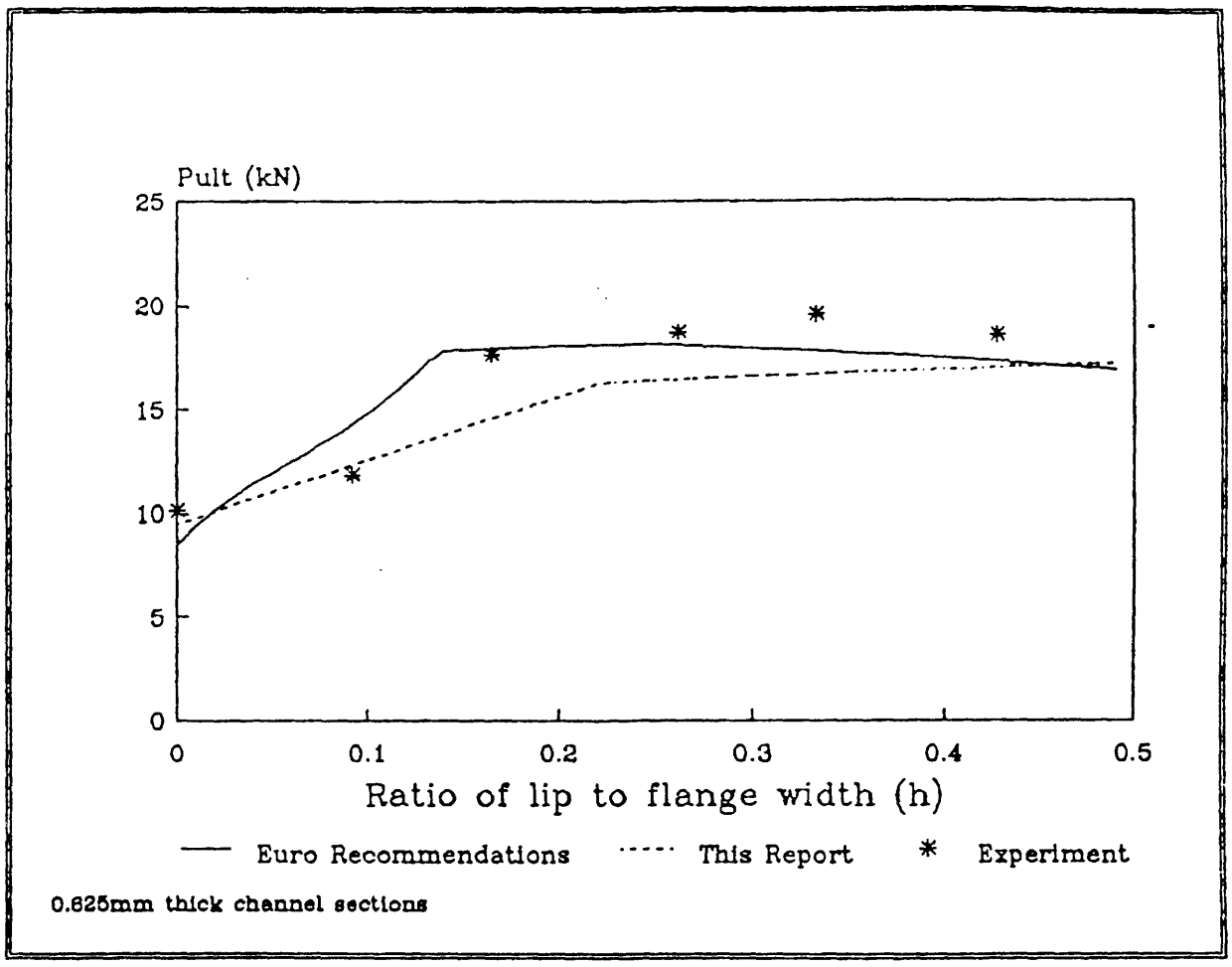
Pult (kN)
25
20
15
10
5
0
0
0.1
0.2
0.3
0.4
0.5
Ratio of lip to flange width (h)
Euro Recommendations
This Report
Experiment
0.625mm thick channel sections

FIGURE 113

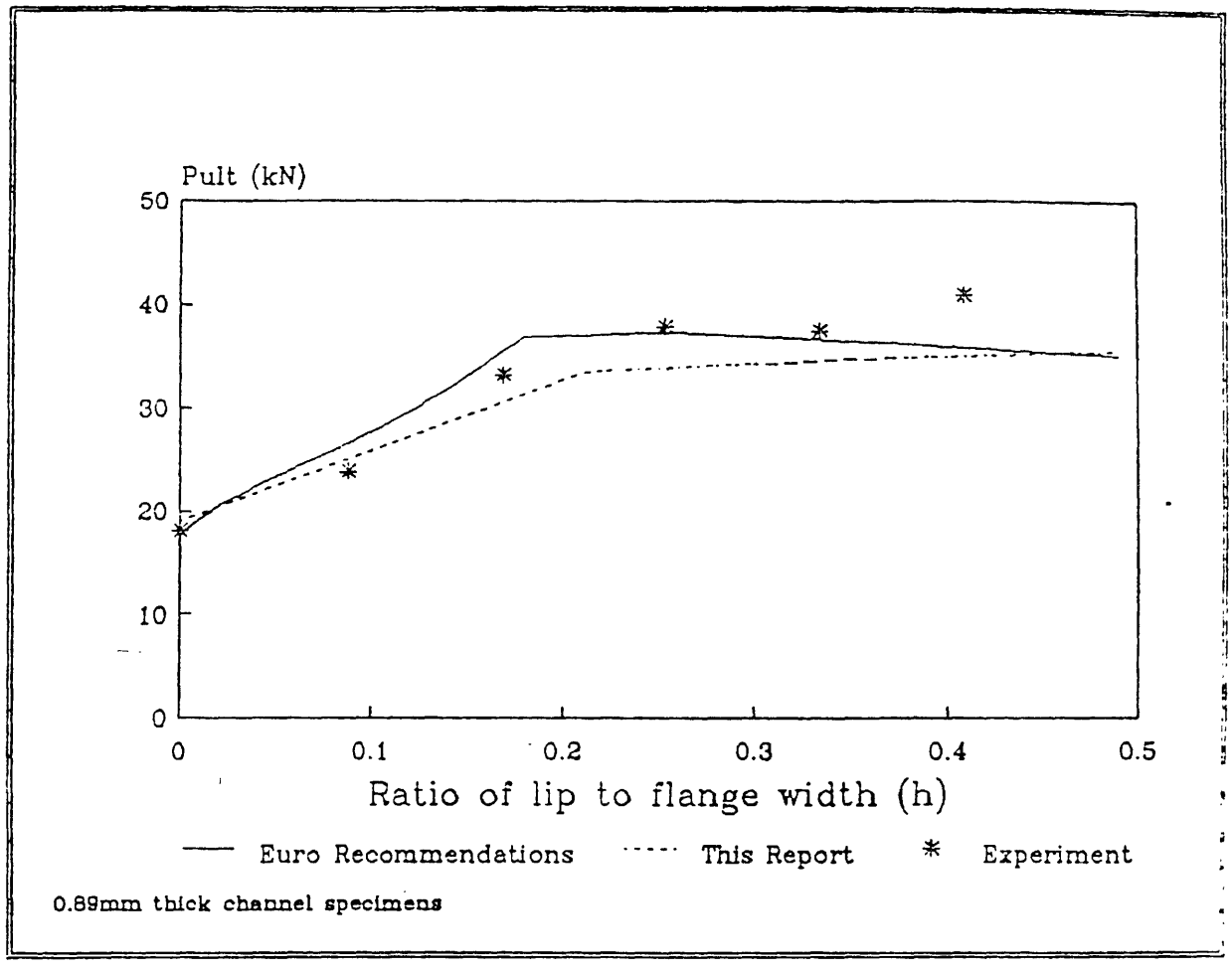
Pult (kN)
50
40
30
20
10
0
0
0.1
0.2
0.3
0.4
0.5
Ratio of lip to flange width (h)
Euro Recommendations
This Report
Experiment
0.89mm thick channel specimens

FIGURE 114

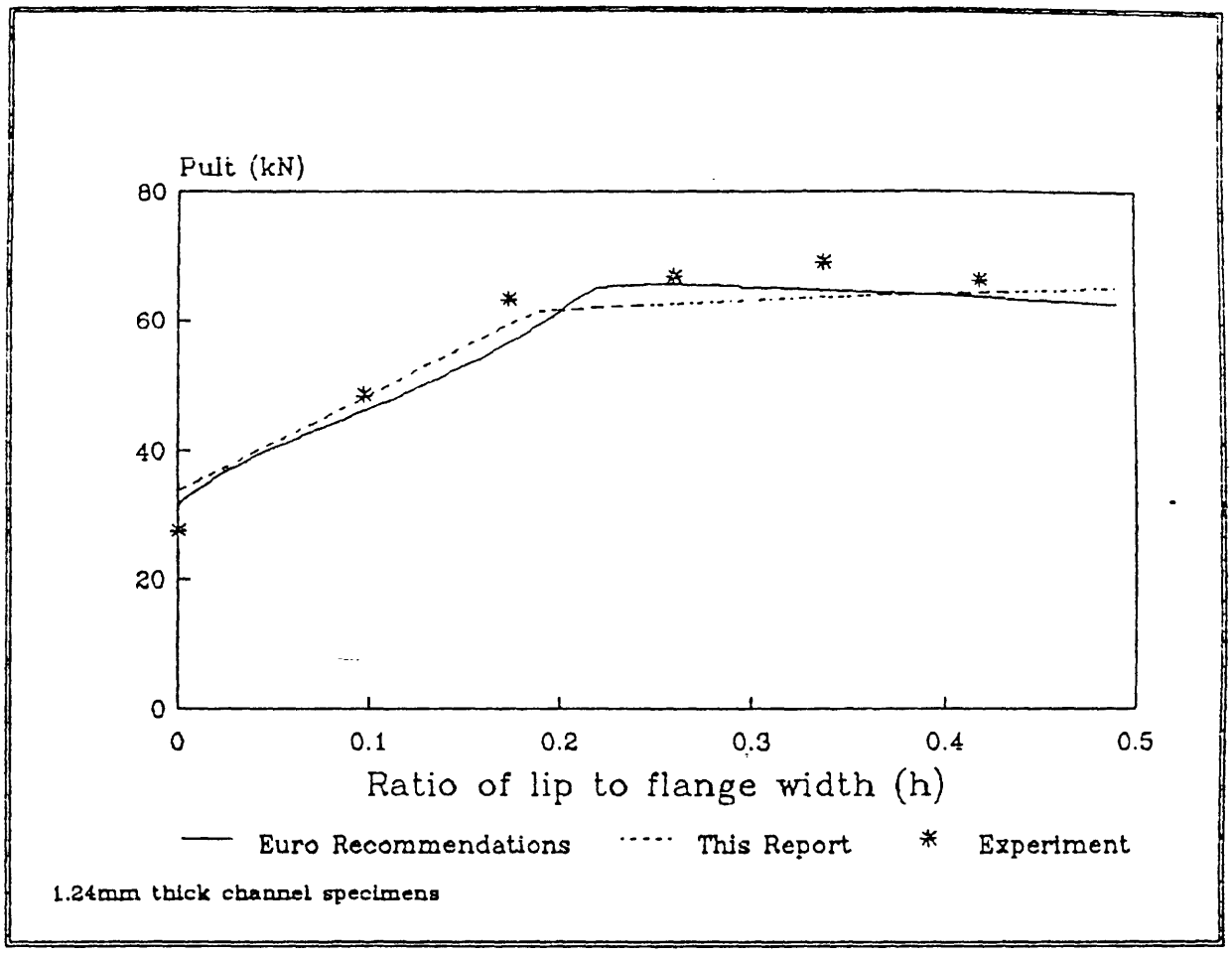
Pult (kN)
80
60
40
20
0
0
0.1
0.2
0.3
0.4
0.5
Ratio of lip to flange width (h)
Euro Recommendations
This Report
Experiment
1.24mm thick channel specimens

FIGURE 115

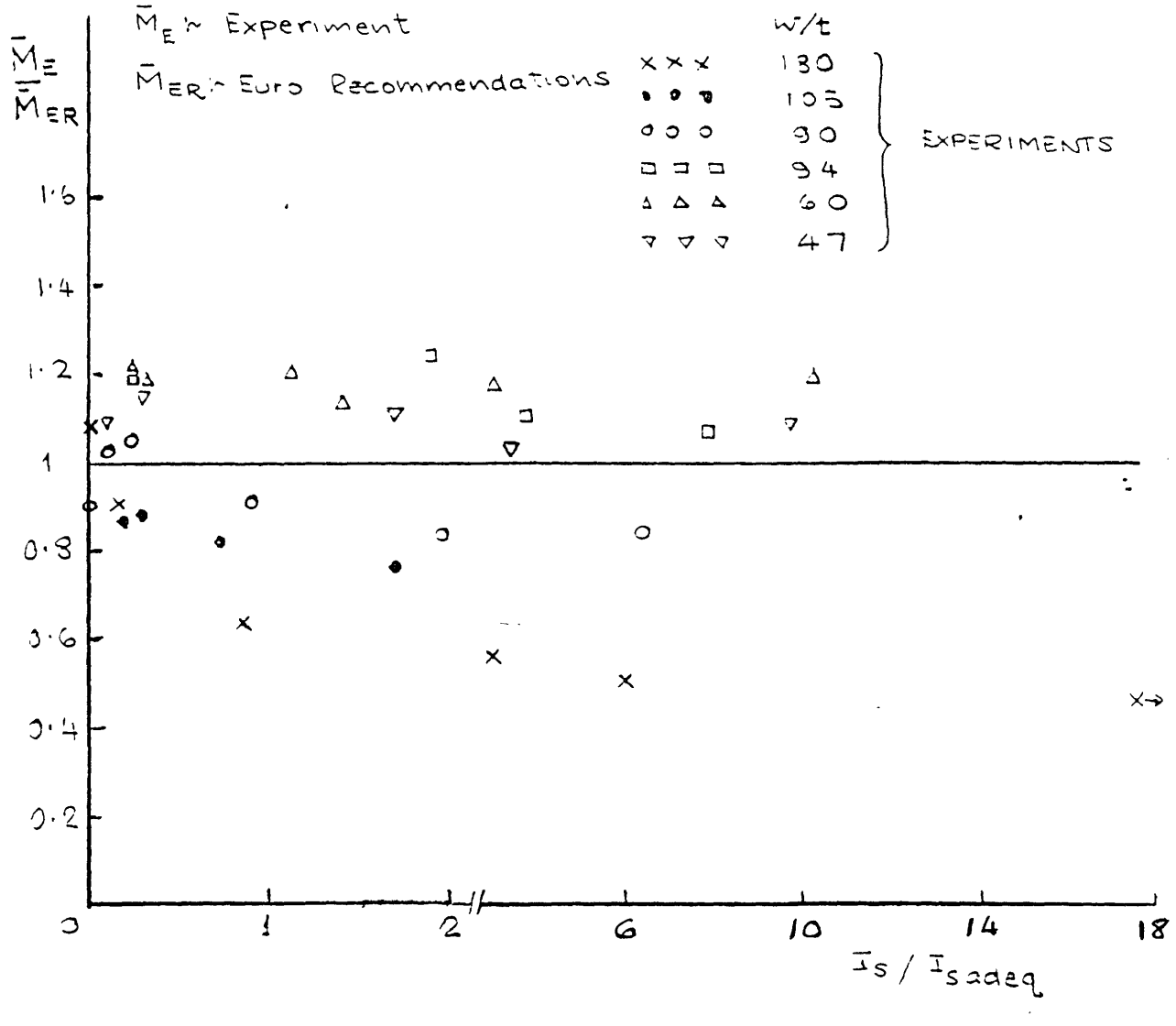

FIGURE 116. Comparison of European Recommendations with Experiments for Beams with Intermediately Stiffened Compression Flanges

SUMMARY OF SPECIMEN TYPES TESTED

1. Unstiffened elements.

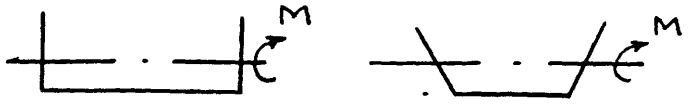

Also reversed moment

115 Tests

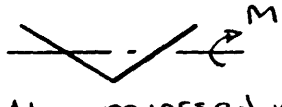

Also reversed moment

36 Tests.

2. Edge stiffened elements

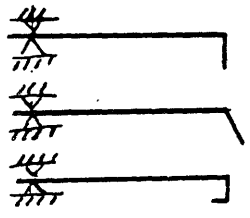

105 Tests

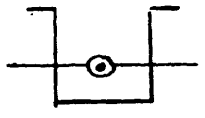

18 Tests

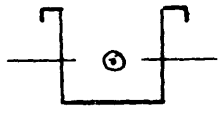

5 Tests

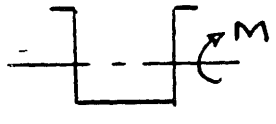

8 Tests

3. Intermediately stiffened elements

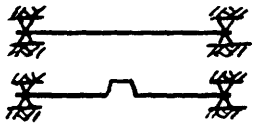

6 Tests

36 Tests

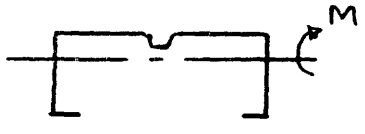

32 Tests

Total 361 Tests

FIGURE 117

ABSTRACT

This report details the research carried out by TNO-IBBC on ECSC contract no. 7210/SA/608.

The theoretical and experimental research concerning the behaviour and load carrying capacity of diaphragm braced beams is ontlined.

Recommendations for a design procedure of diaphragm braced beams of cold-formed sections are presented.

CONTENTS

1. INTRODUCTION 204

2. DESCRIPTION OF STUDY 205
2.1 Literature study 205
2.2 Testing of diaphragm braced beams 207
2.3 Design procedure of diaphragm braced beams (single span) 208
2.4 Design procedure of diaphragm braced beams (continuous system) 212

3. RECOMMENDATIONS FOR A DESIGN PROCEDURE OF DIAPHRAGM BRACED BEMAS OF COLD-FORMED SECTIONS 214

4. SUMMARY 228

REFERENCES 229
Tables 232
Graphs 240
Figures 244

1. INTRODUCTION

Cold-formed sections and thin-walled constructions offer the possibility of an increased use of steel for structual purposes. Cold-formed sections have opened new opportunities for steel that would otherwise be in other materials such as concrete or wood. Examples are purlins, wall studs, shelving that would traditionally be in wood and roofing, cladding, cold-formed steel lintels that would traditionally be in concrete or brick-material. Many possibilities for extension of the market are still open. However, the lack of well presented technical information, comprehensive design recommendations and acceptance criteria have proved to be a severe handicap to the growing application of steel in this market in Europe.

With financial support of the ECSC a research program has been executed concerning the mechanical behaviour of cold-formed sections and drafting of design rules. The contract comprises two main topics executed by two institutes:

- the University of Strathclyde, Glasgow:
  behaviour and load carrying capacity of unstiffened elements, edge stiffened elements and intermediately stiffened elements of cold formed steel sections.
- TNO-IBBC, Delft:
  the load carrying capacity of diaphragm braced cold formed beams.

The forlaying report is the final report concerning the part executed by TNO-IBBC

2. DESCRIPTION OF STUDY

The study executed by TNO-IBBC has been reported in the references [1] -[4]. This chapter will give a summary of the findings in those references.

2.1 Literature study

In reference [1] the results of a literature study have been described. There is started with a survey of existing standards and recommendations in this field:

- American Specifications, 1983
- Swedish Code, 1982
- European Recommendations, draft of 1983.

From the survey of specifications can be concluded that the Swedish Code is the most complete one both for lateral buckling as well as web crippling. Besides for the presence of design rules for different cases also postcritical behaviour is taken into account.

The ECCS Recommendations are much less complete especially for lateral buckling. No provisions are given in the available draft for members with one flange braced and subjected to elastic torsional restraint. The design rules given are very similar to those of the Swedish Code. In the final European Recommendations (1987) the method of Sokol is adopted for purlins braced by sheeting. Ref. [3] gives a discussion of this method.

The design rules of the American Specifications are also less complete compared with the Swedish Code and seem to be much more conservative. For instance, elastic torsional restraint and post-critical behaviour are not taken into account. Besides, the design rules are still based on allowable stresses.

Besides the survey of specifications, an evaluation of literature contributions (theoretical and practical) is made.

As far as the theoretical contributions are concerned, it can be concluded that "new" methods to analyse the flexural-torsional behaviour of cold-formed sections have not been brought forward. In the contributions by Bradford and Hancock [5], Levy and Glassman [7], and Gosowski, Kubica and Rykalyk [8] only modifations of existing methods are given. However, in the contribution by Trahair and Nethercot [6] a number of interesting conclusions are given concerning the similar behaviour of single span resp. two and more span beams and about the effectiveness of bracings.

A few of the practical contributions give rise to a "new" design approach, however only applicable for certain cases. This holds respectively for:

- the contribution by Davies and Thomasson [12], which seems to be the best approach for unbraced beams or beams with discrete bracings;
- the contribution by Schardt and Schrade [15], which is suited for diaphragm braced Z-purlins under gravity loading (and possibly also uplift loading);
- the contribution by Peköz and Soroushian [16], which is dealing with diaphragm braced C- and Z-purlins under uplift loading.

The remaining practical contributions go into details such as:

- the development of some type of section which is carried out by Blanchard [9], Sokol [10], and Bryan, Grant and Muir [13]; interesting with the latter contribution are the concluions about the behaviour of lapped and sleeved purlins;
- the effective length of the compressed flange of Z-purlins by Sokol [11];
- the problems which are met applying cold-formed sections by Kanning [14];
- the effectiveness of the diaphragm restraint for C- and Z-purlins with gravity resp. uplift loading by Celebi [17];
- web crippling as analysed according to the AISI Specifications by Hetrakul and Yu [18];
- the comparison for Z-purlins between three different design methods by Huck [19].

Finally as result of the literature study design rules are proposed for flexural torsional buckling based on a combination of in-plane bending of the entire section and lateral bending of a part of the section. This principle is also incorporated by Pekőz and Soroushian [16], Schardt and Schrade [15] and the Swedish Specification. It is intended to draft design rules which are less section-dependant as the references mentioned. Figure 1 shows that calculation hypothesis in scheme.
It was decided to check the hypothesis at tests on C-, Z- and Σ (sigma)-sections. This testing program has been described in reference [2] and is summarised in 2.2.

2.2 Testing of diaphragm braced beams

In reference [2] the testing program on C-, Z- and Σ-sections has been described. The report comprises also the results of the tests and a comparison of these results.
The choice of test specimens has been determined in such a way that almost every test will be executed in two-fold. Between the different specimens only one parameter has been varied. The combinations of parameters which have been used are:

- single span and double span
- the span about 4 m and 6 m
- shape of the section of the purlins Z, C and Σ
- section height of the purlins h = 140 mm and h = 240 mm
- section thickness of the purlins t = 1,5 mm at the height h = 140 mm and t = 2,0 mm at the height h = 240 mm
- two types of torsional restraint delivered to the purlins by sheeting (type A and B)
- type of loading; gravity and uplift (The test specimens were to be acted upon only by vertical uniformly distributed loading)

Table I gives a survey of the total of 28 testspecimens. The tables Ia-Id show the test program more in detail. For exact dimensions of sections and properties of material see reference [2].
The experiments have been carried out in a box unit made up by steel panels. The bottom of the box consisted of the floor of the laboratory. The specimens were built up in that box. The specimens have been loaded by sucking a vacuum in the box. Deflections have been measured at midspan of every purlin.
Table II gives a survey of the failure loads. The graphs 1-4 give load-deflection diagrams of comparable tests.
The aim of the test program was to check the proposed calculation model. In 2.3 this check has been presented.

2.3 Design procedure of diaphragm braced beams (simple span)

In reference [3] the design procedure for diaphragm braced beams has been derived. Furthermore this procedure has been checked with the results of the test program of reference [2].
The basis for the design procedure to determine the bending moment capacity in the span is shown in figure 2. (Figure 2 comprises some corrections compared with the model of reference [3] which assumed the load q acting in the plane of the web). This means that the stresses in the section are a combination of:

- stresses from in-plane bending of the entire section due to the load q. These generate an axial load N (x) in the free flange of the section (see fig. 1d). This axial load varies along the length of the member due to the in-plane bending moment M (x); with uplift, N (x) is a compressive load and with gravity, N (x) is a tensile load.
- stresses from lateral bending of a part of the section due to the lateral load $k_h q$. The value of k_h is shown in figure 2.

With determining the in-plane bending stresses the effective widths of commpressed parts of the section are applied to account for local buckling effects. The stresses caused by the lateral load of the free flange will be determined without reducing the free flange, which differs also from reference [3].

With diaphragm braced beams rotation of the beam is restrained by respectively:
- the section properties of the diaphragm,
- the section properties of the beam,
- the connection between diaphragm and beam.

Usually this rotational restraint is converted into a lateral restraint as indicated in fig. 1c (taken from [16]), being a linear extensional spring of stiffness K located at the level of the free flange. This means that the part of the section due to lateral bending (and with uplift loading also a compressive load, as explained later) can be calculated as a beam on an elastic foundation (see figure 1d). Chapter 3.2.1 describes the procedure to determine K.

With the energy method the combination of stresses will be applied. In the energy equation is taken into account:
- lateral load energy
- axial load energy
- flexural strain energy of the free flange
- elastic foundation strain energy (caused by the rotational restraint of the sheeting)

In chapter 3 the resulting stress-equations are given depending on the edge conditions, as a part of the design procedure.
As criteria for the ultimate limit state, the above calculated stresses shall be smaller than the yield stress or the ultimate stress for flexural/torsional buckling of the free flange when it is under compression. The ultimate stress for flexural/torsional buckling will be determined in a model based on a beam-column behaviour of a part of the section.
The way to check the load-bearing capactiy of the beam-column is:

$$\omega \sigma_c + \frac{M_f}{W_f} \leq f_{ty}$$

where:

ω = buckling coefficient

σ_c = compressive stress due to in-plane bending of entire (effective) section

M_f = lateral bending moment, second order effects included, acting in the free flange plus $\frac{1}{6}$ of the height of the web.

W_f = section modulus based on moment of inertia (I_f) of a part of the section

f_{ty} = yield stress

The buckling coefficient ω depends on the slenderness $\bar{\lambda}$, for which following has to be taken into account:

- a variable axial load along the length of the bar,
- an elastic foundation, and
- appropriate end conditions.

In chapter 3 the resulting stability check equations are formulated.

In reference [3] also a comparison with existing design methods is given. The relevant metods are those of Sokol (French and ECCS recommendations) in reference [21] and Pekoz (USA) in reference [16]. Differences in [21] compared to the proposed procedure are:

- With uplift loading a constant axial load in the compressed flange is assumed, not varying along the length of the beam (according to the bending moment distribution), which is very conservative.
- The beam-column is considered in compression and not in compression + bending (laterally). Regarding the actual behaviour of the sections this simplification generally is not allowed for.
- Determining the stresses due to in-plane bending of the entire section the widths of the compressed part are <u>not</u> reduced to account for local buckling.
- Determining the slenderness $\bar{\lambda}$ again the constant axial load is used.
- The design formulae for more span purlins under downward load are derived using the displacement function for simply supported beams which is not correct.
- With downward loading and more span beams the design strength of the compressed bottom flange of the beam above the supports is limited by an overall buckling criterion which does not seem very reliable.

Differences in [16] compared to the proposed procedure, are:

- Determining the stresses due to in-plane bending + lateral bending for more span beams the portions between the inflection points are considered as simply supported, which is not conform the actual behaviour of the beam.
- The ultimate axial compressive stresses in the beam-column are not reduced for overall buckling which is not correct (only initial deflection has been assumed)

Due to the above described differences it was observed that the design method of [21] mostly gives very conservative results while the method of [16] varies from very conservative up to sometimes very unconservative results (see also table III).

The proposed design procedure has been checked with the test results described in reference [2] (see chapter 2.2). The results of this check are summarized in table IV. With respect to the results in table IV it can be observed that:

- For single span beams all test results are very well approximated for gravity loading (ratios: 0.96 - 1.03).
- For double span beams the failure loads for gravity loading are higher than the theoretical results.
  If yielding at midsupport, observed during the test, is taken into account the moment capacity of the midsupport is overestimated by 13% in test 25 resp. 3% in test 27, which is due to the support reaction. However, in the tests redistribution of forces after yielding at midsupport occurs, which allows yielding/failure in the span, while theoretically failure is defined as yielding at midsupport. The moment/rotation relationship at midsupport has to be known to take into account redistribution of forces! For that reason additional research has been undertaken. See chapter 2.4 of this final report.
- For single span beams and uplift loading all test results are very well approximated (ratios: 0.87 - 1.00).

- For double span beams and uplift loading theoretically failure occurs with yielding at midsupport, while during the tests failure happened simultaneously at midsupport and in the span. So, similarly to the above described situation with gravity loading, there could have been a redistribution of forces at midsupport, which explains the higher test results particularly with test 28. For reasons of little conservatism ($q_{theor.}$ is smaller than $q_{failure}$ for the midsupport) and because the edge conditions at midsupport for stability check in the span wild change rigorous when midsupport failed following procedure has been proposed:

  "Ultimate uplift load for more span beam can be taken equal to the smallest of the following loads:
  * uplift load belonging to failure of midsupport
  * uplift load belonging to failure of the span when midsupport is still acting"

2.4 Design procedure of diaphragm braced beams (continuous system)

In reference [4] a design procedure for diaphragm braced beams in continuous systems has been derived. Furthermore this procedure has been checked with the results of a testing program which has been described in reference [2] and additional tests in reference [4].
The aim of the additional research was to improve the design procedure of 2.3 for continuous systems under gravity load by:
- Taking into account the redistribution of forces at interior supports of more span beams.
- Introducing the web crippling influence at supports

From the derivation of a design procedure detail support tests (see figure 3) have been executed to determine following aspects:
a. ultimate combinations of bendingmoment capacity over a support and the support reaction
b. moment-rotation behaviour over a support after the maximum capacity of the cross section has been reached (see figure 4)

From reference [2] test results are available for Z-140 purlins as single and double span loaded by gravity. With the results of the detail support test together with the single span tests, the behaviour of the double span tests has been analysed.
Figure 5 and 6 show the load-deflections diagrams of the double span tests no 25 and 27 as reported in reference [2]. Furthermore the results calculated according to the design procedure described in chapter 3 are plotted. This shows a good agreement between test results and proposed design procedure.

3. RECOMMENDATIONS FOR A DESIGN PROCEDURE OF DIAPHRAGM BRACED BEAMS OF COLD-FORMED SECTIONS

3.1 Design criteria

3.1.1 Gravity loaded single span systems

The design procedure for gravity loaded single span systems will be as follows:

a. The ultimate limit state is defined by arriving the ultimate moment capacity in the span. This criterion will be checked as follows:
   - The actual stresses σ_a caused by the design load shall be determined according to chapter 3.2.2
   - The tension stress in the free flange or compression stress in the braced flange has to be smaller than the design value for the yield stress.

b. The serviceability limit state is defined by arriving the allowable deflection in the span. The allowable deflection has to be taken from national regulations. The actual deflection shall be calculated taking into account the effective cross section caused by local buckling according to reference [21]

3.1.2 Uplift loaded single span systems

The design procedure for uplift loaded single span systems will be as follows:

a. The ultimate limit state is defined by arriving the ultimate moment capacity in the span. This criterion will be checked as follows:
   - The actual stresses σ_a caused by the design load shall be determined according to chapter 3.2.2.
   - The compression stress in the free flange or the tension stress in the braced flange has to be smaller than the design value for the yield stress.
   - The stability of the compressed free flange has to be checked according to chapter 3.2.3.

b. See 3.1.1 for uplift load.

3.1.3 Gravity loaded double span continuous systems

With double span is meant that over the midsupport the purlins are fully continued (no overlap or sleeve). The design procedure for the gravity loaded double span continuous systems will be as follows:

a. The ultimate limit state is defined by appearance of a mechanism. Ultimate moment capacity in the field shall be determined theoretically (in principal according to 3.1.1; in practice this means yield stress multiplied by the section modulus of the effective cross section) or by testing (single span tests with a span comparable with the length of the positive moment area). The moment-rotation behaviour over the support should be determined by tests according to 3.2.4. The formulae out of which $q_{failure}$ should be solved, for a double span system with equal spans are:

$$M_{rest} = \frac{q\,\ell}{2}\left(\ell - \sqrt{\frac{8\,M_{span}}{q}}\right) \qquad (1)$$

$$\theta = \frac{\ell}{EI}\left(\frac{1}{12}\,q\,\ell^2 - \frac{2}{3}\,M_{rest}\right) \qquad (2)$$

$$M_{rest} = \text{function of } \theta \qquad (3)$$

Herein:

- q : failure load of the system
- ℓ : distance between supports
- M_{span} : maximum moment capacity in the span determined by testing or theoretically (yield stress multiplied by the section modulus of the effectieve cross section)
- EI : actual bending stiffness belonging to maximum moment capacity in the span
- M_{rest}, θ } design value for the relation between moment and rotation above the support, after failure at that place, according to 3.2.4

b. The serviceability limit state is defined by two items being failure at the support and deflection of midspan.

b1. Failure at the support.

The requirement should be that failure of the beam at the support may appear at a loadfactor of 1.1. Failure should be determined by the governing moment-support reaction combination determined according to 3.2.4. The load, $q_{support}$, at which failure at the support takes place, can be derived from:

$$M_{supp} = \frac{1}{8} q_{supp} \ell^2$$

$$R_{supp} = \frac{5}{4} q_{supp} \ell$$

M_{supp} = function of R_{supp}, determined by tests according to 3.2.4 or by calculation according to ref. [21]

Herein:

q_{supp} : load at which failure above support take place (requirement: $1.1\ q_{service} \leq q_{supp}$)

ℓ : distance between supports

M_{supp}, R_{supp} } combination of moment capacity above support and the support reaction at failure of the support

b2. Deflection of midspan.

The deflection of midspan may be calculated assuming an elastic behaviour. For the bending stiffness the actual value ($I_{effective}$) should be taken.

3.1.4 Uplift loaded double span continuous systems

The design procedure for the uplift loaded double span continuous systems will be as follows:

a. the ultimate limit state is defined by the smallest of following loads:
   - The load at which the maximum moment at the support is reached. Only local buckling should be taken into account according to reference [21].
     The interaction of the support reaction with the moment may be neglected because it is introduced as a "tension" force.
   - The load at which the maximum moment in the span is reached according to 3.1.1.

   For the force distribution an elastic behaviour may be assumed.

b. See 3.1.3 b2 for uplift load.

3.1.5 More span beams with overlap or sleeve

- Detail support tests according to 3.2.4 should be executed. Only the raising part of the load-deflection curve is of interest.
- From the tests can be derived:
  a. the stiffness of the overlapping or sleeved part
  b. failure combination of bending moment + support reaction (in overlapped or sleeved part) or bending moment + shear force (besides overlapped or sleeved part).
- With item "a" the force distribution in the system can be determined (also taking into account local buckling of the cross section in the span).
- The force distribution shall be checked to:
  * failure combinations of bending moment + support reaction or bending moment + shear force (near support)
  * maximum span capacity according to 3.1.1. or 3.1.2 neglecting the influence of overlap or sleeve
  * the allowable deflections

3.2. Calculations rules and descriptions of tests used for the design criteria

3.2.1 Determination of lateral spring stiffness K

a. Determination by testing.
Figure 7 shows the test set up for experimental determination of the spring stiffness K. The value of K follows from:

$$K = \frac{F}{\delta}$$

Herein:
F = load per unity of test purlin length [N/mm]
δ = displacement in direction of load F
K = spring stiffness [N/mm^2]

The parameters involved are:
- number of fasteners per unity of purlin length
- width of the flange of the sheeting through which the connection with the purlin is made
- distance of fastener to rotation point of the purlin
- dimensions (H and t) of the purlin
- thickness of the sheeting

b. Determination of K from a combination of testing and calculation.
From a test according to "a" the rotation constant (C_D [Nmm/mm/rad]) of the connection between purlin and sheeting shall be determined:

case I: uplift load situation and Z-purlin:

$$C_D = \frac{H^2}{\frac{1}{K} - \frac{4\,H^2\,(H + a)}{E\,t^3}}$$

case II: gravity load situation and Z-purlin:

$$C_D = \frac{H^2}{\frac{1}{K} - \frac{4\,H^2\,(b + 2a + H)}{E\,t^3}}$$

For H, a and t see figure 2. The symbol b is the flat part of the purlin flange against the sheeting (b is distance between possible centres of rotation).

When value of K_n is wanted for an other purlin but same sheeting as in test and same distance "a" (in case I) or "b-a" (in case II):

case I:

$$K_n = \frac{1}{\frac{4\ H_n^2\ (H_n + a_n)}{E\ t_n^3} + \frac{H_n^2}{C_D}}$$

required condition: $a_n = a$

case II:

$$K_n = \frac{1}{\frac{4\ H_n^2\ (b_n + 2\ a_n + H_n)}{E\ t_n^3} + \frac{H_n^2}{C_D}}$$

required condition : $(b - a)_n = b - a$

The index "n" belongs to the wanted purlin values.
When testresults are not available, a conservative value for C_D may be taken as: $C_D = p * 130$ [Nm/m/rad]
herein: p = number of fasteners between purlin and sheeting per m' (per sheeting flange at maximum 1 fastener)
As edge conditions are valid for this value of C_D:
- flange width of sheeting through which is fastened: $b \leq 120$ mm
- core thickness of sheeting: $t \geq 0{,}66$ mm
- distance between fastener and point of rotation of the purlin (a or b - a) larger than 25 mm.

3.2.2. Determination of actual stresses

The actual stresses in a cross section in the field follows from:

$$\sigma_a = \frac{M\ (x)}{W_{ef}} \quad \text{(for braced flange)}$$

$$\sigma_a = \frac{M\ (x)}{W_{ef}} + \frac{M\ (y)}{W_{fy}} \quad \text{(for free flange)}$$

Herein:

$M(x)$: bending moment at a place x in the field due to the component of the design load acting in web direction

W_{ef} : section modulus for the effective cross section according to ref. [21]

W_{fy} : section modulus of the free flange plus 1/6 of the height of the web against lateral bending (for gross section of free flange)

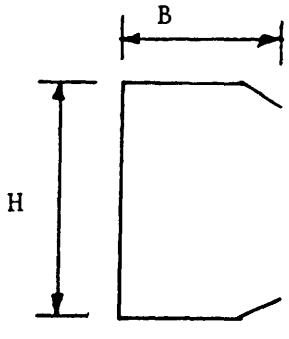

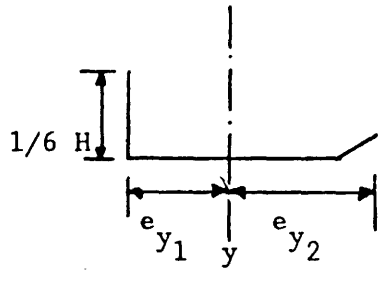

$$W_{fy_1} = \frac{I_{fy}}{e_{y_1}}$$

$$W_{fy_2} = \frac{I_{fy}}{e_{y_2}}$$

$$M(y) = \frac{EI_{fy}\,\pi^2}{\ell^2} A_1 \quad \text{(lateral bending moment)}$$

with :

E = Young's modulus

I_{fy} = moment of inertia (of gross section) of the free flange plus 1/6 of the height of the web against lateral bending

ℓ = span of the purlin

A_1 = constant depending on edge conditions of the purlin in lateral direction

At midspan and compression stress in the free flange, for A_1 may be taken:

- Simply supported beam:

$$A_1 = \frac{4k_h\, q\, \ell^4}{EI_{fy}\, \pi^5 + K\, \ell^4\, \pi - 1.8\, \frac{S_f}{I_{ef}}\, q\, \ell^4}$$

- Beams, both ends fixed:

$$A_1 = \frac{4\, k_h\, q\, \ell^4}{16\, EI_{fy}\, \pi^4 + 3\, K\, \ell^4 - 3.54\, \frac{S_f}{I_{ef}}\, q\, \ell^4}$$

- Beams, one end fixed and one end simply supported:

$$A_1 = \frac{4\, k_h\, q\, \ell^4}{EI_{fy}\, \pi^5 + K\, \ell^4\, \pi - 1.22\, \frac{S_f}{I_{ef}}\, q\, \ell^4}$$

Herein:

k_h : according to figure 2

q : the component of the design load acting in web direction

ℓ : span of the beam

I_{fy} : see before

K : lateral spring stiffness according to 3.2.1.; depending on place of centre of rotation of the beam

S_f : static moment of the free flange plus 1/6 of the height of the web about the neutral axis (the effective cross section is governing)

I_{ef} : the moment of inertia of the effective cross section of the whole beam.

Remark

When the free flange is in tension, then the "-" sign in the denominater should be a "+" sign.

3.2.3 Stability check of free flange in compression

The stability of the free flange in compression shall be checked as follows:

$$\omega \frac{M(x)}{W_{ef}} + \frac{M(y)}{W_{fy}} \leq f_{ty}$$

Herein:

M (x) : see 3.2.2

M (y) : see 3.2.2

W_{ef} : see 3.2.2 (for free flange)

W_{fy} : see 3.2.2

f_{ty} : design value for the yield stress

ω : buckling coëfficiënt

$$\omega = \frac{Q}{F - \sqrt{F^2 - \frac{Q}{\bar{\lambda}^2}}}$$

$$Q = \frac{A_{eff}}{A_g}$$

$$F = 1/2 \{Q + \frac{1 + \eta (\bar{\lambda} - 0.2)}{\bar{\lambda}^2}\}$$

$$\eta = 0.34 (4 - 3Q) \geq 0.76$$

$$\lambda = \frac{\ell_{cr}}{i_{fg}} \cdot \frac{1}{\pi} \sqrt{\frac{f_{ty}}{E}}$$

A_g - area of gross cross section

A_{eff} - area of effective cross section belonging to M(x)

i_{fg} - radius of gyration of gross cross section of free flange plus 1/6 of web height against lateral bending

ℓ_{cr} - buckling length depending on edge conditions in lateral deflections

- simply supported beam

$$\ell_{cr} = \frac{\ell}{\pi} \sqrt{\frac{\frac{2}{3} n^2 \pi^2 - 2}{n^4 + R}}$$

$$n_a = \sqrt{0.3 + \sqrt{0.09 + R}}$$

n = next higher integer value of n_a

- beams, both ends fixed

$$\ell_{cr} = \frac{\ell}{\pi} \sqrt{\frac{\frac{8}{9} n^2 \pi^2 + \frac{2}{3}}{\frac{16}{3} n^4 + R}}$$

$$n_a = 0.66 \sqrt[4]{R}$$

n = next higher integer value of n_a

- beams, one end fixed and one end simply supported

$$\ell_{cr} = \frac{\ell}{\pi} \sqrt{\frac{\frac{20}{27} n^2 \pi^2 - \frac{48}{27}}{n^4 + R}}$$

$$n_a = \sqrt{0.24 + \sqrt{0.06 + R}}$$

n = next higher integer value of n_a

ℓ - span of the beam

$$R = \frac{K \ell^4}{\pi^2 E I_{fg}}$$

K - lateral spring stiffness according to 3.2.1; depending on place of centre of rotation of the beam

I_{fg} - moment of inertia of gross cross section of free flange plus 1/6 of web height against lateral bending

3.2.4 Detail support test procedure

Test setup

The test setup for a detail support test is following:

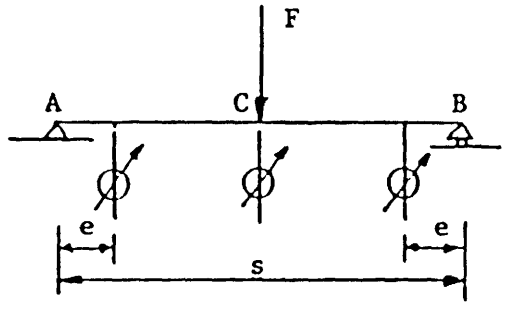

- The supports A and B are resp. a hinge and a roll. Rotation about the axis of the purlin may be prevented (e.g. by a cleat).
- The load introduction at C has to be in accordance with real application. This means mostly that lateral displacement of both flanges is prevented.
- Vertical displacements will be measured in the middle and at a distance "e" from the supports. The latter is necessary to eliminate eventual displacements in the support.
- The span "s" should be choosen in such a way that combinations of moment (M_C) and forces (F) will be produced which are likely to appear in real applications. For double span beams (with span ℓ) with a uniformly distributed load: $s = 0.4\ \ell$.

Execution of test

During testing the load F and the displacements will be recorded. (At least five recordings of almost equal steps up to the maximum of F). After reaching maximum load the recording shall go on (test steering shall be done by controling the displacements). Testing shall go on up to the load is decreased to about 10% - 15% of F_{max} during increasing the displacements.

At every span "s" the test shall be executed in two-fold. When the two values of F_{max} differ more than 5% from the mean value, another test is necessary and the two tests with the lowest value for F_{max} should be used in further evaluation.

Interpretation of testresults

From the tests following data should be derived:

a. $M_{support}$ as a function of $R_{support}$ at failure.
For every test the value of F_{max} should be corrected with factors k_t and k_f to take into account the nominal values for the steel core thickness and the yield stress:

k_f - correctionfactor to take into account the guaranteed yield stress

$$k_f = \frac{f_{ty}}{f_y} \qquad \text{if } f_{ty} < f_y$$

$$k_f = 1 \qquad \text{if } f_{ty} \geq f_y$$

Herein:
f_{ty} : guaranteed design value for the yield stress
f_y : yield stress of the testmaterial

k_t - correctionfactor to take into account the nominal steel core thickness

$$k_t = (t_n/t)^2 \qquad \text{if } t_n < t$$
$$k_t = t_n/t \qquad \text{if } t_n \geq t$$

Herein:
t_n : nominale steel core thickness
t : steel core thickness of test material

For every testspan "s" the mean value of the corrected values of F_{max} shall be defined as R_{supp}. The belonging moment M_{supp} follows from:

$$M_{supp} = \frac{1}{4} s R_{supp}$$

For every s this combination can be shown in a diagram with M and R axis. Intermediate combinations of M_{supp} and R_{supp} may be determined by lineair interpolation.

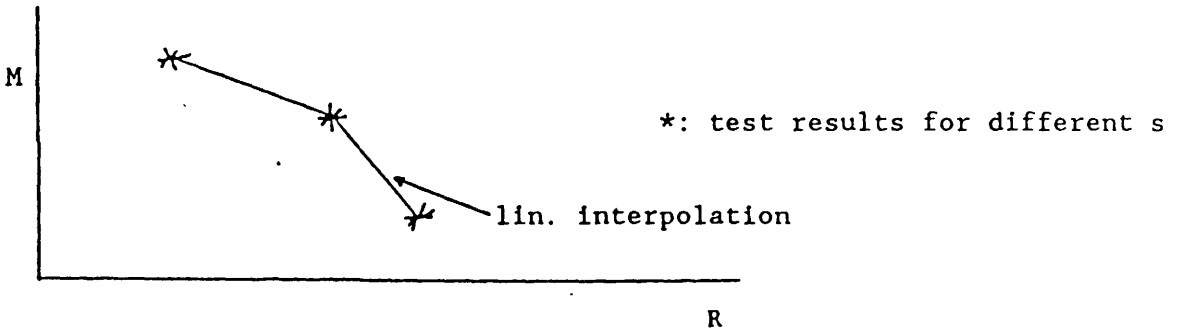

b. Moment-rotation behaviour over the support.

After reaching F_{max} the moment-rotation behaviour is important to determine the rest moment at different rotations θ.

The value of θ for different load levels follows from:

$$\theta = \frac{2\,(\delta_{pl} - \delta_e)}{\frac{1}{2}\,s - e}$$

Herein:

θ : rotation

δ_{pl} : deflection in after-maximum stage corrected with those at "e" (decreasing part of curve)

δ_e : deflection in pre-maximum stage corrected with those at "e" (increasing part of curve)

s : span in test

e : place of dial gauges for elimination of support deformations

For every test (also different values of s) a relation of M and θ can be determined.
As design value for M-θ should be taken the mean of the values of M and multiplied by 0.9. (see following figure).

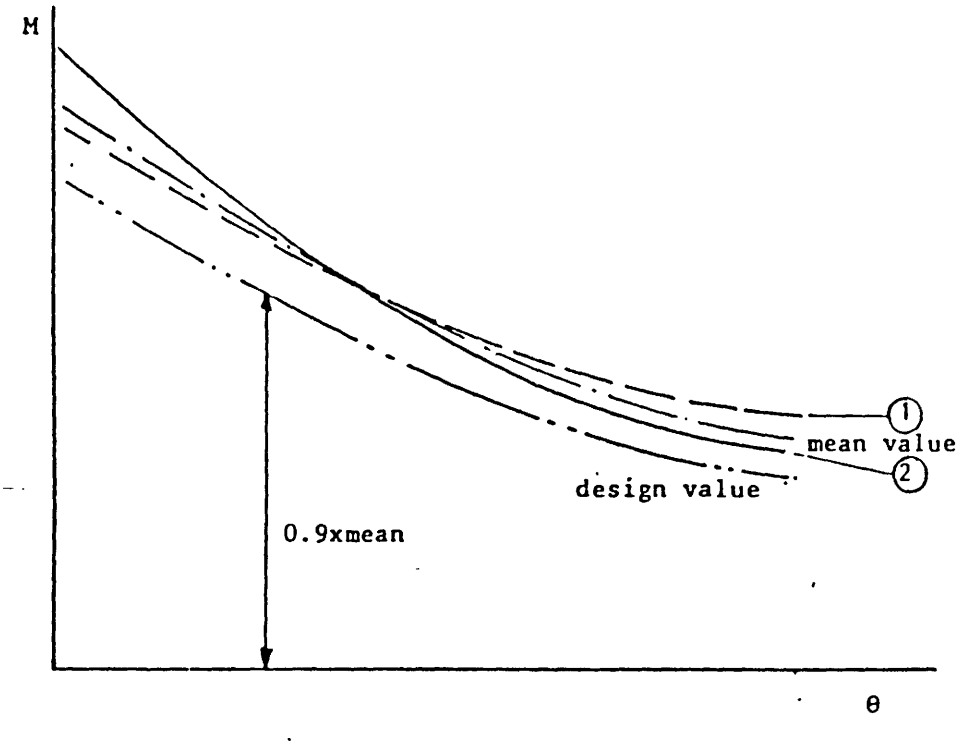

4. SUMMARY

The research carried out in this project has been concentrated on the behaviour and load carrying capacity of diaphragm braced beams of cold-formed sections.

There has been started with a hypothesis for a calculation model. To check that model a number of tests has been executed:
- 24 tests on simply supported beams
- 4 tests on double span beams
- 4 tests on detail supports

On basis of these tests the calculation model has been improved. Finally this has lead to a recommendation for a design procedure for diaphragm braced beams (see chapter 3).

Furthermore it is recommended to use some detail support tests as one of the input parameters for designing purlin-systems. Only then the ultimate load bearing capacity of the system can be predicted. It is also sensible to do tests for the torsional restraint of the purlin delivered by the sheeting. The values given in the report are at the conservative side.

The results of this project will be introduced into committee T7 of the ECCS. This committee is drafting European Recommendations for the design of light gauge steel members.

REFERENCES

[1] F. Soetens and A.W. Tomà
Research for the mechanical behaviour of cold-formed sections and drafting of design rules.
Literature study.
TNO-IBBC report BI-84-55, September 1984.

[2] A.A. Kip and A.W. Tomà
Research for the mechanical behaviour of cold-formed sections and drafting of design rules.
Report of testing of diaphragm braced beams.
TNO-IBBC report BI-86-54, August 1986.

[3] F. Soetens and A.W. Tomà
Research for the mechanical behaviour of cold-formed sections and drafting of design rules.
Design procedure of diaphragm braced beams.
TNO-IBBC report BI-87-12, February 1987.

[4] A.W. Tomà
Research for the mechanical behaviour of cold-formed sections and drafting of design rules.
Detail support tests for continuous systems and the derivation of a design procedure.
TNO-IBBC report BI-87-81, August 1987.

[5] Hancock, G.J., Bradford, M.A., "Elastic interaction of local and lateral buckling in beams", Thin-Walled Structures, Volume 2, 1984.

[6] Trahair, N.S., Nethercot, D.A., "Bracing requirements in thin-walled structures", Development in Thin-Walled Structures, Volume 2, 1984

[7] Levy, M., Glassman, A., "Annäherungsweise Berechnung des Kippens kaltgeformter Profile aus dünnwandigem Stahlblech mit offenem Querschnitt", Acier/Stahl/Steel, Volume 6, 1976.

[8] Gosowski, B., Kubica, E., Rykaluk, K., "Beanspruchung einfeldriger dünnwandiger C-Pfetten, die mit Trapezblechen zusammenwirken", Der Stahlbau 11, 1983.

[9] Blanchard, G., "Profilés en Zed formés a froid", Construction Métallique, no. 1 - 1973.

[10] Sokol, L., "Calcul des pannes en section Z", Constrcution Métallique, no. 1 - 1979.

[11] Sokol, L., "Calcul de la longueur de flambement de la semelle comprimée des pannes en Z", Construction Métallique no. 2 - 1980.

[12] Davies, J.M. and Thomasson, P.O., "Local and overall buckling of light gauge members", Proc. Michael R. Horne Conference, University of Manchester, September, 1983.

[13] Bryan, E.R., Grant, G., Muir, J.A., "Design of cold formed steel members and sheeting", University of Salford.

[14] Kanning, W., "Dachsysteme mit Kaltprofilpfetten", Der Stahlbau 1/1983.

[15] Schardt, R., Schrade, W., "Kaltprofil-Pfetten", Technische Hochschule Darmstadt, Bericht nr. 1, 1982.

[16] Pekőz, T., Soroushian, P., "Behaviour of C- and Z-purlins under wind uplift", Cornell University Ithaca, N.Y., Fabruary, 1981.

[17] Celebi, N., "Diaphragm braced channel and Z-section beams", Cornell University, N.Y., May, 1972.

[18] Hetrakul, N., Yu, W.W., "Structural behaviour on beam webs subjected to web crippling and a combination of web crippling and bending", University of Missouri-Rolla, Missouri, June, 1978.

[19] Huck, G., "Vergleich der Bemessungsvorschriften für Kaltprofile als Dachpfetten", Universität Fridericiana Karlsruhe, February, 1984.

[20] Johnston, G.H., "Design criteria for metal compression members", Third edition, John Wiley and Sons inc., New York, London, Sydney.

[21] European Recommendations for the Design of light gauge steel members, ECCS-TWG 7/1 - First edition 1987.

Table I

Test programme, combinations of parameters							
Test no.	system	appr. span [m]	shape	h [mm]	t [mm]	diaphragm	loading
1, 2	S	6	Z	140	1,5	A	G
3, 4	S	6	Z	140	1,5	A	U
5, 6	S	6	Z	140	1,5	B	G
7, 8	S	6	Z	140	1,5	B	U
9, 10	S	6	Z	240	2,0	A	G
11, 12	S	6	Z	240	2,0	A	U
13, 14	S	4	Z	140	1,5	A	G
15, 16	S	4	Z	140	1,5	A	U
17, 18	S	6	Σ	140	1,5	A	G
19, 20	S	6	Σ	140	1,5	A	U
21, 22	S	6	C	140	1,5	A	G
23, 24	S	6	C	140	1,5	A	U
25	D	4	Z	140	1,5	A	G
26	D	4	Z	140	1,5	A	U
27	D	6	Z	140	1,5	A	G
28	D	6	Z	140	1,5	A	U

For the system S means single span and D means double span.

For the loading G means gravity and U means uplift.

Table Ia

SINGLE SPAN - GRAVITY LOAD

scheme.

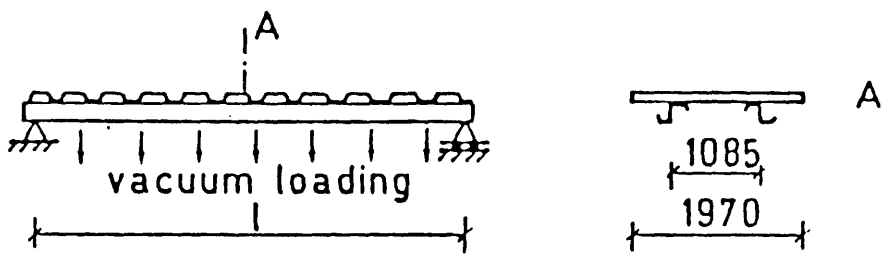

Test parameters

test nr.	purlin	sheeting	span l
1 - 2	⌊ 140 - 1.5	35 - 40 - 0.70	5890
5 - 6	⌊ 140 - 1.5	35 - 119 - 0.70	5890
9 - 10	⌊ 240 - 2.0	35 - 40 - 0.70	5890
13 - 14	⌊ 140 - 1.5	35 - 40 - 0.70	4390
17 - 18	Σ 150 - 1.5	35 - 40 - 0.70	5890
21 - 22	□ 140 - 1.5	35 - 40 - 0.70	5890

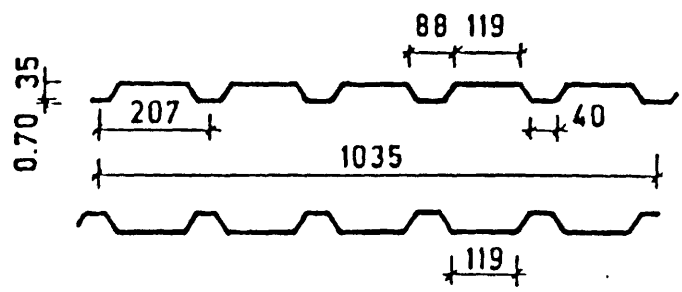

Table Ib

SINGLE SPAN - UPLIFT LOAD

scheme

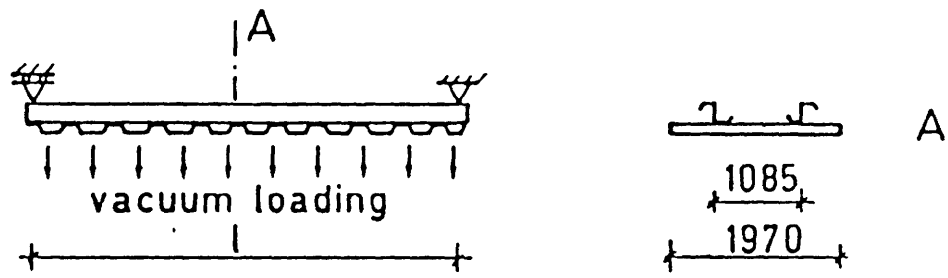

Test parameters

test nr.	purlin	sheeting	span l
3 - 4	⌐ 140 - 1.5	35 - 40 - 0.70	5890
7 - 8	⌐ 140 - 1.5	35 - 119 - 0.70	5890
11 - 12	⌐ 240 - 2.0	35 - 40 - 0.70	5890
15 - 16	⌐ 140 - 1.5	35 - 40 - 0.70	4390
19 - 20	Σ 150 - 1.5	35 - 40 - 0.70	5890
23 - 24	⊏ 140 - 1.5	35 - 40 - 0.70	5890

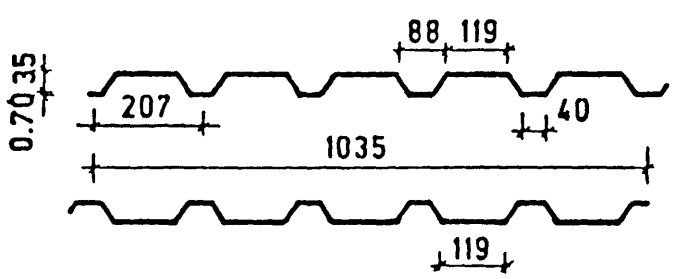

Table Ic

DOUBLE SPAN - GRAVITY LOAD

scheme

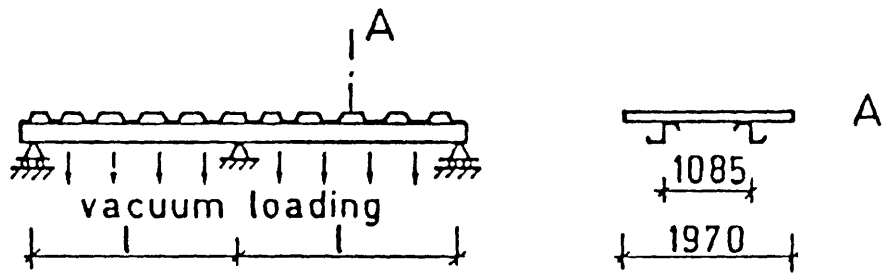

Test parameters

test nr.	purlin	sheeting	span l
25	ℒ140 - 1.5	35 - 40 - 0.70	4195
27	ℒ140 - 1.5	35 - 40 - 0.70	5945

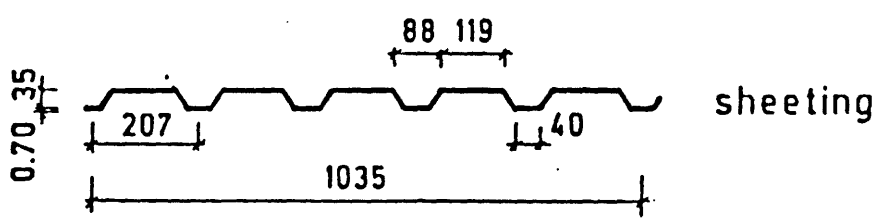

Table Id

DOUBLE SPAN - UPLIFT LOAD

scheme

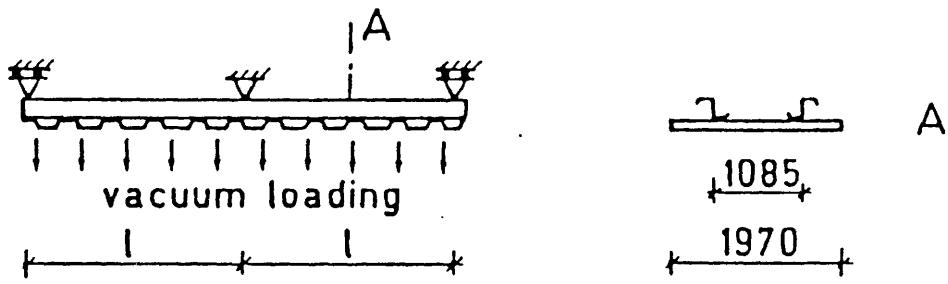

Test parameters

test nr.	purlin	sheeting	span l
26	ℒ 140 - 1.5	35 - 40 - 0.70	4195
28	ℒ 140 - 1.5	35 - 40 - 0.70	5945

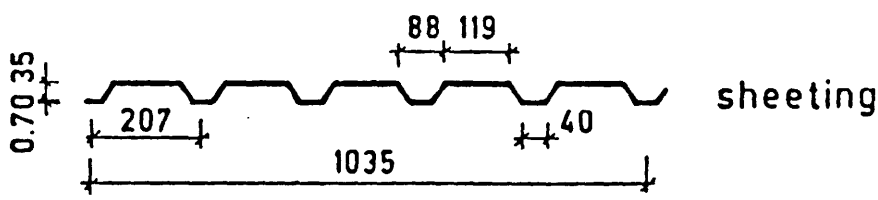

Table II: Failure loads

test no.	dead load (N/m^2)	max. test load (N/m^2)	total failure load (N/m^2)
1	102	1160	1262
2		1180	1282
3		770	872
4	102	860	962
5	102	1140	1242
6		1030	1132
7		780	882
8	102	848	950
9	135	4026*)	4161
10		3826*)	3961
11		2325	2460
12	135	2230	2365
13	102	2100	2202
14		2150	2252
15		1530	1632
16	102	1495	1597
17	110	1575	1685
18		1185	1287
19		1170	1280
20	110	1270	1380
21	102	1175	1277
22		1185	1287
23		825	927
24	102	790	892
25	102	2600	2702
26	102	2300	2402
27	102	1275	1377
28	102	1200	1302

*) inclusive 876 N/m^2 caused by paving tiles

Table III: Comparison between different design procedures

In interim report no. 4, September 1985 the results of the design procedure have been compared already with test results on cold-formed Z-sections of SAB-Profiel B.V.
Except for the above comparison the test results have also been compared with the design method of Sokol [21] and with the method Pekoz [16]. The results are summarized in next table.

	Simply supported, single span beams					
	Z-section span length [m]	F_{theor} [kN]	F_{test} [kN]	$\frac{F_{theor}}{F_{test}}$	Sokol approach	Pekoz approach
Uplift loading	ℓ = 4,0	19,2	20,3	0,95	0,59	0,70
	ℓ = 5,0	14,6	16,5	0,89	0,57	0,86
	ℓ = 6,0	11,8	13,3	0,88	0,67	1,57
Gravity loading	ℓ = 5,0	29,8	26,6	1,12*)	-**)	-

*) If also the effective thickness according to the Swedish Code StBk-N5 is applied, this value reduces to 1,0.
**) Not defined for simply supported, single span beams.

Note: With the design method described in the final report, which is an improved version of the method used to calculate the above results, the theoretical results even better approximate the test results.

Table IV: checking of the proposed design procedure and the results of the test program

Test no.	Shape of cross-section	Span length [mm]	Total failure load [N/m^2]	Failure load q per m purlin length [N/m']	Theoretical load q [N/m']	Ratio $\frac{q_{th}}{q_{test}}$	G = gravity U = uplift
1			1262	1253	1197	0,96	G
2	Z-140	5890	1282				
3			872	903	893	0,99	U
4			961				
5			1242	1223	1197	0,98	G
6	Z-140	5890	1232	1214	1196	0,98	G
7			882	902	903	1,00	U
8			950				
9			4161	4000	3928	0,98	G
10	Z-240	5890	3961				
11			2460	2376	2230	0,94	U
12			2365				
13			2202	2169	2228	1,03	G
14	Z-140	4390	2252	2218	2164	0,98	G
15			1632	1590	1573	0,99	U
16			1597				
17			1686	1678	1673	1,00	G
18	Σ-150	5905	1721				
19			1281	1311	1140	0,87	U
20			1381				
21			1277	1263	1219	0,97	G
22	C-140	5890	1287				
23			927	896	840	0,94	U
24			892				
25			2702	2218*)	2501***)	1,13	G
26	Z-140	4195	2402	2366	2309	0,98	U
27			1377	1125**)	1156***)	1,03	G
28	Z-140	5945	1302	1282	1155	0,90	U

*) yielding midsupport: q_{test} = 2218 N/m', failure midsupport/span: q_{test} = 2661 N/m'

**) yielding midsupport: q_{test} = 1125 N/m'; failure midsupport/span: q_{test} = 1356 N/m'

***) theoretical failure at midsupport

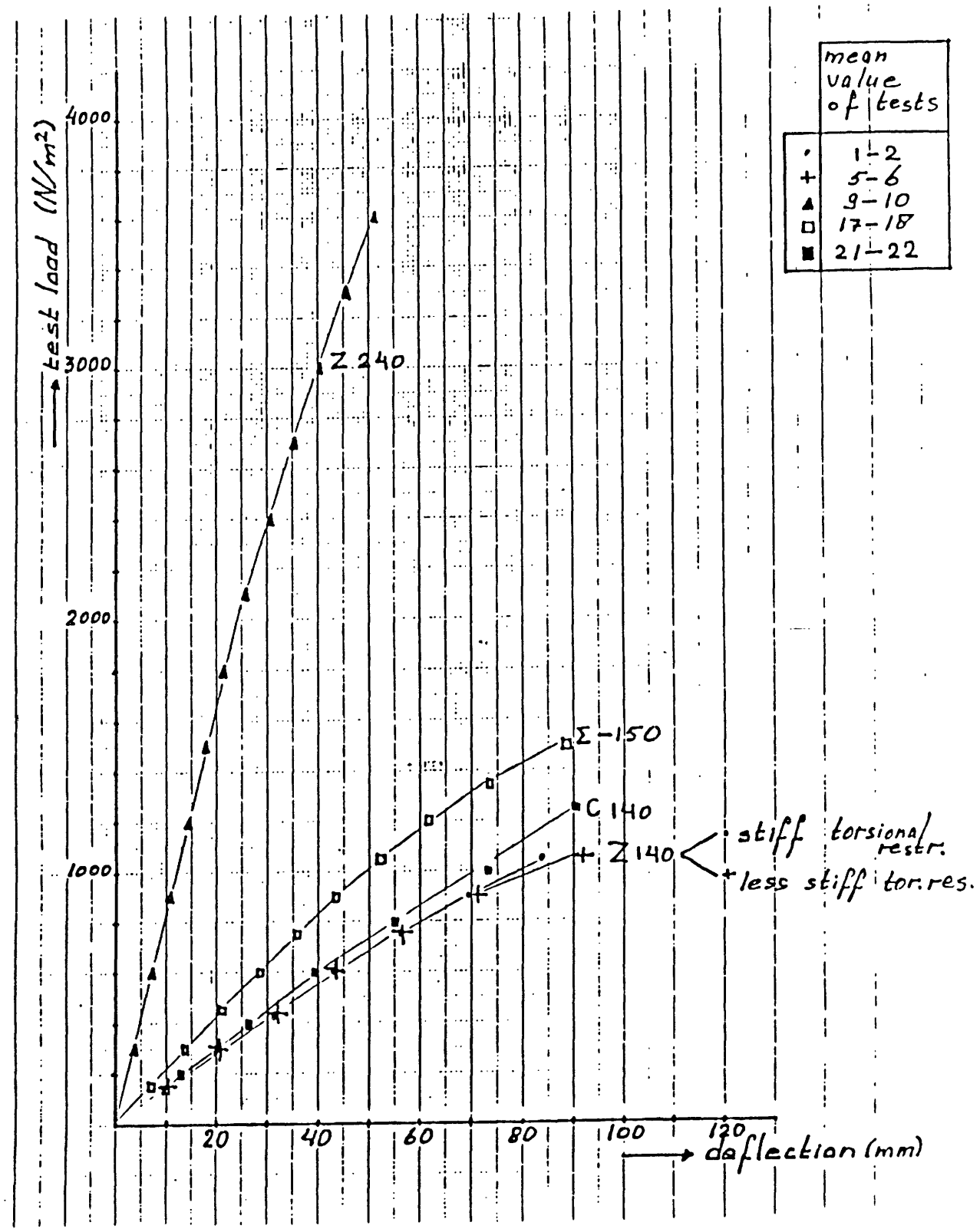

Graph 1: comparison between the load-deflection behaviour for the single span (6 m) gravity loaded tests. (The shown values are mean values of two equivalent tests exclusive the dead weight.)

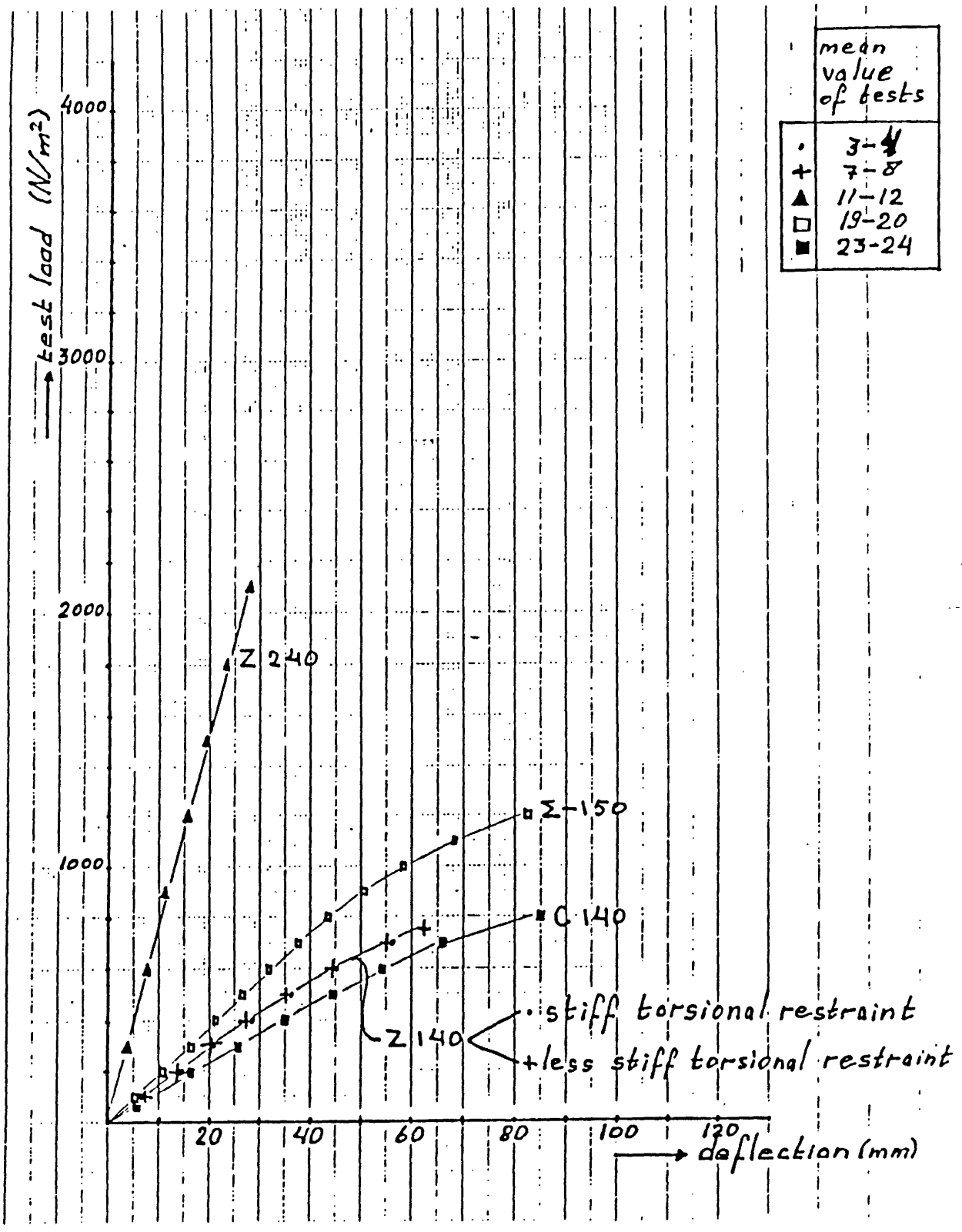

Graph 2: comparison between the load-deflection behaviour for the single span (6 m) uplift loaded tests. (The shown values are mean values of two equivalent tests exclusive the dead weight.)

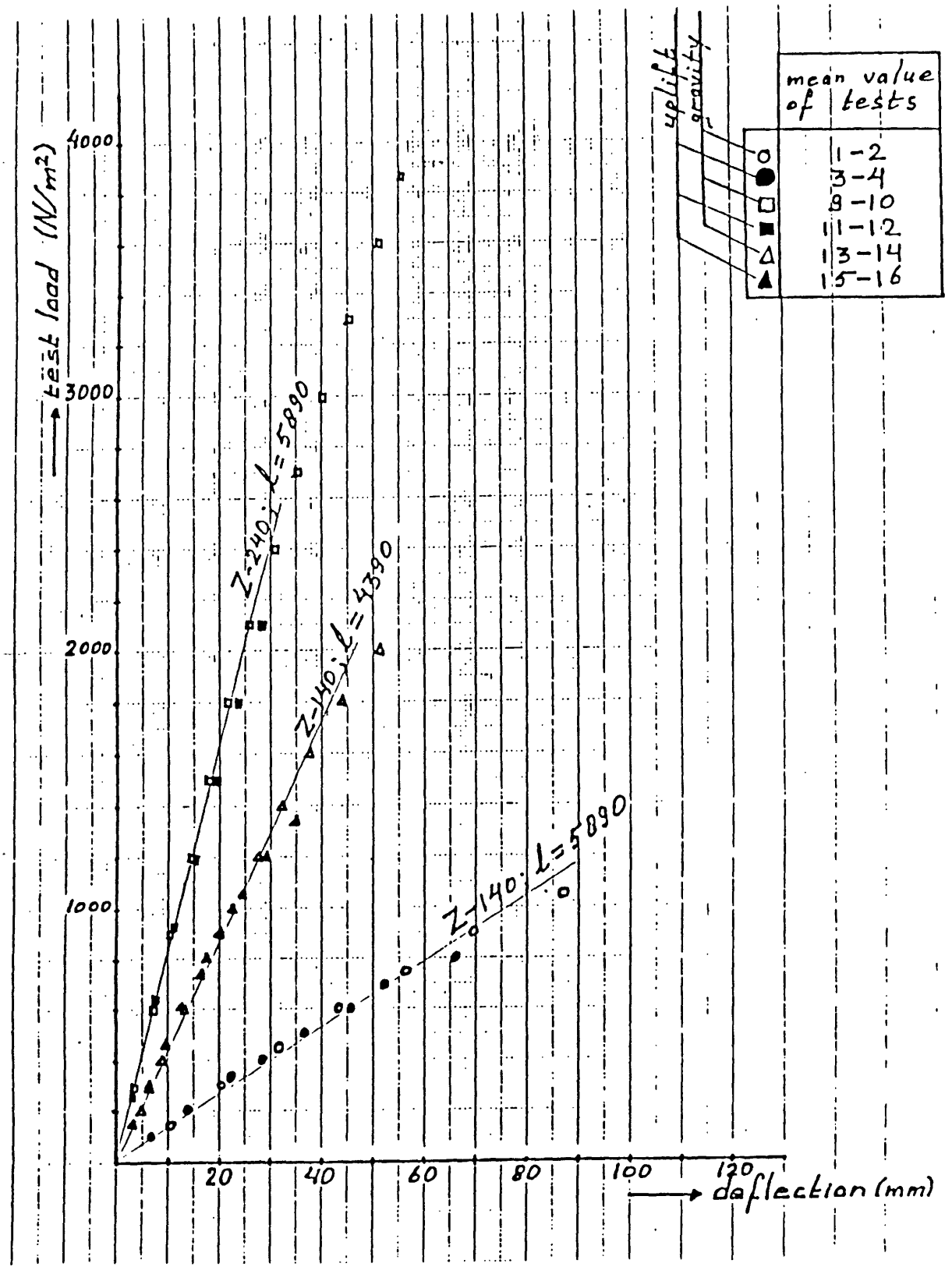

Graph 3: comparison between the load-deflection behaviour for the uplift and gravity loaded Z-sections. (The shown values are mean values of two equivalent tests exclusive the dead weight.)

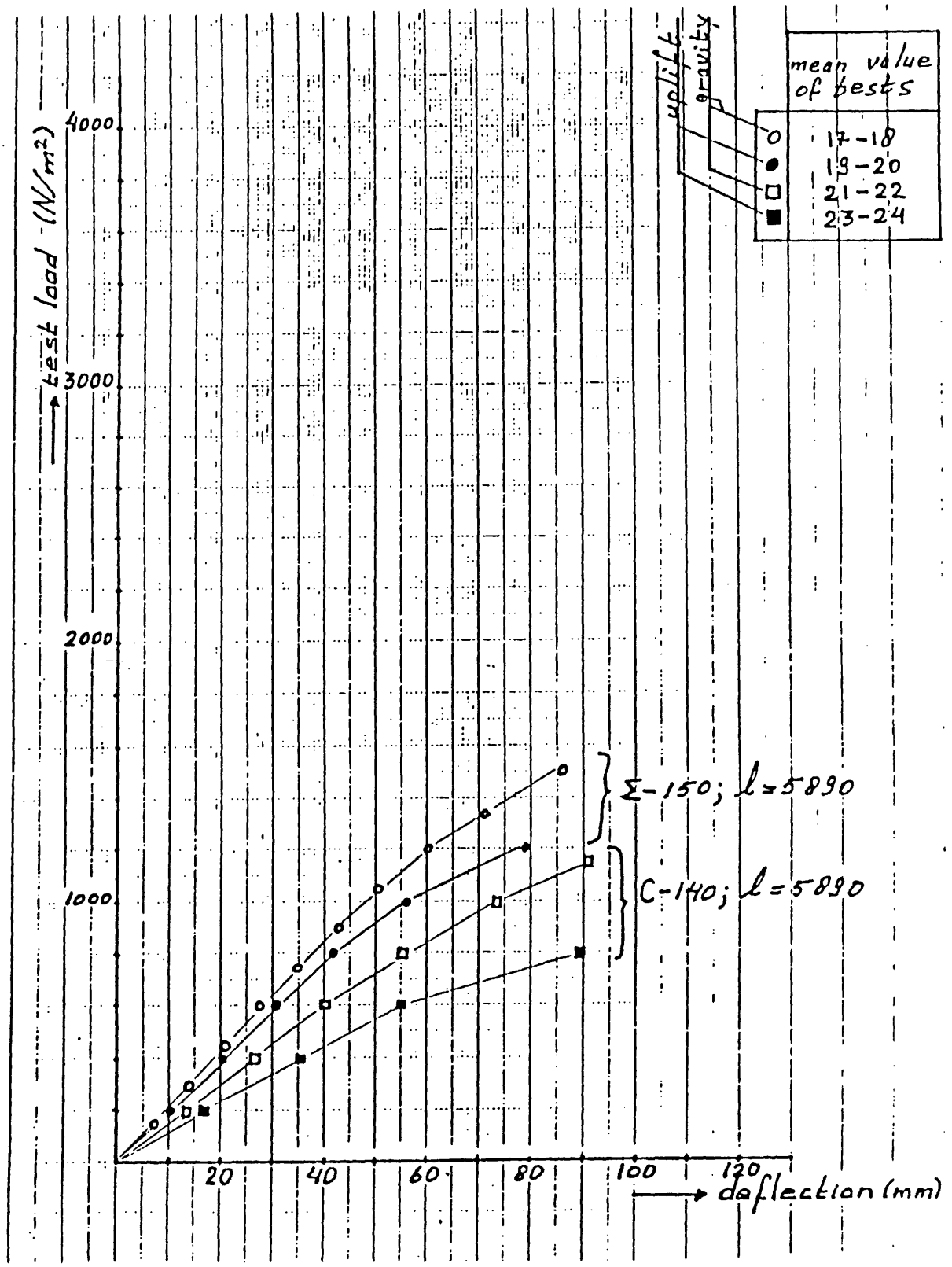

Graph 4: comparison between the load-deflection behaviour for uplift and gravity loaded C- and Σ-sections. (The shown values are mean values of two equivalent tests exclusive the dead weight.)

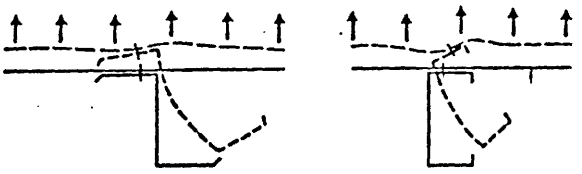

a. Total deflection

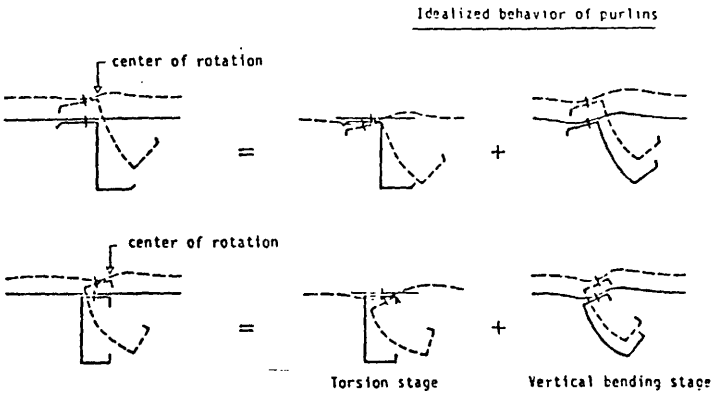

b. Components of total deflection

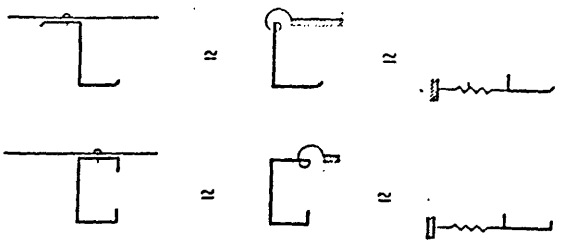

c. Idealisation of rotational restraint

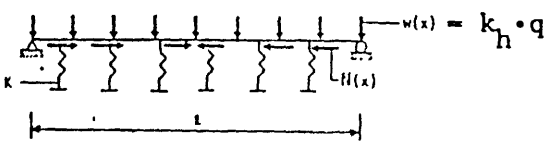

d. Beam-column idealisation

Fig. 1: C- and Z-purlins under uplift loading according to ref. [16]

Gravity load

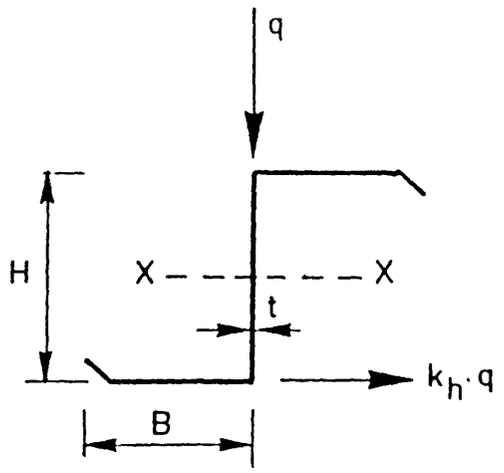

$$k_h = \frac{S_{fl} \cdot B}{2 I_x} = \frac{B^2 Ht}{4 I_x}$$

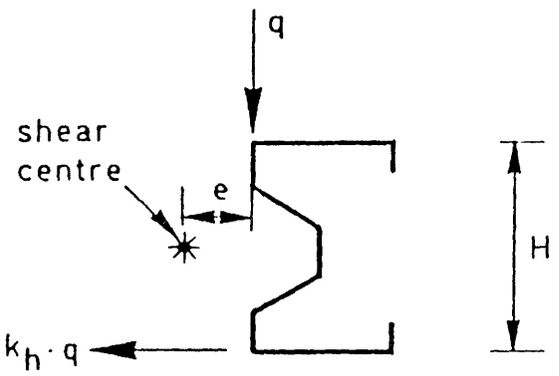

$$k_h = \frac{e}{H}$$

When shear centre at right side of q, than lateral load is working in opposite direction

Uplift load

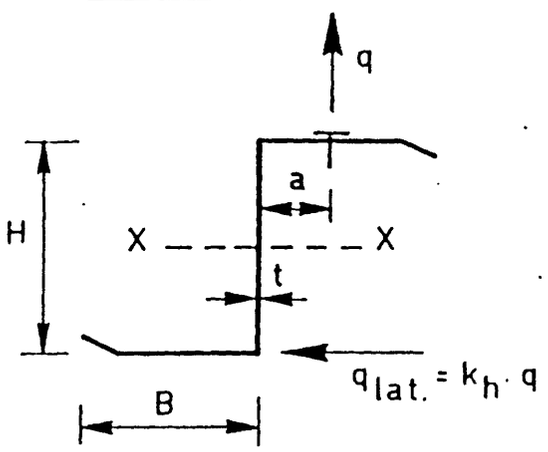

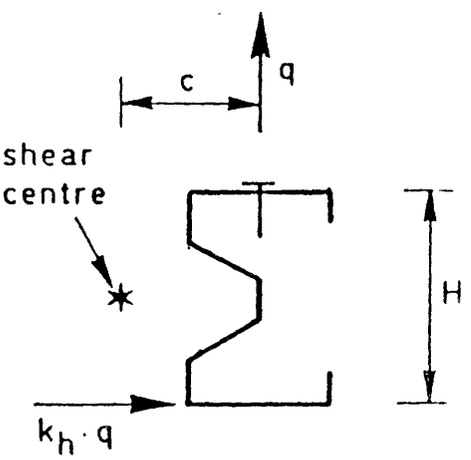

$$k_h = \frac{c}{H}$$

When shear centre at right sideof fastener, than lateral load is working in opposite direction.

$$\text{If } \frac{a}{H} < \frac{B^2 Ht}{4 I_x} \longrightarrow \overleftarrow{k_h} = \frac{B^2 Ht}{4 I_x} - \frac{a}{H}$$

$$\text{If } \frac{a}{H} > \frac{B^2 Ht}{4 I_x} \longrightarrow \overleftarrow{k_h} = \frac{a}{H} - \frac{B^2 Ht}{4 I_x}$$

Fig. 2: Model description, bending + torsion converted into in-plane bending + lateral bending of a part of the section.

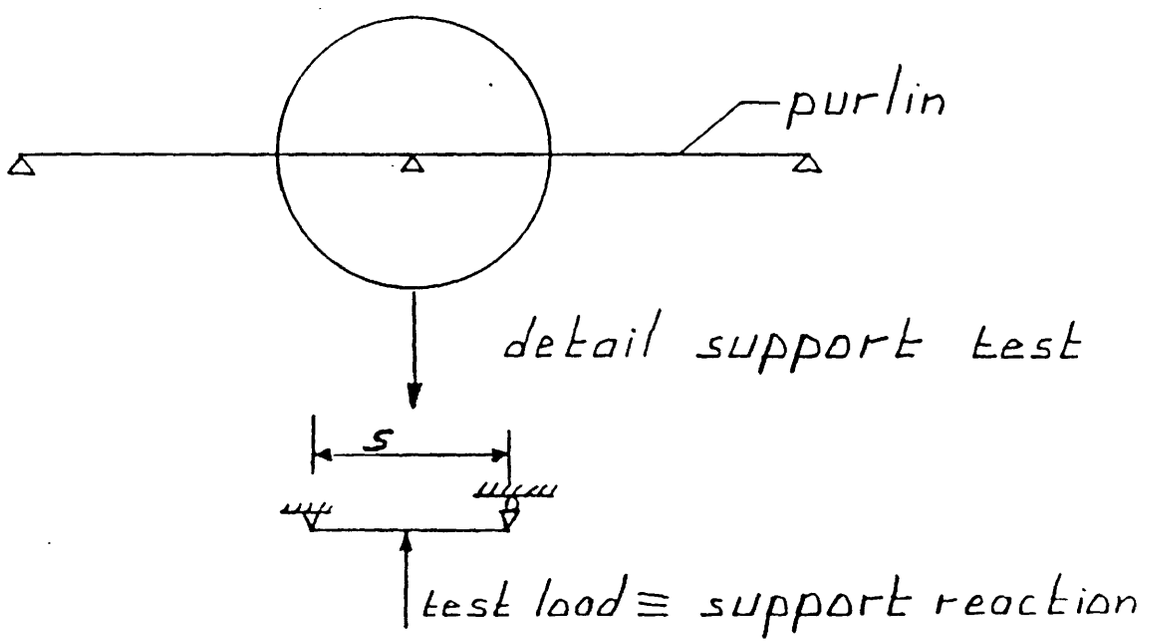

Fig. 3: Scheme of a detail support test

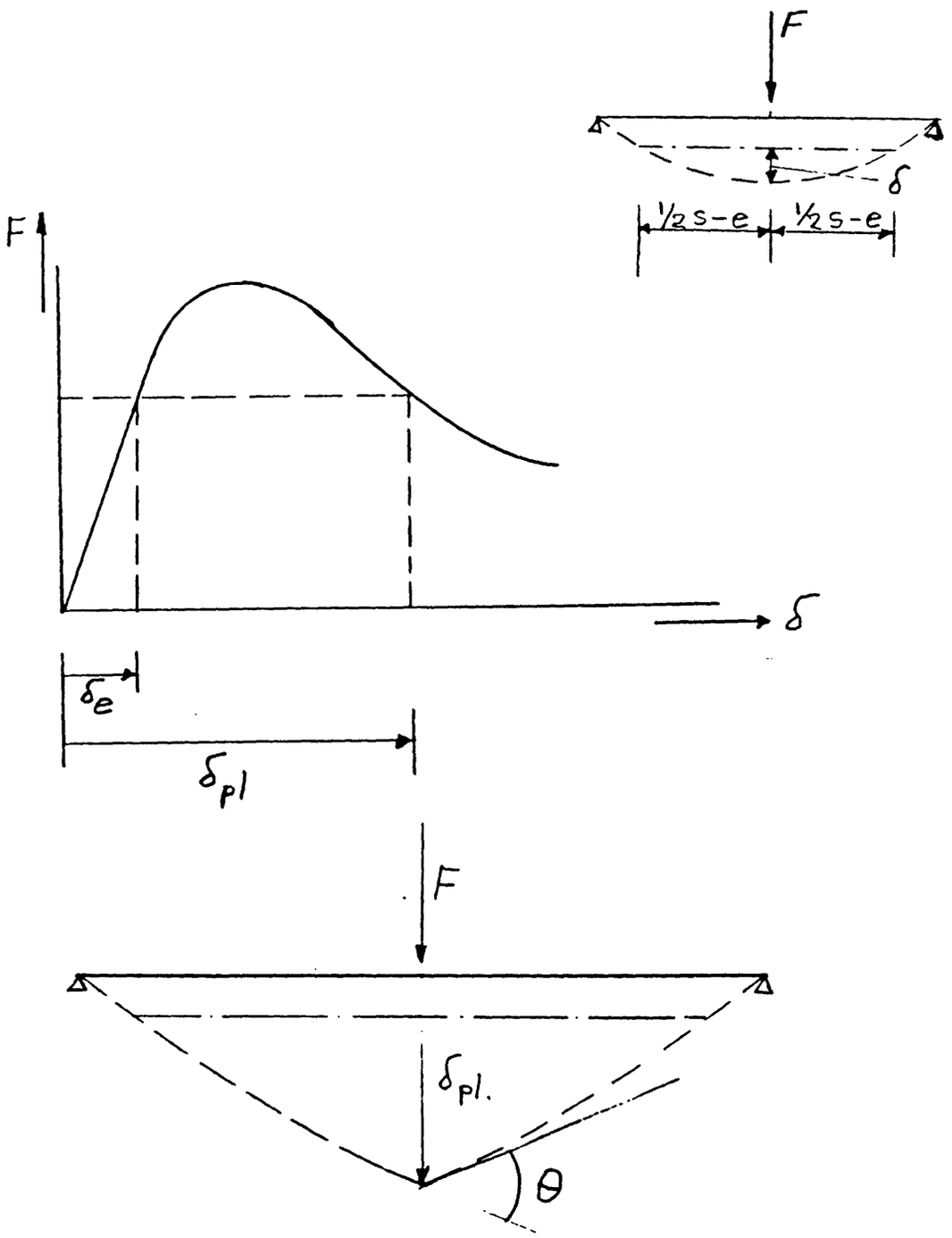

$$\theta = \frac{2(\delta_{pl.} - \delta_e)}{\frac{1}{2}s - e}$$

Fig. 4: Rotation of cross-section under the load in after-maximum stage.

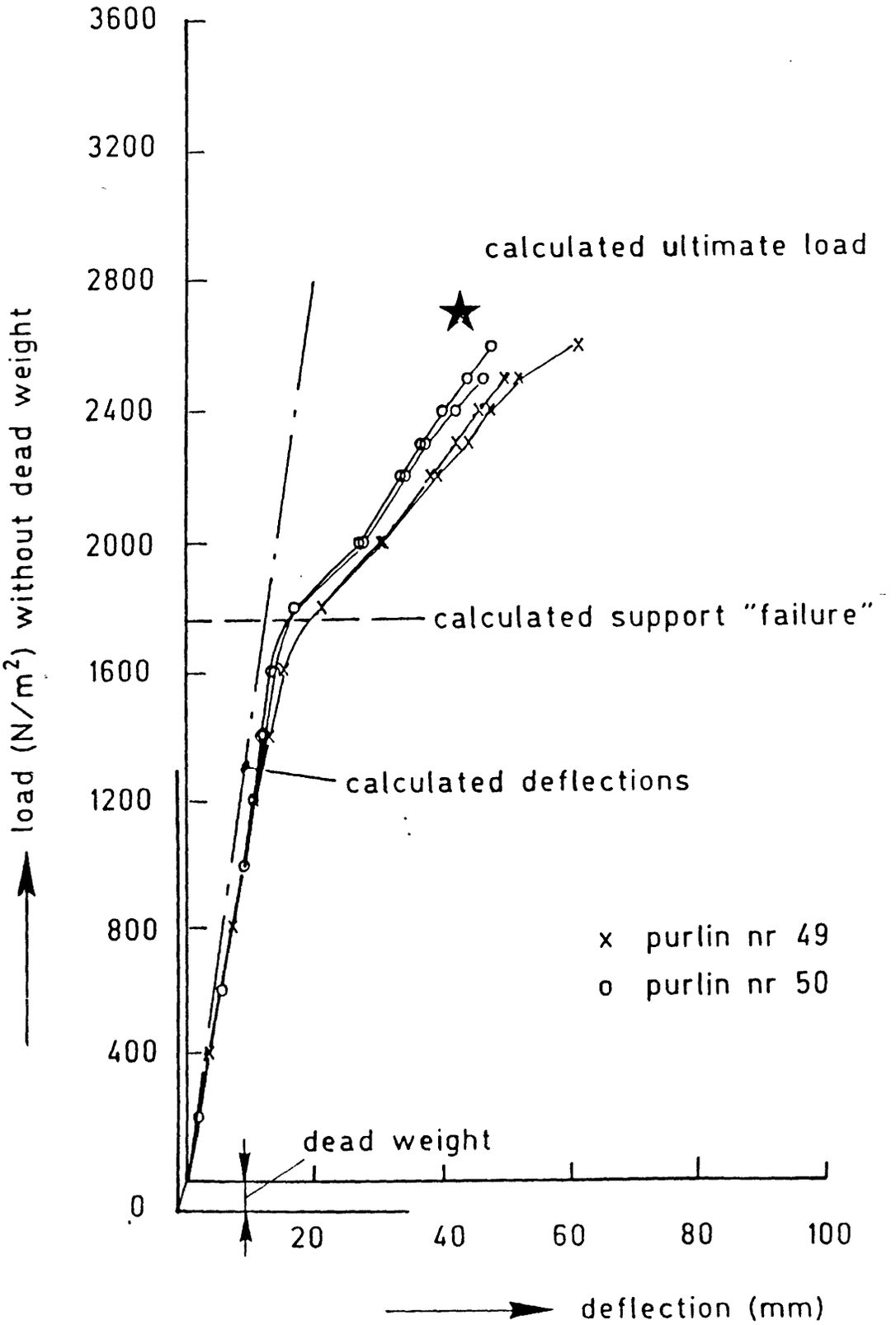

Fig. 5 test and calculation results of a double span beam, gravity load (testno 25 of ref. [2])

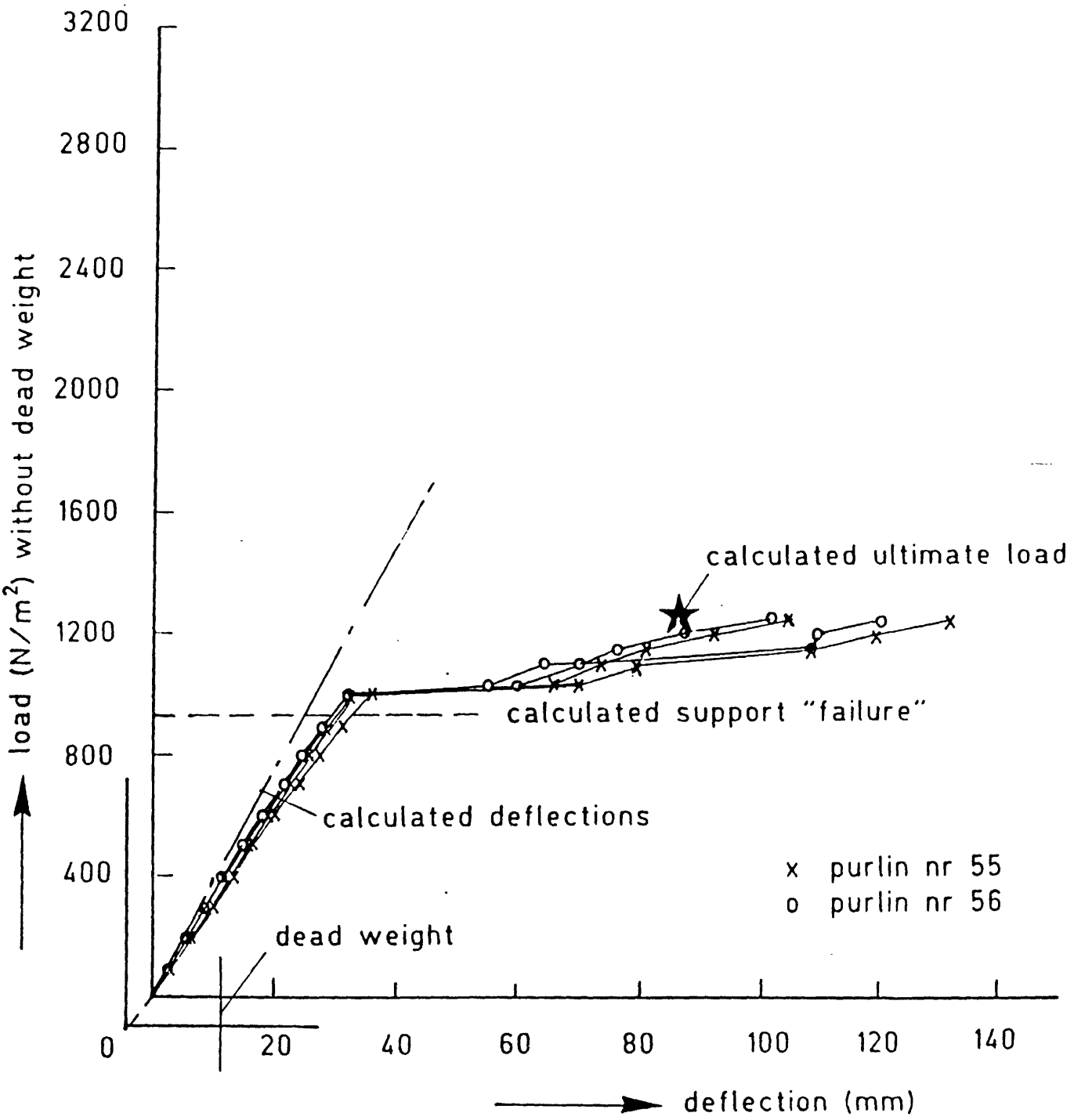

Fig. 6: Test and calculation results of a double span beam, gravity load (testno. 27 of ref. [2])

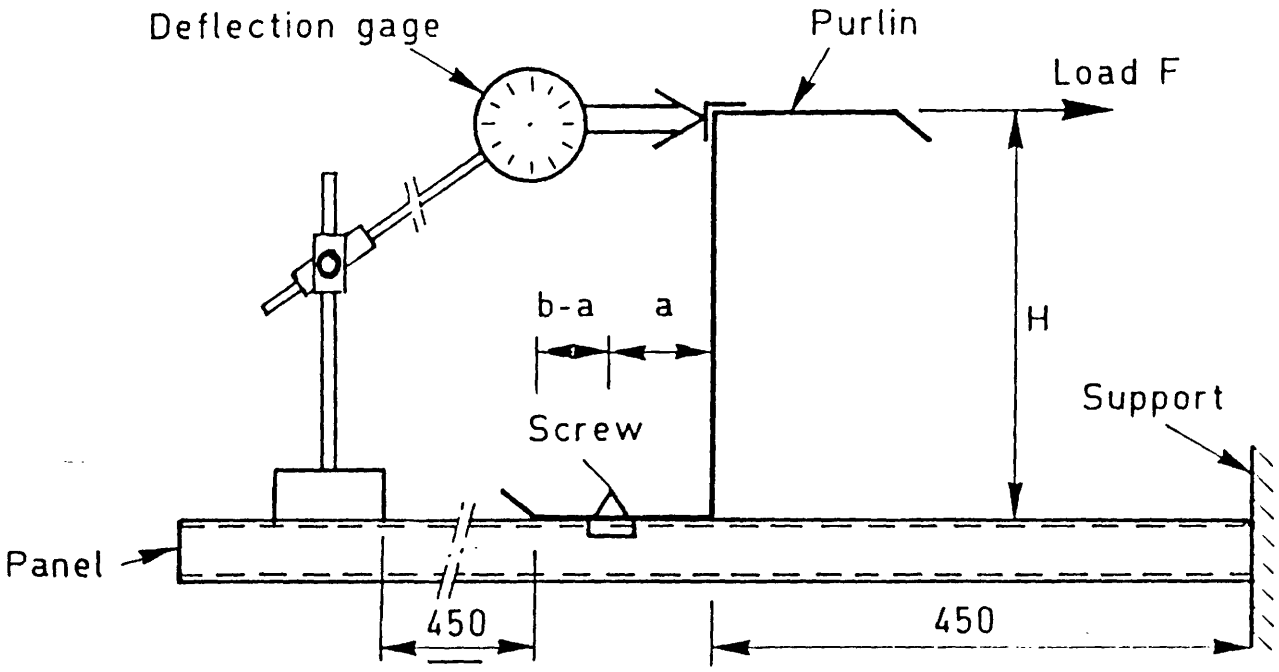

Fig. 7 Experimental determination spring stiffness (K)
The load direction showed concerns the uplift situation

For gravity load the direction of F hasto be opposite.